Effects of land use change from temperate grassland to *Miscanthus* on aspects of hydrology and greenhouse gas emissions

A thesis presented
for the degree of Doctor of Philosophy

Amanda Jane Holder BSc (Hons)
Aberystwyth University

October 2019

Candidate's Surname/Family Name	Holder
Candidate's Forenames (in full)	Amanda Jane
Candidate for the Degree of	PhD (PhD, MPhil, LLM (Res) etc.)
Academic year the work submitted for examination	2018-2019

Summary

This thesis investigates implications of land conversion from agricultural grassland to the bioenergy crop *Miscanthus* on soil nitrous oxide (N_2O) emissions, soil carbon stocks (SOC), and hydrology.

To address concerns of negative impacts on SOC, soils (0-30 cm) were sampled twelve years (T_{12}) after conversion to *Mxg* and four hybrids. T_{12} SOC was not different to six year post-planting stocks, but 8 Mg C ha^{-1} lower than pre-planting.

N_2O fluxes during conversion are poorly studied therefore commercially available *M. x giganteus* (*Mxg*) and a novel hybrid were planted using different tillage methods in a randomised plot trial with an un-cultivated pasture control. Fluxes recorded using static chambers over the first two years revealed no difference between cultivation methods. However, emissions from the *Miscanthus* plots were 550-819% higher than the control in the first year.

Evapotranspiration is important in hydrology. Compared to five years of eddy covariance data from a *Mxg* plantation the Penman-Monteith model provided the closest estimate of four evapotranspiration formulae tested. New seasonal crop coefficient values are presented: 0.63 (early), 0.85 (main), 1.57 (late), and 1.12 (winter). Canopy precipitation interception (C_i) was estimated as 24% (obtained over nine months using stem-flow, through-flow, and rain gauges).

Using the Soil Water Assessment Tool (SWAT) hydrological changes following conversion of 50% and 25% of pasture in west Wales to *Mxg* or short rotation coppice (SRC) were investigated. Soil water content and streamflow were not significantly changed. Surface runoff was reduced for both crops (by up to 40%). Evapotranspiration was increased with SRC (by up to 5%), and reduced with *Mxg* (by up to 2%).

The need to incorporate conversion related changes in N_2O fluxes and SOC into life-cycle analysis assessments is demonstrated. Whilst overall changes to hydrology were minimal, *Miscanthus* C_i and reductions in surface runoff could benefit flood mitigation schemes.

Declarations and statements

Authors declaration and statements

Word Count of thesis: 43,488

DECLARATION

This work has not previously been accepted in substance for any degree and is not being concurrently submitted in candidature for any degree.
Candidate name Amanda Holder

Signature:

Date

STATEMENT 1

This thesis is the result of my own investigations, except where otherwise stated. Where *__correction services__ have been used, the extent and nature of the correction is clearly marked in a footnote(s).
Other sources are acknowledged by footnotes giving explicit references. A bibliography is appended.

Signature:

Date

[*this refers to the extent to which the text has been corrected by others]

STATEMENT 2

I hereby give consent for my thesis, if accepted, to be available for photocopying and for inter-library loan, and for the title and summary to be made available to outside organisations.

Signature:

Date

NB: *Candidates on whose behalf a bar on access (hard copy) has been approved by the University should use the following version of Statement 2:*

I hereby give consent for my thesis, if accepted, to be available for photocopying and for inter-library loans after expiry of a bar on access approved by Aberystwyth University.

Signature:

Date

Co-authors declarations

As senior PhD supervisor and co-author for journal manuscript submissions (Chapters 2, 3, 4 and 5) Iain Donnison provided guidance on overall project direction and comments on thesis content.

Date: 26/3/19

Iain Donnison

As joint PhD supervisor and co-author for journal manuscript submissions (Chapters 2, 3, 4 and 5) Jon McCalmont provided oversight of the project and comments on all chapters of this thesis. Access was also provided to protocols for static chamber sampling of soil greenhouse gas emissions and preparation of soil samples for nutrient analysis (Chapter 3). Unpublished below ground yield data (used in Chapter 2) and above ground yield data (used for model calibration Chapter 5) was also provided by Jon McCalmont. Eddy covariance data (gap-filled and quality controlled) and raw meteo data (from 2012 to 2017) was supplied to myself (Amanda Holder) in order to calculate actual and modelled evapotranspiration (Chapter 4).

Date: 26th March 2019

Jon McCalmont

As joint PhD supervisor and co-author for journal manuscript submissions Niall McNamara provided oversight and comments on Chapters 2, 3, 4 and 5.

Date: 26 march 2019

Niall McNamara

As joint PhD supervisor and co-author for journal manuscript submissions Rebecca Rowe provided comments on Chapters 2, 3, 4 and 5 as well as guidance on statistics. Gas chromatography analysis of soil gas samples (Chapter 3) was carried out by Rebecca Rowe, with assistance from myself (Amanda Holder). Help and instruction was also provided on the use of the Costech elemental analyser for carbon analysis of soil samples (Chapter 2).

Date: 26/03/2019

Rebecca Rowe

As co-author for Chapters 2 and 3, Dafydd Elias provided comments on manuscripts, and advice on statistical methods. Soil samples in Chapter 3 were analysed for nitrate and ammonium by Dafydd Elias with assistance from myself (Amanda Holder). Help and instruction was also provided on the running of soil samples for analysis of carbon via the Costech elemental analyser and Picarro Cavity Ringdown Spectrometer.

Date: 04/04/2019

Dafydd Elias

As co-author for Chapter 2, John Clifton-Brown provided comments on the draft manuscript and also provided access to the methods and raw data for soil samples taken in previous years.

Date: 28/3/19

John Clifton-Brown

As co-author for Chapter 2, Paul Robson provided comments on the draft manuscript and also provided access to unpublished long term yield data.

Date: 2/4/2019

Paul Robson

As co-author for Chapter 2, Marta Dondini provided comments on the draft manuscript and also provided access to the ECOSSE carbon model with verbal instructions of how to run the model.

Date:26/03/19

Marta Dondini

Acknowledgements

Whilst completing a PhD is, essentially, an individual exercise getting to this point has not been achieved without the help and support of others, and there are a number of people in particular that I would like to acknowledge.

Firstly my PhD supervisors Prof. Iain Donnison, Dr Jon McCalmont, Dr Niall McNamara, and Dr Rebecca Rowe, with whom I have enjoyed working and who have always been positive, approachable and available, providing excellent advice and guidance (and swift responses to emails). I would like to thank Jon for inspiring me (from my first introduction to *Miscanthus* at Penglais in 2014), for the patient sharing of technical knowhow, and for imparting infectious enthusiasm and dedication: but most importantly for knowing I could do it before I knew I could. Rebecca I would like to especially thank for teaching me how to talk nicely to the GC and Picarro, and for unravelling the complex world of statistics.

The fellowship and comradery of colleagues in Gogerddan and Pwll Peiran have made it a pleasure to work in and around Aberystwyth. In particular I am grateful to the *Miscanthus* group 'morning tea' sessions where many a problem can be solved: and especially to Laurence 'Mr Fix-it' Jones. Also to the field voles living in the Pwll Peiran plots, a thank you for popping out to say hello and for making me smile while taking measurements.

You could say the PhD journey started six years ago, when I started my Foundation Degree, for which I would like to thank my tutor Dr Graham Harris for the introduction to science and enthusiasm for the countryside. And to my Honours Degree dissertation tutor, Dave Powell, for sharing his passion for geology and ecology, and for the casual comment, "Well you could always stay and do a PhD".

However, influences go back a long way and I would also like to acknowledge and thank my family, especially my parents, for always being supportive and interested in all my endeavours. And a special mention for Steve Holder (without whom I may not have gone to university in the first place), who I thank for sharing the experience and for many years of love and support. In particular a thank you for seeing Lancaster as a great holiday destination, for not minding when I spent weekends or evenings doing 'PhD', and of course for ensuring I survived the three years by not going hungry. I hope to return the favour one day – it's your turn next!

Table of Contents

List of Figures

List of Tables

List of Abbreviations

°′″ N	degree, minutes, seconds north
°′″ W	degree, minutes, seconds west
°C	degree Celsius
‰	per mille
%	percentage
~	approximately
Δ S	change in storage (e.g. soil moisture)
λE	latent heat
µg	microgram
µmol	micromole
χ^2	Wald test, chi-square
1M	one molar
^{13}C	carbon-13
^{14}C	carbon-14
ANOVA	Analysis of variance
a.s.l	above sea level
BG	below ground
BIO	active organic matter (soil carbon pool)
C	carbon
C_3	3-carbon fixation (in photosynthesis)
C_4	4-carbon fixation (in photosynthesis)
C_c	ground area representing plant centre
C_e	ground area representing plant edge
C_i	ground area representing the inter-row
C_i	interception of precipitation by the plant canopy
C_{mis}	*Miscanthus* C percentage contribution to soil carbon
CCC	Committee on Climate Change
CH_4	methane

CI	confidence interval
cm	centimetre
CO	carbon monoxide
CO_2	carbon dioxide
CO_2-eq	carbon dioxide equivalents
DEM	digital elevation model
DM	dry matter
DPM	decomposable plant material
E	evaporation
EC	eddy covariance
ECOSSE	carbon model: Estimate Carbon in Organic Soils – Sequestration and Emissions
ESM	equivalent soil mass
ET	evapotranspiration
ET_a	actual evapotranspiration
ET_c	evapotranspiration for a specific crop type
ET_{EC}	evapotranspiration calculated from eddy covariance data
ET_o	evapotranspiration for a reference crop type
ET_p	potential evapotranspiration
F	ANOVA F-statistic
F	soil moisture function
FB	climate-carbon feedbacks
FAO	Food and Agriculture Organisation of the United Nations
g	gram
G	soil heat flux
GG	Granger-Gray evapotranspiration model
GHG	greenhouse gas
GIS	geographic information system
GJ	gigajoule
GWh	gigawatt hour
GWP	global warming potential
GWQ	baseflow (sub-surface runoff)

H	sensible heat
ha	hectare
HCl	hydrogen chloride
hr	hour
HRU	hydrological response units
HS	Hargreaves-Samani evapotranspiration model
HS.adj	HS adjusted for soil moisture
HSD	in Tukey HSD: honestly significant difference
HUM	humus (soil carbon pool)
Hyb 1	Novel *Miscanthus* hybrid number 1
Hyb 2	Novel *Miscanthus* hybrid number 2
Hyb 3	Novel *Miscanthus* hybrid number 3
Hyb 4	Novel *Miscanthus* hybrid number 4
Hz	Hertz
IOM	inert organic matter (soil carbon pool)
K	kelvin
K_c	crop coefficient
K_s	water stress coefficient
KCl	potassium chloride
kg	kilograms
km	kilometre
km^2	kilometre squared
kPa	kilopascal
LAI	leaf area index
LCA	life cycle analysis
LE	latent heat flux
LUC	land use change
m	metre
m^2	metre squared
m^3	metre cubed
M	million
M25	*Miscanthus* 25% planting scenario

M50	*Miscanthus* 50% planting scenario
MAE	mean absolute error
md	modified Index of Agreement
mg	milligram
Mg	megagram
MJ	megajoule
ml	millilitre
mm	millimetre
mNSE	modified Nash Sutcliffe Efficiency
Mt	million tonnes
Mxg	*M. x giganteus*
N	nitrogen
N_2	dinitrogen
N_2O	nitrous oxide
NH_3^-	ammonia
NH_4^+	ammonium
NO	nitric oxide
NO_2	nitrite
NO_3	nitrate
NO_x	nitrogen oxides
NPP	net primary production
$O(^1D)$	first excited state of the oxygen atom
OH	hydroxyl
OPM-10	novel *Miscanthus* hybrid
p	statistical p-value
P	phosphorus
P	precipitation
PAR	photosynthetically active radiation
PAW	plant available water
PET	potential evapotranspiration
pH	acidity scale (potential of Hydrogen)

PMgrass	simplified Penman-Monteith short grass reference evapotranspiration model
PMK_c	PMgrass adjusted with K_c values calculated for *Miscanthus*
PMsugarcane	PMgrass adjusted with K_c values for sugarcane
PMsugarcane.adj	PMsugarcane adjusted for soil moisture
PT	Priestley-Taylor evapotranspiration model
PT.adj	PT evapotranspiration model adjusted for soil moisture
Q	runoff
r	Pearson correlation coefficient
R^2	coefficient of determination
RCM	resistant plant material
RE	relative error
Rh	Relative humidity
RMSE	root mean square error
Rn	net radiation
Rs	solar/global radiation
s	second
SE / SEM	standard error / standard error of the mean
SOC	soil organic carbon
SOM	soil organic matter
SRC	short rotation coppice
SRC25	short rotation coppice 25% planting scenario
SRC50	short rotation coppice 50% planting scenario
SURQ	surface runoff
SWAT	hydrology model: Soil Water Assessment Tool
T_0	time point corresponding to LUC event
T_6	time point six years after LUC
T_{12}	time point 12 years after LUC
Ta	air temperature
UK	United Kingdom
VPD	vapour pressure deficit
WFPS	water filled pore space (within soil matrix)

Wm^2	watt per metre squared
WY	water yield (amount of water leaving a catchment)
yr	year

1 Climate change, land use change and bioenergy

1.1 The changing climate

The changing climate is a far reaching and pressing environmental and political challenge. In 2015 195 countries agreed a global action plan at the Paris Climate Conference (COP21) with the aim of keeping temperature increases to below 2°C (European Commission, n.d.a). Recently, the need to step up mitigation measures was stressed at the 2018 Climate Change Conference (COP24) where guidelines for implementing agreements were established with the 'Katowice Climate Package' (UNFCCC, n.d.).

To maintain stable temperatures on Earth the flow of incoming energy needs to be balanced by the outgoing flow of energy over the long term. Factors causing a change in the Earth's energy budget can drive climate change (IPCC, 2013), these can result from natural and anthropogenic causes. Naturally occurring greenhouse gasses (GHG) including water vapour, carbon dioxide (CO_2), methane (CH_4) and nitrous oxide (N_2O) maintain the Earth's temperature by trapping solar radiation within the land surface/atmosphere system. Natural processes such as carbon, nitrogen, and water cycling determine these GHG levels in the atmosphere. Soil and vegetation form important long and short term terrestrial carbon (C) stores with CO_2 being exchanged between the biosphere and atmosphere via photosynthesis and respiration (Falkowski *et al*., 2000). Feedback processes within these systems can also act to increase or reduce the effect of GHG's (Figure 1). For example, increased concentrations of atmospheric CO_2 increase the greenhouse effect, warming the climate and subsequently affecting plant production and soil respiration, thus producing both positive and negative feedbacks. Positive feedbacks, such as increased ecosystem respiration, increase warming due to the release of additional

CO_2. In contrast, negative feedbacks, such as carbon sequestration, reduce levels of atmospheric CO_2.

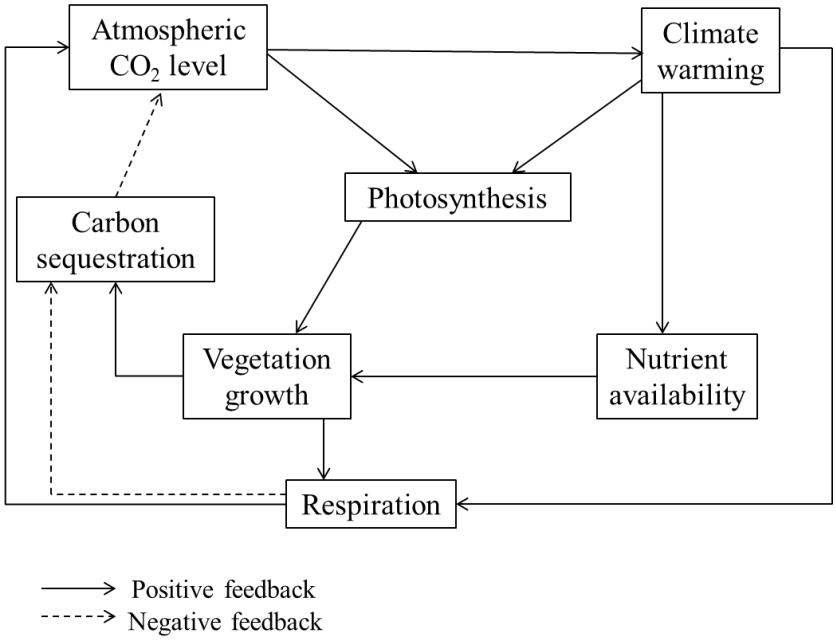

Figure 1 Flow diagram showing terrestrial climate-carbon feedbacks (adapted from Luo *et al*., 2001).

Atmospheric concentrations of GHGs (mainly from fossil fuel combustion, cement production and land use change such as deforestation) have increased at an exponential rate since the Industrial Revolution, with corresponding rises in global mean temperatures. These previously unseen, rapid increases in atmospheric CO_2, CH_4 and N_2O are largely driven by anthropogenic emissions (IPCC, 2013) and have long term consequences. Whilst atmospheric CO_2 moves among different parts of the of the ocean-atmosphere-land system, net CO_2 remaining in the atmosphere is subject to much slower weathering processes and chemical reactions that can impact climate over thousands of years (IPCC, 2007; Archer *et al*., 2009).

Energy production using fossil fuels accounted for 47% of the increase in annual anthropogenic GHG emissions between 2000 and 2010 (IPCC, 2014) and the

growing awareness of the damage this is leading to has resulted in countries aiming to reduce their reliance on fossil fuels. 164 countries have now set targets and policies for increasing renewable forms of energy generation (including wind, solar, hydro and bioenergy) and by 2050 it is suggested that globally the share of the energy generation mix for renewables could be more than 60% (Sen & Ganguly, 2017; IRENA, 2018).

Whilst CO_2 is the most abundant GHG (compared to CH_4 and N_2O, Table 1) CH_4 has a greater ability to absorb and re-emit energy within the atmospheric system, although with a shorter atmospheric lifetime of around 12 years (IPCC, 2007). CH_4 and carbon monoxide (CO) can be removed from the atmosphere via daytime oxidation by hydroxyl (OH), a free radical present in the atmosphere (IPCC, 2014). Although OH acts as a sink for CH_4 and CO the oxidation process can also be a source of CO_2 by starting a sequence of reactions that eventually form CO and CO_2 (as a product of CO reacting with OH). Increases in atmospheric levels of CH_4 and CO can also reduce the oxidising ability of the troposphere due to their consumption of OH. However, OH is also impacted by environmental conditions and increases in nitrogen oxides (NO_x) and ozone levels which can increase OH (Thompson and Cicerone, 1986; Naik *et al*., 2013; IPCC, 2014). Since 2007, after a stable period of ~10 years, atmospheric concentrations of CH_4 have grown and there is debate as to the drivers of this renewed increase (IPCC, 2013). CH_4 emissions are mainly produced from wetlands, agriculture, waste and biomass burning and are related to the exploration for, and transport of, fossil fuels (Heilig, 1994; IPCC, 2013).

N_2O is also a potent GHG, compared to CO_2, with a long lived atmospheric lifetime (of around 120 years) and an ozone destroying action (Ravishankara *et al*., 2009; IPCC, 2013). Inert in the troposphere, atmospheric N_2O is removed mainly by

photolysis in the stratosphere but is also removed by reaction with oxygen atoms ($O(^1D)$), which is the source of the ozone depleting catalyst nitric oxide (NO) (Reay *et al*., 2007). Agricultural management practices combined with natural soil emissions account for 56-70% of global sources of atmospheric N_2O (Reay *et al*., 2012; Butterbach-Bahl *et al*., 2013). It is produced from a range of natural processes (linked to different microbial communities influencing nitrification and denitrification pathways) in soils and water (Butterbach-Bahl *et al*., 2013), but is also produced from agricultural management of soils and fertilizer, animal manure, sewage treatment, the burning of fossil fuels, and chemical industrial processes (Reay *et al*., 2012; IPCC, 2013).

Table 1 An example from the UK (2016) inventory of greenhouse gas (GHG) emissions showing the percentage of total net estimated emissions (Mt CO_2-eq) of three prominent GHG's: carbon dioxide (CO_2); methane (CH_4); and nitrous oxide (N_2O) (Brown, 2018).

GHG	% of total net GHG emissions
CO_2	81%
CH_4	11%
N_2O	5%

The relative impact of CO_2, CH_4 and N_2O can be compared (in reference to CO_2) and expressed in carbon dioxide equivalents (CO_2-eq) calculated in terms of their Global Warming Potential (GWP) (Table 2). GWP can be calculated with or without climate-carbon feedbacks (a measure of the indirect radiative forcing effects, for example, chemical changes of the original gas that produces further GHGs). The use of GWP with feedbacks introduces uncertainties relating to the carbon cycle, but its inclusion does provide a more complete assessment of the relative influences of non-CO_2 gasses (IPCC, 2013).

Table 2 Global Warming Potential (GWP) of CO_2, CH_4 and N_2O. Values are shown over two time scales, 20 years and 100 years, to reflect the variation in radiative forcing (the capacity of the GHG to affect the Earth's energy balance) effect with time due to the different lifetimes of the GHG in the atmosphere. The GWP for each timescale is also shown with and without the inclusion of climate-carbon feedbacks (FB) for non-CO_2 gasses.

	GWP			
	20 years		**100 years**	
	Without FB	**With FB**	**Without FB**	**With FB**
CO_2	1	1	1	1
CH_4	84	86	28	34
N_2O	264	268	265	298

1.2 The water balance and surface energy balance

Atmospheric and oceanic circulations are maintained within the climate system through heat energy captured from incoming solar radiation. Natural processes, land cover, plants, and land management all have an influence on climate and are interlinked. Changes to the water balance (Equation 1) not only have the potential to alter hydrological components such as water table reserves and stream flows, but also impact the climate through changes to the overall energy budget (Equation 2 and Figure 2).

$$P + E + \Delta S + Q = 0 \quad (1)$$

where P is precipitation, E is evaporation, ΔS is change in storage (e.g. soil moisture and groundwater) and Q is runoff.

$$Rn = G + H + \lambda E \quad (2)$$

where Rn is net radiation, G is subsurface soil heat flux, H is the sensible heat flux (heat energy transferred between surface and air when there is a difference in air temperatures), and λE is the latent heat of evaporation (i.e. the energy contained in atmospheric water vapour).

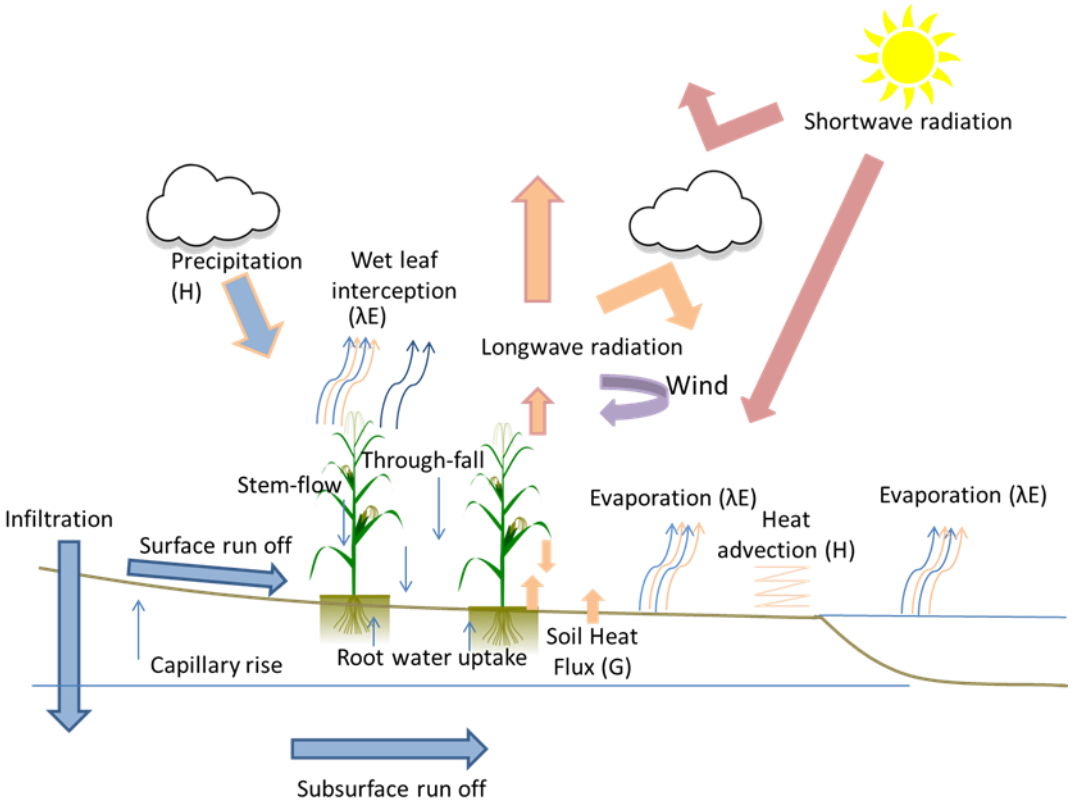

Figure 2 Diagram showing the main elements of the water cycle and equation of energy balance.

Of the three processes removing surface energy (evaporation, convection and thermal radiation) evaporation is the greatest and it is the primary pathway for water to return to the atmosphere (Monteith & Unsworth, 2008).

Water evaporates from water bodies, soil and vegetated surfaces (via wet leaf evaporation: a combination of transpiration and evaporation of water held in the canopy) and diffuses into the atmosphere. Air currents circulate water vapour and energy around the atmospheric system and where this vapour is cooled through heat exchange it condenses and falls as precipitation.

Precipitation falling on vegetation is portioned into through-fall (water falling between the canopy and dripping from leaves) and stem-flow (water funnelled from the leaves down the plant stem). Water remaining on the canopy is subject to

evaporation, the extent to which depends on available energy, wind turbulence and a vapour pressure deficit (VPD, the difference between the vapour pressure of water held in the air at a given time and how much the air could potential hold i.e. the saturated water vapour pressure). The saturated vapour pressure depends on temperature because warmer air has a greater water holding capacity than cooler air. The actual vapour pressure can be derived from relative humidity (Rh, a measure of the percentage saturation of the air at the current air temperature). VPD is an accurate guide to the evaporative capacity of the air and therefore the strain placed on plants to maintain their water balance (Allen *et al*., 1998).

Precipitation reaching the ground infiltrates the soil or is subject to evaporation and surface (over land) runoff. Water moves from low to high potential energy and the amount of water infiltrated and held in soil, and its movement (direction and rate) within it, is dependent on the matric potential (binding of water with the matrix of the solid soil particles due to adsorptive and capillary forces, and drag/shear forces at the surface-water interface), osmotic potential (due to different concentrations of solute molecules), gravitational pressure, and external pressure potential (e.g. from overlying water) (Marshall *et al*., 1996). Water movement is therefore different depending on the soil hydraulic conductivity (ease of water movement) and soil moisture distribution within the soil profile. For example, sandy soils with large pores conduct water more easily than clay soils with smaller pores where there is increased resistance.

Dry soil is infiltrated quickly (unless crusted or highly compacted) due to the attraction of soil particles, but as soils reach saturation gravity becomes the dominant driving force. Therefore ponded water on previously unsaturated soils infiltrates at a rapid rate at first and becomes more constant as the profile becomes saturated and

the percolating wetting front advances (horizontally and vertically) at a decreasing rate with depth (Dingman, 2002). Water that percolates down through the vadose zone (unsaturated soil zone) into the phreatic zone (saturated soil zone) recharges deep water reserves and contributes to subsurface runoff (baseflow).

If water enters the soil at a rate that is less than the saturated hydraulic conductivity of the soil, water content at the surface profile increases but the wetting front does not tend to increase so far. When water is no longer added to soil the advance of the wetting front is much slower and water is held in the soil profile by capillary forces (tension) until the maximum soil water holding capacity is reached (known as the field capacity: the soil water content held after excess water has drained away) (Marshall *et al*., 1996; Dingman, 2002).

Soil water is not restricted to downward movement and evaporation from soil surfaces can be large (Monteith & Unsworth, 2008). When the soil surface is wet atmospheric conditions provide the greater limiting factor, but as the soil dries, movement of water within the profile restricts the evaporation rate.

Soil moisture status and the ease of water movement within the soil profile also effects the extent to which actual evapotranspiration reaches potential evapotranspiration through its impact on plant transpiration (Gardner & Ehlig, 1963; Monteith & Unsworth, 2008). The majority of water used by plants is absorbed via roots and transported upwards through the plant by the negative pressure created from the evaporation of water from the leaves. The rate of water lost to the atmosphere is regulated by turgor pressure in the guard cells at the stomatal opening. In many plants a loss of turgor pressure results in the closure of stomatal openings when the supply of soil water to the plant is not sufficient to meet the evaporation

loss from transpiration, with the effect of reducing the transpiration rate (Marshall *et al*., 1996).

Changes in the partitioning of energy into latent energy (λE) and sensible heat (H), through evaporation and condensation, will influence near-surface air temperature. Water vapour can act to both warm and cool the Earth, through the trapping of long-wave radiation from below (system warming) and reflecting short-wave radiation from above (system cooling). Therefore changes in surface fluxes of water vapour and also the reflectiveness of surfaces (albedo) can produce positive or negative radiative forcing changing the Earth's energy budget (Pielke *et al*., 2002).

The soil heat flux (G, amount of thermal energy moving through and in and out of the soil) couples the surface energy balance with soil energy transfer, and temperature gradients within soil also stimulate water flow via evaporation and condensation. Soil thermal capacity is connected to the soil particle composition (mineral type, particle size, and organic matter content) and soil moisture status (due to the higher heat capacity of water compared to air) and varies with soil surface cover (Monteith & Unsworth, 2008).

1.3 Land use change and impacts on climate

Land use change (LUC), the alteration of the physical composition of the land surface (changes in vegetation or land management), can result in climate forcing through a range of positive and negative impacts. For example, LUC from forest to pasture decreases radiative forcing due to a cooling effect from increased albedo (Claussen *et al.*, 2001; Pitman *et al.*, 2009) however, this is outweighed by an increase in atmospheric CO_2 from release of stored C from previously stable pools, through decomposition and oxidation, and reductions in photosynthetic CO_2 uptake. The amount of C stored in the top 30 cm depth of soil globally is estimated to be twice that of C in atmospheric CO_2 (Batjes, 1996; Powlson *et al.*, 2011). These soil C stocks are very susceptible to losses and gains driven by LUC and changes in management (Guo & Gifford, 2002; Lal, 2004).

Whilst LUC is globally a major contributor to increases in atmospheric CO_2 (mainly from deforestation in the tropics) LUC can also play a role in mitigation, for example in the change from annual to perennial agricultural crops (Smith *et al.*, 2008). In the UK the 'Land Use, Land Use Change and Forestry' sector is currently a net GHG sink (without the inclusion of changes to peatlands, Table 3, Brown, 2018) with forest and grass land uses providing the main two sinks (-23.9 and -9.3 Mt CO_2-eq, respectively). Therefore the effects on GHGs of new land use change scenarios for these two land cover types in particular should be investigated, especially as this sector is highly sensitive to changes in human activities and other disturbances that can lead to increased GHG emissions.

Table 3 UK GHG emissions by sector in 2016 (Brown, 2018). The sector 'Land use, land use change and forestry' is a net sink (not including the full extent of emissions from peatlands which if included could change this to become a net source).

Sector	**Mt CO_2-eq**
Energy	393
Industrial processes	31
Agriculture	42
Land use, land use change and forestry	-15
Waste	20

Land use and management can therefore both drive climate change, through increased GHG emissions, or changes in the water balance (Figure 3) or be driven by climate change (due to the adoption, forced or otherwise, of more suitable crops and management techniques). Crops and management that enable adaptations to changes in climate, or mitigate impacts, are high on the political agenda due to predictions of increased frequency of extreme weather events, including droughts and floods (European Environment Agency, 2014; IPCC, 2014).

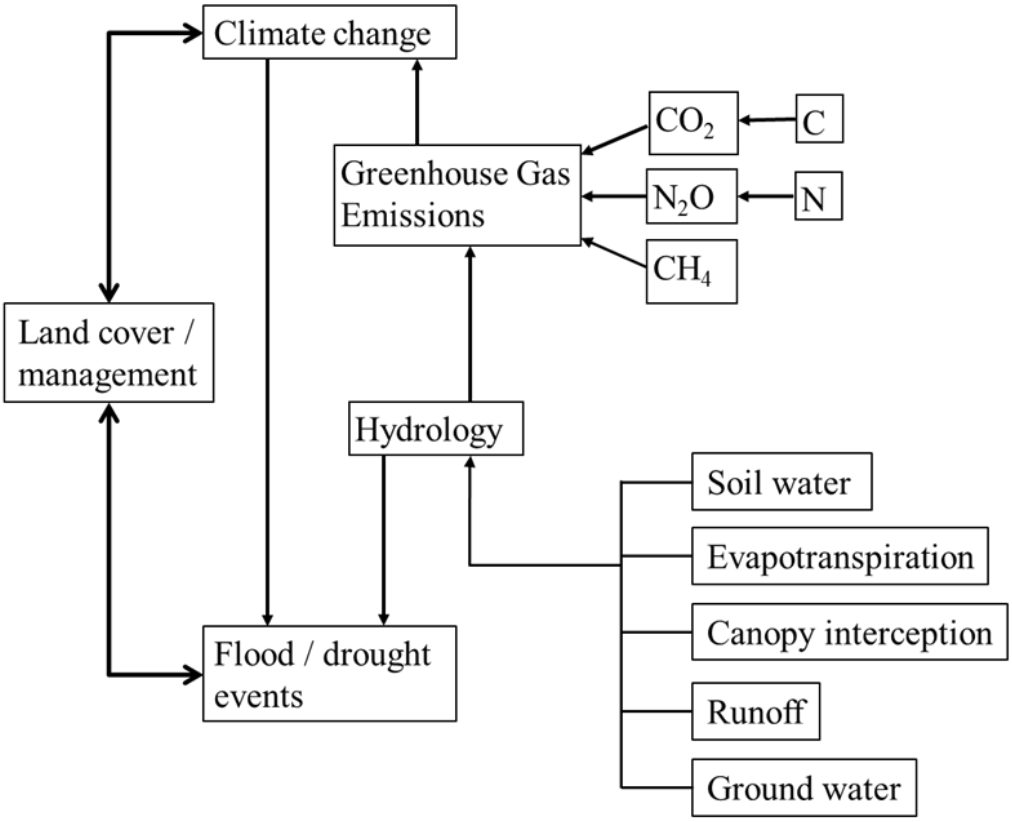

Figure 3 Flow diagram showing links and feedback loops between components of the biosphere/atmosphere system.

1.3.1 Agricultural impacts on CO_2 emissions from arable systems

Change in vegetation and management practices can influence carbon sinks via the level of C stored in soils, plant biomass, and CO_2 taken up through photosynthesis.

CO_2 released is released from soils via mitochondrial respiration (carried out in living root cells), and heterotrophic respiration (from decomposers in the soil) of soil organic matter (SOM, un-decomposed plant material within the soil) and soil organic carbon (SOC, mineralised carbon following decomposition). LUC can stimulate heterotrophic respiration by the input of new plant litter or crop residues, and via changes in the composition and decomposability of dead plant material (e.g. C:N ratios).

Known as the priming effect, the accessibility of C from root exudates or fresh litter can act to increase the rate of decomposition leading to an increase in the release of previously stable carbon pools (Cheng, 2009; Kuzyakov, 2010; Hopkins *et al*., 2013). Soil disturbance events (such as ploughing) can also result in the loss of long term C (Balesdent *et al*., 2000; Conant e*t al*., 2007) through oxidation (due to increased availability of oxygen) and incorporation of SOM stimulating these priming effects. Therefore a move from the repeated disturbances of annual cultivation to perennial systems can lead to increased carbon sequestration in the soil over the long term (Freibauer *et al*., 2004; Qin *et al*., 2016). However, even perennial systems may be routinely cultivated (even if this moves from an annual to a decadal time step) and will have associated SOC losses as a result. As an alternative to deep, conventional ploughing and power harrowing, mitigation measures such as minimum or no-tillage methods (where the soil is not fully turned over during cultivation) can be employed, where appropriate, to reduce these

disturbances to soil ecosystems (Holland, 2004; Conant *et al*., 2007; Lal *et al*., 2007).

Differences in soil N availability arising from changes in fertilizer regimes can have varying positive or negative impacts on net C sequestration (Berg & Matzner, 1997; Neff *et al*., 2002). For example using organic manures (as opposed to chemical N fertilizer) provides a source of C as well as N to the soil and although fertilization can increase crop growth and subsequent residues (thereby increasing SOM), excessive N can result in the use of more stable C as soil microbes strive to maintain their own ideal C:N balance (of ~9:1, requiring a diet ratio of ~24:1 for energy as well as maintenance) (Brady & Weil, 2001; Christopher & Lal, 2007).

1.3.2 Agricultural impacts on trace gas fluxes: nitrous oxide (N_2O) and methane (CH_4) in arable systems

Soil fertilization can increase plant growth and uptake of CO_2, however, soil N_2O emissions have been shown to increase if available N is greater than crop requirements, either through excess application or sub-optimal timing (Oenema *et al*., 1997; Smith *et al*., 2008). Crop uptake of ammonium (NH_4^+) is slower than uptake of nitrate (NO_3) therefore nitrification processes (the conversion of NH_4^+ by soil bacteria to NO_3) can occur, releasing N_2O and nitric oxide (NO) to the atmosphere. In oxygen limited conditions an excess of NO_3 and nitrite (NO_2) can also result in increased atmospheric N_2O due to releases from denitrification (where soil anaerobic bacteria use NO_3 and NO_2 as a substitute for oxygen resulting in the conversion of NO_3 and NO_2 into N_2O, dinitrogen (N_2) and NO). Therefore, soil moisture (affecting the oxygen available to soil microbes) as well as temperature (influencing the rate of microbial activity) and soil pH (nitrification rates are quickest at ~7) can play important roles in the regulation of N_2O fluxes (Maag &

Vinther, 1996; Butterbach-Bahl *et al*., 2013). Soils are usually a net source of N_2O, but temporary negative fluxes can occur (as N_2O is reduced to N_2, or absorbed into soil water) depending on soil conditions (Chapuis-Lardy *et al*., 2007).

Changes in management to deliver N to plants more effectively, a reduction in the use of synthetic nitrogen fertilizers (made from ammonia (NH_3^-) and produced using the energy intensive Haber-Bosch process with associated CO_2 emissions), the use of legumes (to biologically fix N) in rotations, or a change to crops with low nutrient input requirements can be used as a methods to mitigate agricultural GHG emissions (Smith *et al*., 2008; Ashworth *et al*., 2015; Grutzmacher *et al*., 2018; Lal, 2019). However, these options need to be considered in respect of the specific crop and soil conditions as the impact on N_2O emissions may not always be beneficial (Smith *et al*., 2008; Snyder *et al*., 2009; Huang *et al*., 2018). For example, organic fertilizers (with a source of liable C) can increase microbial activity and thus N_2O emissions (Jones *et al*., 2005).

Soils can also be a source or sink for CH_4 depending on the activity of soil methane transforming bacteria (Smith *et al*., 2000; Conrad, 2009). Methanotrophs (bacteria that oxidise CH_4) can be inhibited by increases in N and changes to soil drainage. As soils become waterlogged anaerobic conditions favour methanogens (methane producing bacteria).

1.3.3 Agricultural impacts on the hydrological cycle

Changes in land cover and management can also affect the water cycle through changes in soil structure and differing crop physiology and morphology (Dale, 1997; Vanloocke *et al*., 2010).

Soil structure (the size shape and arrangement of aggregates within the soil matrix) influences aeration, soil water retention and movement, and can be greatly influenced by land management and vegetation. Amount of machinery use and stocking densities of grazing animals can influence soil compaction and bulk density (mass of soil per unit of volume) (Abdel-Magid *et al*., 1987; Burt & Slattery, 2005). Compaction reduces the volume of soil pores thereby restricting water infiltration into, and flow through, the soil which can result in increased overland (surface) flow. Thermal conductivity is also affected by bulk density (conductivity increases as bulk density increases) which can influence temperature effects on soil water movement both as a liquid (through surface tension) and in the gaseous state (by the effect on the vapour pressure of water) (Marshall *et al*., 1996).

High bulk densities can also restrict the access of crop roots to soil water, reducing the return of water to the atmosphere through photosynthetic transpiration. However, this can be dependent on crop type due to differing rooting habits (e.g. fibrous, taproot, or adventitious) and the exertion of turgor pressure employed in enlarging growing root cells. Crop roots tend to create macro-pores increasing infiltration and percolation of water and break down large aggregates into smaller particles which (particularly in perennial crops) become enmeshed within root systems providing increased soil stability and improved hydraulic condition (Gregory, 2006). For crops with rooting systems that penetrate more than one soil layer, hydraulic redistribution of water through soil profiles (along gradients from wet to dry) can occur through uptake and leakage by fine roots (Williams & Scott, 2009). Deeper rooting crops may access groundwater in the phreatic zone with the potential to influence long term water storage and baseflow (Le Maitre *et al*., 1999). Water movement in the soil can also be altered by changes in osmotic potential (result of binding and

dilution of solutes dissolved in soil water) brought about by the filtering of salt from solutes by plant roots (Rowell, 1994; Marshall *et al*., 1996).

Depending on the frequency or method of tillage soils can be loosened resulting in increased infiltration for roots and water. However, regular tillage events can also cause compaction below the plough depth. Bare soil left after cultivation or harvest is also open to damage from rain break down of surface aggregates that seals the immediate surface reducing infiltration (Burt & Slattery, 2005). Surface runoff rates are also influenced by changes in crop height, density, rigidity and residues which alter surface roughness and therefore provide differing mechanical resistance to overland flows (Kort *et al*., 1998; Marshall *et al*., 2009).

Management practices that involve the use of a cover crop, or treatment with mulches (e.g. plastic films, leaf litter, crop residues and overwinter stubble), can improve soil structure making it more stable, increase SOM, and provide protection from the action of rain (Kahlon *et al*., 2013). This encourages higher levels of activity from soil microbes and soil fauna that in turn improve soil structure and allow improved infiltration. Mulches can also increase soil water storage by lessening the evaporative pull on soil water by reducing the amount of radiant energy absorbed by the soil surface (Li *et al*., 2013).

Soil water storage is directly affected by the amount of water required by crops and their capacity to pull against forces holding water in the soil. Plant available water (PAW) for transpiration decreases as the matric potential of soil water decreases. The matric potential at the plant wilting point (minimum level of PAW) is around -1.5 MPa (depending on soil texture) but drought tolerant crops may be able to use water below this (Marshall *et al*., 1996; Bartlett *et al*., 2012). Crops also differ in

their regulation of stomata (to control high rates of transpiration and avoid tension induced breakages of the xylem soil-root-stem-leaf hydraulic connection) in response to soil or atmospheric drought (Tardieu & Simonneau, 1998).

Sufficient soil storage of PAW for crop growth requirements increases evapotranspiration (ET) release of water to the atmosphere and therefore impacts the extent to which actual ET reaches potential ET (PET). ET is also influenced by crop type, with differing canopy characteristics influencing the amount of water returned to the atmosphere in several ways.

Leaf area index (LAI) influences the amount of water stored in the crop canopy which then becomes subject to evaporation (depending on climatic conditions) rather than infiltrating the soil or forming part of surface runoff (Dingman, 2002). Large or closed canopies can also shade soils reducing ground surface evaporation.

Differences in canopy surface roughness (i.e. arising from crop spacing, crop height, leaf dimensions, and stomatal size and arrangement) provide different aerodynamic, boundary layer, and canopy resistances where increased turbulence can remove water vapour from surfaces increasing ET. Surface resistance becomes a smaller factor in the diffusion of water vapour to the atmosphere as the canopy cover increases forming a uniform layer over a large area (Monteith & Unsworth, 2008).

Crops with lower albedo also reflect less solar energy and therefore absorb and retain more heat energy and PAR (photosynthetically active radiation), again with the potential to increase ET (Miller *et al.*, 2016).

1.4 Land use change to biomass energy crops

1.4.1 Miscanthus, a second generation crop

In contrast to fossil fuels, biomass used for energy generation (which can include water and land based vegetation, sewage, manures and residues from forestry and agriculture) is renewable needing only a short time period to replace the resource (Dhillon & von Wuehlisch, 2013). Second generation (inedible portions of food crops and non-food crops) and third generation (aquatic cultivated feedstocks such as algae) bioenergy crops are preferred to first generation crops (derived from edible plants and food based crops such as sugarcane and rapeseed oil) as they reduce direct competition with food production (EASAC, 2012).

Global climate targets, with the increasing prominence of renewable energy generation, are anticipated to result in the increased planting of second generation bioenergy crops (IPCC, 2014; ETI, 2015), and although reductions in overall GHG emissions are expected (Whitaker *et al*., 2018) policy makers need to ensure that the environmental impacts of increased bioenergy demands are fully assessed (Fritsche *et al*., 2010).

Short rotation coppice (e.g. willow, *Salix* spp. and poplar, *Poplus* spp.) and perennial grasses (e.g. switchgrass, *Panicum virgatum* L. and the *Miscanthus* genus), are second generation crops popular for their ability to rapidly gain biomass with few agricultural inputs and their potential to be grown on marginal soil types (Lewandowski *et al.*, 2000; Aylott *et al.*, 2008; Hastings *et al.*, 2014; Cunniff *et al.*, 2015).

Unlike short rotation coppice species that are native to temperate zones (Dickmann, 2006) *Miscanthus* is a perennial grass originating from Asia (Clifton-Brown *et al*.,

2015). Following initial trials across Europe, private sector interest and policies aimed at the advancement of *Miscanthus* as a biomass energy crop began to emerge in the 1990's. Now commercially available, *M. x giganteus* (Greef & Deuter, 1993) is a sterile naturally occurring hybrid (thought to be of *M. sacchariflorus* and *M. sinensis*, Lewandowski *et al.*, 2000) with an estimated economic lifespan of 10 to 15 years (Clifton-Brown *et al*., 2015). In addition to its end use for burning in power stations, *Miscanthus* can also be used in the bio-refining industry (producing liquid fuels, fibre, and chemicals) and as animal bedding (Brosse *et al*., 2012; Van Weyenberg *et al.*, 2015).

Miscanthus utilizes an efficient C_4 photosynthetic pathway that enables the plant to have greater resilience to stresses such as drought or N limitations (Ubierna *et al*., 2013; Sage, 2014). It grows and spreads from underground rhizomes with new shoots emerging from the ground each spring. The rhizomes supply N for the shoots in spring, and N is translocated to the rhizomes at the end of the growing season (Beale & Long, 1997). *Miscanthus* generally has low nutrient requirements compared to annual crops (Cadoux *et al*., 2012) and has been associated with N-fixing bacterial endophytes (Davis *et al*., 2010; Keymer & Kent, 2014).

Rooting habits vary with *Miscanthus* variety, *M. sacchariflorus* genotypes have thick creeping rhizomes that extend horizontally through the soil, whereas *M. sinensis* genotypes have smaller, non-creeping rhizomes, with shoots that tend to form tufts at the plant centre (Richter *et al*., 2015). Roots can reach depths of 2.5 m, depending on soil properties (Neukirchen *et al*., 1999), although the main root mass is generally found within the first 0.5 m (Hansen *et al*., 2004; Monti & Zatta, 2009).

Full establishment is normally obtained after two to three growing seasons (Lewandowski *et al*., 2000) when in established crops stems can reach heights of up to 3.5 m. Stems and large leaves (reaching around LAI 11, Trybula *et al*., 2015) grow over the summer forming a close canopy until winter senescence, triggered by day length and air frosts, causes the leaves to fall. Stems can be harvested from late autumn (after growth has ceased) up to early spring (before the new shoots emerge).

Breeding has also produced newer *Sacchariflorus x Sinensis* hybrids with a range of growth habits, environmental resilience and senescence timing (Clifton-Brown *et al*., 2015; Lewandowski *et al*., 2016; Nunn *et al*., 2017). The choice of hybrid can impact on the plant's suitability for its end use and planting location, for example some hybrids are much drier at harvest which is desirable for combustion, whereas others produce more stems but of a shorter length that can be of benefit to reduce lodging.

M. x giganteus in particular has a high transpiration rate due to rapid biomass production and limited stomatal control (Clifton-Brown *et al*., 2002; Joo *et al*., 2017), and soil PAW has been shown to limit yields (Clifton-Brown & Lewandowski, 2000; Finch *et al*., 2004). It is important that sufficient yields are obtained to ensure the commercial viability of the crop (and maximise SOC sequestration). Richter *et al*. (2008) found that each mm of PAW contributed 55 kg DM ha^{-1} compared with 13 kg DM ha^{-1} per mm of precipitation. However, modelling has shown that *M. x giganteus* would use less crop area and water than other bioenergy crops such as maize (Zhuang *et al*., 2013) and short rotation coppice (SRC) willow (Finch *et al*., 2004) to achieve commercially viable yields.

There may also be potential for making use of the trait of high water demand and full canopy cover in flood mitigation schemes (Stephens *et al*., 2001; Environment Agency, 2015). *Miscanthus* may also provide positive ecosystem services in terms of biodiversity, carbon storage, soil structure and visual appearance (Rowe *et al*., 2009; McCalmont *et al*., 2017a) however, as with hydrology, effects on both yield and ecosystem services will vary depending on location and previous land use (Milner *et al*., 2016).

1.4.2 An overview of the use of models in predicting the impacts of land use change to Miscanthus

Mathematical models encompassing plant-soil interactions are a valuable tool for hypothesis testing, predicting outcomes at temporal and spatial scales beyond the scope of field measurements and ultimately play a role in developing sustainable watershed-management and LUC strategies (Ostle *et al*., 2009; Engel *et al*., 2010; Abbaspour *et al.*, 2015a). Whilst models based on empirical measurements from a single site may provide a good level of accuracy for that site they may not be suitable for use elsewhere, whereas process based models (based on known mechanistic principles) are more effective across a range of sites and scales (Dingman, 2002; Williams & Scott, 2009). Due to the integrated nature of drivers and responses in soil-plant-atmosphere interactions, assumptions of ecosystem albedo, plant phenology, and evapotranspiration can lead to a range of results when modelling the impact of LUC for both GHG emissions and hydrology (Pitman *et al*., 2009). It is therefore important that these parameters are accurately represented and outputs verified for novel crop types.

GHG fluxes are the result of a number of different and interacting drivers that can produce varying responses depending on environmental conditions and this

complexity presents challenges for their representation in models (Smith *et al*., 2003; Li, 2007). However, a number of process based models (e.g. Agro-IBIS (Vanloocke *et al*., 2010), DAYCENT (Davis *et al*., 2010), DeNitrification-DeComposition (DNDC, Gopalakrishnan *et al*., 2012), and Estimate Carbon in Organic Soils – Sequestration and Emissions (ECOSSE, Smith *et al*., 2010)) based on the concept of separate soil C 'pools' have been successfully used to predict soil C and GHG emissions and have been parametrised for use with bioenergy crops (Robertson *et al*., 2015). The compartmentalization of soil C into different pools allows for the representation of varying turnover and decomposition rates and the separation of stable and liable C (Smith *et al*., 2010; Nair *et al*., 2012).

The ECOSSE model has been tested and evaluated at a number of sites within the UK, including LUC conversions to second generation bioenergy crops, and has been found to simulate SOC changes and N_2O emissions to within the level of error obtained from field samples (Dondini *et al*., 2016a, b). However, empirical data from sites with baseline SOC data is lacking (Richter *et al.*, 2015; McCalmont *et al*., 2017a) and is needed to further evaluate the model for future predictions. ECOSSE has been developed for use at different spatial scales, from field to national level, requiring only inputs that are likely to be readily available at the larger scales (Bell *et al.*, 2012). The availability of input data can be a limiting factor in choosing suitable models. For example, several established models exist for calculating potential evapotranspiration (PET) with varying input requirements: the Priestley-Taylor model (Priestley & Taylor, 1972) requires solar radiation, air temperature and relative humidity data whereas the Hargreaves-Samani formula (Hargreaves & Samani, 1985) requires only air temperature as a minimum.

A range of models exist for the estimation of ground surface PET and actual ET based on varying principles (Yang, 2015). These include empirical formulas such as the Hargreaves-Samani model; calculations based on components of the water balance (e.g. Liu *et al*., 2014); micrometeorological models such as Penman-Monteith (Monteith, 1965), and Granger-Gray (Granger & Gray, 1989) and the Bowen-Ratio method (Bowen, 1926); and those based on soil-vegetation-atmosphere transfer (SVAT, e.g. Dickinson, 1984; Sellers *et al*., 1986). 'Complementary models' (such as Granger-Gray) are based on the principle that in the absence of advective heat and moisture, PET and actual ET depend on each other in a complementary way through land and atmosphere feedbacks (Bouchet, 1963; Morton, 1965). It has been found that some models perform better and are therefore more suited to particular regions or climate types (Tabari, 2010; Anayah & Kaluarachchi, 2014).

Micrometeorological methods are the most commonly used (Yang, 2015) although they do not all take account of vegetation impacts, only the effect of atmospheric demand. The Penman-Monteith formula, however, allows for vegetation effects with the inclusion of terms for plant specific parameters and the relationship between atmosphere and surface resistances. Standardised parameters have been developed to produce estimates based on a particular reference crop (normally a well-watered short grass surface) and which can be easily amended for different crop types by the use of a crop coefficient value. The Penman-Monteith formula and simplified versions have been put forward by the Food and Agriculture Organisation of the United Nations (FAO) as the standard method for use with agricultural land (Allen *et al*., 1998). Coefficient values have been established for traditional crops, but to date values used with *Miscanthus* have been based on other crops (e.g. sugarcane,

Stephens *et al*., 2001), or a limited number of empirical measurements (e.g. Beale *et al*., 1999; Triana *et al*., 2015). The accuracy of the various ET models has also not previously been tested with a *Miscanthus* crop.

Actual ET is generally less than PET because of resource and climate restrictions. However, some PET models (e.g. Hargreaves-Samani, Priestley-Taylor, and Penman-Monteith) can be adjusted for soil moisture levels to give a better representation of actual ET, which is needed for greater accuracy in predicting changes to water balances. Whereas models such as Penman-Monteith calculate ET for a uniform vegetation layer, models such as the Shuttleworth-Wallace (Shuttleworth & Wallace, 1985) include the influence of bare soil in estimations of actual ET from sparse canopies.

Although important, ET is only one component of the water cycle and models encompassing all aspects of the water balance have also been used to make predictions relating to LUC to *Miscanthus* at the watershed scale. In Europe the numerical water balance based WaSim (Counsell & Hess, 2000), and the more comprehensive Met. Office Surface Energy Scheme (MOSES, Essery *et al*., 2001), which incorporates the exchange of energy, carbon, and water at the land surface, have been used (Stephens *et al*., 2001; Finch *et al*., 2004; Borek *et al*., 2010). In the US models including the Groundwater Loading Effects of Agricultural Management Systems and National Agricultural Pesticide Risk Analysis (GLEAMS-NAPRA, Leonard *et al*., 1987; Lim *et al*., 2003), Agro-IBIS (Kucharik & Brye, 2003), and the Soil & Water Assessment Tool (SWAT, Arnold *et al*., 1998) have been used to specifically model hydrology in LUC to *Miscanthus* scenarios (e.g. Vanloocke *et al*., 2010; Thomas *et al*., 2014; Cibin *et al*., 2016).

Complex distributed (i.e. with spatial variation of parameters and variables) and physically based (i.e. natural system processes based on mathematical models representing mass momentum and energy) models simulating combined energy and carbon fluxes (including Agro-IBIS, Joint UK Land Environment Simulator (JULES, based on the MOSES model, Best *et al*., 2011), and SWAT) can also provide other related environmental information such as nutrient loadings, sedimentation impacts, and water quality. Using grid based or natural sub-watershed divisions (to take account of spatial differences), and outputs linked to geographic information system (GIS) software (to enable spatial visualisation of results) comprehensive predictions of specific watershed hydrology can be provided.

To date the most commonly used model with bioenergy crops has been SWAT (Engel *et al*., 2010). Watersheds in SWAT are divided into sub-basins and smaller hydrological response units (HRU) based on landscape and management differences. SWAT ultimately uses the water balance equation with sub-models contributing to it from different components within sub-basins that calculate predictions for each HRU separately and are then routed to create total values for each sub-basin. The eight main components are: hydrology, with the choice of runoff calculation (via the Soil Conservation Service (SCS) curve number equation, SCS (1976) or the Green and Ampt Infiltration method, Green & Ampt (1911)) and ET method (via Hargreaves-Samani, Priestley-Taylor, Penman-Monteith, or user defined); crop growth, based on a simplified version of the Erosion-Productivity Impact Calculator (EPIC, Williams *et al*., 1984); weather (driven by precipitation, air temperature, solar radiation, wind speed, and relative humidity); sediments, based on the Modified Universal Soil Loss Equation (MUSLE, Williams, 1975); soil temperature (as a function of damping depth, surface temperature and mean annual air temperature); nutrients (with loading

and partitioning functions); pesticides (based on GLEAMS); and agricultural management. Various water transfer algorithms and channel/reservoir routing commands are used to move the various loadings through the watershed (Arnold *et al*., 1998; Neitsch *et al*., 2011). SWAT can be linked with GIS software (Srinivasan & Arnold, 1994) and has been parametrised to better represent bioenergy crops (Trybula *et al*., 2015).

Modelled LUC scenarios involving *Miscanthus* have predominately been centred in regions of the American mid-West (e.g. Ng *et al*., 2010; Wu & Liu, 2012; Parajuli & Duffy, 2013; Cibin *et al*., 2016; Gassman *et al*., 2017; Panagopoulos *et al*., 2017; Guo *et al*., 2018). However, further watershed scale studies, with GIS based modelling, for different geographical regions are required to improve the accuracy and validation for model predictions in different climatic regions in areas where LUC is likely to occur (Finch *et al*., 2004; Environment Agency, 2015; Trybula *et al*., 2015).

1.4.3 Land use change from agricultural grassland to Miscanthus

Temperate agricultural grasslands are important for farmland biodiversity (Isselstein *et al*., 2005) and as sinks for carbon (Soussana *et al*., 2007) but across the world are facing pressures from urban expansion, conversion to arable, abandonment, and LUC to biofuel crops (Gibon, 2005; Taube *et al*., 2014).

In Europe there are changes in the management of grazing animals leading to the greater use of confinement systems and energy rich animal feeds in places (Taube *et al*., 2014; Xue *et al*., 2017), but a greater reliance on agri-environment schemes has also encouraged the extensification of grazing management in others (Dobbs & Pretty, 2008; Marriott *et al*., 2009; Acs *et al*., 2010). The generally reduced

profitability of grassland agriculture (DEFRA, 2017b; Eurostat, 2018a), and uncertainly around agricultural policy reforms due to changes in the Common Agricultural Policy (European Commission, 2017a), is resulting in increased interest in options for the diversification of grassland.

Although second generation biomass crops like *Miscanthus* are not food crops they can be seen to be in competition with food if grown on good quality land that could otherwise produce edible crops. Therefore the use of economically marginal agricultural land (i.e. low grade and unprofitable) is now preferred for biofuel crop production (Lovett *et al*., 2009; Rathmann *et al*., 2010; Milner *et al*., 2016) and could provide a way to make commercial use of currently underutilized farmland (Donnison & Fraser, 2016).

In LUC from annual crops to *Miscanthus* some benefits have been recorded in terms of biodiversity (Semere & Slater, 2007; Dauber *et al.*, 2010) increased SOC and reduced GHG emissions (Harris *et al*., 2015; McCalmont *et al*., 2017b). In terms of hydrology although *Miscanthus* has been found to use more water than annual crops, (Hickman *et al*., 2010; Vanloocke *et al*., 2010; Zhuang *et al*., 2013) it can also result in improved soil infiltration, hydraulic conductivity and water storage (Blanco-Canqui, 2010; McCalmont *et al*., 2017a). Changes to soil condition could take time and depend on management (past and present) as well as soil type and climate (Stephens *et al*., 2001; Vanloocke *et al*., 2010) and the effects arising from grassland conversions are less well understood.

Changes in soil carbon take place over long time periods and although it has been found that *Miscanthus* plantations generally have lower or similar SOC when compared to grassland controls (e.g. an analysis of 20 datasets showed a

sequestration rate of up to 1.5 Mg C ha^{-1} yr^{-1}, Qin *et al*., 2016), there is still uncertainty regarding the long term (after 10 years) impact (Zang *et al*., 2018).

Fluxes of N_2O respond more rapidly to changes in soil conditions and the resulting influence of the land conversion process from grassland to *Miscanthus* is unclear. Of two studies that have recorded soil N_2O emissions from young *Miscanthus* in comparison to grassland one found that fluxes were six times higher under the year old *Miscanthus* crop (growing season, May to September, cumulative flux of 5.5 kg N ha^{-1} compared to 1 kg N ha^{-1}, Saha *et al*., 2017) and the other found no significant difference with a seven month old *Miscanthus* crop (yearly, November to November, cumulative flux of 0.6 kg N ha^{-1} compared to 0.2 kg N ha^{-1}, Roth *et al*., 2013).

There are no studies covering the actual conversion process from a grazed grassland to *Miscanthus* and as soil disturbance and ploughing can increase soil N_2O fluxes (Drewer *et al.*, 2017) quantifying the impact of this potential "hotspot" is needed to assess the full implications of LUC (Harris *et al.*, 2015; Whitaker *et al*., 2018). Soil CH_4 emissions from temperate agricultural grasslands or from established *Miscanthus* have generally not been found to be significant in terms of GHG balances (Snyder *et al*., 2009; Robertson *et al*., 2017).

Processes such as soil GHG emissions and C sequestration can also be affected by ecosystem hydrology, and soil moisture in particular (Smith *et al*., 2008; Hickman *et al*., 2010), and there are concerns that differences in *Miscanthus* root morphology could lead to a drying of the soil profile and use of water from deep reserves (Stephens *et al.*, 2001; Donnelly *et al.*, 2011). However, a study by Mann *et al.* (2013) concluded that *Miscanthus* survives low water availability through the concentration of nutrients in the rhizome rather than exploiting deep soil water.

Nevertheless, model simulations by (Stephens *et al*., 2001) based on four UK locations and LUC to *Miscanthus* from both grass and wheat, showed that hydrologically effective rainfall (the sum of runoff and percolation) was decreased by 50-60% (a reduction of 100 mm compared to the permanent grass site) and that *Miscanthus* resulted in increased transpiration and interception of precipitation. The role of the canopy in precipitation interception was confirmed by Finch & Riche (2010) who reported measured interception losses of 24% from a *Miscanthus* plot study in south-east England. However, both studies highlight the need for field studies at the commercial scale of planting due to differing effects of advection and wind turbulence compared to small plots. Increased evapotranspiration (along with reduced rainfall) following LUC from grassland to a commercial sized *Miscanthus* plantation (6 ha) in Wales is considered to have played a part in reducing soil moisture over the first three years of growth (McCalmont *et al*., 2017b).

Local conditions as well as extent of planting also influence the impact of LUC. Two studies modelling watershed LUC from marginal mixed land uses (including grassland, corn and soybean) based in the American Midwest found differing levels of effect on streamflow: a reduction of 8% (Cibin *et al*., 2016) compared to 23% (Feng *et al*., 2018). This variation is likely to reflect the different percentages of each land use type and varying topography in the regions.

Data collected from different locations involving LUC from grassland sites to *Miscanthus* is therefore essential to inform modelled projections relating to SOC, GHG emissions, and hydrology to allow for the selection of suitable sites for future crop plantations (Finch *et al*., 2004; Hastings *et al*., 2009; Pallipparambil *et al*., 2015; Dondini *et al*., 2016a).

1.5 Research objectives

The main aim of this research is to investigate the implications of land use change from semi-improved grazed grassland to *Miscanthus* on long term soil carbon stocks, soil N_2O emissions over the conversion and establishment period, and on aspects of hydrology. Land use change to *Miscanthus* is compared to pre-conversion and existing pasture use, and in the case of watershed modelling also to SRC. The main thesis chapters take the form of manuscripts submitted to peer-reviewed journals. The objective was to provide published research in relation to identified knowledge gaps, in a timely manner, in order to provide data to help inform policy decisions regarding potential implications of land use change to bioenergy crops. The main objectives are encapsulated in the following questions posed:

- What are the medium term implications for soil carbon stocks following the LUC from agricultural grassland to *Miscanthus*?
- What are the crop establishment associated N_2O emissions for LUC from semi-improved grazed grassland to *Miscanthus*?
- How does evapotranspiration and canopy precipitation interception from a commercial scale *Miscanthus* plantation differ from a short grass crop?
- Compared to an improved pasture land use what impacts on hydrology could large scale deployment of *Miscanthus* or SRC have?

In order to address these questions a combination of empirical based studies, located in Wales, UK (an area of Europe where agriculture is dominated by grazing pasture, Welsh Government, 2018a), are combined with modelling that enables the wider application of results.

Chapters 2, 3 and 4 provide empirical studies documenting changes in long term SOC stocks and establishment N_2O and CH_4 fluxes in plot based studies following LUC from temperate grassland to *M. x giganteus* and novel hybrids. To provide context, the broader GHG implications of the results are considered through the impact on existing life cycle analyses (LCA). Chapter 2 aims to investigate the change in SOC in a fully established crop and utilizes an existing plot trial (where samples for SOC were taken pre-planting and after six years) to resample for SOC 12 years after conversion. SOC results are compared to estimates obtained using the ECOSSE carbon model which has been used simulate change in SOC in perennial energy crops (Dondini *et al*., 2015; Dondini *et al*., 2016b). The use of ECOSSE also allows for estimations of SOC under a maintained grassland scenario in the absence of a continued grassland control as part of the original trial set up.

Chapter 3 has two main goals: to compare soil N_2O emissions between an established grazed pasture and the establishment period (first two growing seasons) of *M. x giganteus* and a new hybrid*;* and to assess impacts in relation to different reduced tillage methods. This is achieved using multiple static chamber measurements, an established and inexpensive method to provide measurements of soil-atmosphere GHG fluxes (Chadwick *et al*., 2014; Collier *et al*., 2014). Chapter 4 reports the CH_4 fluxes and considers the results in comparison to the grazed grassland counterfactual.

Chapters 5 and 6 provide empirical studies and field measurements to aid modelled estimates of changes to components of the water balance. Any consequential benefits to planting *M. x giganteus* on marginal agricultural land in terms of flood alleviation are considered. Chapter 5 investigates implications for canopy interception of precipitation and evapotranspiration (ET) in a mature commercial scale (~6 ha) field

of *M. x giganteus* in comparison to a reference short grass crop. The studies use in-field eddy covariance instrumentation and manual rain gauges distributed throughout cropped and non-cropped areas. As ET is normally estimated using models, a number are compared and the most accurate determined by comparison to empirically based estimates. Chapter 6 takes this a stage further with the aim of quantifying potential changes to hydrological components following LUC to *M. x giganteus* and SRC (as a potential alternative to *M. x giganteus*) in comparison to existing improved pasture at the watershed level. This case study, based on the west Wales (UK) river basin district, applies the widely used SWAT hydrology model (Engel *et al*., 2010) with a GIS interface to investigate potential large scale LUC scenarios in typical temperate agricultural grassland.

2 Measured and modelled effect of land use change from temperate grassland to *Miscanthus* on soil carbon stocks after 12 years.

Amanda J. Holder[1], John Clifton-Brown[1], Rebecca Rowe[3], Paul Robson[1], Dafydd Elias[3], Marta Dondini[4], Niall P. McNamara[3], Iain S. Donnison[1], and Jon P. McCalmont[2]

[1]Institute of Biological, Environmental and Rural Sciences (IBERS), Aberystwyth University, Gogerddan, Aberystwyth, Wales, SY23 3EQ, UK

[2]College of Life and Environmental Sciences, University of Exeter, Rennes Drive, Exeter, EX4 4RJ, UK

[3]Centre for Ecology & Hydrology, Lancaster Environment Centre, Library Avenue, Bailrigg, Lancaster, LA1 4AP, UK

[4]Institute of Biological and Environmental Sciences, University of Aberdeen, 23 St Machar Drive, Aberdeen, AB24 3UU, UK

Publication Notes

This manuscript, under the same title, was accepted for publication in the peer reviewed journal Global Change Biology Bioenergy on 22 April 2019: GCB Bioenergy (2019) Early view. DOI: 10.1111/ gcbb.12624.

2.1 Abstract

Soil organic carbon (SOC) is an important carbon pool susceptible to land use change. There are concerns that converting grasslands to the C_4 bioenergy crop *Miscanthus* (to meet demands for renewable energy) could negatively impact SOC, resulting in reductions of greenhouse gas mitigation benefits gained from using *Miscanthus* as a fuel. This work addresses these concerns by sampling soils (0-30 cm) from a site twelve years (T_{12}) after conversion from marginal[1] agricultural grassland to *M. x giganteus* and four other novel *Miscanthus* hybrids. Soil samples were analysed for changes in below ground biomass, SOC, and *Miscanthus* contribution to SOC (using a ^{13}C natural abundance approach). Findings are compared to ECOSSE soil carbon model results (run for a land use change from grassland to *Miscanthus* scenario and continued grassland counterfactual), and wider implications are considered in the context of life cycle assessments based on the heating value of the dry matter (DM) feedstock.

Mean T_{12} SOC stock at the site was 8 (+/- 1, standard error) Mg C ha^{-1} lower than baseline time zero stocks (T_0), with assessment of the five individual hybrids showing that whilst all had lower SOC stock than at T_0 the difference was only significant for a single hybrid. Over the longer term, new *Miscanthus* C_4 carbon replaces pre-existing C_3 carbon, though not at a high enough rate to completely offset losses by the end of year 12. At the end of simulated crop lifetime (15 years) the difference in SOC stocks between the two scenarios was 4 Mg C ha^{-1} (5 g CO_2-eq MJ^{-1}). The inclusion of modelled land use change induced SOC loss, along with carbon costs relating to soil nitrous oxide emissions, doubled the greenhouse gas

[1] Described as marginal due to soil depth and type (see section 2.3).

intensity of *Miscanthus* to give a total global warming potential of 10 g CO_2-eq MJ^{-1} (180 kg CO_2-eq Mg^{-1} DM).

2.2 Introduction

Energy generation from fossil fuels (e.g. coal and gas) must be phased out as part of world-wide efforts to combat the impacts of climate change (IPCC, 2014). The European Union has set a target for renewable energy (wind, solar, hydro and bioenergy) to reach a minimum of a 27% share of the energy generation mix by 2030 (European Commission, n.d.b) from the current share of ~17% (European Commission, 2017b). In the UK, renewable energy other than wind, solar, and hydro accounted for 9.4% of the total energy produced in 2017 and there is scope for bioenergy generation (e.g. from biomass crops, landfill and sewage gas and anaerobic digestion) to increase (BEIS, 2018a).

Agricultural grasslands represent a third of the utilized agricultural area across Europe (Eurostat, 2018b) and due to changes in farming subsidies and temperate grassland agricultural management across Europe, areas of lower grade agricultural grassland may become available for biomass crops (Taube *et al*., 2014; Donnison & Fraser, 2016). In the UK, Welsh agriculture is primarily grass based (Welsh Government, 2018a) and spatial modelling has suggested that there may be 0.5 M ha suitable for the planting of perennial bioenergy crops (such as *Miscanthus* and short rotation coppice) (Lovett *et al*., 2014). However, there are concerns that losses of soil carbon (C) caused by soil disturbance (Balesdent *et al*., 2000; Conant *at al*., 2007) could reduce the C mitigation benefits gained from the conversion of grasslands to the production of bioenergy crops (McCalmont *et al*., 2017a; Whitaker *et al*., 2018).

The biomass crop *M. x giganteus* (Greef & Deuter, 1993) is a commercially available hybrid that is a fast growing, tall perennial grass, with an efficient C_4 photosynthetic pathway. It is a low input crop with potential to be grown on

agriculturally marginal land (Lewandowski *et al*., 2000; Clifton-Brown *et al*., 2015). Compared to annual crops, *Miscanthus* has the potential to sequester C due to reduced soil disturbance (tillage is only required as part of the initial cultivation) (Post & Kwon, 2000), the translocation of C from above ground biomass to roots and rhizomes (Kuzyakov & Domanski, 2000) and the provision of soil C inputs from leaf litter (Amougou *et al.*, 2011). New, commercially relevant *Miscanthus* hybrids are being developed with different morphologies and traits (Lewandowski *et al*., 2016; Nunn *et al*., 2017) which may impact on soil organic carbon (SOC), for example though variations in leaf litter and carbon allocation between above and below ground biomass (Clifton-Brown & Lewandowski, 2000; Richter *et al*., 2015).

Land use change from arable crop production to *Miscanthus* generally shows an increase or no change in SOC whereas, in contrast, it has been found that *Miscanthus* plantations have lower or similar SOC when compared to grassland controls (Qin *et al*., 2016). However, to date, most studies have taken grassland sites adjacent to *Miscanthus* plantations as representative of pre-cultivation conditions (Foereid *et al*., 2004; Clifton-Brown *et al*., 2007; Schneckenberger & Kuzyakov, 2007; Zimmermann *et al*., 2012; Rowe *et al.*, 2016; Zang *et al*., 2018) and whilst the use of such sites where soil and climate conditions are similar can provide a reasonable indication they may not accurately replicate baseline SOC stocks (Richter *et al*., 2015; McCalmont *et al*., 2017a). Therefore, there is a need to reduce some of the uncertainty around the impact of this land use change from grassland to *Miscanthus* on SOC (Whitaker *et al*., 2018), especially over the longer term.

Any carbon losses or gains from land use change should be considered over the expected lifespan of the *Miscanthus* crop, currently estimated to be between 10 and 15 years **(**Clifton-Brown *et al.*, 2015). Clifton-Brown *et al*. (2007) found an increase

in SOC under 15 year old *Miscanthus* compared to an adjacent grassland whereas Zang *et al*. (2018) found that although SOC increased between samples taken at the same site 9 and 21 years after conversion, SOC was similar to samples taken from a neighbouring grassland (used to represent pre-conversion conditions). Reducing the uncertainty around the long term impact of SOC using pre-cultivation data from the same site is needed to inform soil carbon model predictions and life cycle analyses (LCA).

Due to the limited number of long term empirical studies of land use conversion to energy crops a number of models have been used to estimate changes in SOC (Robertson *et al*., 2015). ECOSSE (Estimation of Carbon in Organic Soils: Sequestration and Emissions) is a process based model that has been successfully tested and used for simulating SOC under perennial energy crops including grassland and *Miscanthus* in this UK region (Dondini *et al*., 2015; Dondini *et al*., 2016a). However, empirical baseline data of SOC stocks in land use change from grassland to *Miscanthus,* coupled with data of SOC stocks under the mature crop (over 10 years old) would provide further model validation. ECOSSE can be used at the site or regional scale and represents an improvement on a previous model, RothC, due to a new approach to mineral and organic soils whereby the extent of processes occurring are adjusted according to soil conditions and not differentiated solely by soil type (Smith *et al.,* 2010; Robertson *et al*., 2015).

LCA is a tool that can provide an indication of the environmental costs or benefits of producing energy from different methods and by enabling comparisons which help to inform policy decisions relating to proposed land use changes (McManus & Taylor, 2015). LCA's relating to land use change from grassland to *Miscanthus* have not included changes in soil carbon due to a lack of reliable data, and have tended to

assume no change or an increase in SOC stocks (Hillier *et al*., 2009; Hastings *et al*., 2017). LCA estimates involving land use change are sensitive to the initial land use and condition (McManus & Taylor, 2015). For example, Robertson *et al*. (2017) investigated SOC as part of their LCA involving land use change to *Miscanthus* but this was from a previous arable land use with annual cultivation; potential losses at grassland sites, with less regular soil disturbance, could have a significant impact on LCA results (Hillier *et al*., 2009). Changes in SOC over the lifetime of the crop also have the potential to impact on greenhouse gas balances to a greater extent than other land use change associated costs such as increased soil nitrous oxide (N_2O) emissions (Whitaker *et al*., 2018).

Therefore, in this study we aimed to (1) measure the change in SOC stock, and *Miscanthus* contribution to SOC, from a mature (>10 years old) *Miscanthus* crop following land use conversion from an agricultural grassland compared to baseline data of initial SOC stocks; (2) use the empirical data obtained to provide validation for ECOSSE model predictions; (3) use the ECOSSE model to predict SOC stocks following land use change from grassland for an estimated *Miscanthus* crop commercial lifetime of 15 years along with a continued grassland counterfactual, in order to establish the difference in SOC between the two scenarios; and (4) provide context for the predicted difference in SOC between the *Miscanthus* and grassland scenarios at the end of the 15 years by converting the difference to a global warming potential for inclusion in an LCA comparison per unit of energy based on the heating value of the *Miscanthus* biomass.

In order to achieve this we built on previous experimental work reported in Zatta *et al*. (2014) which although from a single site includes baseline SOC data (T_0) and data taken from the same site 6 years (T_6) after land use conversion from grassland

to *M. x giganteus* and four novel *Miscanthus* hybrids. Taking advantage of the difference in $\delta^{13}C$ natural abundance values arising from the contrasting C_3 photosynthetic pathway of temperate grassland species compared to the C_4 pathway of *Miscanthus* (Kuzyakov & Domanski, 2000) we assessed changes in the contribution of *Miscanthus* to SOC between T_6 and T_{12}.

2.3 Materials and methods

Sampling was conducted at a replicated plot trial situated at Aberystwyth, Wales UK (52°26′ N, 4°01′W) on agriculturally marginal shallow dystric cambisol and dystric gleysol classified soil (up to 0.6 m soil depth in places but mainly with a gravel layer at depths >0.3 m). Prior to conversion the site was a mature established perennial ryegrass sward. Historically the site has predominantly been used for grass pasture and silage trials (re-sown ~5 yearly) with occasional oat crops (Zatta *et al*., 2014). The sample area consisted of four blocks of five randomized 25 m^2 plots, each plot contained one of five different *Miscanthus* hybrids. In September 2004, prior to planting, the existing mature perennial ryegrass sward was sprayed with Glyphosate (3 l ha^{-1}) and inversion tilled with mouldboard plough and power harrow before a ryegrass cover crop was sown in October 2004. The cover crop was sprayed with Atrazine (3 l ha^{-1}) on the 5th April 2005 with the *Miscanthus* planted on the 24th of May 2005.

2.3.1 Miscanthus hybrids

Bare root transplants of four novel hybrids (*M. sacchariflorus x M. sinensis*) cloned via in-vitro tillering (hereafter Hyb 1, Hyb 2, Hyb 3, Hyb 4), and rhizome segments of the commercially available *M. x giganteus* (*Mxg*) were slot planted at a density of two plants m^2. Compared to *Mxg*, after three years growth, Hyb 1- 4 had a higher stem density (~39 stems m^2 versus 30 stems m^2), a lower canopy height (~2.05 m versus ~2.50 m), and a lower (~10% verses ~30%) above ground biomass lignin (unpublished data).

The hybrids formed part of an ongoing yield trial with data recorded each year. Percentage differences between the above ground autumn peak harvest and spring

harvest (ripening loss) for each hybrid were calculated from the oven dried weights of 10 stems taken from each plot in November 2007 and February 2008.

2.3.2 Soil cores

Detailed methods regarding the pre-planting (6 May 2005, T_0) soil cores and those taken after 6 years of crop growth (5 May 2011, T_6) can be found in Zatta *et al*. (2014). Briefly, at T_0 five core samples (to 30 cm depth) were taken from two plots in each block, and at T_6 three core samples were taken from each plot. Each of the three T_6 core locations was taken to represent a portion of the overall field area covered by plant centre (8.1%), plant edge (24.5%) and inter-row (67.4%).

On 4 and 5 May 2017, 12 years since the plots were planted (T_{12}), three cores were again taken in each plot following the methods at T_6. The same 8.5 cm diameter cylinder auger (Eijkelkamp, Giesbeek, The Netherlands) was used with a Cobra TT jackhammer (Atlas Copco, Hemel Hempstead, UK) to take intact and uncompressed cores at three locations in each plot taken to represent a percentage of the overall field area. The soil core locations, individual plot heterogeneity, and details of the field cover survey used to calculate the percentage area represented by each core are given in the Appendix (A1). At T_{12} the area represented by the plant centre (C_c) was determined to be 9.82%, the plant edge (C_e) 53.39%, and the inter-row (C_i) 36.79%. Soil cores were taken to a depth of 30 cm at position C_i, 31 cm at C_e, and 32 cm at C_c to allow for soil displacement by rhizome growth (Zatta *et al*., 2014) and were subsequently split at 15 cm, 16 cm, and 17 cm respectively, before air-drying to a constant weight. Soils were sieved (2 mm) to separate soil, stone, and below ground biomass (roots and rhizome). Soil was then ball milled (Planetary Mill, Fritsch GmbH, Idar-Oberstein, Germany). Air dried below ground biomass (roots and rhizome) were pre milled (SM100, Retsch GmbH, Haan, Germany) before being

finely cryo-milled (6870 Cryomill, SPEX, Stan-hope, UK) in liquid nitrogen. Bulk density was calculated using the same method as described in Zatta *et al*. (2014).

2.3.3 Carbon analysis

Inorganic carbon was removed from a 3 g portion of each milled soil sample by adding 30 ml 1M HCl, rinsing and oven drying to constant weight at 40°C (Clifton-Brown *et al*., 2007). 200 mg of the acid treated soil was analysed for percentage carbon content by combustion using a Vario Macro Cube (Elementar Analysensysteme GmbH, Langenselbold, Germany). Total organic carbon was calculated using equation (3):

$$SOC = POC * (ODW_{acid}/ODW_{initial}) \quad (3)$$

where SOC (%) is the total soil organic carbon, POC is the percentage organic carbon in the acid washed sample, ODW_{acid} is the oven dried weight of the sample after acid washing, and $ODW_{initial}$ is the oven dried weight of the same sample before acid washing.

SOC mass was calculated in two ways: to a fixed soil depth (using the soil bulk density[2]); and to an equivalent soil mass (ESM) (Ellert & Bettany, 1995; Wendt & Hauser, 2013). For the ESM approach equations (4) and (5) were used with a fitted cubic spline curve (Wendt & Hauser, 2013) to provide estimates of the cumulative ESM for a layer of soil mass 0-3000 Mg ha^{-1} (SOC_{ESM}). The SOC mass for both methods was then scaled up to Mg ha^{-1} using the percentages relating to the representative area covered by each core location.

[2] See Appendix 4.5.

$$M_{soil(DL)} = (M_{sample}/A_{sample})*10^4 \quad (4)$$

where $M_{soil(DL)}$ is the mass of soil in the depth layer (Mg ha^{-1}), M_{sample} is the dried mass of the soil core sample (g), and A_{sample} is the area of the core sample (mm^2), and 10^4 is the conversion factor from g mm^{-2} to Mg ha^{-1}.

$$SOC_{ESM} = (M_{soil(DL)}*SOC_{cont})/1{,}000 \quad (5)$$

where SOC_{ESM} is the SOC mass in the sample soil mass layer (Mg ha^{-1}), $M_{soil(DL)}$ is the mass of soil in the depth layer (Mg ha^{-1}) (equation 4), SOC_{cont} is the concentration of organic C (kg Mg^{-1}) from equation (3), and 1,000 is the conversion factor from kg ha^{-1} to Mg ha^{-1}.

The carbon content of 5 mg of untreated milled soil and 2 mg of below ground biomass was measured using an ECS 4010 (Costech Analytical Technologies Inc., CA, USA) elemental analyser. Soil and below ground biomass $\delta^{13}C$ was measured using a Picarro Cavity Ringdown Spectrometer G2131-i (Picarro Inc., CA, USA) coupled to the ECS 4010 using a Picarro Caddy split-flow interface (Balslev-Clausen, Dahl, Saad, & Rosing, 2013) and cane (-11.64‰) and beet sugar (-26.03‰) (Iso-Analytical, Crewe, UK) isotopic standards. $\delta^{13}C$ was defined by equation (6):

$$\delta^{13}C = (((^{13}C/^{12}C)/(^{13}C/^{12}C_{PDB}))-1)*1000 \quad (6)$$

where $^{13}C/^{12}C_{PDB}$ is the isotope ratio of the Pee Dee Belemnite standard material (0.0112372) and $^{13}C/^{12}C$ is the isotopic ratio of the measured belowground biomass or soil sample.

The *Miscanthus* contribution to soil carbon (C_{mis}) at T_6 and T_{12} was calculated using equation (7):

$$C_{mis} = (\delta_n - \delta_0/\delta_r - \delta_0) \quad (7)$$

where δ_0 is the soil carbon isotope abundance at T_0, δ_n the abundance at T_6 or T_{12}, and δ_r the abundance of the below ground biomass at T_6 or T_{12} (Balesdent *et al.*, 1987).

2.3.4 *Modelling*

The ECOSSE model (Smith *et al.*, 2010) was run from the conversion year in 2005 and projected to 2020 using the 'limited data site simulation' mode for a continued grassland scenario and a land use change from grassland to *Mxg* scenario.

A default water table depth of 3 m with drainage class 2 was used. Soil texture percentages were sand 58%, silt 24%, and clay 18% with a soil pH of 6[3] (Zatta *et al.*, 2014). Long term monthly averages[4] for precipitation and air temperature as well as monthly 2005 to 2011 data were taken from the nearby (~0.7 km) Gogerddan weather station (Met Office, n.d.a). As data was not available from this station for the years 2012 to 2016, meteorological data to cover this period was taken from another station approximately ~3.5 km distance (McCalmont *et al.*, 2017b). Monthly potential evapotranspiration from 2005 to 2016 was calculated using data from both weather stations using the R (R Core Team, 2015) package 'Evapotranspiration' (Guo & Westra, 2016). Meteorological conditions from 2016 to 2020 were predicted by ECOSSE using the long term monthly averages.

[3] For the grass land use the pH used was 5.9 (0-15 cm depth) & 6.2 (15-30 cm depth) and for the *Miscanthus* land use 6 (0-15 cm depth) and 6.2 (15-30 cm depth).
[4] Averages taken from 17 years of data (2000-2017) from the Gogerddan and Penglais weather stations.

For the continued grassland land use scenario the values for initial carbon content (77 Mg C ha^{-1}), bulk density 1.14 g cm^{-3} and 1.11 g cm^{-3} for the 0-15 and 15-30 cm depths respectively were taken from Zatta *et al*. (2014), along with a yearly plant yield of 8 Mg DM ha^{-1} based on average values for this area given in Smit *et al*. (2008).

For the grassland to *Mxg* land use change scenario the initial carbon content (78.8 Mg C ha^{-1}) was based on the value in Zatta *et al.* (2014) which included inputs from the herbicide killed pasture. All other initial details for the grassland and *Mxg* land use remained the same with the exception of the bulk density under *Mxg* which was taken from T_6 data (1.08 g cm^{-3} and 1.13 g cm^{-3} for the 0-15 and 15-30 cm depths respectively, Zatta *et al*., 2014).

Input of C to the soil from crop residue and below ground biomass is calculated by ECOSSE as a function of net primary production (NPP) modified by empirical parameters within the model relating to each plant type (e.g. to account for harvest offtake). Further details can be found in (Smith *et al.*, 2010) and (Dondini *et al*., 2016b). Briefly, plant inputs enter the soil as RPM (resistant plant material) and DPM (decomposable plant material) with a DPM:RPM ratio set depending on land use category (e.g. grassland or *Miscanthus*). There are five pools of soil organic matter (SOM) that each decompose at a specific rate constant and are sensitive to soil and climate data. There are specific C and N cycles within the model for grassland and *Miscanthus*. Decomposition is simulated by a number of equations into either BIO ('biomass' or active organic matter) or HUM ('humus' or more slowly turning over soil organic matter) pools, with inert organic matter (IOM) not contributing to the decomposition processes. In land use change scenarios protected SOM (soil organic matter) is released from HUM to DPM and RPM. For the land

use change to *Mxg* scenario NPP (Table 4) was calculated from the spring harvested yield (unpublished data) plus 33% to account for over winter ripening loss (primarily leaf litter drop, based on the relationship outlined in Clifton-Brown *et al*., 2007) and 20% to account for below ground biomass gain (estimated from the weight of oven-dried coarse roots and rhizomes sampled over a four year period from a nearby established *Mxg* plantation (unpublished data). As in Zatta *et al*. (2014), for the conversion year, 1.5 Mg DM ha^{-1} was added to account for the input from the herbicide sprayed pasture and an estimated NPP of 16 Mg DM ha^{-1} (approximate mean NPP for years 11 and 12) was used for the projected growing seasons (2017 to 2020), when yields are expected to reduce towards the end of the commercial crop lifespan (Larsen *et al*., 2014; Clifton-Brown *et al*., 2015).

Root Mean Square Error and Relative Error were used to evaluate the accuracy of the model outcomes compared to estimates of SOC derived from soil cores at T_6 and T_{12}.

Table 4 Estimated net primary production (NPP) of biomass (as dry matter, DM) calculated from the peak yield plus 20% as an approximation of below biomass gain for the land use change from grassland to *M. x giganteus* scenario.

Growing season	NPP (Mg ha^{-1})
2005	1.9
2006	2.2
2007	16.7
2008	23.2
2009	21.2
2010	22.0
2011	26.3
2012	22.9
2013	21.7
2014	18.3
2015	14.3
2016	19.3
2017-2020	16.0

2.3.5 Global warming potential

The difference between the ECOSSE predicted grassland and *Mxg* SOC at the end of 2020 (15 years after land use change) was converted from Mg C ha^{-1} to Mg CO_2-eq ha^{-1} [5] using the molecular weight (IPCC, 2007). This was converted to a global warming potential (GWP, g CO_2-eq MJ^{-1}) using an estimated cumulative yield for a fifteen year period of 180 Mg DM ha^{-1} (Larsen *et al*., 2014) and an energy content of 17.95 GJ Mg^{-1} DM (Felten *et al*., 2013)[6].

This GWP, relating to the difference in SOC, is compared and added to a previously published LCA value for *Miscanthus* cultivation that excluded changes in SOC stocks (4.4 g CO_2-eq MJ^{-1} [7], Hastings *et al*., 2017), but included the entire supply

[5] See Appendix A4.3.
[6] See Appendix A4.4.
[7] See Appendix A4.1 for conversion from CO_2-C to CO_2.

chain (propagation, harvest, pelleting and transport) with a *Miscanthus* higher heating value of 18 GJ Mg^{-1} DM (Collura *et al*., 2006; Hastings *et al*., 2017)

To consider the inclusion of other GHG costs relating to the land use change, the carbon cost of increased soil N_2O emissions over the establishment to *Miscanthus* (4.13 Mg CO_2-eq ha^{-1} (8.83 kg N_2O-N ha^{-1}), Holder *et al.*, 2019), and reversion process back to grassland (3.41 Mg CO_2-eq ha^{-1} (7.29 kg N_2O-N ha^{-1}), McCalmont *et al*., 2018), were converted to g CO_2-eq MJ^{-1} using the cumulative fifteen year yield. In both N_2O studies referred to no fertilizer was used during the *Miscanthus* management or LUC, and emissions were estimated from weekly (over a 20 month period, McCalmont *et al*., 2018) or bi-weekly (over an 18 month period, Holder *et al*., 2019) static chamber sampling.

2.3.6 Data analysis

Data analysis was performed in R version 3.5.1 (R Core Team, 2015), and model assumptions were tested using Levene's and Shapiro-Wilk Tests. At T_0 the mean of the five soil core samples per plot was used to provide one value for each plot sampled. At T_6 and T_{12}, the three cores samples per plot were scaled (as detailed in the methods) and added together to give one value per plot.

To assess the effect of land use change on soil carbon stock mean block level T_0 SOC was compared to mean block level T_6 and T_{12} SOC using a linear mixed effect model from package 'nlme' (Pinheiro *et al.*, 2017) with time point as the fixed factor (T_0, T_6, T_{12}), the random effect of block, and an auto correlation structure (AR1). The data was subsequently split into two groups (T_0 with T_6, and T_0 with T_{12}) to allow the influence of hybrid on changes in total scaled SOC stock compared to pre-conversion values (T_0). Land use (*Mxg*, Hyb 1-4, and pre-conversion grassland) was used as a fixed factor with the random effect of block. Finally T_6 and T_{12} data

were grouped to test the impacts on SOC stocks of the fixed factors: time point, hybrid, and depth and their interactions, with block included as a random factor. Model results were summarised using type III ANOVA (package 'car', Fox & Weisberg, 2011) and Tukey HSD (package 'multcomp', Hothorn *et al*., 2008) post-hoc tests.

Miscanthus C percentage contribution (C_{mis}) data was split into 0-15 cm and 15-30 cm depths. Data for the 15-30 cm depth was log transformed to improve residuals. The contribution of C_{mis} to the total SOC stock was then explored with the hybrid, time point (T_6, T_{12}), and sampling position (C_i, C_e, C_c) included as fixed factors with the random effect of block.

Below ground biomass for each depth and sample position was analysed separately using non-parametric paired Wilcoxon tests as residuals were not significantly improved using transformations. Correlations between SOC and C_{mis} versus belowground biomass, and SOC versus ripening loss were completed using the linear model function.

2.4 Results

2.4.1 Soil Organic Carbon

Mean SOC (0-30 cm depth) at T_{12} was 71 +/-1 (SE, standard error) Mg ha^{-1}, (SOC_{ESM} 67 +/- 1 (SE) Mg ha^{-1}, for a reference soil mass layer of 0-3000 Mg ha^{-1}). Soil bulk density results for each time point are summarised in Table 5. SOC was effected by year (χ^2 (2) = 16.52, p<0.001) with post hoc testing showing that both T_6 and T_{12} were significantly lower than T_0 (79 +/-1 (SE) Mg ha^{-1}), but that T_{12} was not significantly different to T_6 (71 +/-1 (SE) Mg ha^{-1}). However, in subsequent analysis by hybrid the difference to T_0 is only significant (p<0.05) for Hyb 2 (Figure 4). Between T_6 and T_{12} SOC both reduced in 0-15 cm layer and increased in the 15-30 cm layer by 4 Mg ha^{-1} (χ^2 (1) = 18.08, p<0.0001).

Miscanthus contribution (C_{mis}) to SOC in the 0-15 cm layer (Figure 5a) was effected by sample position (χ^2 (2) = 19.78, p<0.001) decreasing with distance from the plant centre. However, at T_{12} C_{mis} was spread out more evenly across the three sampling positions than at T_6 (χ^2 (2) = 8.08, p = 0.02). In contrast, in the 15-30 cm layer C_{mis} was similar in all positions (Figure 5b), although it decreased with Hyb 2 and Hyb 4 by 2% (χ^2 (4) = 22.36, p<0.001).

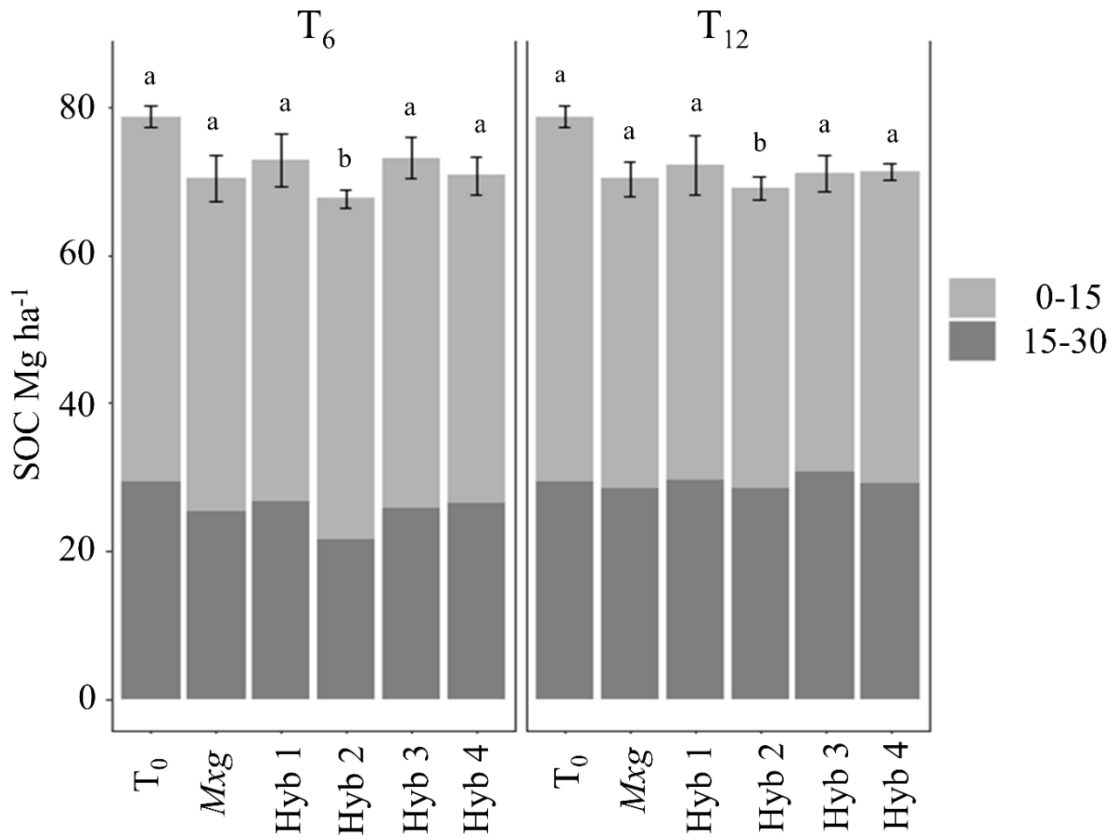

Figure 4 Soil organic carbon (SOC)[8] in the 0-15 and 15-30 cm depths, pre-conversion (T_0) from grassland to *M. x giganteus* (*Mxg*) and four *Miscanthus* hybrids (Hyb 1-4), six years after conversion (T_6) and 12 years after conversion (T_{12}). Error bars show the standard error of the mean for the total 0-30 cm values, and the same letter indicates non-significant difference ($p>0.05$).

Table 5 Soil bulk density for the two soil depths at each sampling occasion (T_0 and T_6 from Zatta *et al*., 2014).

Depth (cm)	T_0	T_6	T_{12}
0-15	1.14	1.08	1.04
15-30	1.11	1.13	1.21

[8] Measured soil organic carbon at the three sampling time points.

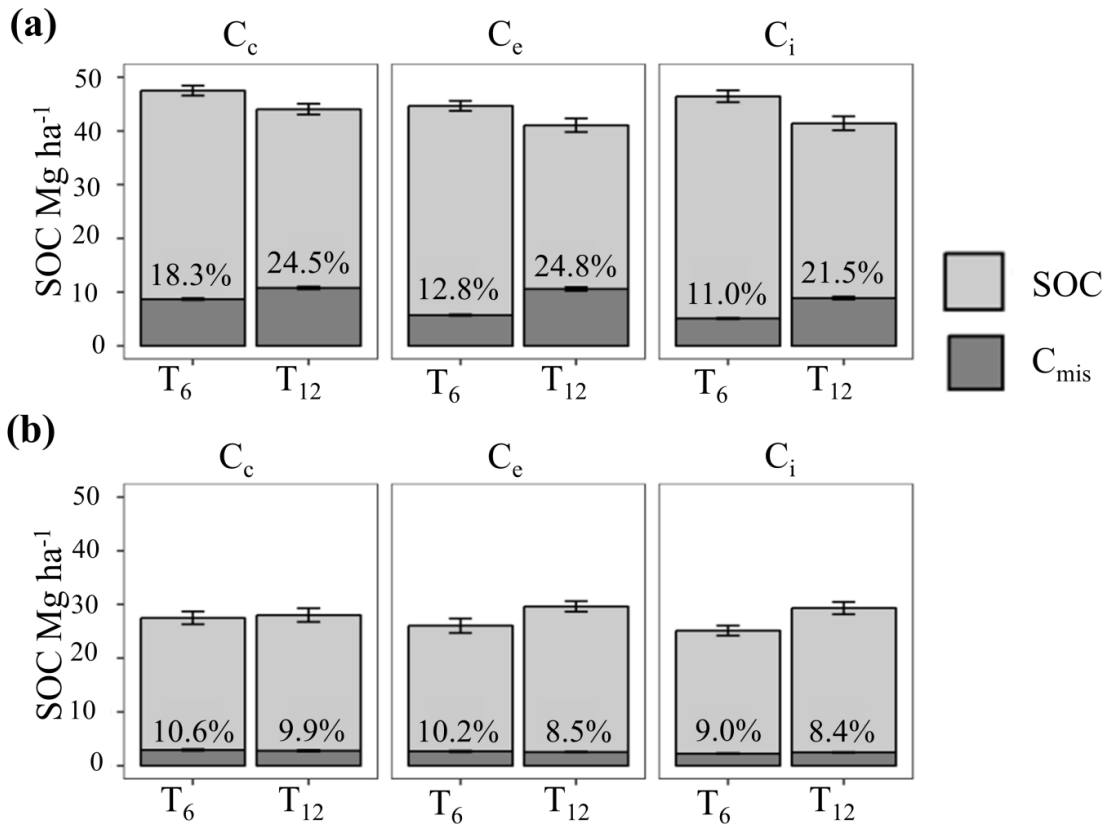

Figure 5 Total soil organic carbon (SOC)[9] and *Miscanthus* derived carbon (C_{mis}) after 6 (T_6) and 12 (T_{12}) years at each sample position (plant centre (C_c), plant edge (C_e), and inter-row (C_i)) for **(a)** 0-15 cm depth and **(b)** 15-30 cm depth. Percentages shown are the C_{mis} portion of SOC. Error bars show the standard error for separate C_{mis} and C_3 derived carbon.

2.4.2 Biomass

The distribution of below ground biomass (roots and rhizome) also changed from T_6 to T_{12} with outward spread from the original planting position towards the inter-row in the upper soil depth (Figure 6).

[9] Measured soil organic carbon and *Miscanthus* derived carbon.

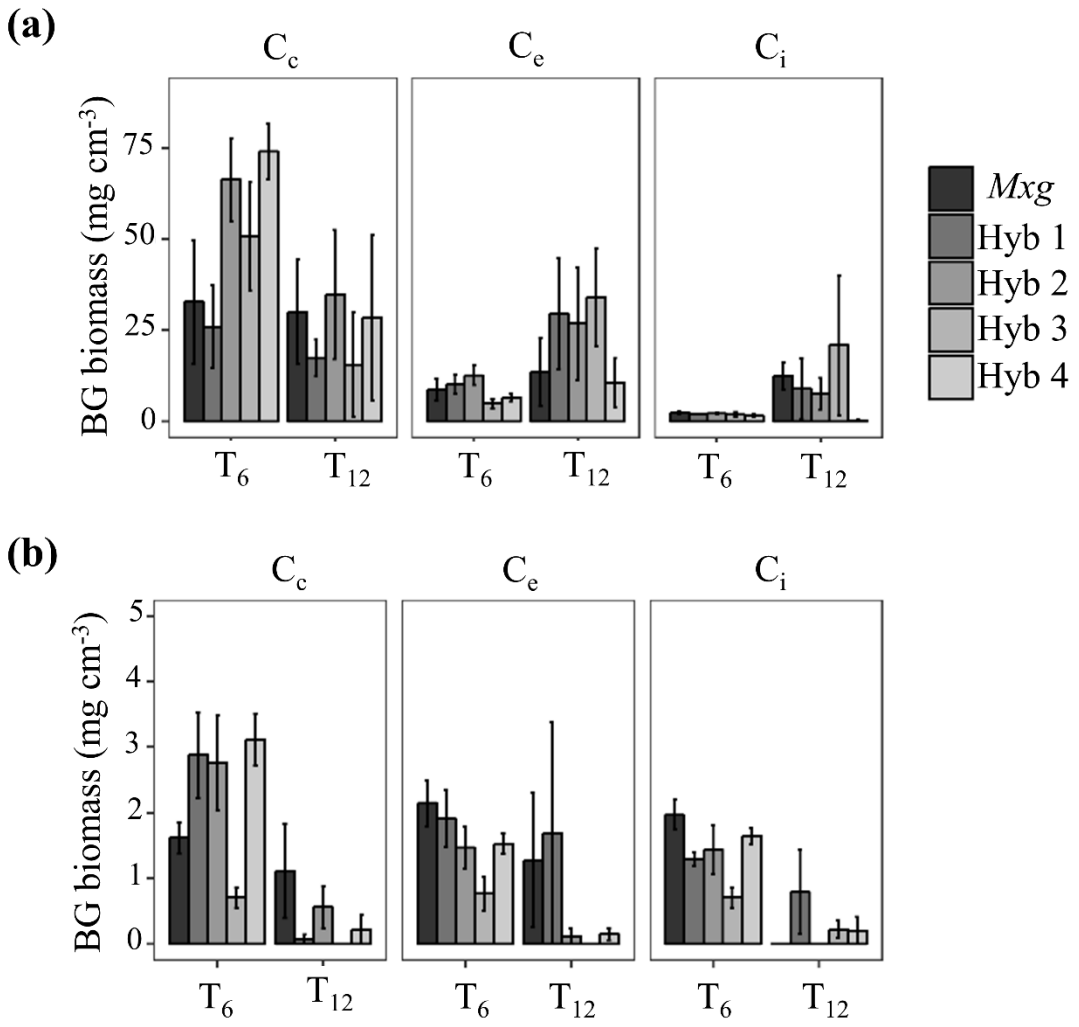

Figure 6 Mean below ground (BG) biomass (roots and rhizomes) found after 6 (T_6) and 12 (T_{12}) years of growth for *Miscanthus* hybrids (*M. x giganteus* (*Mxg*) and Hyb 1-4) at each sample position (plant centre (C_c), plant edge (C_e) and inter-row (C_i)) at the **(a)** 0-15 cm depth and **(b)** 15-30 cm depth. Error bars show the standard error.

At the 0-15 cm depth below ground biomass was only reduced at position C_c ($p=0.02$) between time points T_6 and T_{12} (by 37+/-10 (SE) Mg ha^{-1}), whereas there was a reduction in all positions in the lower 15-30 cm layer ($p<0.05$) (Figure 6).

No correlation was found between below ground biomass and SOC at T_{12} as was found in T_6 (Zatta *et al.*, 2014). However, C_{mis} was positively and significantly correlated with below ground biomass at both time points ($r = 0.67$ at T_6; and $r =$

0.65, p<0.0001 at T_{12}) in the upper 0-15cm soil depth (Figure 7). Roots were not separated from rhizome in T_6 or T_{12} but only small fragments of rhizome were found in samples from the lower depth at both time points.

Hyb 4 had the greatest reduction in below ground biomass in the 0-15 cm soil depth between time points (-14 +/- 12 mg cm^{-3}, T_6 to T_{12}) and also had the highest percentage inputs from ripening losses (leaf/litter drop) (36%, Table 6).

Hyb 2 had the lowest over winter ripening loss although no significant difference was found between ripening loss for the different *Miscanthus* hybrids. Ripening loss was positively, but not significantly, correlated with change in SOC (between T_0 and T_{12}) in the 0-15 cm depth layer (r 0.77, p = 0.13, Figure 8).

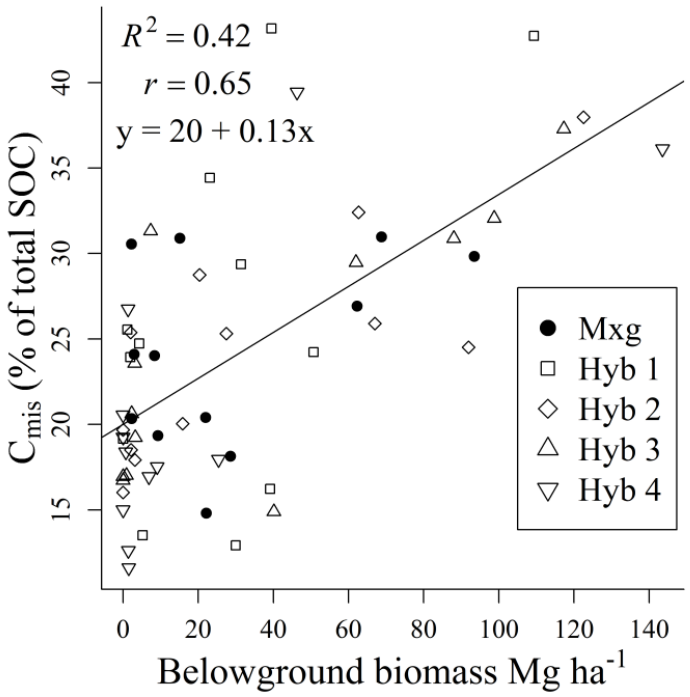

Figure 7 *Miscanthus* derived soil carbon as a percentage of total soil organic carbon (SOC) against below ground biomass for hybrids *M. x giganteus* (*Mxg*) and Hyb 1-4. Data includes all sample positions in the 0-15 cm soil layer at 12 years after planting.

Table 6 The change in below ground (BG) biomass and *Miscanthus* derived soil carbon (as a percentage of total soil organic carbon (SOC)) at 0-15cm depth after 6 (T_6) and 12 (T_{12}) years of land conversion from grassland to *Miscanthus*. Biomass and C_{mis} differences are taken from mean values across all three sampling positions (C_c, C_e, C_i). Above ground ripening loss is the difference between autumn peak and spring harvest yields. The standard error is shown in brackets.

Hybrid	BG biomass (mg cm^3): Difference T_6 to T_{12}	C_{mis} (% of SOC): Difference T_6 to T_{12}	Above ground ripening loss (%)
Mxg	+4 (+/- 10)	+10 (+/- 2)	26 (+/- 9)
Hyb 1	+6 (+/- 6)	+10 (+/- 3)	31 (+/- 4)
Hyb 2	-4 (+/- 9)	+5 (+/- 1)	19 (+/- 1)
Hyb 3	+4 (+/- 12)	+8 (+/- 3)	25 (+/- 8)
Hyb 4	-14 (+/- 12)	+7 (+/- 3)	36 (+/- 4)

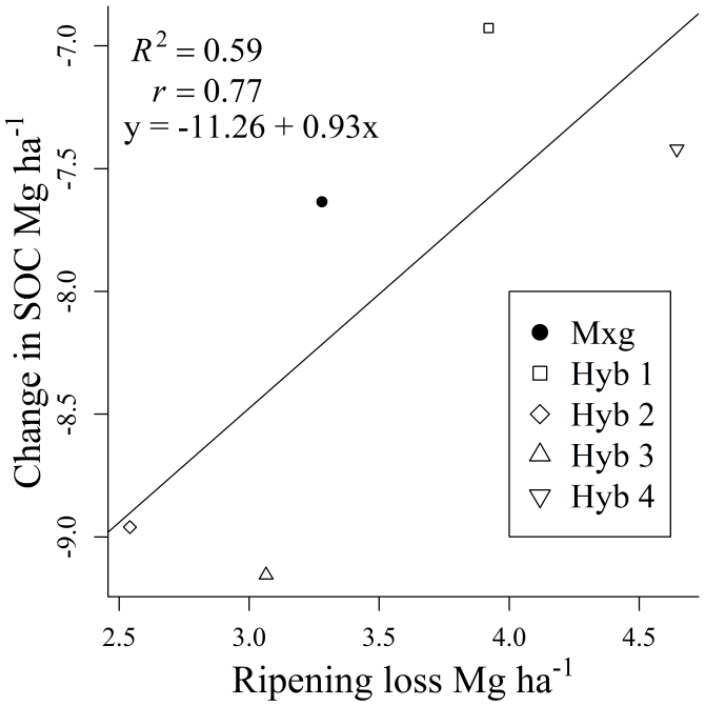

Figure 8 Correlation between change in T_0 and T_{12} mean soil organic carbon (SOC) and estimated ripening loss at the 0-15cm depth for hybrids *M. x giganteus* (*Mxg*) and Hyb 1-4.

2.4.3 Modelling

Measured SOC at T_6 and T_{12} was within the 95% confidence interval (CI) of the ECOSSE model predictions for all the hybrids[10]. For the land use change from grassland to *Mxg* scenario the model Root Mean Square Error (RMSE) of 5.49% was within the RMSE 95% CI of 9.67%, and the Relative Error (RE) of 5.41% was within the RE 95% CI of 9.62% (based on soil core results from T_6 and T_{12}).

At the beginning of the 15 year simulation the land use change to *Mxg* scenario shows slightly higher SOC than the continued grassland scenario (reflecting the higher initial C value used). After this there is a clear drop in levels of SOC under *Miscanthus* before they begin to level out. After 15 years the predicted loss compared to T_0 was 12 Mg ha^{-1}, however, the model suggests there is also a slow decline in the SOC under the continued grassland scenario which shows a loss of 7 Mg ha^{-1} after 15 years (Figure 9). At the end of 2020 the difference in SOC stocks between the continued grassland scenario, and land use change to *Mxg* scenario is 4 Mg C ha^{-1}.

[10] i.e. the ECOSSE simulations matched the empirical measurements.

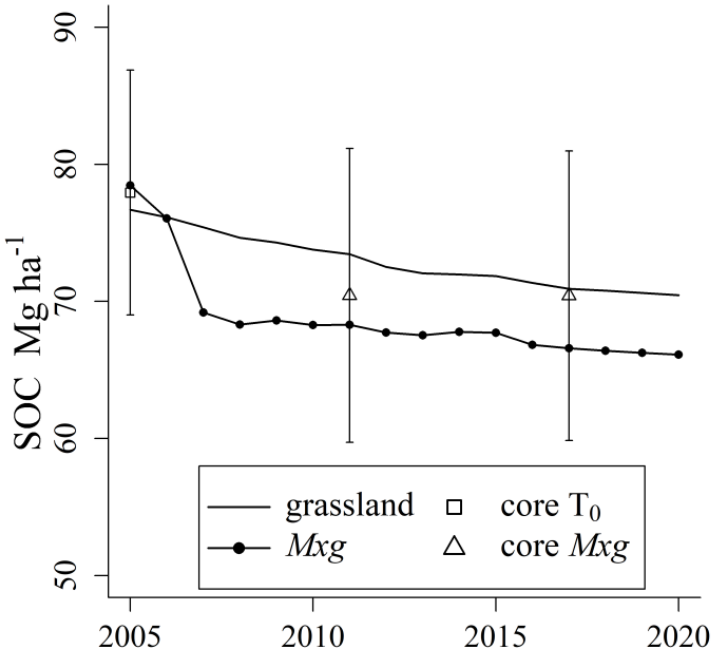

Figure 9 Results of the 15 year (2005-2020) ECOSSE simulation of soil organic carbon (SOC) under a continued grassland scenario (grassland) and a land use change from grassland to *M. x giganteus* (*Mxg*) scenario. Mean SOC from soil cores taken immediately pre-conversion (T_0) and from under *Mxg* in 2011 and 2017 are shown with error bars indicating the 95% confidence intervals.

2.4.4 Life cycle analysis

The carbon cost relating to the difference in predicted SOC stocks between the continued grassland and land use change to *Mxg* scenarios of 4 Mg C ha^{-1} (or 15 Mg CO_2-eq ha^{-1}) equates to 5 g CO_2-eq MJ^{-1} based on the energy content of the estimated 15 year yield. This represents a 125% increase when added to a previous LCA that excluded soil carbon changes (Table 7).

Table 7 Global warming potential (GWP) over a 15 year crop lifetime of the estimated carbon costs associated with the *Miscanthus* production chain, predicted difference in soil organic carbon (SOC) stocks (compared to a grassland counterfactual), and estimated increases in soil nitrous oxide (N_2O) emissions related to the land conversion and reversion.

Cost association	**GWP (g CO_2-eq)**	**GWP (sum, g CO_2-eq)**
Production chain (Hastings *et al*., 2017)	4	
Difference in SOC	5	9
Establishment N_2O (Holder *et al*., 2019)	1	10
Reversion N_2O (McCalmont *et al*., 2018)	1	11

2.5 Discussion

2.5.1 Total soil organic carbon

In the light of concerns over the impact on soil carbon when planting bioenergy crops into grassland (McCalmont *et al*., 2017a; Whitaker *et al*., 2018), this study has shown a 10% loss in SOC after 12 years of land use change from this temperate marginal grassland to *Miscanthus* at this site. In this new analysis, unlike Zatta *et al*. (2014), we did find a reduction in soil carbon stock at T_6 compared to T_0 but the breakdown by hybrid confirmed that the difference was only significant for a single hybrid (at T_6 and T_{12}, Figure 4). The overall reduction in carbon from T_0 to T_{12}, of 8 Mg ha^{-1}, is within the range +4 to -9 Mg ha^{-1} reported in other grassland to *Miscanthus* field based studies (Clifton-Brown *et al*., 2007; Schneckenberger & Kuzyakov, 2007; Zimmermann *et al*., 2012; Zang *et al*., 2018). There was also no difference between carbon stocks at the two sampling points (T_6 and T_{12}) suggesting a reasonably stable carbon state. However, this is in contrast to Zang *et al*. (2018) where soil organic matter increased between sampling occasions (9 and 21 years after *Miscanthus* planting). This difference may be as a result of different soil pH and nutrient levels, or the slightly cooler (annual average air temperature 6.7°C vs. 10.4°C) and wetter (annual average precipitation 1074 mm vs. 654 mm) climate in this study, which could all influence *Miscanthus* derived carbon (Zimmermann *et al*., 2012).

The initial tillage and planting of the cover crop in this study occurred in the autumn (October 2004) before the T_0 samples were taken in early May 2005 (prior to *Miscanthus* planting). It is therefore possible that if the original sampling had taken place in the autumn, estimated SOC stock may have been higher. Tillage results in releases of SOC due to the change in conditions that are created in the soil matrix

and the creation of newly available substrate that can stimulate soil bacteria/microbial activity and decomposition rates. However, initial increases in CO_2 immediately following autumn ploughing have mainly been attributed to the release of soil CO_2 from large soil pores and from the release of dissolved CO_2 from soil water, and there is generally a lag time before CO_2 from bacterial decomposition of soil organic matter and SOC is released (Reicosky & Lindstrom, 1995). Turnover times for light fraction SOC are generally in terms of months to years (Post & Kwon, 2000) and are connected to soil moisture and temperature, with temperature increases stimulating turnover (La Scala Jr. *et al*., 2008). During the winter months following tillage at this experimental site microbial activity and decomposition could be expected to be slow, due to low air and soil temperatures (mean air temperature at the site October 2004 – April 2005 was 8°C) and therefore changes in SOC from October to April minimal. Baseline soil carbon stocks at our site were also remarkably similar to another nearby periodically re-seeded grassland site used for a land use transition experiment (see McCalmont *et al.* 2017b), which contained 79 Mg C ha^{-1} in the top 30 cm. Results presented here might, therefore, be assumed to be reasonably representative of land use transitions on these typical improved marginal grassland systems in the UK. Grasslands with deeper soils have shown contrasting changes to SOC following LUC to *Miscanthus*. In empirical studies that sampled soils to a depth of 1 m across a range of soil types, Rowe *et al*. (2016) found that significant SOC losses were only found in the top 30 cm whereas Qin *et al*. (2016) found SOC was generally increased in the top 30 cm. However, both studies conclude that taken over the whole 1 m soil profile SOC was not significantly lost. In some cases surface losses were offset by increases lower in the profile and in others changes were limited to the surface and therefore impacts were diluted when

considered over the whole depth. Impacts may be different for longer term, semi-natural grassland sites where initial carbon stocks may be higher (Guo & Gifford, 2002).

2.5.2 Miscanthus derived carbon and spatial distribution

C_{mis} mirrored the ground cover survey and below ground biomass found (with the spreading of *Miscanthus* into the outer C_e and C_i sampling positions) supporting the use of multiple coring positions when scaling up from small samples to Mg ha^{-1} (Neukirchen *et al*., 1999).

The land use change is clearly seen in the increase of C_{mis} between T_0 and T_6. Although new *Miscanthus* C_4 carbon replaced pre-existing C_3 carbon, this was not at a high enough rate to completely offset losses by the end of year 12. The impact of land use change on SOC generally differs with soil depth (Poeplau & Don, 2014; Rowe *et al.*, 2016; Zang *et al*., 2018). In this study it was found that between T_6 and T_{12} C_{mis} increased in the top layer, although SOC also declined (Figure 5). A higher percentage of C_{mis} in the topsoil (0-10 cm) compared to deeper soil layers is in accordance with findings by Poeplau & Don, (2014) and Hu *et al*. (2018). This is likely to be attributed to the distribution of the main *Miscanthus* root and rhizome biomass, which are concentrated in the upper layer (Figure 6) and positively correlated to C_{mis} at T_6 and T_{12} (Figure 7). However, SOC also declined in this upper layer, which may be in part attributed to the 'priming effect' where increased microbial activity (stimulated by ploughing and an increase in accessible C generated from higher plant biomass, root exudates and litter) leads to the use of more stable soil carbon (Cheng, 2009; Kuzyakov, 2010; Hopkins *et al.*, 2013). In contrast, between T_6 and T_{12}, SOC in the lower 15-30 cm depth increased despite C_{mis} remaining at a similar level (Figure 5). The reason for this difference is unclear,

but it may be a legacy of the cultivation where although ploughing could be expected to add C_3 inputs from dead roots/residues in both soil depths there are slower turnover rates at the lower 15-30 cm layer due to the higher bulk density (Table 5) resulting in less aeration for microbial activity. The increase in SOC in this lower layer was only seen at the plant edge and inter-row positions where there is also the increased possibility of weeds providing C_3 inputs to the soil, but further research would be needed to confirm these possibilities.

2.5.3 Influence of hybrid

Despite the novel hybrids (Hyb 1-4) having lower lignin content than *Mxg*, and 3 out of the 4 novel hybrids having a lower C:N ratio, the influence of hybrid was small. This is in contrast to the suggestion made in Zatta *et al*. (2014) that after a longer time period differences in the SOC levels for the hybrids would reflect differences in carbon partitioning. All five hybrids sequestered similar amounts of C_{mis} and only Hyb 2 had lower overall SOC compared to the baseline (at T_6 and T_{12}). Therefore this study suggests that for this type of interspecies hybrid (*M. sacchariflorus x M. sinensis*) the potential of yield improvements are not generally at the cost of soil carbon losses compared to the commercial standard (*M. x giganteus*). However, investigation into differences in the chemical and physical properties of the root biomass of Hyb 2 may provide more insights.

Leaf litter inputs to the soil are an important part of carbon cycling (Amougou *et al*., 2011) and we found that Hyb 4, which lost the most below ground biomass between T_6 and T_{12}, also had the highest ripening loss which may have acted as compensation. Hyb 2, the only hybrid with significantly lower SOC than at T_0, also had low ripening loss inputs (Table 6). The correlation between ripening loss and change in SOC found in this study after 12 years (Figure 8), although not significant

is in line with the prediction from the RothC model in Zatta *et al*. (2014) where ripening loss for each hybrid was correlated to projected SOC in 2025.

2.5.4 Modelling

The ECOSSE model predicted SOC under *Miscanthus* within the statistical error of the field measurements and no bias was found. However, SOC under *Mxg* projected to 2020 with ECOSSE (66 Mg C ha^{-1}) is less than was predicted using the RothC model (72 Mg C ha^{-1}, Zatta *et al*., 2014). The initial drop in SOC following land use conversion to *Mxg* is greater with ECOSSE, which may be attributed to the land use change routine within ECOSSE which aims to simulate carbon loss from cultivation. Differences in predictions may also be as a result of differences in weather data used in the two models after 2011. However both models predicted the SOC to within the 95% confidence intervals at T_6 and T_{12} when soil core samples were taken. Although the model can be run using different yield results for the novel hybrids, differences in decomposition rates for above and below ground biomass would allow for greater accuracy in comparisons of genotypic differences.

In this work it was not possible to compare samples from maintained grassland at the same site or within an acceptable distance but the ECOSSE model suggests SOC under continued grassland also has a steady decline of 7 Mg ha^{-1} over 15 years (Figure 9). It should not therefore be assumed that even without any cultivation (whether to *Miscanthus* or a new grass ley) SOC would remain the same as baseline levels over time. UK wide surveys recording trends in soil carbon over time (at the 0-15 cm depth) have also reported significant reductions (~6%) in soil carbon under managed fertile grasslands between 1998 and 2007 (Bellamy *et al*., 2005; Emmett *et al*., 2010). These losses may be attributable to a number of factors including climate change and changes in management methods that have resulted in more efficient

harvesting and a reduced use of organic manures (Bellamy *et al*., 2005; Smith *et al*., 2007). The grassland scenario is run with the same yearly biomass yield input, whereas changes in weather and management would in reality impact on yields, and hence carbon inputs, resulting in differences in SOC.

The difference in predicted SOC between the land use change and continued grassland scenarios (-6%, at 2020, the end of the estimated *Mxg* crop lifetime) was within the range of -48% to +15% found for eight established (>5 years) *Miscanthus* plantations compared to neighbouring grassland sites (Rowe *et al*., 2016). The contrasting results for the different sites within Rowe *et al*. (2016), along with the results of this study, show that significant losses in SOC can occur, and whilst Qin *et al*., (2016) found no overall change in SOC in relation to grassland to *Miscanthus* conversions, confidence intervals ranged from -9% to +21% (for the mean of five datasets reflecting the change in SOC in *Miscanthus* crops >10 years).

2.5.5 Global Warming Potential impacts

Soil sustainability is an important consideration when assessing the impacts of potential land use change scenarios (UNFAO, n.d.; Hillier *et al*., 2009). In this long term land use change study where initial SOC stocks are similar to that expected for temperate grasslands in this climate (European Commission Joint Research Centre, n.d.; McCalmont *et al*., 2017b) we have seen decreases in SOC (compared to baseline levels, and between modelled predictions of grassland and *Miscanthus*), which more than doubled a production cost LCA result (Table 7). Similarly soil N_2O emissions during crop establishment and reversion to the next crop have recently been shown to represent a significant portion of the greenhouse gas balance (McCalmont *et al*., 2018; Holder *et al*., 2019).

The starting *Miscanthus* production Global Warming Potential (GWP) figure used of 4 g CO_2-eq MJ^{-1} from Hastings *et al*. (2017) does not include changes in soil carbon stocks or soil greenhouse gas fluxes, based on the premise that on average C would be sequestered or at worst maintained. However, when the cost of change in soil carbon (4 Mg C ha^{-1}, 5 g CO_2-eq MJ^{-1}, compared to a continued grassland counterfactual), along with the cost of soil N_2O emissions from land conversion (1 g CO_2-eq MJ^{-1}, Holder *et al*. 2019) were added to the original GWP, the resulting cost of producing a *Miscanthus* crop over a 15 year period (10 g CO_2-eq MJ^{-1} or 180 kg CO_2-eq Mg^{-1} DM) still remained far lower than estimates for producing energy from natural gas (59 g CO_2-eq MJ^{-1}), currently the highest consumed fossil fuel energy source (BEIS, 2018b), and coal (121 g CO_2-eq MJ^{-1}) (Hastings *et al*., 2017).

Whether the bioenergy crop itself should bear the greenhouse gas cost of land conversion at the beginning of the cropping cycle (Holder *et al*., 2019) or reversion at the end (McCalmont *et al*., 2018), or indeed both, is open to debate. It may also be the case that any losses in SOC are temporary depending on the land use change after *Miscanthus*, if for example the land is re-converted to a permanent pasture. As shown in McCalmont *et al*. (2018) soil N_2O emissions connected to cultivation disturbances are strongly driven by the legacy of the previous crop species, and losses or gains in soil carbon are also sensitive to the initial land condition (Qin *et al*., 2016; Richards *et al*., 2017) suggesting a case for LCA studies to attribute conversion period greenhouse gas emissions to the previous crop and incorporate projected reversion costs into the GWP balance of the current one.

3 Soil N_2O emissions with different reduced tillage methods during the establishment of *Miscanthus* in temperate grassland.

Amanda J. Holder[1], Jon P. McCalmont[2], Rebecca Rowe[3], Niall P. McNamara[3], Dafydd Elias[3] and Iain S. Donnison[1]

[1]Institute of Biological, Environmental and Rural Sciences (IBERS), Aberystwyth University, Gogerddan, Aberystwyth, Wales, SY23 3EQ, UK

[2]College of Life and Environmental Sciences, University of Exeter, Rennes Drive, Exeter, EX4 4RJ, UK

[3]Centre for Ecology & Hydrology, Lancaster Environment Centre, Library Avenue, Bailrigg, Lancaster, LA1 4AP, UK

Publication Note

This manuscript, under the same title, was accepted for publication in the peer reviewed journal Global Change Biology Bioenergy on 24 September 2018: GCB Bioenergy (2019) 11 (3) DOI: 10.1111/gcbb.12570.

3.1 Abstract

An increase in renewable energy and the planting of perennial bioenergy crops is expected in order to meet global greenhouse gas (GHG) targets. Nitrous oxide (N_2O) is a potent greenhouse gas, and this paper addresses a knowledge gap concerning soil N_2O emissions over the possible 'hotspot' of land-use conversion from established pasture to the biofuel crop *Miscanthus*. The work aims to quantify the impacts of this land use change on N_2O fluxes using three different cultivation methods. Three replicates of four treatments were established: *M. x giganteus* (*Mxg*) planted without tillage; *Mxg* planted with light tillage; a novel seed-based *Miscanthus* hybrid planted with light tillage under bio-degradable mulch film; and a control of un-cultivated established grass pasture with sheep grazing. Soil N_2O fluxes were recorded every two weeks using static chambers starting from pre-conversion in April 2016 and continuing until the end of October 2017. Monthly soil samples were also taken and analysed for nitrate and ammonium.

There was no significant difference in N_2O emissions between the different cultivation methods. However, in comparison to the un-cultivated pasture N_2O emissions from the cultivated *Miscanthus* plots were 550-819% higher in the first year (April to December 2016) and 469-485% higher in the second year (January to October 2017). When added to an estimated carbon cost for production over a 10 year crop life-time (including crop management, harvest, and transportation) the measured N_2O conversion cost of 4.13 Mg CO_2-eq. ha^{-1} represents a 44% increase in emission compared to the base case.

This paper clearly shows the need to incorporate N_2O fluxes during *Miscanthus* establishment into assessments of GHG balances and life-cycle analysis and

provides vital knowledge needed for this process. This work therefore also helps to support policy decisions regarding the costs and benefits of land use change to *Miscanthus*.

3.2 Introduction

Nitrous oxide (N_2O) is a potent atmospheric greenhouse gas (GHG), and agriculture is the largest contributor of N_2O to the atmosphere (Smith *et al*., 2008; Reay *et al*., 2012; IPCC, 2014). Soil management and tillage can impact on N_2O emissions via the addition of fertilizers, plant residues, and changes to soil structure. These interventions influence microbial activity and thereby N_2O emission through changes in water holding capacity, pore spaces, nutrient availability and temperature (Maag & Vinther, 1996; Dobbie & Smith, 2003; Smith *et al.*, 2003; Butterbach-Bahl *et al.*, 2013). Similar to conventional crops the establishment practices for perennial bioenergy crops such as *Miscanthus* and short rotation coppice also require weed control (normally via herbicide applications) and soil tillage during the cultivation. With little further soil disturbance or inputs during the crop's life-time this is a likely 'hotspot' for GHG emission. The planting of perennial bioenergy crops is expected to increase in order to meet global greenhouse gas emission targets (IPCC, 2014; Energy Technologies Institute, 2015), and therefore it is important that the establishment associated GHG impacts of land use change are understood.

To avoid competition with food, the use of economically marginal agricultural land (low grade and unprofitable) is preferred for biofuel crops (Lovett *et al*., 2009; Rathmann *et al*., 2010; Milner *et al*., 2016). Agricultural grasslands make up a third of the utilized agricultural area across Europe, with higher proportions in some member states (e.g. Ireland, UK, Slovenia and Luxemburg) and could represent a key land use for conversion (Eurostat, 2018b). With changes in the management of grazing animals (Taube *et al.*, 2014; Xue *et al.*, 2017), reduced profitability of grassland agriculture (Department for Environment Food & Rural Affairs (DEFRA), 2017a; Eurostat, 2018a), and uncertainly around agricultural policy reforms due to

changes in the Common Agricultural Policy (European Commission, 2017a), there is likely to be an increased interest in options for the diversification of grassland and especially more marginal grassland (Donnison & Fraser, 2016). Use of these lands for the growth of bioenergy crops including *Miscanthus* may be one option for this diversification, and could also play a role in reducing overall agricultural GHG emission.

The *Miscanthus* genus (Greef & Deuter, 1993) is a perennial grass biomass feedstock with the commercially available sterile clone *M. x giganteus* (*Mxg*) attractive for its rapid biomass production, low nitrogen input requirements and ability to be grown on poorer agricultural soils (Lewandowski *et al.*, 2000; Clifton-Brown *et al.*, 2015). *Mxg* is thought to be a natural hybrid of *M. sacchariflorus* and *M. sinensis* (Lewandowski *et al.*, 2000) and newer *Sacchariflorus x Sinensis* hybrids are also being developed for growth on marginal sites (Lewandowski *et al*., 2016; Nunn *et al*., 2017). However the impact on soil N_2O emissions during the time of conversion from grasslands to *Miscanthus* production are generally poorly studied and require attention to quantify the environmental sustainability of this crop.

Experiments to date on GHGs resulting from conversion to *Miscanthus* are centred around establishment into arable land rather than grassland, finding lower or similar levels of N_2O emissions compared to annual crops (Smith *et al*., 2013; Davis *et al*., 2015; Oates *et al*., 2016). In contrast there are no published studies documenting N_2O emissions over the actual conversion process to *Miscanthus* from a grazed grassland, revealing a significant knowledge gap (Harris *et al.*, 2015; Whitaker *et al*., 2018). Two studies have looked at N_2O emissions from *Miscanthus* established on grass but have only measured fluxes in crops during their second and third growing

seasons, and hence uncertainties remain about the flux levels that can be expected. Saha *et al*. (2017) measured N_2O in the second growing season for *Miscanthus* planted into grassland in various locations within a conservation area (in the USA) and found that N_2O fluxes were six times higher for *Miscanthus* compared to the grassland in some places, but similar to the existing grassland in others. Roth *et al*. (2013) measured N_2O fluxes in 2 and 14 year old *Miscanthus* (in Ireland) and compared this to established grassland (with a bi-annual cut) finding that although the fluxes were higher in the 2 year old *Miscanthus*, this was not significantly different to the grassland site. In a review of the research to date on land use change to bioenergy crops, Whitaker *et al.* (2018) also highlight the need for more work relating to grassland transitions to *Miscanthus* and planting methods that may reduce emissions.

Establishment options exist for *Miscanthus* and these could play a role in reducing the cultivation associated N_2O emissions. Reduced tillage methods involving either planting directly into the soil without any form of ploughing (no till) or minimum tillage (cultivation to a shallow depth generally not more than 10 cm) are generally recognised to have the benefits of reduced soil erosion and water runoff, and can lead to increases in soil organic matter and soil biological activity (Holland, 2004; Lal *et al*., 2007). However, the impact of no till cultivation on N_2O emissions can vary and seems to be linked to soil type and water content (Chatskikh & Olesen, 2007; Rochette, 2008; Grave *et al*., 2018). The use of a bio-degradable film mulch has shown improved agricultural and economic performance of *Miscanthus* by increasing shoot density during establishment in cool temperate climates through increased soil temperature and conservation of moisture (Olave *et al*., 2017; Ashman *et al*., 2018). Although not currently routinely employed with *Miscanthus*, the use of

this type of film may expand as an aid in establishment, with increasing use of lower agricultural grade land at higher altitudes (Lovett *et al*., 2009; Clifton-Brown *et al.*, 2011; Alexander *et al.*, 2014). Rapid commercial scaling of *Miscanthus* is also currently limited by the need for clonal propagation by rhizome so new inter-species seed-based hybrids are being developed to maximise production of the crop (Clifton-Brown *et al*., 2017; Lewandowski *et al*., 2016). These new varieties are now at the stage of large, pre-commercial trials across Europe in marginal soils and have been developed in tandem with these new mulch film based agronomies (GRACE, n.d.).

In this work we address both the N_2O impacts of *Miscanthus* establishment on marginal upland semi-improved grassland, and the potential for different establishment methods to mitigate these. We compare the soil N_2O emission during the cultivation and first two growing seasons of *M. x giganteus* and a novel *Miscanthus* hybrid planted using three different low soil disturbance methods. The trial site was at a higher altitude than generally used commercially for growing *Miscanthus* and was chosen as being representative of the kind of poorer quality semi-improved grassland that is likely to be most in need of diversification opportunities under growing economic pressures.

The *Miscanthus* hybrid chosen (OPM-10) was selected from a range of new seed-based hybrids previously tested in multi-location trials across Europe (Lewandowski *et al*., 2016; Nunn *et al*., 2017). This particular hybrid (*Sacchariflorus x Sinensis*) has previously shown strong resilience in cooler environmental conditions and was thought likely to be suitable for these upland sites. This study has two main aims: firstly to compare soil N_2O emissions between an established grazed pasture and the initial cultivation, planting and first two growing seasons of *Miscanthus;* and

secondly to assess impacts on, and potential drivers of soil N_2O emissions in different reduced tillage methods (no till, minimum till, and minimum till with the addition of a film mulch layer). To check establishment with the different cultivation methods, over-winter survivorship is also considered.

3.3 Materials and methods

3.3.1 Location and experimental plots

The experimental site is located near Cwmystwyth, Wales, UK (52.349 °N 3.806 °W) and is approximately 250 m a.s.l. on a 1:10 east facing slope. Formed over bedrock of interbedded mudstone/sandstone the soil texture is a clay loam/silty clay loam with a pH of 5. Field capacity was calculated to be approximately 38% volumetric water content following the methodology in Saxton & Rawls (2006). The land has been used for cattle/sheep grazing and silage crops for at least the last 25 years. No fertilizer or lime has been used since 2006 and since then the field has been used for extensive sheep grazing. An in-field weather station (MiniMet Automatic, Skye Instruments Ltd, UK and Delta-T RG-2 rain gauge, UK) recorded a total rainfall of 1049 mm from June to December 2016, and 2158 mm for January to December 2017. The precipitation recorded was within the normal range for upland grassland in the UK (2000-3000 mm yr^{-1}), but very wet compared to the UK national annual average of 1154 mm (Met Office, n.d.b). Air temperatures ranged from -4°C to 30°C over the two year period. The average minimum and maximum air temperatures (2 and 19.3°C respectively) were slightly cooler and warmer than the UK 30 year average of 5.3 and 12.4°C (Met Office, n.d.b).

Twelve plots of 7 m x 7 m, were established in April 2016 using a randomised block design (Figure 10).

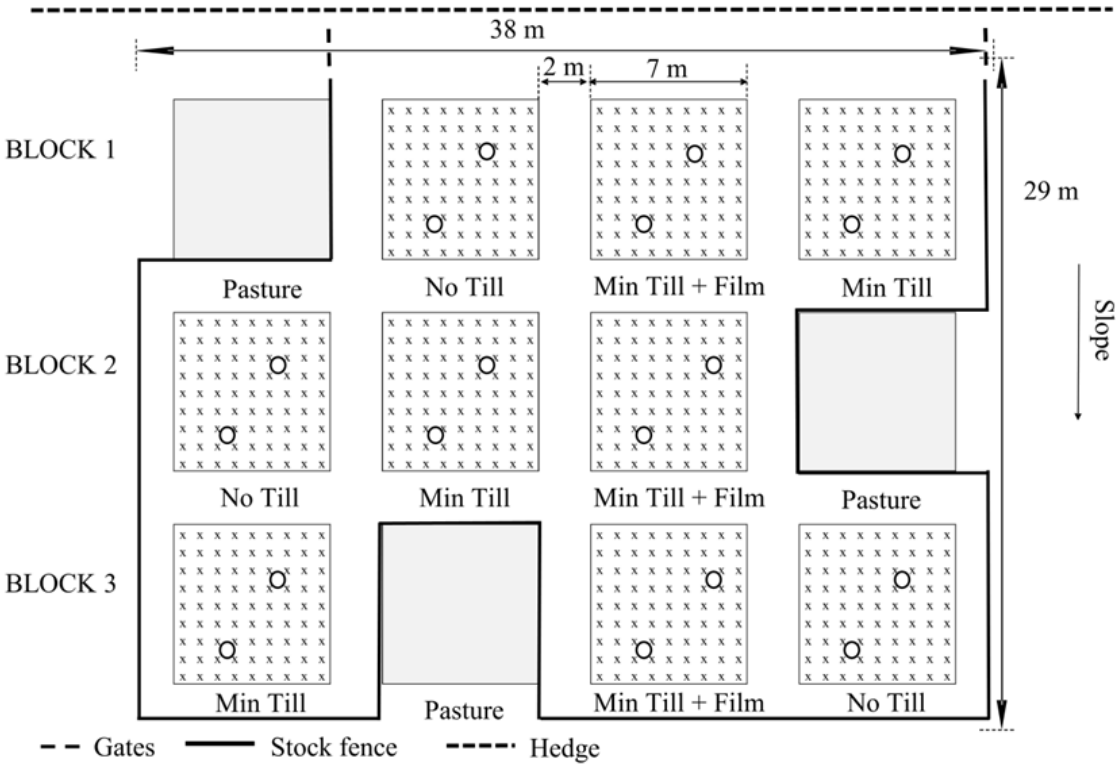

Figure 10 Plan of the experimental plot layout. 'x' represents the planting positions and the circles represent locations of the static chamber collars. Each block contains a plot of existing undisturbed pasture (Pasture) and each of the three treatments: *M. x giganteus* rhizomes slot planted (No Till); *M. x giganteus* rhizomes planted with a minimum till method (Min Till); and *Miscanthus* hybrid OPM-10 planted with a minimum till method and covered with a clear bio-degradable film (Min Till + Film).

The following treatments were included in each block: *M. x giganteus* (*Mxg*) planted via a no tillage method (No Till); *Mxg* planted via minimum tillage (Min Till); *Miscanthus* hybrid (OPM-10) planted via minimum tillage and under a film layer (Min Till + Film); and an untreated plot of existing grass pasture (Pasture). Fencing allowed continuation of extensive sheep grazing on the pasture plots (Figure 10). Cultivation began on 14 April 2016 when all except the pasture plots were sprayed with glyphosate (1.5 kg ha^{-1}) to kill off existing vegetation. Planting of the *Miscanthus* plots took place on 13 May 2016 at a density of ~1.6 plants m^{-2} (81

plants per 49 m^{-2} plot). The No Till plots were slot planted with *Mxg* rhizomes by hand. The Min Till plots were rotavated to a depth of approximately 10 cm using a small tractor and rotavator. Three of the rotavated plots were planted by hand with *Mxg* rhizomes and the other three were planted by hand with OPM-10 as tissue cultured plug plants (plug size 4 cm x 4 cm x 8 cm). The OPM-10 plants were then covered with a clear bio-degradable maize film layer (Samco 'Grey', pin hole 20 aeration, Samco Agricultural Manufacturing Ltd, Limerick, Ireland) (Figure 11).

Figure 11 The bio-degradable maize film layer being laid over the newly planted *Miscanthus* OPM-10 hybrid plug plants on 13 May 2016.

Each sheet of film covered two rows together which left one row in each plot uncovered. The film layer had mostly degraded after a month when the remainder was removed. In July 2016 any plants that had failed to establish were replaced with the appropriate *Mxg* rhizome or OPM-10 plug.

3.3.2 Sampling of N_2O soil emissions

Fortnightly static chamber gas sampling following the methods in Parkin & Venterea (2010) and Collier *et al*. (2014) began on 12 April 2016 and continued until 24 October 2017 (41 occasions). Two chamber collars, each covering an area of 0.12 m^2 were inserted into the ground of each plot (Figure 10) to a depth of 5-6 cm. Collars

were removed for cultivation, but otherwise remained in place throughout the study. In the Min Till + Film plots, holes to match the area of the collars were made in the mulch film to allow re-insertion.

Equipment and sampling methodology followed those in McCalmont *et al.* (2018). On each sampling occasion chamber lids (area 0.0251 m^3) with an external reflective surface and butyl rubber septum were attached to the collars with spring clamps. Every sampling event commenced with Block 1 between 10 and 11 am (Alves *et al*., 2012), all treatments within the block were sampled at four time series before moving to the next block. 10 ml gas samples from each chamber were taken at 0, 15, 30 and 45 minute intervals and injected into pre-evacuated 3 ml glass vials sealed with rubber septa (Labco, Lampeter, UK). Concurrent chamber level air temperature was taken with a temperature probe (Testo 104, Testo Ltd. Hampshire, UK). Soil volumetric water content (ML3 soil moisture probe, Delta-T Devices, Cambridge, UK, calibrated to the specific field soil) and soil temperature measurements (Testo 104, Testo Ltd, Hampshire, UK) were taken from within 1 m of each chamber using 10 cm hand held probes.

N_2O concentrations were determined by gas chromatography (Perkin Elmer Autosystem XL Gas Chromatograph, USA) and the N_2O fluxes were calculated using R version 3.2.3 (R Core Team, 2015) package 'flux' v3.0-0 (Jurasinski *et al*., 2014).

3.3.3 Soil sampling

Pre-cultivation soil samples were taken in April 2016, followed by regular monthly soil samples (one from each plot) to a depth of 30 cm from June 2016 until October 2017. Samples were taken using a 4.8 cm internal diameter split tube soil auger

(Eijkelkamp Agrisearch Equipment BV, Giesbeek, The Netherlands) and separated into 0-15 cm and 15-30 cm depths. Soil cores were sub-sampled for use in different analyses.

Fresh sub-samples (5 g), used to assess nutrient availability, were mixed on a shaking table with 25 ml 1 M solution of KCl (potassium chloride) and then filtered (150 mm diameter hardened ashless filter papers, Whatman, UK) into 250 ml sterilin bottles and frozen at -20 °C. The samples were later defrosted and analysed for nitrate (NO_3^-) and ammonium (NH_4^+) using continuous flow colorimetry with an AA3 HR AutoAnalyser (SEAL Analytical Ltd, Southampton, UK).

Bulk densities for the two depths were calculated (following the method outlined in Emmett *et al*., 2008) for the samples taken in April 2016, June 2016, March 2017, and July 2017 to account for changes occurring due to the tillage.

Gravimetric moisture was calculated from oven drying sub-samples to constant weight (at 105°C) and then converted to volumetric water content using the bulk density measurement.

3.3.4 Global Warming Potential

To assess the impacts of cultivation driven N_2O fluxes on previous estimates of the Global Warming Potential (GWP) costs per ha of biomass production (Hastings *et al* 2017), the total sum of the N_2O fluxes for each of the cultivation methods was converted to CO_2 equivalent (CO_2-eq) and put into the context of a simulated 10 year crop life-time.

Daily N_2O totals were created by multiplying the mean hourly fluxes (mg N_2O m^{-2} hr^{-1}) by 24 and converting to Mg ha^{-1} [11]. Linear interpolation was used to fill in the gaps between the 41 fortnightly values and results for each treatment were summed to a total flux following the method in McCalmont *et al*. (2018). Finally totals were converted to CO_2-eq using IPCC (2007) conversion factor of 298[12].

Carbon intensity of producing biomass (including crop management, harvest, transport and fuel preparation) over the lifetime of the crop was based on value of 4.40 g CO_2-eq MJ^{-1} (Hastings *et al.*, 2017). This was converted to Mg CO_2-eq ha^{-1} using yield estimate of 12 Mg DM ha^{-1} yr^{-1}, or 120 Mg DM ha^{-1} for the full 10 year period (Larsen *et al*., 2014). Whilst yields can vary and are typically reduced at the start and end of a crops' life-time, the figure used is taken as a representative mean for the 10 year timespan, being at the lower end of a range of reported mean yields (Clifton-Brown *et al.*, 2004; Larsen *et al.*, 2014; McCalmont *et al*., 2018). The energy content used was 17.95 GJ Mg^{-1} DM (Felten *et al*., 2013).

3.3.5 Statistical analysis

Data was analysed using R version 3.2.3 (R Core Team, 2015). Cumulative N_2O fluxes and over winter plant survivorship were tested using ANOVA and Tukey HSD post-hoc tests with tillage (cultivation method) as the fixed factor and the random effect of block. Baseline fluxes (recorded on 12 April 2016) were compared with fluxes on 11 April 2017 using ANOVA with sample date and tillage as the fixed factors, the random effect of block, and a cube transformation to improve model residuals. As the two growing seasons represented very different stages in the establishment, N_2O fluxes for the two seasons were tested separately and statistics

[11] See Appendix A4.2.
[12] See Appendix A4.3.

were carried out on cube transformed data. To explore potential drivers of N_2O emissions Akaike's information criterion (AIC) was used for selection of linear models with the random effects of block and sample date and fixed factors of: tillage; NO_3^- and NH_4^+ (each to a depth of 15 cm); air temperature; soil temperature (0-10 cm depth); and water filled pore space; with fixed factor selection restricted to avoid co-correlated factors (air and soil temperature) within a single model (R packages 'nlme', Pinheiro *et al*., 2017; and 'MuMIn', Barton, 2018). In addition impacts of tillage method on these drivers was explored using ANOVA and Tukey HSD post hoc tests using tillage method as a fixed factor and the random effect of block and sample date.

3.4 Results

3.4.1 Establishment

In the OPM-10 plots 15% of the hybrids planted under film failed to establish after the initial planting whereas all of the hybrid plants (100%) that were outside of the film failed. Across all the *Mxg* plots, 33% of the No Till treatment and 29% of the Min Till treatment failed to establish. All gaps were replaced in July 2016 and the survivorship after the first winter was 87% for the hybrid plants, 83% for the No Till treatment, and 78% for the Min Till treatment. There was no significant difference in the survivorship between the different treatments ($F_{2, 5} = 3.96$, $p = 0.09$).

3.4.2 N_2O fluxes

N_2O spikes were observed in all the *Miscanthus* plots compared to the pasture control, regardless of tillage method (Figure 12a). However, whilst cumulative N_2O fluxes over the 18 month period were higher under *Miscanthus* cultivation compared to the retained grassland controls ($F_{3, 7} = 8.51$, $p = 0.01$) post-hoc testing confirmed no significant difference in fluxes between the tillage methods for the *Miscanthus* (Figure 13).

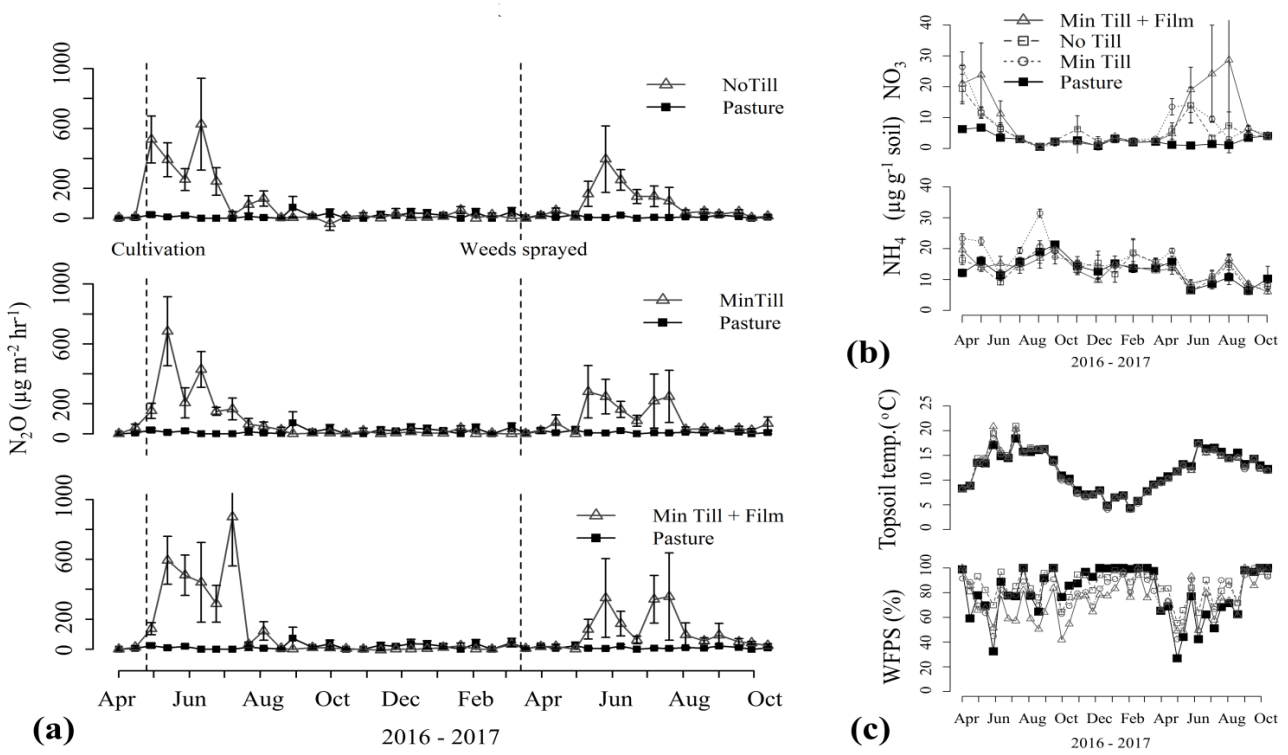

Figure 12 (a) Mean N_2O flux over the sampling period (12 April 2016 to 24 October 2017) for the no tillage (No Till), minimum tillage (Min Till) and minimum tillage with film (Min Till + Film) treatment in comparison to the established pasture control (Pasture). The dotted lines show the time of cultivation in 2016 and the herbicide sprayed in 2017. **(b)** Mean levels of NO_3^- and NH_4^+ in soil samples (0-15 cm depth) taken monthly from June 2016 to October 2017. **(c)** The mean soil temperature (0-10 cm depth) and water filled pore space (WFPS) (0-15 cm depth) across the treatments. The error bars in all the charts show the standard error of the mean.

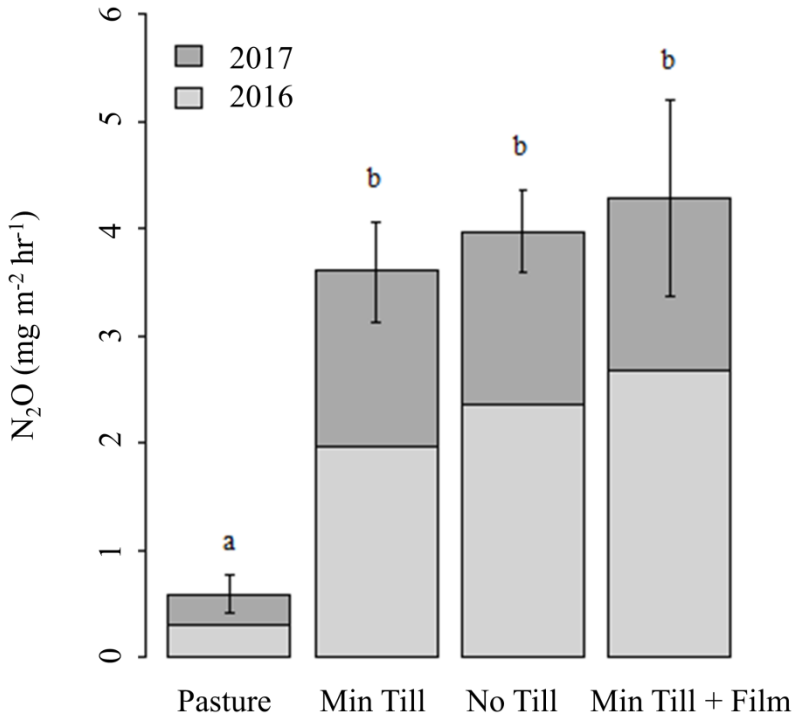

Figure 13 Mean cumulative N_2O flux from 12 April 2016 to 24 October 2017. Error bars show standard error of the mean. The same letter indicates non-significant difference based on post hoc testing of the significant main effect of treatment.

Gas samples taken on 11 April 2017 from all the treatments and control showed a higher N_2O flux ($F_{1,14}$ = 13.83 p = 0.00) than was recorded in the pre-conversion baseline samples taken on 12 April 2016. However, fluxes were low in both instances (Figure 12a). On 11 April 2016 there was a zero flux rate in all the designated treatments (pre-conversion) with the exception of the No Till treatment, where a mean flux of 0.01 mg N_2O m^{-2} hr^{-1} was recorded. A year later (12 April 2017) mean fluxes ranged from 0.01 to 0.03 mg N_2O m^{-2} hr^{-1}. There was no significant difference between the treatments at either of these time points.

The highest N_2O peak recorded over the period (882.9 µg m^{-2} hr^{-1} on 19 July 2016) was seen in the Min Till + Film plots in the first growing season. The highest peak

flux rates (μg N_2O m^{-2} hr^{-1}) recorded for the other treatments were: Min Till 684.22 on 24 May 2016; No Till 628.10 on 22 June 2016; and Pasture 73.13 on 9 September 2016, again all in the first growing season. Flux rates reduced over the winter months but increased again in the tillage plots during the second growing season (Figure 12).

3.4.3 N_2O drivers

Temperature and nutrient levels varied with season and between plots (Figure 12b, 12c). Model selection was conducted on each growing season separately but the same combination of drivers in each season achieved the closest fit with R^2 (marginal) values of 0.40 for the 2016 season and 0.39 for the 2017 season. The best combination of fixed factors for both growing seasons suggests that N_2O fluxes were positively driven by NO_3^- (0-15 cm depth) and soil temperature (0-10 cm depth), as well as tillage (equation 8, asterisks denote interactions between the factors):

$$NO_3^- + soil\ temperature + tillage + NO_3^- * soil\ temperature + NO_3^- * tillage + 1 \quad (8)$$

Reflecting model selection, differences were found in soil temperature and NO_3^- levels between the treatments in both growing seasons. The Min Till + Film and No Till treatments had higher soil temperatures than the Pasture ($F_{3, 115} = 3.97$, $p = 0.03$) for the first growing season. However for the second season, when differences are more apparent in plant morphology between *Miscanthus* and the Pasture grass, all the cultivated treatments had lower soil temperatures than the Pasture ($F_{3, 125} = 22.61$, $p<0.001$). Differences were also found in levels of NO_3^- in treatments with extra disturbance and the addition of the film layer. In the first growing season the Min Till + Film treatment had higher levels of NO_3^- than the Pasture ($F_{3, 115} = 4.13$, $p< 0.001$). This trend was also found in the second season where the Min Till + Film

treatment had the highest levels compared to all the other treatments (including Pasture). In addition the Min Till treatment was also higher than the Pasture ($F_{3, 125}$ = 10.54, $p<0.001$). Although the potential driver of water filled pore space was not selected for in the best model combination, the Min Till + Film treatment was drier than all the other treatments during the first growing season ($F_{3, 115}$ = 12.02, $p<0.001$). However, this was not observed in the second season where the Pasture was drier than the No Till and Min Till treatments, although the Min Till + Film treatment was drier than the No Till treatment ($F_{3, 125}$ = 9.39 $p<0.001$). All the plots were above field capacity for the majority of the sampling period.

3.4.4 Global Warming Potential

The N_2O emission resulting from cultivation (differences from grassland control) equated to a GWP (Mg CO_2-eq ha^{-1}) of 3.91 ±0.13 for the No Till treatment, 3.57 ±0.12 for the Min Till treatment and 4.90 ±0.18 for the Min Till + Film treatment. The carbon cost of biomass production for *Miscanthus* over a 10 year crop life-time was estimated as 9.49 Mg CO_2-eq ha^{-1}. When the mean N_2O land-use conversion cost of 4.13 Mg CO_2-eq ha^{-1} is added to the life-time cost of production the overall cost of 13.62 Mg CO_2-eq ha^{-1} represents an increase of 44%.

3.5 Discussion

This study highlights that regardless of cultivation method the establishment of *Miscanthus* on grassland is associated with increased N_2O fluxes compared to un-cultivated, unfertilised pasture. There are no other studies capturing fluxes during the initial cultivation for *Miscanthus* but studies of grassland tillage for reseeding do show similar flux levels to those we recorded in the *Miscanthus* cultivation (Drewer *et al*., 2017). This suggests that it may be the land disturbance itself and the residues of the previous crop rather than the following crop that is driving these increased emissions. The N_2O fluxes from the retained pasture in this study were also similar to mean fluxes found across a number of European grazed and fertilized grasslands (Flechard *et al*., 2007).

N_2O emissions have been considered to be a small part of the overall GHG balance in established plantations, with highest reported values (excluding cultivation/conversion) contributing 6% of total GHG balances (Dondini *et al.*, 2016a; Robertson *et al*., 2017). Our study shows that the land-use conversion cost of N_2O (4.13 Mg CO_2-eq. ha^{-1}) represented approximately 30% of the total CO_2-eq. cost of producing the energy in the crop over 10 years (13.62 Mg CO_2-eq ha^{-1}). Whilst more studies are needed to understand potential impact over a wider range of sites (and soil types) this work does clearly show the importance of taking this initial increase in N_2O into account when calculating GHG balances relating to land use change. However, it should be noted that this is a one off cost and the relative magnitude of its impact per unit of energy produced by the crop reduces in the long run. Yield predictions suggest that the life-span of a commercial *Miscanthus* crop could be around 15 years depending on site conditions (Clifton-Brown *et al.*, 2015). Even including the carbon cost of the increased N_2O fluxes during land conversion

from grassland to *Miscanthus* the GWP of the energy produced over a 10 year crop lifetime (6 g CO_2-eq MJ^{-1}) is lower than estimates for producing energy from coal (121 g CO_2-eq MJ^{-1}) and natural gas (59 g CO_2-eq MJ^{-1}) (Hastings *et al*., 2017).

The initial soil N_2O fluxes we recorded are in line with the prediction made by Roth *et al*. (2013) who suggested that fluxes may be higher during earlier stages of cultivation than from under 7 month old *Miscanthus*. However, while they found no significant difference between pasture N_2O emissions and *Miscanthus* our results did show a significant difference and higher peak flux rates. The deeper plough depth in Roth *et al*. (2013) may have had an impact, allowing more time for N_2O to be reduced to N_2 before reaching the surface (Baggs *et al.*, 2000), but higher fluxes are just as likely to be the result of different edaphic and climatic site conditions. The water filled pore space in our study was in the optimum range for N_2O emissions (~80%) (Maag & Vinther, 1996; Butterbach-Bahl *et al*., 2013) and rainfall at the site was above the UK national average which may in part have also contributed to the higher fluxes and highlights the need for more work across a range of climatic conditions.

Whilst N_2O fluxes can vary between years (Jorgensen *et al*., 1997; Drewer *et al.*, 2012) the trend for a reduction in the second year after establishment seen in this experiment (despite higher second year early season fluxes) is in line with Roth *et al*. (2013), and fits with the generally low fluxes reported for mature *Miscanthus* plantations in studies by Gauder *et al*. (2012) and Drewer *et al*. (2012). This suggests that fluxes in mature crops are likely to be lower than those recorded here for the conversion period, a point also noted in review by Whitaker *et al*. (2018).

Models predicted around 40% of the variance, values higher than those reported by Roth *et al.* (2013), where only 27% of fluxes could be explained by a large number of factors and Gauder *et al*. (2012) where soil temperature explained less than 10%. N_2O fluxes are known to be volatile so higher frequency monitoring of N_2O fluxes (in this study once every two weeks) with chambers, or continuous monitoring with the capture of larger ground areas via eddy covariance methods may reveal more about N_2O drivers (Jones *et al.*, 2011; Alves *et al*., 2012). The limited spatial nature of the chambers may be a reason that an effect of periods of grazing was not seen in the N_2O emissions. However, the plots were extensively grazed and Flechard *et al*. (2007) found that while grazing tended to increase N_2O emissions the effect was not clear and more noticeable only on fields that were also artificially fertilized.

Model selection showed NO_3^- and soil temperature as well as tillage to be significant in predicting fluxes. The use of herbicide to control weeds (used during initial cultivation and in mid-March of the second year) provided plant material with the likely effect of stimulating microbial activity through increased carbon and substrate for nitrification/denitrification (Baggs *et al*., 2000; Huang *et al.*, 2004; Palmer *et al*., 2014). The significant increases in N_2O we found following cultivation suggest that methods of planting that enable establishment with reduced herbicide use could provide benefits of reduced N_2O emissions. For example, Xue *et al*. (2017) proposed a method where only small strips of grassland (rather than the entire planting area) are sprayed with herbicide to enable the slot planting of *Miscanthus*. This aims to reduce immediate competition from weeds but also allow continued grassland productivity in the early years of *Miscanthus* establishment. This may provide early season opportunities for grazing prior to the *Miscanthus* shoot emergence in late April/early May.

Fluxes were higher in April 2017 across all the treatments and control compared to the pre-conversion rates recorded in April 2016 and this early season increase is likely to be related to the slightly higher soil temperature in April 2017. Soil and air temperature also have known links to N_2O fluxes, often influencing processes that result in a 'multiplier effect' on emissions (Butterbach-Bahl *et al.*, 2013); therefore the higher temperatures found in the Min Till + Film and No Till treatments (compared to the Pasture) could have had a disproportionate impact on N_2O emissions. However, despite concerns that the use of a film layer can increase N_2O emissions (Nishimura *et al.*, 2012; Cuello *et al.*, 2015) we found that although the film layer did increase soil temperature and NO_3^- levels and reduce soil moisture, this did not create significantly higher N_2O emissions compared to the other tillage methods. The film layer also proved to be beneficial for establishment which would therefore contribute to better future yields and hence reductions in yield scaled emissions (Kim *et al.*, 2017; Olave *et al.*, 2017).

It was expected that the Min Till treatment would aid establishment and over-winter survivorship compared to the No Till treatment by de-compacting the soil and allowing easier rhizome/root growth, however, there was no significant difference in the over-winter survivorship between the treatments. Overall survivorship at this upland site (at around 70%) was lower than has been recorded in a nearby lower altitude site (89% at 100 m a.s.l., McCalmont *et al.*, 2017b) so it is possible that impacts of tillage were masked by site conditions. However, there are other benefits from no till planting to be considered, such as reduced soil erosion and the retention of soil organic matter (Holland, 2004; Lal *et al.*, 2007). Whilst no till cultivation can sometimes increase N_2O emissions compared to conventional tillage in wet and

poorly aerated soils (Rochette, 2008; Grave *et al*., 2018), we found no significant difference between the low impact cultivation methods tested.

Although there were increased N_2O emissions from land use change to *Miscanthus* due to the cultivation of the soil, this is to be expected in the planting of any new crop requiring the killing off of a previous crop and subsequent soil disturbance. There was a clear reduction in emissions over the second growing season suggesting that the higher fluxes (compared to uncultivated pasture) are not likely to last in the long term. The use of the mulch film did not significantly increase N_2O emissions compared to the other tillage methods tested suggesting that its benefit in extending the possibilities for *Miscanthus* to be grown on agriculturally marginal land does not come at an increased N_2O cost.

4 Soil CH_4 emissions with different reduced tillage methods during the establishment of *Miscanthus* in temperate grassland.

4.1 Introduction

Results from the static chamber sampling conducted in Chapter 3 were also analysed for carbon dioxide (CO_2) and methane (CH_4) as well as nitrous oxide (N_2O). The CO_2 levels recorded were used as a basis for quality control of the biweekly samples indicating, for example, any problems with leaking chambers or vials.

CH_4 soil and enteric emissions form an important part of the greenhouse gas budget for grazed pasture systems (IPCC 2006) and are included as key indicators within the agricultural sector used to check progress towards meeting the UK governments target of net zero emissions by 2050 (CCC 2019). The soil CH_4 emissions results recorded from the static chambers for the land use change and continued grazed grassland plots are therefore shown here (please see Chapter 3 for a description of the experimental site and methods used).

4.2 Results

The CH_4 results are presented below (Table 8 and Figure 14), and show the low soil emissions recorded at the site. Each of the cultivation plots resulted in a CH_4 sink when calculated over the first year (April to April).

Table 8 Weight of CH_4 emission from the experimental site in Chapter 3, calculated from April 2016 to April 2017 using linear interpolation between sampling points.

Treatment	CH_4 (kg ha^{-1} yr^{-1})
Pasture	0.5
No Till	-0.2
Min Till	-0.4
Min Till + Film	-1.1

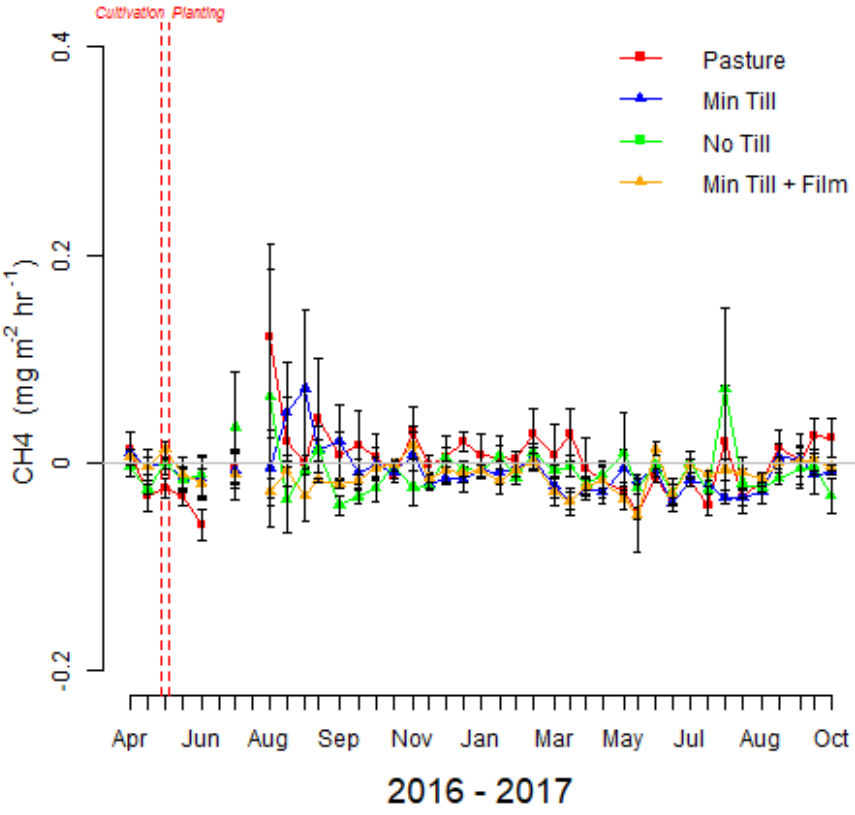

Figure 14 Mean methane flux recorded using static chambers comparing plots of *Miscanthus* planted with no tillage (Min Till), *Miscanthus* planted with no tillage (No Till), a novel *Miscanthus* hybrid planted with minimum tillage under a mulch film layer (Min Till + Film), and an uncultivated pasture control (Pasture), as detailed in Chapter 3. The gaps in the data relate to issues with the gas chromatography machine. Error bars show the standard error.

4.3 Discussion

CH_4 fluxes from temperate agricultural soils are generally low in relation to CO_2 and N_2O (Drewer *et al*., 2012; Gauder *et al*., 2012; Robertson *et al*., 2017), and this was also the case at this site with the highest value of 0.5 kg CH_4 ha^{-1} yr^{-1} coming from the uncultivated grassland control. Over the establishment year (April to April) the cultivated plots did not have higher CH_4 emissions than the uncultivated grassland control and CH_4 levels were similar to those recorded from an established *Miscanthus* site at a different UK location of 0.51 kg CH_4 ha^{-1} yr^{-1} (Robertson *et al*., 2017).

It should also be considered that in a land use change scenario from grazed grassland to *Miscanthus*, there would also be a reduction in eneteric CH_4 emissions due to the land no longer being grazed. For comparison the eneteric CH_4 emission factor from an intensively grazed sheep pasture in a similar location (Scotland, UK) was calculated to be 7.4 kg CH_4 $sheep^{-1}$ yr^{-1} (Dengel *et al*., 2011), and the IPCC emission factor for sheep grazed pasture in developed countries is 8 kg CH_4 $sheep^{-1}$ yr^{-1} (IPCC 2006).

5 Evapotranspiration model comparison and an estimate of field scale *Miscanthus* canopy precipitation interception.

Amanda J. Holder[1], Jon P. McCalmont[1], Niall P. McNamara[2], Rebecca Rowe[2] and Iain S. Donnison[1]

[1]Institute of Biological, Environmental and Rural Sciences (IBERS), Aberystwyth University, Gogerddan, Aberystwyth, Wales, SY23 3EQ, UK

[2]Centre for Ecology & Hydrology, Lancaster Environment Centre, Library Avenue, Bailrigg, Lancaster, LA1 4AP, UK

Publication Notes

This manuscript, under the same title, was accepted for publication in the peer reviewed journal Global Change Biology Bioenergy on 13 January 2018: GCB Bioenergy (2018) 10, 353–366, DOI: 10.1111/gcbb.12503

5.1 Abstract

The bioenergy crop *M. x giganteus* has a high water demand to quickly increase biomass with rapid canopy closure and effective rainfall interception, traits that are likely to impact on hydrology in land use change. Evapotranspiration (ET, the combination of plant and ground surface transpiration and evaporation) forms an important part of the water balance and few ET models have been tested with *Miscanthus*. Therefore this study uses field measurements to determine the most accurate ET model and to establish the interception of precipitation by the canopy (C_i).

Daily ET estimates from 2012 to 2016 using the Hargreaves-Samani, Priestley-Taylor, Granger-Gray and Penman-Monteith (short grass) models were calculated using data from a weather station situated in a 6 ha *Miscanthus* crop. Results from these models were compared to data from on-site eddy covariance (EC) instrumentation to determine accuracy and calculate the crop coefficient (K_c) model parameter. C_i was measured from June 2016 to March 2017 using stem-flow and through-flow gauges within the crop and rain gauges outside the crop.

The closest estimated ET to the EC data was the Penman-Monteith (short grass) model. The K_c values proposed are 0.63 for the early season (March and April), 0.85 for the main growing season (May to September), 1.57 for the late growing season (October and November), and 1.12 over the winter (December to February). These more accurate K_c values will enable better ET estimates with the use of the Penman-Monteith (short grass) model improving estimates of potential yields and hydrological impacts of land use change. C_i was 24% and remained high during the

autumn and winter thereby sustaining significant levels of canopy evaporation and suggesting benefits for winter flood mitigation.

5.2 Introduction

The planting of perennial bioenergy crops is expected to grow following an increased focus on renewable energy generation in order to meet global greenhouse gas emission targets (IPCC, 2014; Energy Technologies Institute (ETI), 2015). Adaptations to changes in climate are also being considered as it is now anticipated that some of the predicted impacts of climate change are unavoidable (IPCC, 2007; IPCC, 2014). In the UK repeated flooding events have stimulated interest in identifying mitigation strategies and have highlighted the potential role for farmland and upland areas for buffering against high rainfall (Marshall *et al*., 2009; Christen & Dalgaard, 2013; Wynne-Jones, 2016). This need is leading to an interest in finding commercially viable climate change resilient crops (Environment Agency, 2015) that can be located within these landscapes to provide wide ranging environmental benefits. *M. x giganteus* Greef et Deu (Greef & Deuter, 1993) is a low input biomass feedstock that, beyond simply burning in power stations, is also marketable in the bio-refining industry (producing liquid fuels and chemicals) and as animal bedding (Brosse *et al*., 2012; Van Weyenberg *et al.*, 2015).

The current commercial clone, *M. x giganteus* (hereafter *Miscanthus*) is a tall growing (up to ~3 m) sterile perennial grass hybrid with an efficient C_4 photosynthetic pathway. Requiring few agricultural inputs, it has the potential to grow on poorer soils (Lewandowski *et al.*, 2000; Hastings *et al.*, 2008; Lovett *et al.*, 2009; Cadoux *et al*., 2012). *Miscanthus* has limited stomatal control, a high water demand used to quickly increase biomass, and rapid canopy closure with a large leaf area index providing effective rainfall interception (Clifton-Brown *et al.*, 2002; Joo *et al.*, 2017). The site specific impacts of land use change to *Miscanthus* on water balances vary depending on factors including altitude, climate, and stage of crop

maturity (Dunkerley, 2000; Stephens *et al*., 2001). Increased planting of *Miscanthus* could potentially increase evapotranspiration (ET) and affect ecosystem water dynamics through impacts on boundary layer temperatures, humidity, and solar radiation to the ground (Hickman *et al.*, 2010; Milner *et al*., 2016). However, these traits may also reduce flooding, soil erosion and nutrient runoff. Information regarding these potential impacts is vital for accurate modelling of land use change scenarios in order to fully inform policy-makers.

ET is mainly estimated using models due to the cost of equipment and time consuming nature of field studies. A number of models can be used to calculate estimates of actual ET (ET_a, evaporation from all surfaces under natural conditions), potential ET (ET_p, the ET rate where there is no shortfall in soil water for vegetation use) and reference crop ET (ET_o, ET_p from a specific reference crop type (e.g. short grass) with no water shortage) (Allen *et al.*, 1998; Xu & Chen, 2005; McMahon *et al.*, 2013).

Different models require varying levels of data and have different approaches to the basis of the calculations and the impacts of these differences for the prediction of ET rates for a novel crop like *Miscanthus* are not clear. The Hargreaves-Samani (HS, Hargreaves & Samani, 1985) model is based on air temperature, Priestley-Taylor (PT, Priestley & Taylor, 1972) on solar radiation, and the Granger-Gray (GG, Granger & Gray, 1989) model uses a complementary relationship where land and atmosphere feedbacks lead to a mutual dependency between ET_a and ET_p (Bouchet, 1963; Morton, 1965). The simplified Penman-Monteith model (PMgrass, Allen *et al*., 1998) uses net incoming radiation and atmospheric and surface resistance terms to provide an estimate of ET_o for a reference short green crop. PMgrass results can

be further adapted to provide estimates of ET for a specific crop type (ET_c) with the use of a crop coefficient value (K_c) (Allen *et al.*, 1998).

To our knowledge there are no published studies comparing different ET models with a *Miscanthus* crop. The PMgrass model in conjunction with K_c values has been used for *Miscanthus* plants by Beale *et al*. (1999) in a water-use efficiency study, and by Triana *et al.* (2015) and Liu *et al.* (2014) in water-balance studies. K_c values reported for *Miscanthus* range from 0.31 to 1.20 (Beale *et al.,* 1999; Stephens *et al*., 2001; Triana *et al*., 2015), based on data obtained from locations with different climates, and do not always include the full *Miscanthus* growing season. Hydrology models incorporating ET have also been used to model land use change to *Miscanthus*: Stephens *et al.* (2001) and Borek *et al.* (2010) used the WaSim model (calculating ET using PMgrass with the option of K_c values); Finch *et al.* (2004) the Met. Office Surface Energy Scheme (MOSES) model; Vanloocke *et al.* (2010) the Agro-IBIS model; and Cibin, *et al.* (2016) the Soil & Water Assessment Tool (SWAT) model. The SWAT model can calculate ET_p via the Penman-Monteith equation (Monteith 1965), PT or HS methods (SWAT, n.d.). Only Stephens *et al.* (2001) and Finch *et al.* (2004) model hydrology for *Miscanthus* in a UK climate type. Simulations by Stephens *et al.* (2001) show reductions in runoff and groundwater recharge under *Miscanthus* compared to grass, whereas simulations by Finch *et al.* (2004) show *Miscanthus* having lower water use than grass, whilst pointing out that measurements over a full year are required to confirm this. More crop specific measurements for energy grasses are required to provide accurate estimates of ET and validate model predictions (Stephens *et al.,* 2001; Finch *et al*., 2004; Vanloocke *et al.*, 2010; McCalmont *et al.*, 2017a). Of the few studies that have measured ET for *Miscanthus*, Finch *et al.* (2004) recorded growing season

highs of ~5 mm day^{-1} with eddy covariance (EC) equipment, Hickman *et al.* (2010) measured highs of ~7 mm day^{-1} using a residual energy balance approach and Triana *et al.* (2015) report a maximum 11 mm day^{-1} using lysimeters.

Knowledge of the accuracy of commonly used ET formulae is not only of use in modelling the hydrological impacts of land use change but will also be of benefit in the modelling of potential yields and other environmental impacts such as greenhouse gas emissions where models require ET_p as an input (Richter *et al.*, 2008; Hastings *et al.*, 2009; Dondini *et al.*, 2016b).

In addition to ET, canopy precipitation interception (C_i) is an important metric in understanding winter evaporation and soil moisture re-charge. To date there have been few studies relating to tall grass energy crops and interception, with only one UK *Miscanthus* study. Finch and Riche (2010) reported measured *Miscanthus* C_i of 24%. However, measurements took place in small trial plots and the effect cannot be assumed to be the same at field scale as surface resistance becomes a smaller factor in water vapour diffusion to the atmosphere with increasing canopy cover forming a uniform layer (Monteith & Unsworth, 2008; Finch & Riche, 2010).

This study aims to:

a) determine the most accurate ET model compared to EC ET data (ET_{EC}) for use with *Miscanthus*; and
b) establish C_i in a commercial scale *Miscanthus* plantation under UK climate conditions.

To achieve this four base ET models, with further adjustments taking account of soil moisture status, were used to compare to ET_{EC} at a commercial scale mature

Miscanthus plantation in Wales, UK, where in-situ weather station and EC equipment have been recording since land-use conversion from grassland in 2012. A field study was set up in the plantation to record C_i from June 2016 to March 2017.

5.3 Materials and methods

5.3.1 Site Description

Field experiments, EC measurements, and weather data collection took place at a 6 ha plantation of *Miscanthus* located in Aberystwyth, Wales (52°25'17″ N 4°04'14″ W) (Figure 15). The site elevation is ~110 m a.s.l. with coastal cliffs ~0.5 miles west of the field boundary. It is predominantly flat with a slight slope (7°) to the south. The soil, a mixture of clay loam and sandy/silty clay loam, is formed over Denbigh series bedrock. The field capacity is 0.38 m^3m^{-3}, as shown in Saxton & Rawls (2006) and confirmed from in-situ soil moisture probes (2x CS616 Campbell Scientific (CSI), Logan, UT, USA, soil water content reflectometer installed at 25 cm depth). Permanent wilting point is 0.22 m^3m^{-3} (Saxton & Rawls, 2006). The field was converted from semi-improved grass pasture to *Miscanthus* in April 2012.

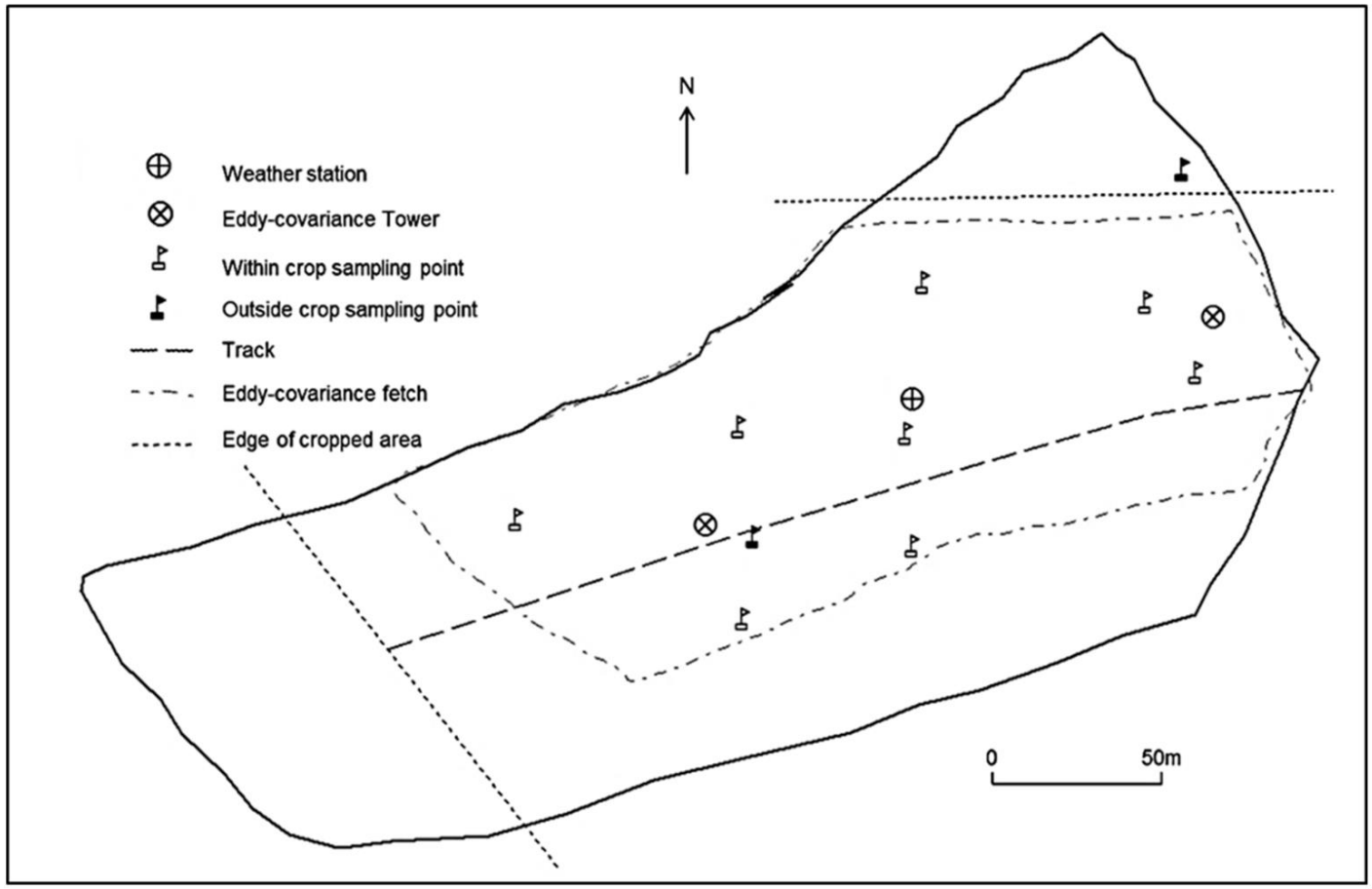

Figure 15 Map showing the outline of the 6 ha (approx.) *Miscanthus* field with the cropped area, sampling points, and meteorological and atmospheric measuring equipment locations marked.

5.3.2 Meteorological data

EC data were recorded by two open path systems (EC150/CSAT3A OPEC system, CSI, Logan, UT, USA) located at two towers (Figure 15) covering the central and most level 3.9 ha portion of the cropped area. Sensors were raised during the growing season to maintain a height of 2 m above the canopy. The systems included a sonic anemometer (CSAT-3A, CSI), infrared gas analyser (EC150, CSI), and air temperature (Ta, °C) and relative humidity (Rh, %) probes (HMP155A, CSI) recording to data-loggers (CR3000, CSI) at 20 Hz and processed to 30 min averages using EddyPro software (EddyPro version 4.2.0, LI-COR bioscience, Lincoln, NE, USA). Data was quality controlled and gap filled as described in McCalmont *et al.* (2017b). Latent heat flux (LE) values surrounding gap filled values were further checked for abnormally high figures caused by wet instrumentation, and were replaced using averages of nearby non gap filled values. ET figures were determined from LE using equation 9, and were converted to mm day^{-1}.

$$ET_{EC} = \frac{LE}{\lambda} \quad (9)$$

where ET_{EC} is the ET flux (mm hour^{-1}), LE is the 30 min latent heat flux after corrections and gap filling (Wm^2) and λ is the latent heat of vaporization constant. The value used for the hourly rate constant was 690.42 Wm^2 (2.4855 MJ m^2), as determined by the EddyPro software.

Excepting Rh and Ta (measured at each eddy covariance tower) meteorological data was collected from a station located in the centre of the field (Figure 15) and logged

in 30 minute intervals using a CR1000 (CSI) data logger. Precipitation (mm) was recorded using a tipping bucket rain gauge (52203, R.M. Young, Michigan, USA). Photosynthetic photon flux density (µmol m^{-2} s^{-1}) was measured with a SKP215 Photosynthetically Active Radiation (PAR) Quantum sensor (Skye systems, Llandrindod Wells, UK). Wind speed (ms^{-1}) and direction (º from north) was collected using a 05013 wind monitor (R.M. Young, Michigan, USA). Small gaps in the weather data (less than 1% overall) were filled from a nearby weather station[13].

5.3.3 ET models

Four ET models[14] were calculated using equations 10-18 with the R (R Core Team, 2015) package 'Evapotranspiration' (Guo & Westra, 2016). Results were output on a daily (24 hour) time-step.

The Granger-Gray (GG) formula (McMahon *et al.*, 2013) calculates actual ET (equation 10).

$$GG = \frac{\Delta Gg}{\Delta Gg+\gamma}\frac{Rn-G}{\lambda} + \frac{\gamma Gg}{\Delta Gg+\gamma}Ea \qquad (10)$$

where GG is the Granger-Gray ET model (mm day^{-1}), Gg is based on equations 11 and 12, G is the soil heat flux (MJ m^{-2} day^{-1}), γ the psychrometric constant (kPa °C^{-1}), R_n the net daily radiation (MJ m^{-2} day^{-1}), λ the latent heat of vaporization (MJ kg^{-1}), and Ea the drying power of the air calculated from equation 13.

[13] Located 3.6 km distance away from the field site.
[14] A large number of PET & ET models exist and the ones selected here were chosen to reflect the different calculation methods.

$$Gg = \frac{1}{0.793+0.20e^{4.902Dp}} + 0.006\,Dp \quad (11)$$

where Dp is calculated using equation 12.

$$Dp = \frac{Ea}{Ea+\frac{Rn-G}{\lambda}} \quad (12)$$

where Ea is calculated using equation 13.

$$Ea = f(u)\,(v^*a - va) \quad (13)$$

where $f(u)$ is the wind function shown in equation 14, v^*a the daily saturation vapour pressure (kPa) and va the mean daily actual vapour pressure (kPa).

$$f(u) = 1.313 + 1.381\,u_2 \quad (14)$$

where u_2 is the average daily wind speed (m s^{-1}) at 2 m.

The Priestley-Taylor (PT) formula (McMahon *et al.*, 2013) calculates potential ET (equation 15).

$$PT = \alpha PT\left[\frac{\Delta}{\Delta+\gamma}\,\frac{Rn}{\lambda} - \frac{G}{\lambda}\right] \quad (15)$$

where PT is the Priestley-Taylor ET model (mm day^{-1}), αPT is a constant of 1.26 for advection free saturated surfaces, Δ is the slope of vapour pressure curve (kPa $°C^{-1}$), γ the psychrometric constant (kPa $°C^{-1}$), R_n the net daily radiation (MJ m^{-2} day^{-1}), λ the latent heat of vaporization (MJ kg^{-1}), and G the soil heat flux (MJ m^{-2} day^{-1}).

The Hargreaves-Samani (HS) formula (McMahon *et al.*, 2013) calculates reference ET for a short grass crop with no water shortage (equation 16).

$$HS = 0.0135 C_{HS} \frac{R_a}{\lambda} (T_{max} - T_{min})^{0.5} (T_a + 7.8) \quad (16)$$

where HS is the Hargreaves-Samani ET model (mm day^{-1}), C_{HS} is a coefficient based on equation 17, R_a is extra-terrestrial radiation (MJ m^{-2} day^{-1}), λ the latent heat of vaporization (MJ kg^{-1}), T_{max} and T_{min} the maximum and minimum daily temperatures (°C) and T_a the average daily temperature (°C).

$$C_{HS} = 0.00185 (T_{max} - T_{min})^2 - 0.0433 (T_{max} - T_{min}) \quad (17)$$

where C_{HS} is the Hargreaves-Samani coefficient and T_{max} and T_{min} are the maximum and minimum daily temperatures (°C).

The Penman-Monteith (PMgrass) formula (Allen *et al.*, 1998) calculates reference ET for a short grass crop with no water shortage (equation 18)

$$\frac{0.408\Delta(R_n - G) + \gamma \frac{900}{T_a + 273} u_2 (V_a^* - V_a)}{\Delta + \gamma(1 + 0.34 u_2)} \quad (18)$$

where Δ is the slope of the vapour pressure curve (kPa °C^{-1}), R_n the net radiation (MJ m^{-2} day^{-1}), G the soil heat flux (MJ m^{-2} day^{-1}), γ the psychrometric constant (kPa

°C^{-1}) , T_a the mean daily air temperature (°C), u_2 the average daily wind speed (at 2 m) (m s^{-1}), v^*a the daily saturation vapour pressure (kPa), and va the mean daily actual vapour pressure (kPa).

The inputs required for the models along with the values used for the constants are shown in Table 9. Global radiation, also known as solar radiation (Rs) (Allen *et al*., 1998), was calculated as 2x PAR (Monteith & Unsworth, 2008) and converted to MJ m^2 day^{-1}.

Table 9 Data input requirements for the Hargreaves-Samani (HS), Priestley-Taylor (PT), Granger Gray (GG), and Penman-Monteith (short grass) (PMgrass) evapotranspiration models. The options and values for the constants used in this study are shown in italics.

Inputs	**HS**	**PT**	**GG**	**PMgrass**
Date, time, and day of the year of each record	✓	✓	✓	✓
Air temperature, Ta (°c)	✓	✓	✓	✓
Relative humidity, Rh (%)	✓	✓	✓	✓
Wind speed at 2 m height, u_2 (m s^{-1})		✓	✓	
Solar radiation, Rs (MJ m^{-2} day^{-1})	✓	✓	✓	✓
Precipitation (mm)	✓	✓	✓	✓
Alpha (*0.23*)		✓	✓	
Alpha PT (*1.26*)		✓		
1948 Penman wind function version			✓	
Short crop				✓
Elevation (*115 m*)	✓	✓	✓	✓
Latent heat of vaporization, Lambda (*2.45 MJ kg^{-1} at 20 °C*)	✓	✓	✓	✓
Latitude (*0.914902 radians*)	✓	✓	✓	✓
Solar constant, Gsc, (*0.082 MJ m^{-2} min^{-1}*)	✓	✓	✓	✓
Stefan-Boltzmann constant, Sigma (*4.903 10^{9} MJ K^{-4} m^{-2} day^{-1}*)		✓	✓	✓
Soil heat flux, G (*0, negligible for daily time-step*)		✓	✓	✓
Height of wind instrument, Z (2 m)			✓	✓

5.3.4 Adjustment from ET_p to ET_a

The PT and HS models were adjusted daily to provide a prediction of ET_a via the use of a soil moisture function (Mintz & Walker, 1993; Dingman, 2002; Xu & Chen, 2005) which reduces ET estimates as soil water becomes depleted to critical levels. The relationship between ET_p, precipitation, the soil moisture function (*F*), and ET_a is as follows:

if ET_p > precipitation then $ET_a = ET_p \times F$

if ET_p = precipitation then $ET_a = ET_p$

if ET_p < precipitation then $ET_a = ET_p$

The soil moisture function is calculated from a basic soil water balance using equations 19-21.

$$F\ [0\text{-}1] = \frac{W}{W*} \qquad (19)$$

where F is the soil moisture function restricted to between 0 and 1, W the soil moisture estimated from equation 20, and W the soil storage capacity calculated from equation 21.*

$$W_t\ [0\text{-}96] = W_{t-1} + (P_t - ET_{pt}) \qquad (20)$$

where W_t is the soil moisture (mm) restricted to between 0 and the field capacity (96 mm, from equation 21), W_{t-1} the soil moisture (mm) from the previous day, P_t the precipitation (mm) and ET_{pt} the calculated ET_p (mm).

$$W^* = 1000(0.38-0.22)0.60 \quad (21)$$

where W is the site specific soil moisture storage capacity (mm), 1000 the conversion to mm, 0.38 the site specific field capacity (m^3m^{-2}), 0.22 the site specific wilting point (m^3m^{-2}) and 0.60 the site specific approximate soil/rooting depth (m).*

Following the method in Allen *et al.* (1998) the PMgrass results were adjusted with a water stress coefficient (K_s) and a crop coefficient (K_c) to provide an estimate of ET_a, as shown in equation 22. The K_c values for sugarcane, also a C_4 plant with tall stems and a large leaf area index, were used. Sugarcane published K_c values are 0.40 for the early growth stage, 1.25 for the main growing season, and 0.75 for the late season (Allen *et al.*, 1998). 0.75 was also used for the winter season.

$$ET_a = K_sK_c\ ET_o \quad (22)$$

where ET_a is the PMgrass results adjusted for the soil moisture depletion and crop type, K_s the water stress coefficient calculated from equations 23-25, K_c the crop specific coefficient, and ET_o the PMgrass result.

$$K_s\ [0\text{-}1] = \frac{TAW-Dr}{TAW-RAW} \quad (23)$$

where K_s is the water stress coefficient (between 0 and 1), TAW the total available water (mm) calculated in the same way as W (equation 21), Dr the root zone moisture depletion calculated from equation 24, and RAW the readily available water (mm) calculated from equation 25.*

$$Dr_t = Dr_{t-1}, - P_t + ET_{ct} \quad (24)$$

where Dr is the root zone depletion (mm), Dr_{t-1} the water content in the root zone on the previous day (mm), P_t the precipitation (mm) and ET_{ct} the crop evapotranspiration (mm).

$$RAW = pTAW \quad (25)$$

where RAW is the readily available water (mm), TAW the total available water (mm) calculated in equation 21, and p the fraction of TAW that the plant can extract without suffering water stress applied on a seasonal basis (values of p used were 0.76 for the early and late season, 0.67 for the main season, and 0.77 for the winter - based on the values and adjustments given for sugarcane in Allen et al. (1998)).

5.3.5 Miscanthus crop coefficient (K_c)

To calculate the *Miscanthus* specific K_c, ET_{EC} and PMgrass daily ET rates were divided to approximately correspond to the relevant stages of plant growth (Table 10).

Table 10 Months allocated to each seasonal stage of *Miscanthus* plant growth for calculation of the crop coefficient (K_c).

Season	Month
Early	March and April
Main	May, June, July, August, and September
Late	October and November
Winter	December, January, and February

The K_c value for each season was calculated using equation 26 and the value multiplied by the results of PMgrass to provide the Penman-Monteith K_c (PMK_c) estimated ET.

$$K_c = \frac{ET_{EC}}{PM} \quad (26)$$

where K_c is the crop coefficient, ET_{EC} the mean daily EC calculated evapotranspiration for the season, and PM the mean daily evapotranspiration calculated by the Penman-Monteith (short grass) model.

5.3.6 Canopy precipitation interception

Measurements took place from 23rd June 2016 until 13th March 2017 using methods similar to those used by Riche and Christian (2001). Eight sampling locations (2 m^2) within the cropped area (Figure 15) were selected by stratified random sampling using a pre-conversion topsoil moisture map to take account of wetter and drier areas. Three stem-flow and three through-fall gauges (Figure 16a, b, c) were randomly placed within each sampling location.

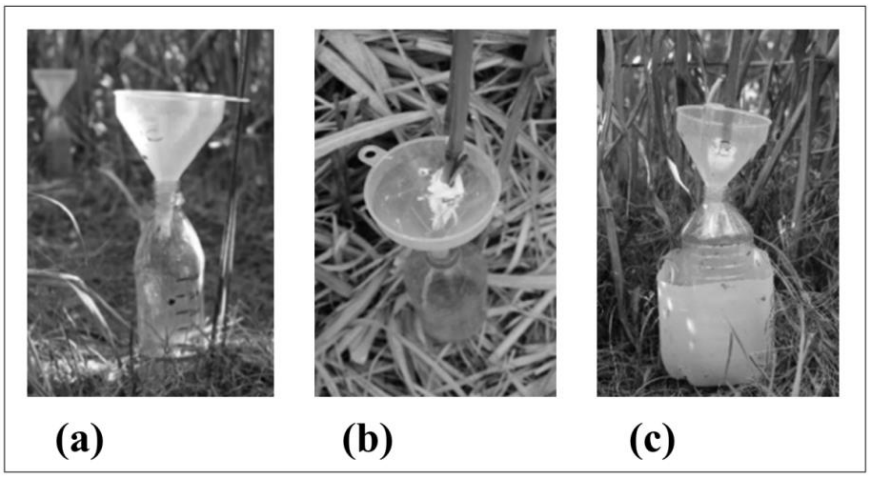

Figure 16 (a) Through-fall within the crop and precipitation outside the crop canopy was measured using 500 ml plastic bottles with 95 mm diameter funnels. The funnel and bottle were attached to a garden stake and secured with an elastic band and tent peg. **(b)** Stem-flow was measured using 750 ml plastic bottles (of the same height as the 500 ml bottles) with a 95 mm diameter funnel adapted to fit around the stem and sealed with silicon sealant. **(c)** As a precaution against overflowing the stem-flow bottle was placed inside a plastic container.

Two further sampling areas to collect gross precipitation were located outside the crop canopy - one to the north and the other in a clearing along the centre track (Figure 15). A monthly count of the number of mature stems in 1 m^2 along with the average stem thickness was carried out in an area immediately adjoining the sampling locations. Gauges were checked approximately twice weekly with measurements taken in dry weather when water levels were high enough in the gauges for accurate measurement with the use of a graduated cylinder. After the first few weeks of data collection an error level of less than or equal to 4.75% was calculated from the sums of squares and coefficient of variation using the means of the eight zones within the crop (Raghunath, 2006).

The C_i was taken to be the difference between the gross precipitation recorded outside the crop and the net precipitation recorded within the crop (equation 27).

$$C_i = GP - (TF + SF) \quad (27)$$

where C_i is the interception (mm), GP the measured gross precipitation (mm), TF the measured through-fall (mm) and SF the measured stem-flow (mm).

For each recording event the amount of precipitation collected in the through-fall bottles was converted into a depth measurement based on the area of the funnel. Gross rainfall was collected and converted to a depth measurement in the same way as the through-fall using the four gauges located in each of the two locations outside the crop. For each recording event stem-flow amounts were adjusted for the average size of the stem and reduced by the amount collected by the closest through fall bottle to account for through-fall that would also have been collected by the funnel (equation 28). Total stem-flow was then calculated as a mean depth measurement (equation 29). During measurement 19 samples out of a total of 2856 (2.62%) were rejected as a result of broken stems or damage to the collecting system.

$$SFA = SFC - (TFC - SP) \quad (28)$$

where SFA is the stem-flow amount (ml), SFC the amount collected in the stem-flow bottle (ml), TFC the amount collected in the closest through-fall bottle (ml) and SP the percentage of the funnel/overflow bottle area taken up by the stem (%).

$$SFD = \frac{(SFA \times S)*1000}{SA} \quad (29)$$

where SFD is the total stem-flow depth (mm), SFA the mean stem-flow amount (calculated from the mean stem-flow amount in each sampling area) (ml), S the mean number of stems in 1m^2, 1000 the conversion to mm^3, and SA the surface area of the stem count (mm^2).

5.3.7 Statistics

Statistics were carried out using R version 3.2.3 (R Core Team, 2015). Model residual plots were checked for the appropriateness of linear regression and the linear model function was used to obtain the R^2 values (with ET_{EC} as the independent variable). The seasonal daily means, standard deviation and standard error of the mean were calculated for all the daily ET results. The HydroGof (Zambrano-Bigiarini, 2017) R package was used to calculate the Mean Absolute Error (MAE), Root Mean Square Error (RMSE), modified Index of Agreement (md) (return of between 0 and 1 where 1= a perfect match) and the modified Nash Sutcliffe Efficiency (mNSE) (return of between –infinity and 1 where 1= a perfect match and 0= predictions as accurate as the mean of the observed data) as described in Legates & McCabe (2005)[15].

[15] See also Appendix A2.1 for more information regarding the model evaluation statistics.

5.4 Results

5.4.1 Experimental data

Meteorological data from the weather station and eddy covariance instrumentation is shown in Figure 17. Wind direction at the site is predominantly from the west with mean wind speeds and annual precipitation of 2.45 ms^{-1} and 871 mm for the period 2012 to 2016. Over the C_i study period (23rd June 2016 to 13th March 2017) the total precipitation was 776 mm. Conditions at the site during the C_i sampling period were generally within the five year average with the exception of short periods of high wind speeds due to seasonal storms, and particularly high rainfall during the summer of 2016 caused by shifts in the gulf stream (Figure 17a, Met Office, 2016a). Most precipitation was received during the winter with the exception of 2012 and 2016 where high rainfall was also received during the summer. 2012 was the wettest of the 5 years reflecting national conditions with 2012 being one of the wettest years on record (Met Office, 2016b). Ta was similar across the years with 2013 and 2016 having the highest summer and winter temperatures (Figure 17b). Rh was mostly above 80% for all of the 5 years (Figure 17d). Soil moisture only dropped below the wilting point from 24th July 2014 to 20th October 2014 (Figure 17e). Rs levels and LE and sensible heat (H) fluxes were comparable across each of the five years (Figure 17f, g, h).

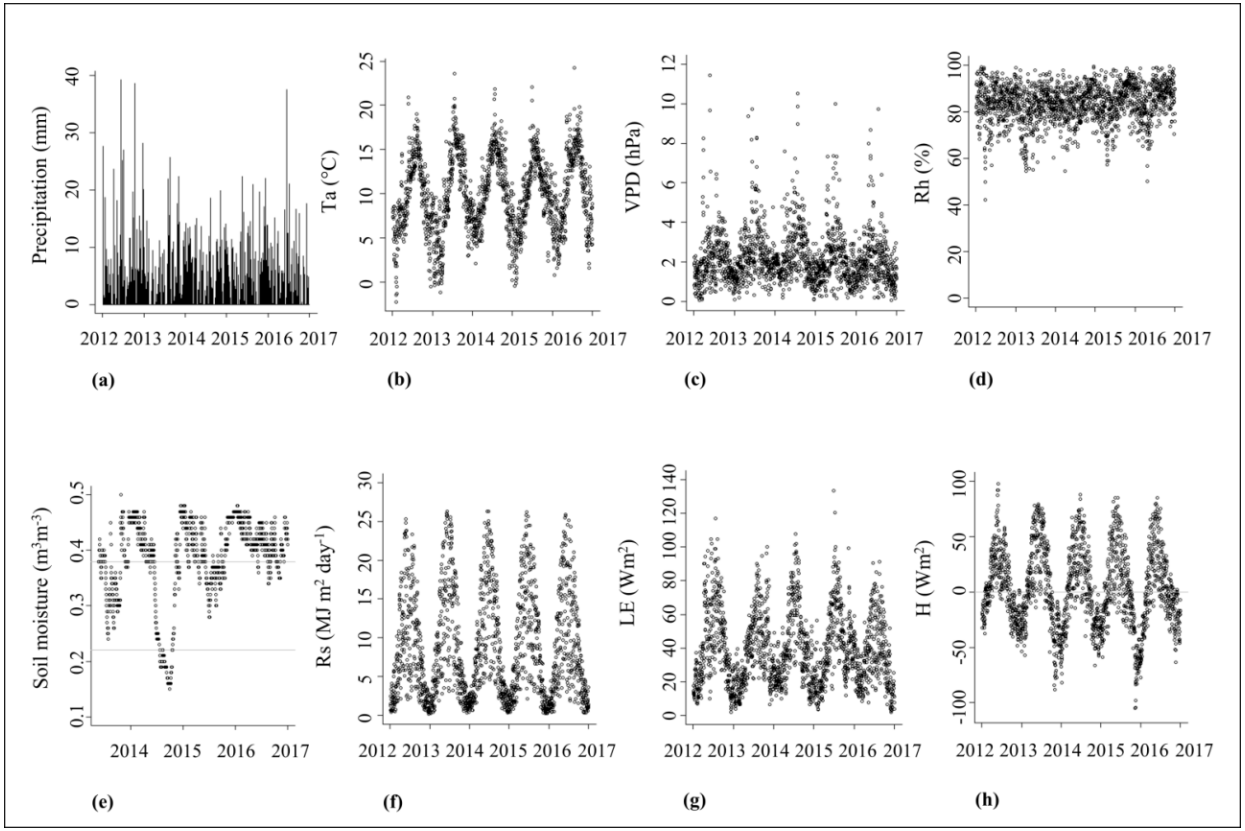

Figure 17 Daily (24 hour) data for the period 2012 to 2016: **(a)** total daily precipitation (mm); **(b)** mean daily air temperature (°C); **(c)** mean daily vapour pressure deficit (hPa); **(d)** mean daily relative humidity (%); **(e)** mean daily soil moisture (m^3m^{-3}) at 25 cm depth (available data is from 22/05/2013 to end 2016) with the grey lines showing the field capacity (0.38) and wilting point (0.22); **(f)** mean daily solar radiation (calculated as 2x Photosynthetically Active Radiation) (MJ m^2 day^{-1}); **(g)** mean daily latent heat flux (Wm^2) and **(h)** mean daily sensible heat flux (Wm^2).

5.4.2 ET results

The mean annual ET rates (mm year^{-1}) from 2013 to 2016 (excluding the conversion year) were ET_{EC} 483, GG 432, PMgrass 545, PMsugarcane 552, PMsugarcane.adj 408, HS 698, HS.adj 327, PT 547, PT.adj 295, and PMK_c (*Miscanthus*) 494[16]. The highest daily ET_{EC} was 4.65 (mm day^{-1}) in the main 2015 growing season.

Monthly trends in ET_{EC} (Figure 18) were similar over the five year study period with 2014 and 2015 showing the highest summer peaks, and the winters of 2012/13 and 2014/15 showing the lowest drops. ET_{EC} was higher in the winter than predicted by all the models. There was no drop in ET_{EC} during the period when the soil moisture was below wilting point, although there was a drop over the following late and winter seasons. GG, PMgrass and PT.adj correspond well to the summer peak of 2012 which was the conversion year, but all the potential ET models overestimate the summer peaks.

Adjustments for soil moisture with HS.adj and PT.adj reduce the main growing season levels too much compared to ET_{EC}, but PMsugarcane.adj overestimates them. Whilst HS results are considerably higher in the summer, the model performs better over the winter. PMgrass and PMsugarcane results are also close to ET_{EC} over the winter, although the late growing season higher values are not captured by any of the models.

[16] Yearly values for the whole time period (2012-2016) are shown in Appendix A2.2.

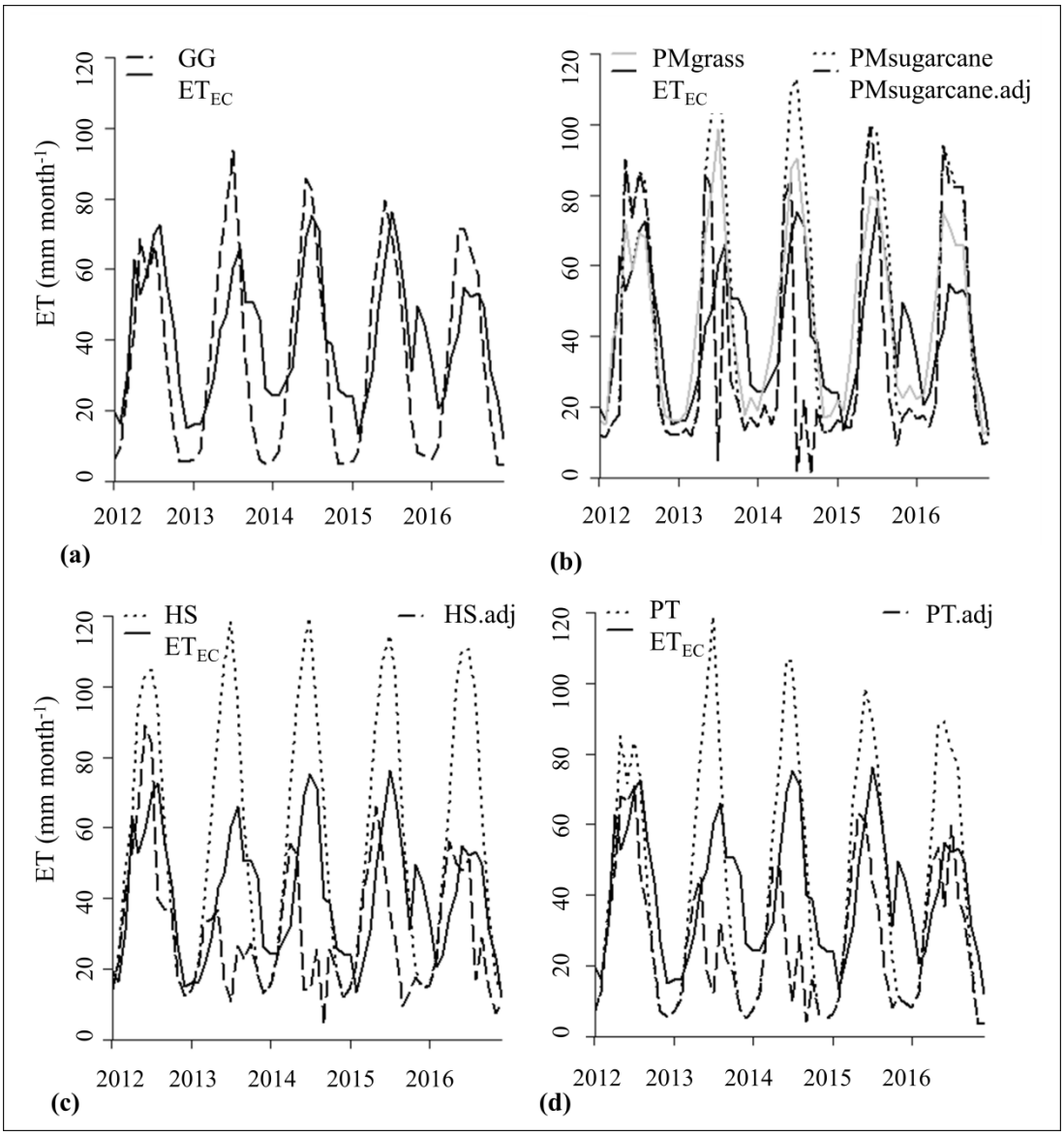

Figure 18 Results of the daily evapotranspiration (ET) model predictions and eddy covariance ET (ET_{EC}) summed to provide monthly values: **(a)** Granger-Gray (GG) actual ET model predictions and ET_{EC}; **(b)** Penman-Monteith short grass reference ET (PMgrass), Penman-Monteith sugarcane crop ET (PMsugarcane), Penman-Monteith sugarcane crop ET adjusted with a water stress coefficient (K_s) (PMsugarcane.adj) and ET_{EC}; **(c)** Hargreaves-Samani grass reference ET (HS), Hargreaves-Samani grass reference ET adjusted with a soil moisture function (F) (HS.adj) and ET_{EC}; **(d)** Priestley-Taylor potential ET (PT), Priestley-Taylor potential ET adjusted with a soil moisture function (F) (PT.adj) and ET_{EC}.

Statistics carried out for the early season (Table 11) show low R^2 values for all the models compared to ET_{EC}. The seasonal daily mean of the GG results is the closest to ET_{EC}, and is followed by PT.adj. All the model predictions over-estimate with the exception of PMsugarcane. HS is shown to be the worst model for the early season with the most unfavourable outcomes of all the statistical tests performed compared to the other models. Adjustments for soil moisture during the early season improved PT and HS results (mean F values for the early season for PT and HS were 0.89 and 0.84 respectively) but made no difference to PMsugarcane (mean K_s for the early season was 1). PT.adj, GG, PMsugarcane and PMsugarcane.adj show a moderate fit using the modified Index of Agreement (md), however the modified Nash Sutcliffe Efficiency (mNSE) test results in below zero values for all the models, with PT.adj being closest to it at -0.04. Overall for the early season PT.adj performs the best, closely followed by GG. Comparing the potential ET models shows the PT results to be closest to PMgrass.

Table 11 Mean daily evapotranspiration for the early season (2012 to 2016[17], number of observations 305) with the standard deviation (SD), standard error of the mean (SEM), R^2 , mean absolute error (MAE), root mean square error (RMSE), modified Index of Agreement (md) and modified Nash Sutcliffe Efficiency (mNSE). The models are: GG, Granger-Gray; PMsugarcane.adj, PMgrass adjusted with a water stress coefficient and the crop coefficient for sugarcane; PMsugarcane, PMgrass adjusted with the crop coefficient for sugarcane; PMgrass, Penman-Monteith (short grass); HS, Hargreaves-Samani; HS.adj, HS adjusted with a soil moisture function; PT, Priestley-Taylor; PT.adj, PT adjusted with a soil moisture function. Model results are compared to eddy covariance (EC).

	EC	**GG**	**PMsugar-cane.adj**	**PMsugar-cane**	**PMgrass**	**HS**	**HS. adj**	**PT**	**PT. adj**
Mean (mm day^{-1})	1.03	1.17	0.57	0.57	1.43	1.78	1.48	1.44	1.26
SD (mm day^{-1})	0.52	0.54	0.23	0.23	0.57	0.48	0.38	0.64	0.47
SEM (mm day^{-1})	0.03	0.03	0.01	0.01	0.03	0.03	0.02	0.04	0.03
R^2 [0-1]		0.27	0.21	0.21	0.21	0.19	0.22	0.28	0.37
MAE (mm day^{-1})		0.43	0.47	0.47	0.55	0.81	0.57	0.56	0.40
RMSE (mm day^{-1})		0.54	0.65	0.65	0.69	0.92	0.66	0.71	0.50
md [0-1]		0.48	0.45	0.45	0.38	0.29	0.34	0.41	0.49
mNSE [-INF - 1]		-0.12	-0.22	-0.22	-0.44	-1.12	-0.47	-0.45	-0.04

[17] There is an error in the published paper (currently awaiting the addition of an amendment notice) with the Table caption incorrectly showing the dates 2012 to 2013.

The mean values and statistics for the main season (Table 12) show PMgrass to be the best model compared to ET_{EC}, followed by GG. All the model means (except HS.adj and PT.adj) show an over-estimation for the season but GG and PMsugarcane.adj show the smallest difference to ET_{EC}. However, PMsugarcane.adj has a high MAE and low mNSE compared to the other models. PMgrass is the only model to have a mNSE value above zero (0.08). The impact of soil moisture across the adjusted models is not the same with the mean *F* values for the season for HS and PT as 0.25 and 0.42 respectively whereas the seasonal mean K_s value is 0.74. Comparing the potential ET models to PMgrass again shows the PT results to be closest. The model with the worst fit to ET_{EC} for the main season is the HS model.

Table 12 Mean daily evapotranspiration for the main season (2012 to 2016[18], number of observations 765) with the standard deviation (SD), standard error of the mean (SEM), R^2 , mean absolute error (MAE), root mean square error (RMSE), modified Index of Agreement (md) and modified Nash Sutcliffe Efficiency (mNSE). The models are: GG, Granger-Gray; PMsugarcane.adj, PMgrass adjusted with a water stress coefficient and the crop coefficient for sugarcane; PMsugarcane, PMgrass adjusted with the crop coefficient for sugarcane; PMgrass, Penman-Monteith (short grass) model; HS, Hargreaves-Samani; HS.adj, HS adjusted with a soil moisture function; PT, Priestley-Taylor; PT.adj, PT adjusted with a soil moisture function. Model results are compared to eddy covariance (EC).

	EC	**GG**	**PMsugar-cane.adj**	**PMsugar-cane**	**PMgrass**	**HS**	**HS. adj**	**PT**	**PT. adj**
Mean (mm day^{-1})	1.89	2.03	2.05	2.79	2.23	3.11	1.21	2.58	1.27
SD (mm day^{-1})	0.68	0.87	1.36	1.06	0.85	0.67	1.23	1.07	0.93
SEM (mm day^{-1})	0.02	0.03	0.05	0.04	0.03	0.02	0.04	0.04	0.03
R^2 [0-1]		0.40	0.12	0.49	0.49	0.11	0.02	0.43	0.05
MAE (mm day^{-1})		0.54	1.04	0.93	0.51	1.25	1.41	0.81	0.92
RMSE (mm day^{-1})		0.70	1.31	1.18	0.71	1.45	1.63	1.06	1.19
md [0-1]		0.58	0.39	0.44	0.60	0.30	0.23	0.48	0.39
mNSE [-INF - 1]		-0.03	-0.87	-0.67	0.08	-1.25	-1.53	-0.45	-0.65

[18] There is an error in the published paper (currently awaiting the addition of an amendment notice) with the Table caption incorrectly showing the dates 2012 to 2013.

During the late season the means for all the models under-estimate ET_{EC}, including the potential ET formulae (Table 13). Only the Penman-Monteith derived models have mediocre R^2 values whereas the values for the other models are low. Results of the md test for all the models are in a similar range although PMgrass shows the best fit at 0.49. All of the results of the mNSE test are below zero although PMgrass and HS are slightly better than the other models with values of -0.06 and -0.09 respectively. Out of the potential ET models PMgrass performs better than HS and PT, but HS is closest to the PMgrass results. The means of the models adjusted for soil moisture were further away from the mean ET_{EC} than their unadjusted potential ET base models. Overall for the late season PMgrass shows the best fit, followed by HS. GG is the worst fit for the season.

Table 13 Mean daily evapotranspiration for the late season (2012 to 2016[19], number of observations 305) with the standard deviation (SD), standard error of the mean (SEM), R^2 , mean absolute error (MAE), root mean square error (RMSE), modified Index of Agreement (md) and modified Nash Sutcliffe Efficiency (mNSE). The models are: GG, Granger-Gray; PMsugarcane.adj, PMgrass adjusted with a water stress coefficient and the crop coefficient for sugarcane; PMsugarcane, PMgrass adjusted with the crop coefficient for sugarcane; PMgrass, Penman-Monteith (short grass) model; HS, Hargreaves-Samani; HS.adj, HS adjusted with a soil moisture function; PT, Priestley-Taylor; PT.adj, PT adjusted with a soil moisture function. Model results are compared to eddy covariance (EC).

	EC	**GG**	**PMsugar-cane.adj**	**PMsugar-cane**	**PMgrass**	**HS**	**HS. adj**	**PT**	**PT .adj**
Mean ($mm\ day^{-1}$)	1.21	0.36	0.52	0.58	0.77	0.95	0.65	0.48	0.38
SD ($mm\ day^{-1}$)	0.59	0.22	0.27	0.27	0.36	0.37	0.42	0.33	0.30
SEM ($mm\ day^{-1}$)	0.03	0.01	0.02	0.02	0.02	0.02	0.02	0.02	0.02
R^2 [0-1]		0.02	0.41	0.37	0.37	0.03	0.12	0.06	0.12
MAE ($mm\ day^{-1}$)		0.85	0.69	0.64	0.48	0.49	0.63	0.74	0.83
RMSE ($mm\ day^{-1}$)		1.04	0.83	0.79	0.64	0.69	0.82	0.94	1.00
md [0-1]		0.34	0.39	0.42	0.49	0.41	0.41	0.37	0.35
mNSE [-INF - 1]		-0.88	-0.53	-0.40	-0.06	-0.09	-0.39	-0.63	-0.83

[19] There is an error in the published paper (currently awaiting the addition of an amendment notice) with the Table caption incorrectly showing the dates 2012 to 2013.

During the winter season, as in the late season, all the models means were less than the ET_{EC} mean (Table 14). PMgrass was closest mean to ET_{EC} and also had the most favourable md result of 0.51. PMsugarcane, and PMsugarcane.adj were similar to PMgrass with md values of 0.48. PMgrass was the only model with a mNSE result above zero (0.10). Both the PMsugarcane models mNSE results were zero. Adjustments for moisture were minimal for this season with only HS being adjusted (the winter seasonal mean *F* value for HS was 0.97 and for PT was 1, and the mean K_s value for adjusting PMsugarcane was also 1). Overall for the winter season PMgrass showed the most favourable fit of the models tested, followed by PMsugarcane. The worst fit for the season was GG.

Table 14 Mean daily evapotranspiration for the winter season (2012 to 2016[20], number of observations 449) with the standard deviation (SD), standard error of the mean (SEM), R^2 , mean absolute error (MAE), root mean square error (RMSE), modified Index of Agreement (md) and modified Nash Sutcliffe Efficiency (mNSE). The models are: GG, Granger-Gray; PMsugarcane.adj, PMgrass adjusted with a water stress coefficient and the crop coefficient for sugarcane; PMsugarcane, PMgrass adjusted with the crop coefficient for sugarcane; PMgrass, Penman-Monteith (short grass) model; HS, Hargreaves-Samani; HS.adj, HS adjusted with a soil moisture function; PT, Priestley-Taylor; PT.adj, PT adjusted with a soil moisture function. Model results are compared to eddy covariance (EC).

	EC	**GG**	**PMsugar-cane.adj**	**PMsugar-cane**	**PMgrass**	**HS**	**HS .adj**	**PT**	**PT .adj**
Mean (mm day^{-1})	0.74	0.23	0.49	0.49	0.66	0.56	0.54	0.27	0.27
SD (mm day^{-1})	0.39	0.14	0.23	0.23	0.31	0.19	0.19	0.23	0.23
SEM (mm day^{-1})	0.02	0.01	0.01	0.01	0.01	0.01	0.01	0.01	0.01
R^2 [0-1]		0.00	0.23	0.23	0.23	0.00	0.00	0.00	0.00
MAE (mm day^{-1})		0.53	0.31	0.31	0.28	0.36	0.36	0.51	0.51
RMSE (mm day^{-1})		0.66	0.43	0.43	0.37	0.48	0.48	0.65	0.65
md [0-1]		0.35	0.48	0.48	0.51	0.34	0.35	0.35	0.35
mNSE [-INF - 1]		-0.71	0.00	0.00	0.10	-0.18	-0.16	-0.64	-0.63

[20] There is an error in the published paper (currently awaiting the addition of an amendment notice) with the Table caption incorrectly showing the dates 2012 to 2013.

5.4.3 Miscanthus K_c value

In the early and main growing seasons there is a difference in the *Miscanthus* K_c values (calculated from the eddy covariance data and the PMgrass results) when data is used from the whole five year period compared to just 2013 to 2016, but values are almost the same for the late and winter seasons (Table 15). The early season in 2012 represents an atypical period being the time of land conversion to *Miscanthus* with a dominance of bare soil during the crop's initial establishment. Figure 19 shows ET_{EC} results in comparison with PMgrass adjusted with the calculated K_c values (PMK_c).

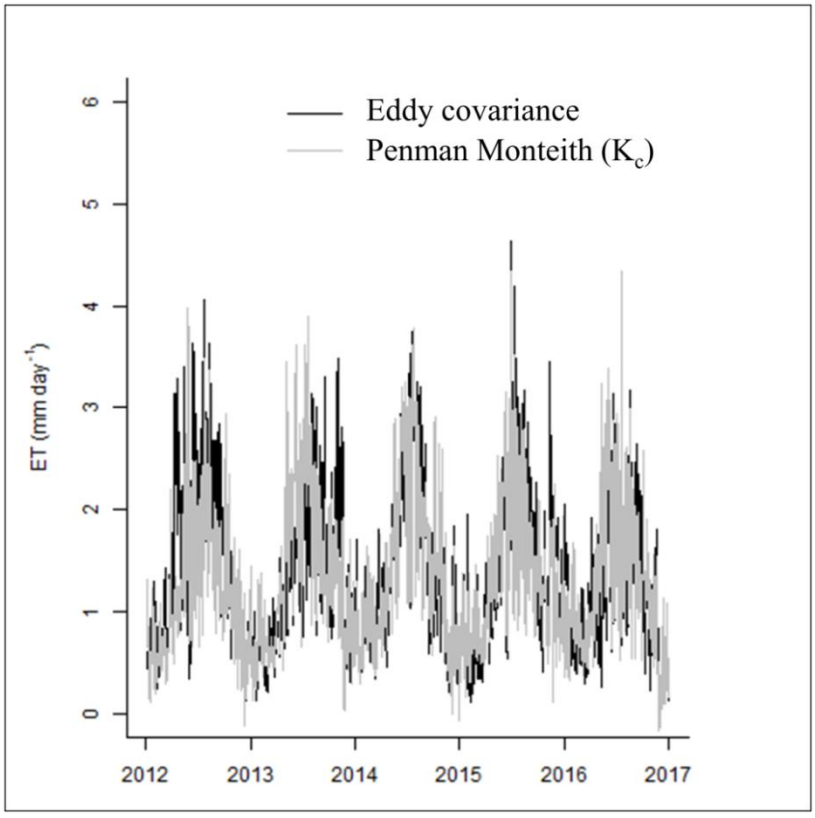

Figure 19 Results of eddy covariance calculated evapotranspiration (ET) and the Penman-Monteith (short grass) model adjusted with *Miscanthus* calculated K_c values of 0.63 for the early season (March and April), 0.85 for the main season (May to September), 1.57 for the late season (October and November) and 1.12 over the winter (December to February).

Table 15 K_c calculated using the Penman-Monteith (short grass) model and eddy covariance results for the seasons in the periods 2012 to 2016, and 2013 to 2016.

	2012-2016	2013-2016
Early	0.72	0.63
Main	0.85	0.81
Late	1.57	1.58
Winter	1.12	1.13

5.4.4 Canopy Interception

51 recording events took place over the sampling period June 2016 to March 2017. Data was only removed from one of these occasions due to the high winds in November 2016 causing damage to the gauges. Measured C_i was 24% for the period. The total gross precipitation (outside of the crop) was 776 mm and the net precipitation (a combination of stem flow and through-fall) was 588 mm. The net precipitation was made up of 133 mm stem-flow and 455 mm through-fall. Gross precipitation was related to net precipitation with an R^2 value of 0.9 (Figure 20a).

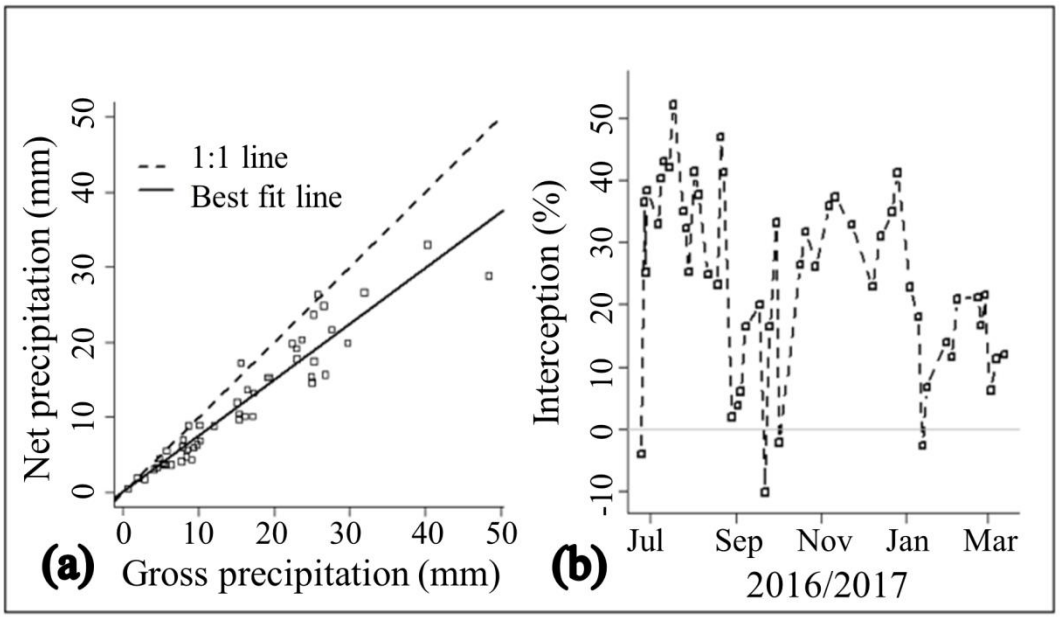

Figure 20 Extent of canopy precipitation interception from June 2016 to March 2017 **(a)** Net precipitation recorded within the *Miscanthus* crop (a combination of stem-flow and through-flow) regressed against gross precipitation received outside of the crop; **(b)** percentage of interception loss on each measuring occasion.

Interception is highest from July to September when the canopy is mature (Figure 20b). The highest level of interception for a measuring occasion was 52% recorded during the period 15th – 18th July, and the highest mean monthly level of interception was 34% recorded for the month of August. Whilst the interception levels drop over the autumn and winter as leaves are dropped in senescence, the remaining canes continue to intercept rainfall until the harvest at the end of March. There are four instances where there was a higher net than gross precipitation (Figure 20b). Examination of the data suggests these are related to occasions when wind direction may have caused gauges to record higher levels in the within-crop sampling due to the canopy intercepting rain being blown horizontally by the wind.

5.5 Discussion

5.5.1 ET models

The mean ET_{EC} of 483 mm $year^{-1}$ was over half of the mean annual rainfall demonstrating the importance of obtaining accurate estimates of ET in hydrological modelling. The maximum measured ET_{EC} value of 4.65 mm day^{-1} was considerably lower than the highs of 7 and 11 mm day^{-1} found in the USA by Hickman *et al*. (2010) and in Italy by Triana *et al*. (2015). This is as expected for the very different climatic conditions of the studies. However, it was similar to the ET_{EC} of around 5 mm day^{-1} obtained in Hereford, UK and within the range of the MOSES model predictions both shown in the study carried out by Finch *et al*. (2004).

The eddy covariance technique is a recognized method for obtaining field estimates of ET and is regarded as having a good level of accuracy - provided careful data processing and gap-filling strategies are employed (Aubinet *et al.*, 2012; Gebler *et al*., 2015; Wagle *et al.*, 2016). The use of daily ET results has provided a detailed insight into the performance of the models within each season. Although none of the ET models provide a good fit compared to ET_{EC} , the highest modified Index of Agreement (md) results for each season were generally in the medium range (early 0.49, main 0.60, late 0.49 and winter 0.51).

A combination of factors in this study have allowed for reasonable comparisons of reference and potential ET models to ET_{EC} in this study. Whilst reference and potential ET models calculate ET on the basis of no crop water shortage this was the case at the field site for the majority of the study period, with only a short time when the soil moisture status was below wilting point. Adjustments to the HS and PT base models to account for soil moisture stress generally resulted in ET rates less than

ET_{EC} (Figure 18). This *Miscanthus* genotype has also been shown to have a slower initial response to drought, with limited stomatal control (Clifton-Brown *et al*., 2002; Joo *et al*., 2017) and the ability to exploit the maximum soil depth and hence available water (Neukirchen *et al*., 1999) enabling the maintenance of high ET rates compared to other crops. However, prolonged water stress is likely to reduce *Miscanthus* ET rates (Joo *et al.,* 2017).

PMgrass performed the best in all the seasons with the exception of the early season. This model had the highest md result for the main, late and winter seasons and was the only model to achieve a mNSE score of above zero (main 0.08 and winter 0.10). *Miscanthus* emerges later than the start of the grass pasture growing season and can continue transpiring to the end of October (in favourable years). These are likely to be factors in differing early and late season ET rates of *Miscanthus* compared to grass.

GG was the second best model for both the early and main season (early: MAE 0.43, md 0.48, mNSE -0.12; main: MAE 0.54, md 0.58, mNSE -0.03), but it was the worst performing model for the late and winter seasons (late: MAE 0.85, md 0.34, mNSE -0.88; winter: MAE 0.53, md 0.35, mNSE -0.71). For the early season GG closely followed the best performing model which was PT.adj (MAE, 0.40, md 0.49, mNSE -0.04).

Both GG and PMgrass require wind speed data as an input whereas this is not required by PT and HS. PT and HS models can also be used within the SWAT hydrology model to calculate ET in the absence of wind speed data (Arnold *et al.*, 2012) making them suitable for sites with more limited instrumentation. Comparing PT and HS to ET_{EC} has shown that PT performs better than HS over the early (PT,

md 0.41; HS, md 0.29) and main growing seasons (PT, md 0.48; HS, md 0.30) but that over the late (PT, md 0.37; HS, md 0.41) and winter (PT, MAE 0.51, md 0.35, mNSE -0.64; HS, MAE 0.36, md 0.34, mNSE 0.36) seasons HS out performs PT. HS is more commonly used for warmer climates (Tabari, 2010) so was least suited to the UK climate type.

Winter ET_{EC} values were higher than all of the model predictions - an important point to consider when modelling the impacts on water balance and potential flood mitigation benefits. Winter precipitation interception by stalks and dead leaves in the field are not taken into account in PMgrass. Interception is an important factor in ET rates where differences of 30% between ET calculated with and without adjustment for the impact of C_i have been observed (Robinson *et al*., 2017). The field site's coastal proximity and localized weather systems could also be impacting on lower model results compared to ET_{EC}. ET_a may be higher at times on site due to advection of sensible heat energy either from the sea or the presence of nearby hilly terrain causing localized wetter and drier air systems creating greater mixing in boundary layers (Van Dijk *et al*., 2015).

Whilst the use of the more complex Penman-Monteith formulae (Monteith, 1965), may provide better results the detailed data input requirements are not always available, and the simplified short grass equation (PMgrass) in conjunction with crop specific K_c values have been used (Stephens *et al.*, 2001; Borek *et al*., 2010; Triana *et al.*, 2015). The use of K_c values for sugarcane did not perform as well as using the PMgrass base model (Figure 18). Based on the data in this study the following *Miscanthus* specific K_c values are suggested: early season 0.63; main season 0.85; late season 1.57; and 1.12 over winter. The main growing season K_c value is the

same as the 0.85 proposed by Beale *et al*. (1999) and within the wide range of 0.31 to 1.93 found by Triana *et al*. (2015). However, it is lower than the 1.20 suggested by Stephens *et al*. (2001) and the 1.15 for maize and 1.25 for sugarcane given by Allen *et al*. (1998). Clearly these measurement will to a degree be site specific and would benefit from testing at a wider number of sites, however they do represent an improvement in our knowledge especially for the non-growing season (Hay & Irmak, 2009).

5.5.2 Canopy precipitation interception

This study has shown that the *Miscanthus* crop is having a greater impact than short grass pasture on precipitation reaching the ground surface from the months of June (with the growth of leaves) through to the spring harvest date. High interception over July to September reflects the time when the canopy is at its fullest. However, it remains high into the autumn when the crop continues to intercept moisture after senescence due to stem density and some dead leaves remaining attached to stems until the end of January.

The measured interception of 24% from June to March is similar in value to the annual interception estimated for a mixed deciduous forest of 25% (Herbst *et al*., 2008), 21% for short rotation coppice (SRC) poplar (Hall & Allen, 1982), and the model prediction for SRC willow of 20% (Stephens *et al*., 2001), suggesting benefits for flood alleviation by reducing soil moisture recharge (Marshall *et al*., 2009). However, in contrast to forestry, the *Miscanthus* crop has a period after harvest each year when there is no, or very little, interception with only short stubble left in the field before spring regrowth. Nonetheless, interception by the *Miscanthus* canopy

will play a role in reducing soil moisture, particularly in the late autumn and early winter when higher rainfalls can occur.

Data collected in this study compares well to the measured results in plots of *Miscanthus* found by Riche and Christian (2001) of 25% in 1997/8, and 24% in 1998/9. There was a longer period of interception in this study due to the late harvest date in March as opposed to the more typical harvest time of early February. When the interception is calculated over a shorter timescale of June to January, as in the study by Riche and Christian (2001), the result is slightly higher at 26%. Use of the Gash interception model by Finch and Riche (2010) suggested that interception might be reduced by as much as 6% in larger scale plantations, but the results of this study do not support this suggestion. This may be due to an estimated value for field scale wet canopy evaporation used in the Gash model and obtained from the full Penman-Monteith equation (Monteith, 1965). This component has a large influence in the result (Gash *et al*., 1995; Gash *et al.*, 1999) and therefore the accuracy of the estimated evaporation rate will impact on the predicted interception. Higher measured interception than obtained via the Penman-Monteith equation has been noted before (Van Dijk *et al*., 2015) and shows the importance of this field estimate for accurate hydrological modelling. Another possible reason for this higher interception (and therefore wet leaf evaporation) than modelled is the lower albedo of 0.21 (Miller *et al.*, 2016) for *Miscanthus* during October and November compared to 0.23 for grass (Allen *et al*., 1998). This means the crop is reflecting less solar energy and retaining more heat energy.

This study shows the potential benefits for flood mitigation of *Miscanthus* compared to a short grass pasture with similar levels of interception to forestry and SRC, which

are coupled with the crop's high water use and conversion efficiency and higher winter ET rates. The most accurate of the formulae considered to predict ET rates was the simplified Penman-Monteith (short grass) equation. The *Miscanthus* specific K_c values suggested would benefit from being tested against other commercial scale plantations where ET_{EC} or other field measurements of ET are available. However, information from this study can be used to increase accuracy of yield models and in determining suitable areas for planting.

6 Soil & Water Assessment Tool (SWAT) simulated hydrological impacts of land use change from temperate grassland to energy crops: a case study in western UK

Amanda J. Holder[1], Jon P. McCalmont[2], Niall P. McNamara[3], Rebecca Rowe[3] and Iain S. Donnison[1]

[1]Institute of Biological, Environmental and Rural Sciences (IBERS), Aberystwyth University, Gogerddan, Aberystwyth, Wales, SY23 3EQ, UK

[2]College of Life and Environmental Sciences, University of Exeter, Rennes Drive, Exeter, EX4 4RJ, UK

[3]Centre for Ecology & Hydrology, Lancaster Environment Centre, Library Avenue, Bailrigg, Lancaster, LA1 4AP, UK

Publication Notes

This manuscript, under the same title, was accepted for publication in the peer reviewed journal Global Change Biology Bioenergy on 9 May 2019: GCB Bioenergy (2019) Early View. DOI: 10.1111/gcbb.12628

6.1 Abstract

When considering the large-scale deployment of bioenergy crops, it is important to understand the implication for ecosystem hydrological processes and the influences of crop type and location. Based on the potential for future land use change (LUC), the 10,280 km^2 West Wales Water Framework Directive River Basin District (UK) was selected as a typical grassland dominated district, and the Soil & Water Assessment Tool (SWAT) hydrology model with a geographic information systems interface was used to investigate implications for different bioenergy deployment scenarios. The study area was delineated into 855 sub-basins and 7,108 hydrological response units based on rivers, soil type, land use, and slope. Changes in hydrological components for two bioenergy crops (*Miscanthus* and short rotation coppice, SRC) planted on 50% (2,192 km^2) or 25% (1,096 km^2) of existing improved pasture are quantified. Across the study area as a whole, only surface runoff with SRC planted at the 50% level was significantly impacted, where it was reduced by up to 23% (during April). However, results varied spatially and a comparison of annual means for each sub-basin and scenario revealed surface runoff was significantly decreased and baseflow significantly increased (by a maximum of 40%) with both *Miscanthus* and SRC. Evapotranspiration was significantly increased with SRC (at both planting levels) and water yield was significantly reduced with SRC (at the 50% level) by up to 5%. Effects on streamflow were limited, varying between −5% and +5% change (compared to baseline) in the majority of sub-basins. The results suggest that for mesic temperate grasslands, adverse effects from the drying of soil and alterations to streamflow may not arise, and with surface runoff reduced and baseflow increased, there could, depending on crop location, be potential benefits for flood and erosion mitigation.

6.2 Introduction

Land use change (LUC) involving different crop types or management can influence ecosystem level hydrological processes. Quantification of these impacts is necessary to inform policy decisions based on trade-offs between a range of potential positive and negative environmental impacts (DeFries & Eshleman, 2004; Foley *et al*., 2005; Mohr & Raman, 2013). The use of bioenergy crops for renewable energy generation can help to reduce reliance on fossil fuels and attain climate change objectives (Chum *et al*., 2011; CCC, 2018a). Although large-scale uptake of dedicated energy crops in Europe has been slow to date (Lindegaard *et al*., 2016), their use as part of the energy generation mix is increasing (BEIS, 2018a) and renewable energy from biomass remains part of international and European climate mitigation policies (CCC, 2018b; IPCC, 2014). In Europe, as part of the long-term strategy and vision for a 'Climate neutral Europe by 2050', sustainable expansion of bioenergy crops is likely to target economically marginal lands, avoiding any perceived competition with food crops whilst maximizing returns for land owners (CCC, 2018b; European Commission, 2018). However, the implication of this LUC for ecosystem hydrological processing is not fully understood, particularly for second-generation (nonfood) bioenergy crops such as short rotation coppice (SRC; e.g. willow, *Salix spp*. and poplar, *Populus* spp.) and perennial grasses (e.g. switchgrass, *Panicum virgatum L*. and *Miscanthus, M. x giganteus*). Temperate grasslands comprise a third of the utilized agricultural area across Europe and present a large potential area for the deployment of energy crops (Eurostat, 2018a). Changes in grazing management and reductions in agricultural subsidies, combined with typically poorer quality soils, are resulting in large areas of grassland becoming economically unprofitable (Donnison & Fraser, 2016; Eurostat, 2018b; Taube *et al*., 2014). This is particularly

noticeable for European regions such as Wales (UK) with a grass-dominated agricultural landscape and a high proportion of land (80%) designated by the European Commission as 'Less Favoured Areas' (LFAs, agriculturally disadvantaged land in terms of soils, relief, aspect or climate, and receiving funding under the European Agricultural Fund for Rural Development, European Commission, n.d.b). Land suitability modelling suggests large areas (2,093 km^2, 36% of west Wales) are suitable for bioenergy crops *Miscanthus* and SRC (Lovett *et al*., 2014). Ambitious planting rates of up 50 km^2 yr^{-1} have also been proposed as attainable with the potential for rural employment and diversification highlighted (ADAS UK Ltd [ADAS] & Energy Technologies Institute [ETI], 2016), which is especially relevant in the light of the uncertain future of UK (and indeed European) agricultural subsidies.

In comparison with grazed grassland, *Miscanthus* and SRC have the potential to impact on soil hydrological balance through an increased demand for water (Clifton-Brown *et al*., 2002; Weih & Nordh, 2002), changes in root morphologies impacting water access through the soil profile (Crow & Houston, 2004; Neukirchen *et al*., 1999), differences in leaf development and morphology influencing evapotranspiration and precipitation interception (Finch & Riche, 2010; Holder *et al*., 2018; Stephens *et al*., 2001), and taller, stronger stems changing hydraulic resistance to overland flows (Kort *et al*., 1998; Marshall *et al*., 2009). As a result, there is generally an increase in evapotranspiration and a reduction in soil water recharge and surface runoff, compared to existing land uses (Holder *et al*., 2018; McCalmont *et al*., 2017; Rowe *et al*., 2009). These traits could be of benefit in landscape flood mitigation schemes (Environment Agency, 2015; Stephens *et al*., 2001) but can alter river flows and environments for aquatic and riparian species

(Arthington *et al*., 2010; Poff & Zimmerman, 2010) and adversely affect dryland areas (Langeveld *et al*., 2012). Resulting impacts of LUC to energy crops will be dependent on the extent of the area planted within river catchments and on regional climate, soil type, slope and altitude and stage of crop maturity (Hastings *et al*., 2014; Stephens *et al*., 2001; Vanloocke *et al*., 2010). This is reflected in previous studies of the impacts of land use conversions involving grassland to *Miscanthus* and SRC. For example, in modelled conversions from mixed land uses (grassland, corn and soybean) to *Miscanthus* in different regions of the American Midwest, Cibin *et al*. (2016) found that streamflow was reduced by around 8%, whereas Feng *et al*. (2018) found a mean reduction in streamflow of 23% (reflecting differing percentages of each land use type and varying topography). For SRC compared to conventional pasture, Hartwich *et al*. (2016) found that decreases in modelled surface runoff varied from 20% to 78% in their study of the Northern German Plain with regional differences in climate and soils. These differences highlight the need for location-specific modelling for the quantification of the potential impacts, positive or negative, of large-scale bioenergy cultivation. Hydrology simulation models linked to geographic information systems (GIS) can be used to gauge the effects of different LUC scenarios over varying spatial and temporal scales for specific locations, and a number of different models have been used in connection with biofuel scenarios (Engel *et al*., 2010; Finch *et al*., 2004; Vanloocke *et al*., 2010). The Soil & Water Assessment Tool (SWAT) is a physically based (i.e. representation of hydrological processes based on known principles of energy and water flux) hydrology model (Arnold *et al*., 1998) that can be incorporated into GIS software (Dile *et al*., 2016). SWAT has been widely used to assess the impacts on hydrology and water quality of different land use management strategies (Engel *et*

al., 2010) and has been successfully improved and used to represent *Miscanthus* and SRC crops (Hartwich *et al*., 2016; Trybula *et al*., 2015) enabling the use of the model for grassland LUC scenarios in Europe where the implications are unclear. In this study, we aim to utilize the SWAT model with a GIS interface to quantify how water yield (amount of water leaving the catchment), soil water storage, evapotranspiration, surface runoff, baseflow (groundwater flow) and streamflow respond to LUC from grassland to *Miscanthus* and SRC in a typical temperate agricultural grassland region at two planting levels: an ambitious 'maximum' (50% of available improved pasture) and more 'limited' (25% of improved pasture) level. Differences in responses between planting levels and bioenergy crop are also considered.

6.3 Materials and methods

6.3.1 West Wales River Basin and model description

The West Wales Water Framework Directive River Basin District (area 10,280 km^2), hereafter referred to as the watershed (Figure 21; Environment Agency, 2014), is located in the western part of the UK and was chosen as a temperate region of Europe dominated by grass-based agriculture and classed agriculturally as an 'LFA'.

Figure 21 Environment Agency England and Wales Water Framework Directive river basin districts. The area covered by the West Wales River Basin used in this study is shown in black. This figure contains public sector information licensed under the Open Government Licence v3.0

Hydrology for the watershed was modelled using the QSWAT v1.5 (rev. 664) extension with QGIS software (QGIS, 2014) and SWAT 2012 Editor interface (Arnold *et al.*, 1998; Dile *et al.*, 2016). A physical description of the watershed within the model (representing the baseline scenario of existing land use and conditions) was built up using the GIS layers detailed in Table 16.

Table 16 Description of data used within the SWAT hydrology model with source reference.

Data type	Resolution	Source
Digital Elevation Model	50 m	OS Terrain 50 (Ordnance Survey, 2018)
Soil	1 km	Soil Parent Material (British Geological Survey Materials, 2018)
	5 km	The Digital Soil Map of the World v3.6 (UNFAO, 2003)
Land use	25 m	Land Cover Map 2015 (Rowland *et al*., 2017)
River network	15-30 m	OS Open Rivers (Ordnance Survey, 2018)
Inland water bodies	—	UK Lakes Portal (CEH, n.d.)
	—	GB Lakes Inventory (NRW, 2018)
Streamflow	7 locations	National River Flow Archive 2018 (NERC & CEH, n.d.)
Climate	19 locations	National Centres for Environment Prediction (NCEP, n.d.)
	4 locations	Met Office climate data (Met Office, 2014)

The United Nations Food and Agriculture Organisation's map (UNFAO, 2003), showing dominant soil types, was matched to the soil types given in the British Geological Survey soils map (British Geological Survey Materials, 2018) and the SWAT database soil codes. The watershed consists of mainly loamy soils with varying amounts of clay, silt and sand. Dystric Cambisols account for 50% of the area, Dystric Gleysols 23% and Gleyic Cambisols 19%. The remainder consists of small areas of Podzol (5%) and Humic Gleysols (2%). The watershed is

predominately made up of low quality agricultural land (Welsh Government, n.d.), 40% of the watershed is >15% slope and 42% is >200 m a.s.l. (Ordnance Survey, 2018). The dominant agricultural land is improved grass pasture (52%), with only 4% of the area designated as arable or horticulture. Urban areas account for 3% of the watershed with the remainder of the land cover made up of natural grasslands (19%), woodlands (18%), and small pockets of heath and marsh (4%; Rowland *et al*., 2017). The watershed was delineated into 855 sub-basins based on the digital elevation model and river data. hydrological response units (HRUs) within each sub-basin were divided based on soil type, land use and slope (divided into two bands, above and below 15%). Insignificant HRUs were excluded using the following threshold filters to ignore areas of less than: 10% land use; 20% soil class; and 10% slope band; and redistributed proportionally among those remaining (Dile *et al*., 2018). Climate data[21] were obtained for 15 years from 1999 to 2013, the most recent period with all required data available (Table 16). The SWAT model was run on a monthly time step for the full duration using 1999 to 2003 as a 5 year warm up period (no results from the warm up period are used in the analysis). Climate data (precipitation, wind, relative humidity and solar radiation) obtained from the National Centers for Environmental Prediction (NCEP, n.d.) were checked for accuracy with long-term weather data ranges using four UK Met Office climate stations (Met Office, 2014) located within the watershed (Figure 22). Mean annual precipitation in the watershed from 2004 to 2013 was 1,532 mm (Met Office, n.d.b). Potential evapotranspiration (PET) was calculated with the r (R Core Team, 2015) package 'Evapotranspiration' Penman Monteith formula for short grass (Guo & Westra, 2016) using data from a representative weather station (Figure 22; Appendix

[21] Climate data on a daily basis.

A3.1) and read into the SWAT model (Neitsch *et al*., 2011). This resulted in the mean watershed PET being within estimates for the location and land cover type (based on Nisbet, 2005). Actual evapotranspiration was calculated within the SWAT model taking account of evaporation of canopy intercepted precipitation, crop transpiration and soil evaporation and sublimation, as detailed in the SWAT theoretical documentation (Neitsch *et al*., 2011).

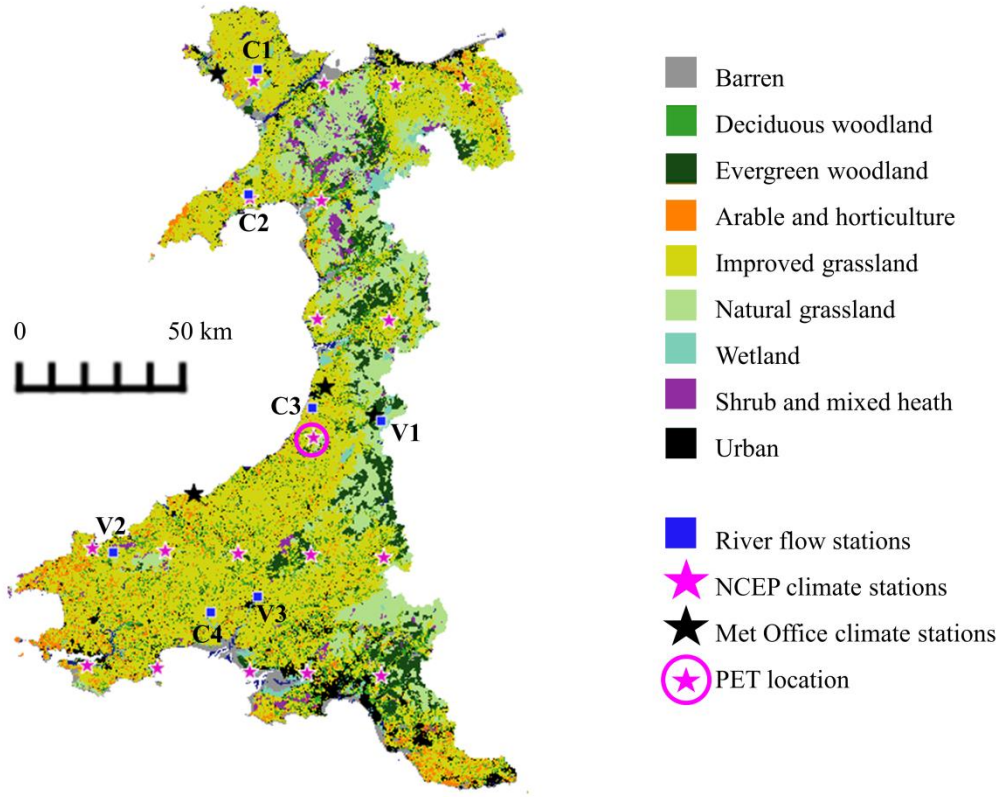

Figure 22 Land use as represented in the baseline Soil & Water Assessment Tool (SWAT) model for west Wales watershed (based on the Land Cover Map 2015, Table 16). Observed river flow from calibration (C1–C4) and validation (V1– V3) gauging stations was used to calibrate SWAT model predictions. Weather data were obtained from the National Centers for Environmental Prediction (NCEP) climate locations and UK Met Office climate stations. Potential evapotranspiration (PET) was calculated using data from the circled climate location

The curve number (CN) method (USDA, 1986) was used in relation to simulation of surface runoff within the model with adjustments allowed based on the steepness of the slope.

6.3.2 Plant growth simulation and management

In order to reflect expected growth rates for the region, plant inputs for the different land cover types were adjusted from the SWAT default values using values from the literature and, in the case of *Miscanthus*, some data was also obtained from measurements taken at a field-scale trial site within the watershed. The main plant inputs used for the LUC crops and other land use cover plant types are shown in Tables 17 and 18, respectively. Arable agriculture in the watershed was based on typical crops grown in the region: wheat, barley, oats and oilseed rape (Welsh Government, 2018b). Woodland biomass at the start of the simulations was input as 153 Mg DM ha^{-1} for evergreen forests and 136 Mg DM ha^{-1} for deciduous woodland (Forestry Commission, 2011, 2017).

Table 17 Main plant growth inputs for the land use change crops used in the simulations: Pasture (based on the SWAT land use code CRDY), *Miscanthus* and short rotation coppice. Values were taken from the SWAT database (SWAT: crop), measurements) or from the ranges suggested in the references. Where no reference is listed, a best estimation value was used

Input description	**Pasture (CRDY)**	***Miscanthus***	**Short Rotation Coppice**
Radiation use efficiency (kg ha^{-1}/MJ m^{-2})	10 (Belanger *et al.*, 1994; Cristiano *et al.*, 2015)	42 (Trybula *et al.*, 2015) Measurements	28 (Bullard *et al.*, 2002; Linderson *et al.*, 2007; Verlinden *et al.*, 2013)
Max. stomatal conductance (m s^{-1})	0.005 (SWAT: Tall Fescue)	0.005 (Beale *et al.*, 1996; Clifton-Brown & Lewandowski, 2000)	0.004 (SWAT: poplar)
Light extinction coefficient	0 (SWAT: Tall Fescue)	0.68 (Clifton-Brown & Lewandowski, 2000)	0.5 (Linderson *et al.*, 2007)
Max. leaf area index	4 (Asner *et al.*, 2003)	11 (Trybula *et al.*, 2015)	9 (Pellis *et al.*, 2004; Schmidt-Walter & Lamersdorf, 2012; Hartwich *et al.*, 2016)
Min. leaf area index during dormancy	0.8	0 (Trybula *et al.*, 2015; Guo *et al.*, 2018)	0.75 (SWAT: poplar)
Max. canopy storage (mm)	0	2.2 (Stephens *et al.*, 2001)	2.2 (Stephens *et al.*, 2001; Schmidt-Walter & Lamersdorf, 2012)
Max. canopy height (m)	0.75	3 Measurements	8 (Hartwich *et al.*, 2016)
Max. root depth (m)	2 (SWAT: Tall Fescue)	2.5 (Neukirchen *et al.*, 1999)	2 (Hartwich *et al.*, 2016)
Optimum temperature (°C)	15 (SWAT: Tall Fescue)	20	15
Base temperature (°C)	0 (SWAT: Tall Fescue; Hurtado-Uria *et al.*, 2013)	8 (Hastings *et al.*, 2009)	5 (Hartwich *et al.*, 2016)

Table 18 Main plant growth values used in the simulations for the land use types of arable (AGRL), lawn grass (BERM), natural grassland (FESC), evergreen forest (FRSE), heather/shrub grassland (MIGS), deciduous woodland (OAK), heather (SHRB) and fen/marsh/bog/saltmarsh (WETL). The model input variable name (Code) and references are shown where used (SWAT denotes the SWAT database)

Description	Code	AGRL	BERM	FESC	FRSE	MIGS	OAK	SHRB	WETL
Radiation use efficiency (kg ha^{-1}/MJ m^{-2})	BIO_E	33.5 (SWAT)	10 (Belanger *et al.*, 1994)	15 (Belanger *et al.*, 1994; Cristiano *et al.*, 2015)	15 (SWAT)	2 (Garbulsky *et al.*, 2010)	2 (Garbulsky *et al.*, 2010)	2 (Garbulsky *et al.*, 2010)	5 (Garbulsky *et al.*, 2010)
Max. leaf area index	BLAI	5 (Asner *et al.*, 2003; AHDB 2018)	4 (SWAT)	4 (SWAT)	6 (Asner *et al.*, 2003)	4 (Asner *et al.*, 2003)	6.5 (Asner *et al.*, 2003; ORNL DAAC, n.d.)	3.5 (Asner *et al.*, 2003; Gonzalez *et al.*, 2013)	5 (Asner *et al.*, 2003)
Max. canopy storage (mm)	CANMX	0.8 (Wang *et al.*, 2006)	—	1.2 (Burgy *et al.*, 1958)	3.7 (Hörmann *et al.*, 1996)	1.5 (Dunkerley, 2000)	2.3 (Hörmann *et al.*, 1996)	1.5 (Dunkerley, 2000)	1.2 (Burgy *et al.*, 1958)
Optimum temperature (°C)	TOPT	20 (Finch *et al.*, 2002)	15 (SWAT: FESC)	15 (SWAT)	20	15 (SWAT: FESC)	15 (Bequet *et al.*, 2011)	15	15
Base temperature (°C)	TBASE	5 (Finch *et al.*, 2002)	0 (SWAT: FESC)	0 (SWAT)	0 (SWAT)	0 (SWAT: FESC)	5 (Bequet *et al.*, 2011)	0	5
Fraction of tree biomass converted to residue	BIO_LEAF	—	—	—	0.0045 (Yang & Zhang, 2016)	—	0.003 (Yang & Zhang, 2016)	—	—
No. years to tree maturity	MAT_YRS	—	—	—	30 (SWAT)	—	100	—	—

6.3.3 *Miscanthus field measurements*

A number of plant growth input values available in the literature for *Miscanthus* are based on measurements made in the American Midwest region from fertilized crops. Therefore, to check the suitability for their use in the region simulated in this project, the main *Miscanthus* growth values were checked using data obtained from an established *Miscanthus* plantation (~6 ha) located within the watershed. A full description of the field site (planted in 2012) and methods used for biomass sampling are given in McCalmont *et al*. (2017). Mean annual harvest yields simulated by the model (14.74 Mg ha^{-1}, 2004–2013) were checked against the mean peak autumn yield (14.95 Mg ha^{-1}, 2014–2016, J. P. McCalmont, unpublished data) recorded at the site. The value used for radiation use efficiency (BIO_E: 41, Trybula *et al*., 2015) was found to be similar to an estimate of 42 made using measurements of photosynthetically active radiation and gains in *Miscanthus* above and belowground biomass between May 2015 and November 2016 (J. P. McCalmont, unpublished data). Canopy height was recorded weekly during the 2017 growing season at eight randomly located measuring points within the crop (locations as shown in Holder *et al.*, 2018) and reached a maximum of 3 m.

Above ground biomass samples taken in February, June and August 2017 (from locations close to the eight measuring points) were freeze dried and subsequently ground to <2 mm using a Retsch mill (SM100; Retsch, Haan, Germany) before being further cryomilled in liquid nitrogen to a fine powder (6870 Cryomill; SPEX, Stan-hope, UK). Samples were then analysed for total nitrogen (N) using a Vario Macro Cube Elementar (Analysensysteme GmbH, Langenselbold, Germany). Analysis of total phosphorus (P) was carried out by IBERS Analytical Chemistry

(Aberystwyth, UK). This provided estimates of N and P at three seasonal time points (Table 19).

Table 19 Model inputs relating to *Miscanthus* above ground biomass nutrient contents (N, nitrogen; P, phosphorus) and residue decomposition rate. 'Source reference' details whether the value used for the SWAT model input (Code) was sourced from the literature (reference given) or derived from sampling at the field site within the watershed (measurement, with month samples taken).

Description	Code	Value	Source reference
fraction N in yield	CNYLD	0.0032	measurement (February)
fraction P in yield	CPYLD	0.0005	measurement (February)
fraction N in biomass at emergence	BN1	0.024	measurement (June)
fraction N in biomass at 50% maturity	BN2	0.009	measurement (August)
fraction N in biomass at maturity	BN3	0.005	(Ng *et al*., 2010; Trybula *et al*., 2015; Guo *et al*., 2018)
fraction P in biomass at emergence	BP1	0.0024	measurement (June)
fraction P in biomass at 50% maturity	BP2	0.0016	measurement (August)
fraction P in biomass at maturity	BP3	0.0009	(Trybula *et al*., 2015)
plant residue decomposition coefficient (fraction)	RDSCO_PL	0.002	(Amougou *et al*., 2012)

6.3.4 Management operations

The following management operations were employed within the model depending on the land use/scenario for each HRU.

6.3.4.1 Improved grassland

Sheep grazing at a stocking density of two livestock units starting in April for a duration of 212 days (to a minimum biomass of 1.5 Mg DM ha^{-1}; Genever & Buckingham, 2016). The daily dry weight of biomass eaten and trampled was set to

18 kg ha^{-1} (each), and fresh manure inputs to 60% of biomass consumed. Nitrogen fertilizer was added in March, April and July (40, 50, 20 kg N ha^{-1} respectively) and phosphorus was added in March, April and September (25, 15, 10 kg P ha^{-1} respectively; DEFRA, 2017c)[22].

Pesticides were applied on a 2 year rotation: Year 1, Fluroxypyr MHE, Clopyralid and Triclopyr amine (0.32, 0.23, 0.42 kg ha^{-1}) were added in mid-April based on the contents of Pastor®; Year 2, Glyphosate amine (0.54 kg ha^{-1}) was added at the beginning of October based on Roundup 360® (Ballingall, 2014; Fera Science Ltd, 2018)[23].

6.3.4.2 Miscanthus

Fertilizer was automatically added by SWAT (according to crop N stress levels) to a maximum of 60 kg N ha^{-1} $year^{-1}$ (amount required to obtain realistic yields within the model) and the above ground biomass was harvested annually in November at a 90% efficiency (based on field observations).

6.3.4.3 Short rotation coppice

Fertilizer was automatically added by SWAT (according to crop N stress levels) to a maximum of 5 kg N ha^{-1} $year^{-1}$ (being the amount required to obtain realistic yields within the model) and above ground biomass harvested in November on a 3 year rotation with a 70% efficiency (based on the SWAT database and Guo *et al*., 2015).

[22] and
[23] Management practices are likely to vary and these values reflect ideal practice used to maximise productivity.

6.3.4.4 Lawn grass

Fertilizer was automatically added to a maximum of 40 kg N ha^{-1} $year^{-1}$. Grass was cut from April to August every 2 weeks, and then once a month during September and October.

6.3.4.5 Arable

Fertilizer was automatically added to a maximum of 26 kg P ha^{-1} $year^{-1}$ and 111 kg N ha^{-1} $year^{-1}$ (DEFRA, 2017). All above ground biomass harvested (and plant growth killed) annually on 1 August (AHDB, 2018).

6.3.4.6 Natural grassland

Light cattle grazing at a stocking density of 1.2 livestock units from mid-May for a duration of 90 days (to a minimum biomass of 3 Mg DM ha^{-1}; Genever & Buckingham, 2016). The daily dry weight of biomass eaten and trampled was set as 22.5 kg ha^{-1} (each), and fresh manure inputs were 60% of biomass consumed. Beef fresh manure was also automatically added to a maximum of 25 kg ha^{-1} $year^{-1}$ (DEFRA, 2017; Welsh Government, 2018b).

6.3.5 Calibration

The initial model (representing existing land use) was calibrated for streamflow using the SWAT-CUP 2012 v.5.1.6 Sequential Uncertainty Fitting (SUFI2) procedure (Abbaspour, 2015) and the protocol outlined in Abbaspour *et al*. (2015). Water flow calibration and validation stations were selected from the National River Flow Archive (NERC & CEH, n.d.), discarding those with outside factors that may influence flow (e.g. private ground water extraction). To achieve calibration, only watershed level parameters were amended (Table A-25). Observed streamflow from gauging stations C1 to C4 (Figure 22) was compared to modelled streamflow from

the relevant sub-basin outlet and accuracy was assessed using R^2 and Nash–Sutcliffe efficiency results. Gauging stations located at V1–V3 (Figure 22) were used to validate the modelled streamflow data.

6.3.6 Scenarios

The baseline scenario is the calibrated model with existing land use. Four further simulations were run by splitting and changing the existing improved pasture land use and management to include the relevant percentage of energy crop (restricted to <15% slope, DEFRA, 2002; Lovett *et al*., 2014). *Miscanthus* planted on 50% (M50) and 25% (M25) and SRC planted on 50% (SRC50) and 25% (SRC25) of existing improved grass pasture within each sub-basin. The maximum LUC scenario using 50% of existing pasture (2,192 km^2) is based on the potentially suitable land in the district suggested in Lovett *et al*. (2014). The reduced, limited, level of LUC at 25% (1,096 km^2) reflects a level that could be reached in ~20 years if potential ambitious planting schemes (ADAS & ETI, 2016) were taken up.

6.3.7 Analysis of results

Data analysis was performed in r version 3.5.1 (R Core Team, 2015) using linear models and linear mixed models (package 'nlme', Pinheiro *et al*., 2017), with Tukey HSD (package 'multcomp', Hothorn *et al*., 2008) post-hoc tests for significant results. Model residual plots were checked for the appropriateness of each model. Linear mixed model results were summarized using type III ANOVA (package 'car', Fox & Weisberg, 2011) which performs a Wald chi-square test[24]. For each level of planting, maximum (50%) or limited (25%), impacts of the crop type (baseline, *Miscanthus* and SRC) and season on the hydrological components of surface runoff,

[24] denoted as χ^2

baseflow, soil water content, evapotranspiration and water yield were explored using whole watershed means calculated for each month (2004–2013). For surface runoff, baseflow and water yield transformations were used to improve model residuals (cube root with surface runoff and square root with baseflow and water yield). Analysis was conducted separately for each planting level with models including crop type and month (and their interactions) as fixed factors and year as a random effect, with an auto correlation structure (AR1). In addition, to compare between planting levels and bioenergy crop type, differences to the baseline (mm change in monthly means) were used. Linear mixed models included the fixed factors of LUC level (25% and 50%), crop type (*Miscanthus* and SRC), month, and the random effect of year and an auto correlation structure (AR1). Surface runoff and baseflow data were transformed before testing (cube root and natural logarithm transformations respectively). To allow for spatial effects to be examined, mean annual values (2004–2013) for all sub-basins were produced and impacts on surface runoff, baseflow, soil water content, evapotranspiration, water yield and streamflow were examined separately for each level of planting (50% or 25%) using linear models with crop type (SRC, *Miscanthus*, baseline) as a fixed factor. Streamflow data were transformed using the natural logarithm to improve residuals.

6.4 Results

6.4.1 Model calibration

The watershed area was delineated into 855 sub-basins (Figure 23) and 7,108 HRUs. Satisfactory calibration between observed and modelled streamflow was achieved with Nash–Sutcliffe efficiency coefficient values of >0.50 for the baseline scenario representing existing land cover (Table 20; Figure A-33–A-38). The CNs were increased from starting values for land in good hydrological condition in order to improve the correlation between observed and modelled streamflow. The final values used are shown in Table 21. Following amendments to plant growth parameters, simulated yields were checked against published data (Table 22; Figure A-40–A-43).

Table 20 Results of the correlation (R^2 and Nash–Sutcliffe [NS] values) between the observed streamflow at the calibration (C1–C4) and validation (V1–V3) locations (Figure 22) and the streamflow predictions for the relevant sub-basin

Location	R^2	NS
C1	0.65	0.50
C2	0.73	0.67
C3	0.84	0.67
C4	0.83	0.81
V1	0.87	0.56
V2	0.76	0.59
V3	0.88	0.76

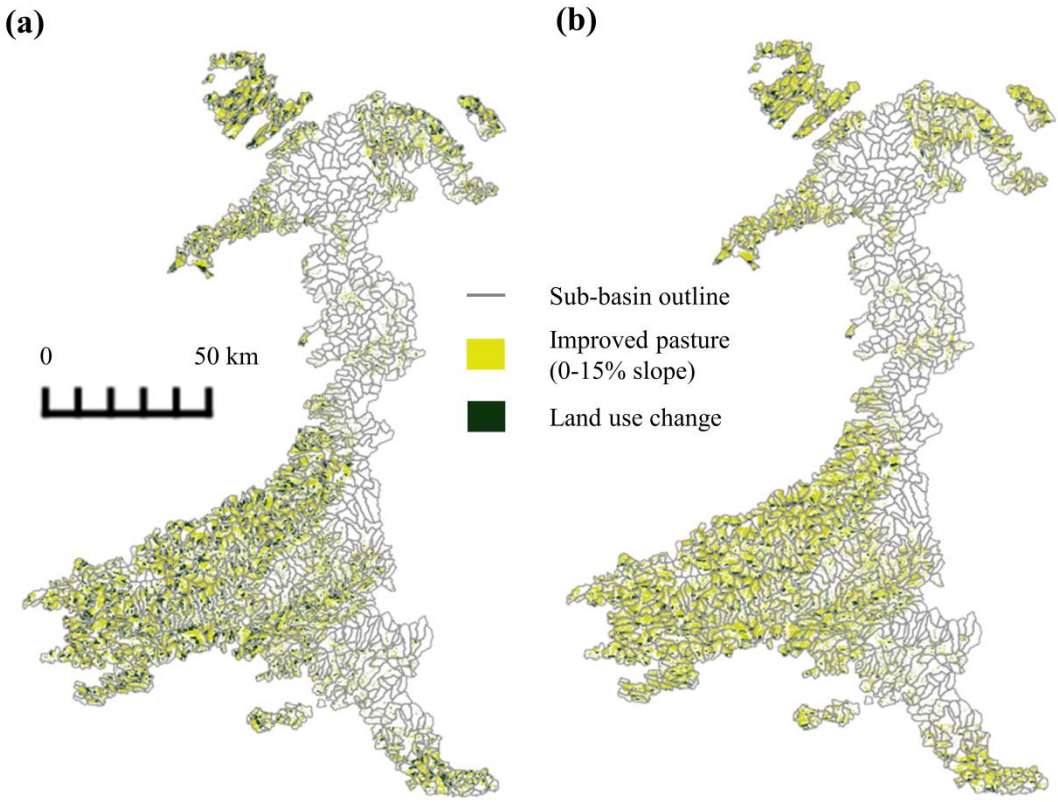

Figure 23 The West Wales River Basin District watershed delineated into 855 sub-basins. The spread of the (a) maximum and (b) limited land use change scenarios (50% and 25%, respectively, of improved pasture in each sub-basin) is represented

Table 21 Values used for the SWAT input codes (Code) controlling water erosion (USLE_C) and surface runoff via Manning's N roughness coefficient (OV_N) and Soil Conservation Service Curve Number for each hydrological soil group (SCS A–D, USDA, 1986). Details shown are for the land use types of arable (AGRL), lawn grass (BERM), improved grass pasture (CRDY), natural grassland (FESC), evergreen forest (FRSE), heather/shrub grassland (MIGS), deciduous woodland (OAK), heather (SHRB) and fen/marsh/bog/saltmarsh (WETL). Source reference or SWAT database crop type are shown for the land use change crops of CRDY, *Miscanthus* (MSXG) and short rotation coppice (WSRC).

Code	AGRL	BERM	CRDY	FESC	FRSE	MIGS	MSXG	OAK	SHRB	WETL	WSRC
USLE_C	0.2	0.003	0.003 (SWAT: pasture)	0.003	0.001	0.003	0.003 (SWAT: alamo)	0.001	0.003	0.003	0.001 (SWAT: poplar)
OV_N	0.14	0.1	0.15 (SWAT: pasture)	0.1	0.1	0.15	0.24 (Cibin *et al.*, 2016)	0.14	0.15	0.05	0.14 (SWAT: poplar)
SCS_A	72	49	68	49	45	48	31	45	48	49	30
SCS_B	81	69	79	69	66	67	59	66	67	69	55
SCS_C	88	79	86	79	77	77	72	77	77	79	70
SCS_D	91	84	89 (Hess *et al.*, 2010; USDA, 1986: grazed, no mulch)	84	83	83	79 (Cibin *et al.*, 2016)	83	83	84	77 (USDA, 1986: trees, good)

Table 22 SWAT simulated and reference mean biomass (for the month of August, 2004–2013) or yield (Y and harvest month) in dry mass units of Mg DM ha^{-1}. The SWAT database code used as the basis for each land use is shown; short rotation coppice (WSRC) and *Miscanthus* (MSXG) were added to the internal project database.

Land Use	**Code**	**Simulated** (Standard Deviation)	**Reference**
Cereals/Oil Seed Rape	AGRL	Y Aug: 4 (2.5)	7 Cereals, 3 Oil Seed Rape (DEFRA, 2017b)
Urban grass (mowed)	BERM	1.5 (0.4)	~4 cm sward height
Improved pasture (grazed)	CRDY	2.86 (2.6)	~2 depending on grazing strategy (Genever & Buckingham, 2016)
Natural grassland (light grazing)	FESC	3.5 (0.3)	3-7 (Mills, 2016); 1-3 (Milne, *et al.*, 2002)
Heather/shrub grassland	MIGS	9.75 (2.78)	6-27 (Mills, 2016) ; 5-10 (Milne *et al.*, 2002)
Heather	SHRB	9.10 (2.26)	6-10 (Mills, 2016); 5-10 (Milne *et al.*, 2002)
Fen/marsh/bog/saltmarsh	WETL	14.78 (10.74)	1-22 (Mills, 2016)
Short rotation coppice	(WSRC)	Y Nov: 13.71 (8.02)	5-16 (Aylott *et al.*, 2008); 10-15 (Cunniff *et al.*, 2015)
M. x giganteus	(MSXG)	Y Nov: 14.74 (9.92)	14 (Larsen *et al.*, 2014); 15 measurements

6.4.2 Effects at the West Wales River Basin watershed level

Impacts for the whole 10,280 km^2 watershed varied across the months with the greatest differences occurring during the growing season (May–September, Figure 24). However, of the hydrological components tested (surface runoff, baseflow, soil water content, evapotranspiration and water yield), only surface runoff was significantly different compared to the baseline, where planting SRC at the 50% level resulted in significant reductions ($p = 0.03$) ranging from 17% (8 mm, January) to 23% (3 mm, April; Figure 24a).

Using the percentage change (compared to the baseline) to assess impacts of planting levels and bioenergy crop types, the 50% planting level (with both *Miscanthus* and SRC) led to greater reductions in overall surface runoff than at the 25% level ($\chi^2(1) = 4.56$, $p = 0.03$). In contrast, although the 50% planting level resulted in greater increases in baseflow than the 25% level ($\chi^2(1) = 49.94$, $p < 0.001$), impacts were significantly different between the bioenergy crop types, where baseflow was increased more during the spring with *Miscanthus* than with SRC ($\chi^2(1) = 10.21$, $p = 0.001$; Figure 24b). The direction of change for evapotranspiration following LUC differed with bioenergy crop type, where it was increased with SRC during the early part of the year (January–May), but decreased with *Miscanthus* during the same period ($\chi^2(11) = 118.42$, $p < 0.001$; Figure 24c). From October to December, both crop types showed a decrease following higher evapotranspiration over the growing season. Greater impacts generally resulted from the 50% planting level compared to the 25% level, although this also depended on crop species with greater differences found with *Miscanthus* than SRC ($\chi^2(1) = 10.86$, $p = 0.001$). Water yield showed a decrease during the growing season with both bioenergy crops; however, during the early part of the year, the *Miscanthus* crop resulted in an increase, which was in

contrast to the decreasing trend with SRC ($\chi^2(11) = 27.85$, $p = 0.003$). Impacts were again greater at the 50% planting level compared to the 25% but differences between crop types and planting levels were low from October to December ($\chi^2(1) = 10.92$, $p = 0.001$).

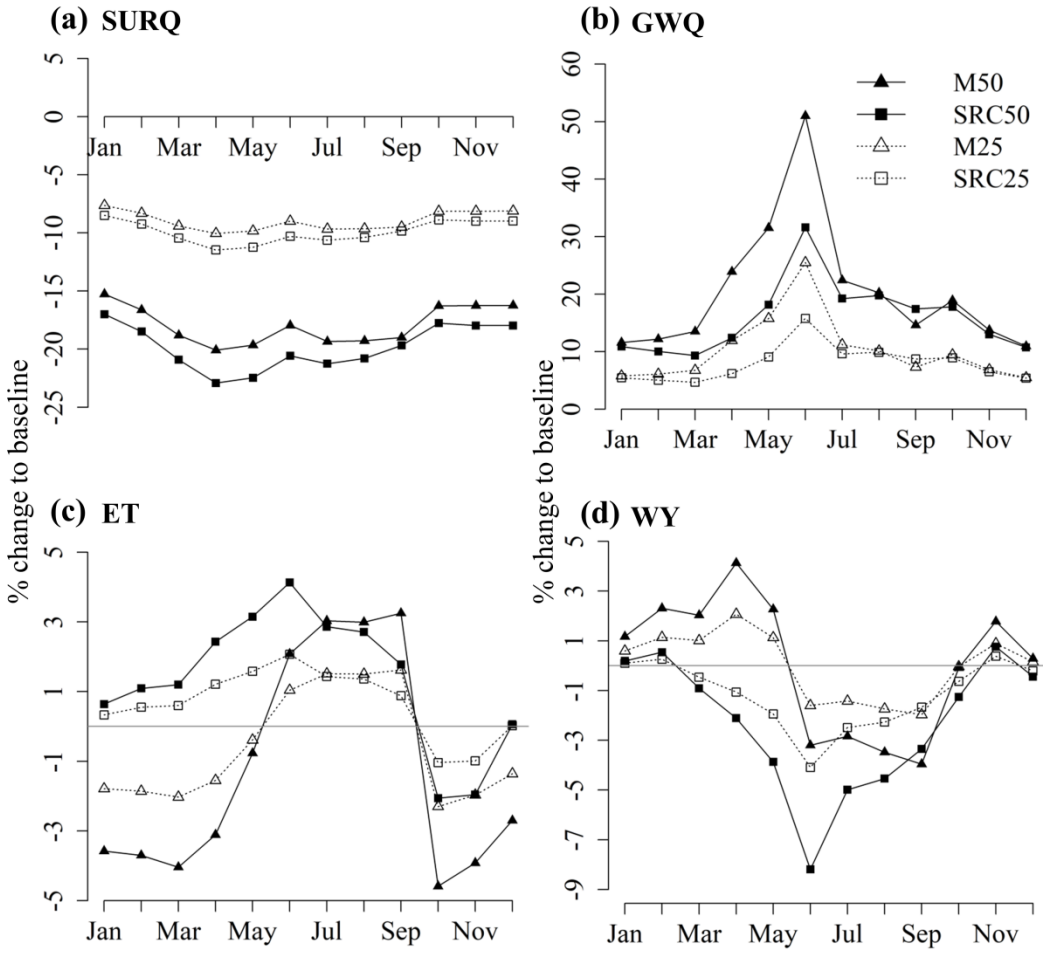

Figure 24 Percentage difference in the mean monthly (a) surface runoff (SURQ), (b) baseflow (GWQ), (c) evapotranspiration (ET) and (d) water yield (WY), based on the 10 year simulation period, for each of the land use change scenarios compared to the baseline scenario of no land use conversion. The scenarios shown are *Miscanthus* (M50 and M25) and short rotation coppice (SRC50 and SRC25) planted on approximately 50% (2,192 km^2) or 25% (1,096 km^2) of improved pasture areas on or below a 15% slope

6.4.3 Sub-basin variation

Land use change was simulated in 726 of the 855 sub-basins (Figure 23), although it is also possible for non-LUC sub-basins to be impacted if, for example, they are downstream of the change. As changes in streamflow were limited in the majority of sub-basins (Figure 25) and maximum changes in soil water content ranged from −3% to +2% across all the sub-basins, these components were not found to significantly vary spatially (soil water content $F_{2,2562} = 0.46$, $p = 0.63$; $F_{2,2562} = 1.83$, $p = 0.16$; streamflow $F_{2,2562} = 0.30$, $p = 0.74$; $F_{2,2562} = 0.38$, $p = 0.68$; at the 25% and 50% levels respectively). However, reductions in streamflow of more than 50% were found in the same 10 sub-basins for each LUC scenario. Streamflow in these 10 sub-basins ranged from 0.5 to 1.6 $m^3 s^{-1}$ (daily mean) in the baseline (existing land use) scenario.

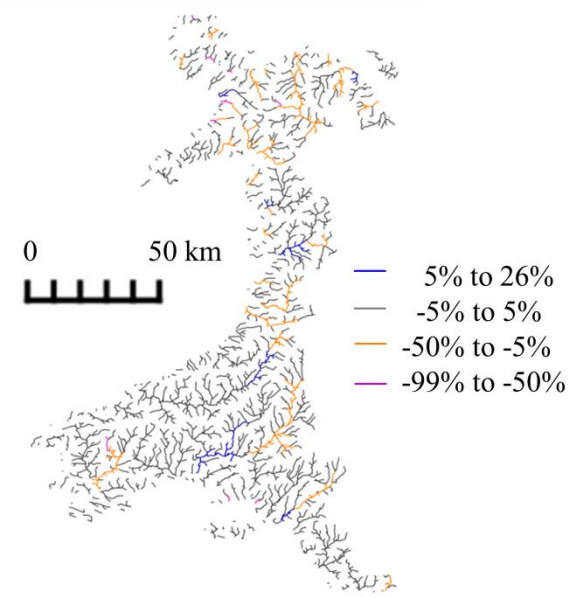

Figure 25 Mean percentage change in streamflow compared to the baseline. The change was the similar for each of the land use change (LUC) scenarios, and the percentage shown is the same for each crop type and LUC level.

The different LUC levels and crops had varying impacts on the other hydrological components (Figure 26; Table 23). Surface runoff was significantly lower than the baseline scenario for *Miscanthus* and SRC in both the 25% ($F_{2,2562}$ = 32.77, $p < 0.001$) and 50% ($F_{2,2562}$ = 156.8, $p < 0.001$) scenarios, with differences ranging from 0 to −182 mm (0% to −40%, Figure 26a). No significant differences in surface runoff were found between *Miscanthus* and SRC.

Baseflow results also showed greater differences in *Miscanthus* compared to SRC in the 50% LUC scenario where a significant difference ($p = 0.02$) was found between the two crops (Figure 26b). Eighty-four sub-basins in the M50 scenario increased baseflow by more than 30%, compared to 11 sub-basins in the SRC50 scenario. The maximum amount of the increase was 39% (136 mm) for M50 and 36% (127 mm) for SRC50. Baseflow was significantly higher than the baseline scenario for both *Miscanthus* and SRC in the 25% ($F_{2,2562}$ = 70.29, $p < 0.001$) and 50% ($F_{2,2562}$ = 233.6, $p < 0.001$) LUC scenarios.

Changes in evapotranspiration with *Miscanthus* and SRC compared to the pasture baseline ranged from −2% (−15 mm, M50) to 5% (+32 mm, SRC50) and whilst the difference was only significant for SRC ($p < 0.001$), a distinct difference was seen between the two crops ($p < 0.001$). Where changes in evapotranspiration relating to the *Miscanthus* scenarios occurred, the result was a small reduction; however, with SRC increases were produced (Figure 26c). The same trend was identified in the 25% LUC scenarios. It was also found that some of the sub-basins with the highest increase in evapotranspiration also had the highest reductions in water yield (Figure 26c,d). Changes in water yield compared to the baseline scenario were not significant at the 25% LUC level. However, for the 50% LUC scenarios, SRC was

significantly lower than both the *Miscanthus* (p = 0.001) and baseline (p = 0.01) scenarios (Figure 26d). Differences in water yield ranged from a reduction of 4% (−30 mm, SRC50) to an increase of 2% (+16 mm, M50).

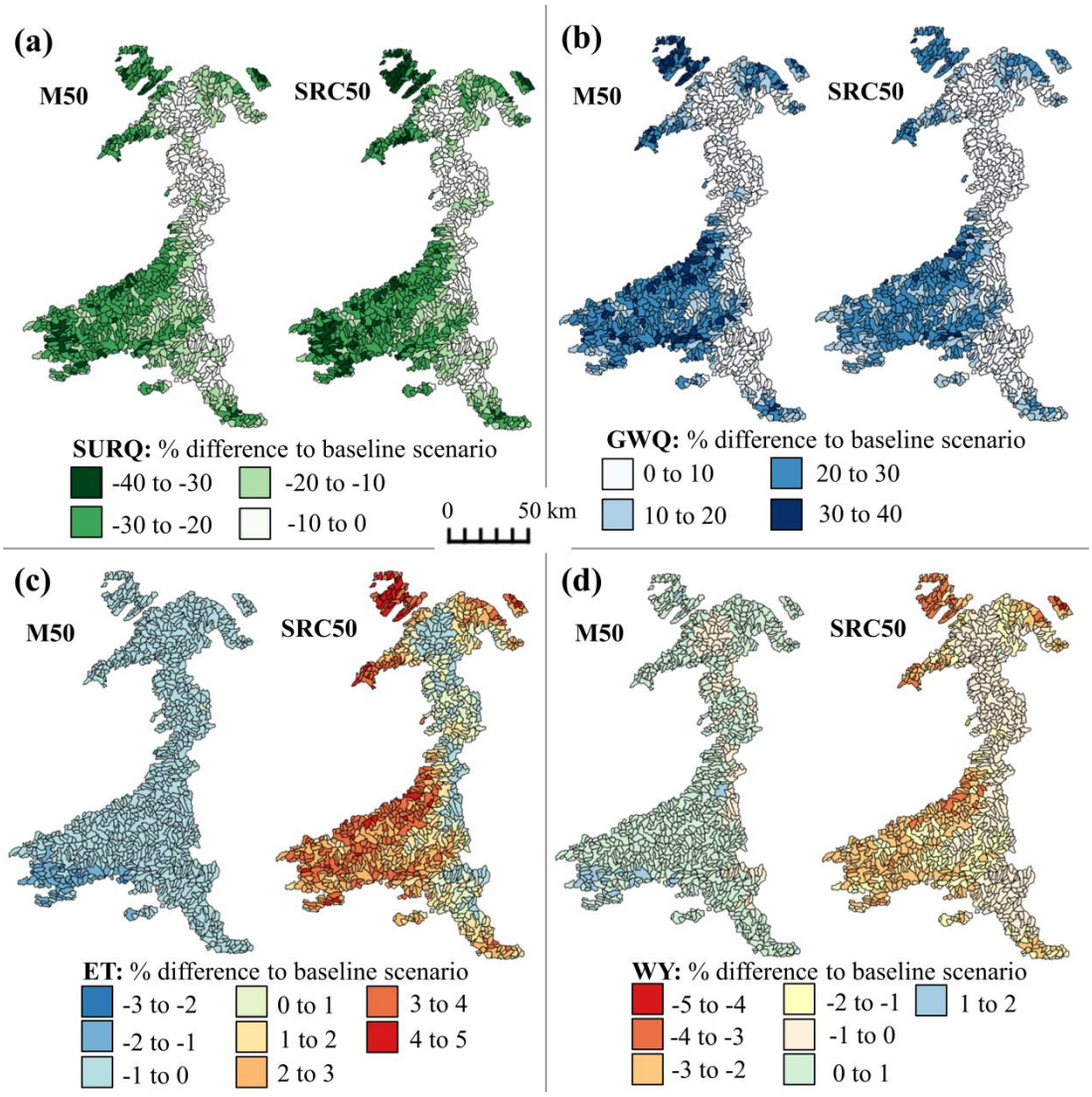

Figure 26 Percentage difference in mean annual (a) surface runoff (SURQ), (b) baseflow (GWQ), (c) evapotranspiration (ET) and (d) water yield (WY) over the 10 year simulation period for the maximum land use change scenarios compared to the baseline case of no land use conversion. The scenarios shown are *Miscanthus* (M50) and short rotation coppice (SRC50) planted on approximately 50% (2,192 km^2) of improved pasture areas on or below a 15% slope.

Table 23 Mean annual sub-basin surface runoff (SURQ), baseflow (GWQ), soil water content (SW), evapotranspiration (ET) and water yield (WY) in mm, and streamflow (daily mean, m^3 s^{-1}) for each of the scenarios (SE shown in brackets). The scenarios reflect planting *Miscanthus* (M) or short rotation coppice (SRC) on approximately 50% (2,192 km^2) and 25% (1,096 km^2) of existing improved pasture areas compared to the baseline (Base) of no land use change. Significance ($p < 0.001$) is shown for Base versus M/SRC.

	Base	**25%**		**50%**	
	(mm)	**M**	**SRC**	**M**	**SRC**
SURQ	344 (4)	314 (3) ***	311 (3) ***	284 (3) ***	278 (3) ***
GWQ	387 (2)	417 (2) ***	413 (2) ***	477 (2)***	439 (2) ***
SW	166 (0.3)	166 (0.3)	166 (0.3)	167 (0.3)	167 (0.3)
ET	678 (1)	677 (1)	684 (1) ***	676 (1)	691 (1) ***
WY	851 (3)	852 (3)	845 (3)	853 (3)	838 (3) ***
Flow out	1.27 (0.13)	1.25 (0.14)	1.24 (0.13)	1.25 (0.14)	1.24 (0.13)

*Significance denoted by "***"*

6.5 Discussion

This study has shown that large-scale planting of *Miscanthus* or SRC crops does have a significant impact on the hydrological cycle for the West Wales River Basin. The simulated reductions in surface runoff and increases in baseflow for *Miscanthus* and SRC (at the limited and maximum LUC levels) correspond with previous predictions relating to LUC to *Miscanthus* and SRC (Environment Agency, 2015; Stephens *et al*., 2001) where changes to these hydrological components followed a similar trend. The maximum monthly reduction (in mm) across the watershed for surface runoff with *Miscanthus*, 17 mm (in November, a 17% reduction compared to the baseline scenario), was similar to the 18 mm maximum reduction simulated by Cibin *et al*. (2016) in modelled LUC from grassland to *Miscanthus* within a U.S. catchment. The 20%–30% reduction in surface runoff found for the majority of the sub-basins is also within the range of 20%–78% predicted by Hartwich *et al.* (2016) in modelled LUC from grassland to SRC (in different regions of the Northern German Plain).

It should be noted that the surface runoff calculations used in the model simulations are based on the CN method (Soil Conservation Service, 1976) and Manning's roughness coefficients (e.g. Chow, 1959). These are well established for traditional crops, grassland and woodland but empirical measurements (to act as a basis for coefficient values) are lacking for *Miscanthus* and SRC (Environment Agency, 2015). The values we adopted for *Miscanthus* were previously used by Cibin *et al*. (2016) and are based on values for Alamo switchgrass (*P. virgatum L.*). Switchgrass is a similar perennial grass to *Miscanthus* but may exhibit morphological differences, for example an increased stem density compared to *Miscanthus* (Cassida *et al*., 2005) that could result in differences in hydraulic resistance and hence surface

runoff rates. Similarly, new *Miscanthus* varieties (currently in pre-commercial trials, Lewandowski *et al*., 2016) can have significantly different morphologies. SRC CNs used were based on existing values for trees, but an SRC plantation differs in stand layout and density compared to natural woodland and therefore (for both SRC and *Miscanthus*) empirical measurements would improve model inputs. However, whilst accuracy of the model could be improved in this respect, replacing grassland in comparison with grassland with the more rigid stems and greater height of both *Miscanthus* and SRC means that these crops would be expected to reduce runoff and sediment flow.

Due to both physiological and physical factors (e.g. higher water use and greater leaf area index [LAI]), energy crops are generally associated with higher evapotranspiration than grassland, especially during the growing season (Cibin *et al*., 2016; Guo *et al*., 2018; Hartwich *et al*., 2016), something also found in this study. Differences in SRC compared to *Miscanthus* in evapotranspiration and water yield are slightly more complex. Whilst the longer SRC growing season can, in part, account for the greater impact of SRC than Miscanthus, modelled differences are also likely to be linked to specific parameters used for the LAI value during plant dormancy. In the *Miscanthus* scenarios this was set to zero (as in Trybula *et al*., 2015), whereas the LAI for the SRC scenarios during dormancy was set to 0.75 (as per the SWAT database for willow and poplar species). Although SRC and *Miscanthus* are not transpiring during winter months, LAI influences calculations of canopy storage and hence the evaporation of intercepted precipitation.

Whilst changes in water quality were not modelled, measured soil N losses following the establishment of *Miscanthus* and SRC have been found to reduce in

comparison with annual crops and grassland due to lower fertilizer use and differences in N use efficiency (Christian & Riche, 1998; Schmidt-Walter & Lamersdorf, 2012). Therefore, the reduction in fertilizer use with both *Miscanthus* and SRC (110, 60 and 5 kg N ha^{-1} $year^{-1}$ for pasture, *Miscanthus* and SRC respectively) could be expected to reduce nitrate leaching. In addition, whilst the model required the addition of fertilizer to obtain expected crop growth based on published data (Aylott *et al*., 2008; Cunniff *et al*., 2015; Larsen *et al*., 2014), fertilizer use is not routine in UK commercial production of these crops, particularly when cultivating on previously fertilized pasture land (Aylott *et al*., 2008; Terravesta Ltd, 2018). Fertilizer applications have been used in other SWAT-based studies (e.g. 122 kg urea ha^{-1} $year^{-1}$ with *Miscanthus*, Cibin *et al*., 2016, and 50 kg N ha^{-1} $year^{-1}$ with willow, Wang *et al*., 2018) and although the best yield responses to N fertilization are generally achieved at around 60–100 kg N ha^{-1}, *Miscanthus* and SRC do not always show a response to fertilization (Aronsson *et al*., 2014; Cadoux *et al*., 2012; Quaye & Volk, 2013).

The different rooting structures and water requirements of SRC and *Miscanthus* have the potential to cause drying of the soil profile under rain-limited conditions (Donnelly *et al*., 2011; Stephens *et al*., 2001). Such drying could have negative impacts such as reductions in yields (Knapp *et al*., 2001; Richter *et al*., 2008) and changes in microbial processes and associated nutrient availability with implications for soil carbon stocks and greenhouse gas emissions (Jensen *et al*., 2003; Smith *et al*., 2008). However, such drying did not occur in either scenario modelled in this study with soil moisture levels remaining similar to the pasture baseline. This is in contrast to Hartwich *et al*. (2016) where soil water content was reduced in simulated LUC from pasture to SRC crops in the drier Northern German Plain, where soils are

likely to have a higher sand content. Rainfall levels in west Wales (1,532 mm yr^{-1}) are also towards the top end of the range (of between 1,000 and 1,600mm yr^{-1}) for areas including Ireland, western Great Britain, northern Italy, Switzerland, Austria and northern Spain (European Environment Agency, 2012). The soils in this study also have a high clay and silt content, factors that are likely to limit drying impacts compared to drier locations or free-draining, lighter soils (Balogh *et al*., 2011; Marshall *et al*., 1996). Therefore, in assessing the land suitability for the cultivation of energy crops, local conditions should be considered to ensure rainfall rates are sufficient to meet crop demand (Richter *et al*., 2008). The fact that the majority of grasslands in Europe (as a fraction of total agricultural land area) tend to be located in wetter areas (Smit *et al*., 2008) confirms that these locations should perhaps be targeted for this kind of agricultural diversification.

Reductions in the amount of water leaving the sub-basins (water yield) were only significant for the maximum SRC LUC scenario, and changes in streamflow were not significant for any of the LUC scenarios. This indicates that changes in aquatic environments are likely to be limited across the whole watershed. However, some sub-basins did show reductions in streamflow of over 50% which, when coupled with the difficulties in understanding and predicting biotic responses to altered flow rates (Bunn & Arthington, 2002; Shafroth *et al*., 2010), demonstrates the importance of local environmental flow assessments in proposed large-scale energy crop planting (Poff *et al*., 2010).

The significant reduction in surface runoff and increase in baseflow found for both LUC levels and crop types could also impact on aquatic and riparian species (Gurnell *et al*., 2012), which should be considered when selecting suitable locations

for energy crop deployment. However, improvements in soil water infiltration seen in this study may also benefit flood mitigation by increasing soil water capacity during periods of high rainfall, as has been found with the use of young trees (<7 years old) in shelterbelts (Marshall *et al*., 2009).

Although increases in baseflow were higher with *Miscanthus* than with SRC during the spring (possibly as a result of increased soil infiltration with *Miscanthus* due to the later leaf development), overall SRC in our modelling performed better than *Miscanthus* in terms of potential flood mitigation benefits. This is largely due to overall reductions in water yield (at the 50% LUC scenario) and increases in evapotranspiration (at both LUC levels). The annual *Miscanthus* harvest is also in contrast to SRC where the 3 year harvest cycle results in more overwinter standing plant material for 2 out of 3 years. However, the timing of the harvest for *Miscanthus* in the model was simulated as occurring in November, but *Miscanthus* can be (and often is in the UK) harvested as late as early spring where the presence of the senesced biomass continues to intercept precipitation (Holder *et al*., 2018), and tall stalks would provide further resistance to overland flows and may reduce some of the differences between the two crops. Reductions in surface runoff and increases in baseflow brought about by LUC can also act to slow and buffer high overland flows (Bronstert *et al*., 2002; Marshall *et al*., 2009; OECD, 2016) with the predicted impact of slowing the flow rate across floodplains. This factor could therefore potentially release currently excluded land in flood zone areas for the planting of biomass crops (Environment Agency, 2015). In the scenarios we tested, slope was restricted to below 15% in order to allow for crop management and harvest, but if the crops were planted with the main aim of flood mitigation or nutrient buffering (e.g. as land margin buffer strips, Ferrarini *et al*., 2017) with less

demand for commercial return, this assumption could be relaxed somewhat with the acknowledgment that annual harvest may sometimes be lost due to prevailing conditions preventing land access.

The large-scale planting areas considered in this study were chosen to highlight the maximum effects of the land conversion scenarios. To set the more limited LUC scenario (1,096 km^2) in context, it has the potential to provide 12%, 1,639 GWh (assuming a yield of 12 Mg DM ha^{-1}, Larsen *et al*., 2014; an energy content of 17.95 GJ Mg^{-1} DM, Felten *et al*., 2013; with a conversion efficiency of 25%, Nguyen & Hermansen, 2015) of the Welsh Government target for 70%, 13,431 GWh (BEIS, 2018b) of Welsh electricity consumed to come from renewables (National Assembly for Wales, 2017).

Specific locations for planting of energy crops within the watershed will ultimately be based on economic and social constraints and it is not likely that just *Miscanthus* or SRC would be grown but rather a mix chosen to suit local conditions and opportunities. Projections based on profitability (using existing farm scales and energy crop prices) have suggested a commercially viable planting area of 390 km^2 of energy crops in Wales (Alexander *et al*., 2014). However, there is scope for this to increase (by as much as 300 km^2 yr^{-1} across the UK) due to improvements in agronomy, changes to climate resulting in greater yields, boosts in demand, and increases in prices paid for supply or if incentivized with subsidies (ADAS & ETI, 2016; Alexander *et al*., 2014; Hastings *et al*., 2017). Overall, whilst there is potential for negative impacts in a small number of sub-basins, this study shows that even with very ambitious levels of LUC the production of bioenergy crops within this catchment is unlikely to result in damaging impacts on basin-level hydrological

processes. The impacts on other ecosystem services however were not addressed and would need to be considered in any policies that seek to support large-scale planting of energy crops.

7 Synthesis and conclusions

This thesis aimed to address the four questions posed in section 1.5:

- What are the medium term implications for soil carbon stocks following the LUC from agricultural grassland to *Miscanthus*?
- What are the crop establishment associated N_2O emissions for LUC from semi-improved grazed grassland to *Miscanthus*?
- How does evapotranspiration and canopy precipitation interception from a commercial scale *Miscanthus* plantation differ from a short grass crop?
- Compared to an improved pasture land use what impacts on hydrology could large scaled deployment of *Miscanthus* or SRC have?

Whereas Chapters 2 to 6 provide detailed responses to these identified knowledge gaps, the following sections provide a review and discussion of the main findings in relation to these questions.

The aim of this work was also to provide published data to help inform policy decisions. In respect of this, as well as manuscripts being submitted to a peer-reviewed journal, results relating to the GHG work (Chapters 2 and 3) fed into a joint policy workshop by the Committee on Climate Change (CCC) and the Centre for Ecology & Hydrology entitled "Steps to scaling up UK sustainable bioenergy supply" (held on 16th July 2018, London), which in turn informed the CCC's recommendations to government in their report 'Biomass in a Low Carbon Economy' (CCC, 2018a).

7.1 Review and discussion

A recent report (CCC, 2018b) showed that agricultural diversification, including LUC from grassland to bioenergy crops, would be needed to meet climate targets and could save 2 Mt CO_2-eq of GHG emissions compared to 2016 by 2050. This study has shown that in LUC from temperate agricultural grassland to the production of *Miscanthus* there are GHG costs that need to be considered in terms of soil N_2O emissions and changes in soil C arising as a result of land disturbance caused by cultivation. However, also presented is the potential for this type of LUC to play a role in reducing Energy and Agricultural Sector GHG emissions with limited effects on hydrological balances (for mesic temperate grasslands), and with a promising potential role for *Miscanthus* as part of landscape climate resilience schemes.

Methods to increase and protect soil C stocks are necessary if climate targets set at Paris (COP21 meeting) are to be met (Rumpel *et al*., 2018). In providing much needed long term SOC data from field measurements with baseline values, results in Chapter 2 find that the overall change in SOC twelve years after LUC from grassland to *Miscanthus* was a reduction of 8 Mg ha^{-1}. The potential for SOC losses from grassland sites should therefore be considered in determining suitable locations for *Miscanthus* plantations with sites of high SOC or biodiversity avoided.

However, model predictions with ECOSSE suggest that at the end of the anticipated crop commercial lifetime the difference in SOC in comparison to a continued grassland counterfactual could be 4 Mg C ha^{-1}, due to a reduction also predicted within the grassland scenario. Due to the limitations of using an existing experimental set up (necessary to obtain an estimate of the long term SOC impact), it was not possible to obtain field samples of retained grassland from within the site itself or from within a reasonable distance. However, it is possible for SOC under a

continued grassland use to change due natural processes affecting C cycling and pasture yields (Post & Kwon, 2000). The modelling also assumes no soil intervention, for example if the land was cultivated and reseeded for a new grass ley, which if included would be likely to reduce the grassland SOC prediction due to the soil disturbance (Balesdent *et al*., 2000; Conant *et al*., 2007).

Trends in ECOSSE are influence by soil organic matter inputs, so it is important that the values used represent reality as much as possible. The starting SOC used for the continued grassland scenario (77 Mg C ha^{-1}) is as predicted by the RothC model in Zatta *et al.* (2014) and is within the range of 1-6% SOC reported for similar grasslands (European Commission Joint Research Centre, n.d.; Kiely *et al*., 2009; McCalmont *et al*., 2017b). The yearly plant input was based on yield values given in Smit *et al*. (2008) for the general western area of Wales, however more detailed yield values from the specific site location could have improved the predictions. Higher yield values would increase the predicted SOC under the grassland scenario with lower yield values having the opposite effect.

The starting SOC for the land use change scenario (78.8 Mg C ha^{-1}) was slightly higher than the grassland (77 Mg C ha^{-1}) to account for the additional inputs from the initial herbicide application and cultivation to plant the cover crop (that would otherwise not be included in the simulation). The ECOSSE model includes one cultivation routine during a land use change that would account for the second herbicide application. Whilst the 78.8 Mg C ha^{-1} is from the time zero (T_0) soil core samples (which were taken after the second herbicide application) due to the low temperatures between the application of herbicide in April, and the samples being taken in May, decomposition was likely to have been slow and therefore its effect minimal in the soil cores and therefore the ECOSSE predictions. The T_0 core results

were also remarkably similar to another nearby periodically re-seeded grassland site used for a land use transition experiment (see McCalmont *et al*. 2017b), which contained 79 Mg C ha^{-1} in the top 30 cm.

Whilst the ECOSSE carbon model has been evaluated for use with grassland and *Miscanthus* crops in various locations Flattery *et al*. (2018) found that for their experimental site ECOSSE did not accurately represent observed soil respiration. Nevertheless, ECOSSE performed well with predictions of SOC stocks found within the 95% confidence intervals obtained from field sampling data.

The analysis of field soil samples for $\delta^{13}C$ (Chapter 2) showed the importance of the root systems and biomass in all the *Miscanthus* hybrids (with an increase in *Miscanthus* derived C in the 6 years between sampling dates and the positive correlation of SOC with below ground biomass), a factor confirmed by Gregory *et al*., (2018) where SOC was matched to *Miscanthus* root mass. The concentration of below ground biomass was found in the 0-15 cm soil depth, which reflects the site conditions where shallow soils and sufficient rainfall means the roots have less need to find water from depth. In this study the soil was only sampled to a maximum depth of 32 cm, however, Rowe *et al*. (2016) found that in 1 m depth soil sampling SOC was only significantly lower than paired grassland sites at the 0-30 cm depth. It has also been found that although conventional tillage (as employed in this experiment) results in losses at the top 30 cm of soil, at lower depths higher SOC concentrations may occur (Baker *et al*., 2007). However, the sampling depth used was appropriate for the site where there are shallow soils with a gravel layer at depths shortly after 0.3 m and where the main root biomass was found to be concentrated in the top 0-15 cm.

The reduction of soil disturbance with use of minimum or no till methods can be a practical way to help meet climate goals by reducing SOC cultivation related losses (Smith *et al*., 2008). However, caution is needed with conservation tillage methods to ensure their suitability as their use can conversely cause higher soil GHG emissions, particularly in anaerobic, clayey soils (Rochette, 2008; Lal, 2011). In Chapter 3, which provides the first literature publication of soil N_2O fluxes over the conversion period from grassland to *Miscanthus,* it was found that the different levels of soil disturbance, and the addition of a clear film mulch layer, did not significantly increase emissions.

The results in Chapter 3 are comparable to those from a recent study (Krol *et al*., 2019) where a similar static chamber method was used to record fluxes for the two years covering land conversion and *Miscanthus* establishment. In this new study Krol *et al*. (2019) recorded first year (April to April) emissions of 12.1 +/- 2.5 kg N_2O ha^{-1} yr^{-1} which is similar to the emissions shown in Chapter 3 of 8.61 +/- 3.5 kg N_2O ha^{-1} yr^{-1} (when calculated over the same period) from the LUC *Miscanthus* plots. Their study found that in the first year of conversion (from organic cattle grazed temperate grassland to *M. x giganteus*) fluxes were comparable to grazed or fertilized grasslands, whereas in the second year emissions were comparable to un-grazed or unfertilized grasslands. This downward trend adds further weight to the premise in Chapter 3 that emissions would return to grassland levels after a few years.

The use of static chambers for measuring soil GHG emissions is a commonly used technique (Chadwick *et al*., 2014; Collier *et al*., 2014) although there are a few limitations to the method that should be taken into account. The chambers only provide a snapshot of the daily soil fluxes within the period of sampling, and whilst

care was taken to ensure samples were taken at a representative time of the day interpolation between data points is necessary to provide daily and annual estimates. N_2O is a volatile flux as a result of microbial activity responses to small changes in available substrate, oxygen temperature and moisture in the soil (Butterbach-Bahl *et al*., 2013) and therefore there is the likelihood that peaks and troughs occurring outside the sampling periods are missed which will influence results (Jones *et al*., 2011; Alves *et al*., 2012).

Increase the frequency of sampling events, particularly at times when N_2O spikes are anticipated, for example after rain storm or fertilizer events may help to reduce these inaccuracies. This method was successfully employed by Duncan *et al*. (2018) who increased the regular biweekly sampling after times of fertilization and heavy rainfall and reduced sampling frequency during the winter months when emissions were expected to be low. However, this method is less likely to be helpful for the trial site used in this thesis which was above field capacity for most of the year. Contrary to Chapter 3, where water filled pore space (WFPS) was not found to be a driver of soil N_2O emission, Duncan *et al*. (2018), McGowan *et al*. (2018), and Krol *et al*. (2019) all report WFPS as a driver (along with NO_3^- and soil temperature). This difference is again likely to be related to the high soil moisture at the site in this study.

Static chambers are also limited by the area of ground they cover and could therefore give over or underestimations of fluxes depending on the nature of the soil covered by the chamber, especially in sheep grazed plots. The effect of this in Chapter 3 was reduced by using two chambers per plot in addition to the replicated plot design (Chadwick *et al*., 2014). The use of eddy covariance instrumentation could eliminate spatial and temporal issues of this nature, but comes with a high equipment cost compared to chambers.

A large proportion of GHG emissions from the Agricultural Sector relates to artificial fertilizer use and production (Smith *et al*., 2008; Ashworth *et al*., 2015) and in these field experiments no added fertilizer was used on the *Miscanthus* plots or the grassland controls, which if used would be likely to increase soil N_2O emissions (Bouwman *et al*., 2002; Flechard *et al*., 2007). Whilst N fertilizer is sometimes used with *Miscanthus* crops, high levels of fertilizer do not necessarily increase yields (Lewandowski & Schmidt, 2006; Behnke *et al*., 2012; Cadoux *et al*., 2012) and fertilizer use is not typical in the UK (Terravesta Ltd, n.d.). The grassland controls were extensively managed with grazing sheep (without supplementary feeding) and no increases in N_2O fluxes were recorded corresponding with times of grazing, and fluxes remained low throughout the study period.

As well as N_2O, methane (CH_4) is a potent GHG. However, as found in other studies (Drewer *et al*., 2012; Gauder *et al*., 2012; Robertson *et al*., 2017), CH_4 fluxes were low in relation to N_2O with the highest value of 0.5 kg CH_4 ha^{-1} yr^{-1} coming from the uncultivated grassland control (Chapter 4).

The results in Chapters 2 and 3 suggest that costs relating to SOC change and establishment period N_2O emissions do need to be considered in determining the GHG balance of production when such LUC is involved. However, the benefit for reductions of GHG emissions within the Energy Sector is also shown through the life cycle analysis results. When calculated over a 15 year crop lifetime the total GWP covering LUC from grassland to *Miscanthus* of 10 g CO_2-eq MJ^{-1} (Chapter 2: including the cost of producing a *Miscanthus* crop, 4 g CO_2-eq MJ^{-1} (Hastings *et al.*, 2017); SOC losses, as the difference in SOC compared to a grassland counterfactual, 5 g CO_2-eq MJ^{-1}; and establishment period increases in N_2O emissions, 1 g CO_2-eq MJ^{-1}) is 83% lower than estimates for natural gas (59 g CO_2-eq MJ^{-1}, Hastings *et al.*,

2017), currently the primary fossil fuel energy source in the UK (BEIS, 2018b). The crop lifetime used in the LCA inevitably makes a difference to these one-off GHG costs, and the GWP presented here was calculated using a conservative estimate for the *Miscanthus* crop lifetime (15 years), whereas a recent LCA covering the production of bioethanol from *Miscanthus* used a 20 year crop lifetime (Lask *et al*., 2018). Yields may show a tendency to drop after ~15 years but it is possible for *Miscanthus* to be harvested for 20 years or more in Europe, depending on the location and yield needed for commercial viability (Clifton-Brown *et al*., 2007; Larsen *et al*., 2014).

A mature *Miscanthus* crop exhibits different traits and morphologies compared to a grass pasture with implications for ecosystem hydrology, and with few published UK studies Chapters 5 and 6 provide important insights into different aspects of the water balance and implications for landscape scale hydrology.

Evapotranspiration (ET) forms a large portion of the water balance and there are a number of methods than can be used to obtain field estimates of ET, for example, through calculation of the water balance or the use of lysimetry (Rana & Katerji, 2000). In Chapter 5 we were able to take advantage of previously installed eddy covariance equipment, regarded as having a good level of accuracy at the field scale, (Aubinet *et al*., 2012; Gebler *et al*., 2015; Wagle *et al*., 2016) to calculate ET over a period of 5 years. The rare opportunity of this long term dataset allowed for temporal dynamics to be accommodated in calculations of the coefficient (K_c) values (measured ET compared to a reference short grass crop).

Mathematical models are commonly used to calculate ET and Chapter 5 provides an original comparison of four models in relation to actual ET from eddy covariance data. This showed that the Penman-Monteith (short grass) model was the best

performing, and K_c values calculated from it showed that ET from the *Miscanthus* field was reduced in spring and summer (0.63 and 0.85, respectively) and increased in autumn and winter (1.57 and 1.12, respectively) compared to the standard short grass reference crop.

As the majority of crop ET estimates are only calculated over the growing season this work represents an improvement in knowledge of ET levels over the entire year (Stephens *et al*., 2001; Hay & Irmak, 2009). For example, despite the long term nature (4 years) of a recent ET study (Barco *et al*., 2018), measurements were not taken over winter. In Chapter 5 this was shown to be especially important for *M. x giganteus* (with a late spring harvest date) where the field measurements of canopy precipitation interception remained high over winter (between 20% and 40%) and was therefore assumed to fuel winter evaporation from water held on the tall stems.

However, although the ET measurements and K_c values were calculated over a number of years they came from only one site. As this is located close to the coast, and in a wetter part of the UK, results may vary in other places. Nevertheless, ET ranges were similar to growing season values (60-75 mm month^{-1}) recorded by Finch *et al*. (2004) at another UK location, and the field scale canopy precipitation interception (26% for the period June to January) was similar to that recorded in experimental plots (25%) by Finch & Riche (2010).

Chapter 5 showed that winter evaporation over a *Miscanthus* plantation was higher than a reference short grass crop, but this aspect is not well represented in the landscape hydrology simulations with the application of the SWAT model in Chapter 6. *Miscanthus* within the model was set to be harvested in the autumn as it was not possible within the model to obtain accurate yield simulations and growth patterns with a February harvest. This meant that the dormant LAI for *Miscanthus*

was zero (resulting in no water stored on vegetation to fuel winter evaporation) in comparison to 0.75 LAI for SRC (with harvest taking place on a three year cycle) and 0.80 for pasture. This is therefore the likely reason that *Miscanthus* in the model had low winter evaporation compared to both SRC and pasture and an issue that needs to be resolved if the SWAT model is to be used with crops where a spring harvest is more common.

Potential ET (PET) within the model sets the upper limit for actual ET and results can be inconsistent (Samadi, 2017), however the use of the SWAT option to read in PET values was found to provide realistic PET ranges (compared to estimates for the location and land cover type (Nisbet, 2005)) for the west Wales location of the study (Chapter 6). The SWAT model was also calibrated successfully obtaining a good correlation with observed streamflow data, and the use of SWAT (as one of the most commonly used hydrology models) will allow comparisons to be made between results from different locations around the world.

Other components of the water balance were also explored at a landscape scale in Chapter 6. Despite scenarios representing large scale deployment of *Miscanthus* (50% (2,192 km^2) and 25% (1,096 km^2) of existing pasture <15% slope gradient) the resulting differences in hydrological components were small in comparison to the baseline. The maximum (50%) LUC scenarios resulted in no significant differences to soil water status (ranging between -3% to +2% (across sub-basins) change compared to the baseline scenario of no LUC) and streamflow (mostly varying between -5% and +5%) for both *Miscanthus* and SRC. The lack of impact on soil moisture (likely due to the location of the study area where rainfall is sufficient to replenish crop use of soil water) means that detrimental changes in soil GHG production arising from changes in soil moisture are not likely to occur. However,

this may not be the same for other areas of the UK where less rainfall is received or where there are lighter soils.

Surface runoff was found to decrease monthly within the range of 15% to 20% (percentage change compared to baseline for the maximum LUC scenario to *Miscanthus*, across the whole 10,280 km^2 watershed) whereas baseflow increased in the range of 10% to 50%. This shift in flow from surface runoff to baseflow shows promising benefits for the use of perennial energy crops as part of landscape flood mitigation schemes, especially as reductions in surface runoff were seen throughout year. These percentage differences (calculated over the whole watershed area using values for the 10 year period) retain some influence of the heterogeneity of the sub-basins as within SWAT the land phase of the hydrological cycle controls the amount of water loaded to the main channel for each sub-basin, then a water routing phase of the model moves the water through the channels to the watershed outlet. However model predictions are for an established crop and there will be additional changes in hydrology to consider over the 2/3 year establishment period where crop growth is not so vigorous and, depending on the type of cultivation involved, there may be a period of bare soil (Feng *et al.*, 2017). Whilst the model was run on a daily basis the results were output on a monthly basis which would mask to a certain extent any peaks in runoff relating to individual high rainfall events, however as a continuous long term yield model SWAT is not designed to model single flood events (Neitsch *et al*., 2011).

The availably of long term climate data at a high spatial resolution is lacking for the area modelled which being a hilly region on the western coastal part of the UK is highly variant in altitude and weather patterns. Weather data (especially precipitation

and temperature) from a wider spread of climate locations would improve the simulations.

7.2 Future work

The experimental chapters in this thesis have shown impacts for a wetter western climate, but more studies are needed to understand potential influence on long term SOC and soil N_2O emissions over a wider range of grassland to *Miscanthus* LUC sites. The K_c values suggested (Chapter 5) would also benefit from testing across a range of UK sites. Changes to hydrology may be felt to a greater extent locally and therefore could be significantly different in regions of the UK where soils are generally drier or there is less rainfall (compared to the west Wales region in Chapter 6).

Chapter 3 has shown the potential for *Miscanthus* to be established in a wet climate at a higher altitude (250 m a.s.l) than would usually be considered commercially and therefore future simulations of planting in upland fringes could be considered. For example, SWAT model predictions covering the eastern side of Wales (not covered in this study) would provide valuable information in relation to potential flood mitigation impacts downstream where there are large areas of urbanisation. However, in respect of confirming and quantifying these benefits more empirical data is needed relating to overland hydraulic flow and *Miscanthus* establishment and survival in response to frequently flooded conditions. Whilst Chapter 6 has provided modelled estimates of hydrological parameters, runoff in particular would benefit from field studies with the aim of providing parameterisation for various hydrological models. An exploration of the difference to water yield caused by a later harvest date for *Miscanthus* would be valuable as contrary to claims made that *Miscanthus* uses more water that existing crops it was found in the SWAT simulations that water yield was not impacted.

However, current predictions for the UK are for further warming as well as periods of heavy rain and the increased likelihood of floods (CCC, 2018b). Therefore, if *Miscanthus* is to provide sustainable yields for use in energy (or other markets) and be used as part of flood mitigation initiatives, it is important that the crop can withstand both drought and flooding events in addition to the ability to thrive on marginal land. These are not factors considered in this study, but that would benefit from further research (Kørup *et al*., 2018; Ruf & Emmerling, 2018). This work could also be further developed by analysing and comparing data from wet and dry years in particular, and also testing for future scenarios over the next 30 years where significant changes in climate and land use may occur.

Further work will also be required if hybrids with physiological traits that vary greatly from *M. x giganteus* become commercially viable. For example, differences in root systems and nutrient translocation efficiencies could impact on SOC, and different morphologies on hydrology. Data relating to novel hybrids would also aid model predictions, for instance, in Chapter 2 the knowledge of differences in biomass decomposition rates would be valuable in improving ECOSSE estimates for the different hybrids considered.

Whilst beyond the scope of this study, research into co-cropping agricultural grassland with *Miscanthus* (particularly during the establishment period) may demonstrate reductions in GHG emissions. For example: reducing emission related soil N_2O emissions by planting *Miscanthus* in strips (allowing existing grassland productivity in between) with the aim of reducing the area of land disturbed in cultivation (Xue *et al*., 2017). Similarly, other ecosystem benefits from LUC to *Miscanthus* could be considered including the use of the SWAT model to investigate changes in water quality and sedimentation.

7.3 Concluding summary

In the light of anticipated LUC from mesic agricultural grassland to *Miscanthus*, this research has found there are negative impacts that need to be taken into account when assessing the sustainability and suitability of planting locations, but that there are potential benefits for reductions in energy related GHG emissions and for a role in landscape resilience.

Adding much needed long term empirical data, with time zero values, the study in Chapter 2 showed a reduction in SOC (of 8 Mg C ha^{-1}) after 12 years of LUC to *Miscanthus* from an agricultural grassland. Therefore caution should be exercised in locating *Miscanthus* plantations to avoid long term and semi-natural grassland sites that are likely to have higher initial carbon stocks.

Chapter 3, in an original study providing empirical measurements of soil N_2O fluxes over the initial cultivation and establishment of *Miscanthus* (in a typical upland fringe agricultural grassland) showed that while N_2O fluxes were significantly higher than existing pasture during the cultivation year (550-819% higher for the period April to December), there was a trend for a reduction in second year levels (469-485% higher for the period January to October 2017). The type of low soil disturbance cultivation method, or the addition of the film mulch layer (which proved beneficial for *Miscanthus* establishment), did not create significantly higher N_2O emissions.

However, despite these cultivation related carbon costs, benefits for reducing energy sector GHG emissions were clearly shown in the LCA comparisons between *Miscanthus* and fossils fuel use with a GWP reduction of 83% compared to natural gas. It was also shown that effects on hydrological processes are unlikely to result in

damaging impacts in areas where rainfall is sufficient to meet the higher *Miscanthus* requirements.

In Chapter 5 a unique comparison of empirical *Miscanthus* ET data with four commonly used ET models the Penman Monteith (short grass formula) was found to be the most accurate. Calculation of seasonal crop coefficient values (spring 0.63; summer 0.85; autumn 1.57; winter 1.12), coupled with empirical field data, revealed that winter evaporation and canopy interception (24% for the period June to March) from the field remained high.

Large scale hydrology modelling in Chapter 6, of ambitious LUC from improved agricultural grassland to *Miscanthus* in a previously unassessed representative watershed, revealed that changes to soil moisture and streamflow were not significant. Simulations showed surface runoff was reduced and baseflow increased by up to 40% in some sub-basins. This combination of winter canopy precipitation interception and changes in flow from surface runoff to baseflow has potential benefits for flood mitigation schemes.

References

Abbaspour, K. C. (2015). *SWAT-CUP: SWAT Calibration and Uncertainty Programs - A User Manual*. Department of Systems Analysis, Integrated Assessment and Modelling (SIAM), Eawag. Swiss Federal Institute of Aquatic Science and Technology, Duebendorf, Switzerland. Retrieved from https://swat.tamu.edu/media/114860/usermanual_swatcup.pdf

Abbaspour, K. C., Rouholahnejad, E., Vaghefi, S., Srinivasan, R., Yang, H., & Kløve, B. (2015). A continental-scale hydrology and water quality model for Europe: Calibration and uncertainty of a high-resolution large-scale SWAT model. *Journal of Hydrology*, *524*, 733–752. https://doi.org/10.1016/j.jhydrol.2015.03.027

Abdel-Magid, A. H., Schuman, G. E., & Hart, R. H. (1987). Soil Bulk Density and Water Infiltration as Affected by Grazing Systems. *Journal of Range Management*, *40*(4), 307–309. https://doi.org/10.2307/3898725

Acs, S., Hanley, N., Dallimer, M., Gaston, K.J., Robertson, P., Wilson, P. & Armsworth, P.R. (2010). The effect of decoupling on marginal agricultural systems: Implications for farm incomes, land use and upland ecology. *Land Use Policy*, 27(2), 550-563, doi: 10.1016/j.landusepol.2009.07.009

ADAS UK Ltd, & Energy Technologies Institute. (2016). *Job implications of bioenergy*. Retrieved from https://www.eti.co.uk/library/adas-relb-job-implications-of-establishing-a-bioenergy-market

Agriculture and Horticulture Development Board (AHDB). (2018). Wheat growth guide. *AHDB Cereals & Oilseeds*, 1–44. https://doi.org/https://cereals.ahdb.org.uk/media/185687/g66-wheat-growth-guide.pdf

Alexander, P., Moran, D., Smith, P., Hastings, A., Wang, S., Sünnenberg, G., Lovett, A., Tallis, M.J., Casella, E, Taylor, G., Finch, J. & Cisowska, I. (2014). Estimating UK perennial energy crop supply using farm-scale models with spatially disaggregated data. *GCB Bioenergy*, *6*(2), 142–155. https://doi.org/10.1111/gcbb.12121

Allen, R. G., Pereira, L. S., Raes, D., Smith, M., & Ab, W. (1998). *Crop evapotranspiration - Guidelines for computing crop water requirements - FAO Irrigation and drainage paper 56*. FAO - Food and Agriculture Organization of the United Nations, Rome. https://doi.org/10.1016/j.eja.2010.12.001

Alves, B. J. R., Smith, K. A., Flores, R. A., Cardoso, A. S., Oliveira, W. R. D., Jantalia, C. P., Urquiaga, S. & Boddey, R. M. (2012). Selection of the most suitable sampling time for static chambers for the estimation of daily mean N2O flux from soils. *Soil Biology and Biochemistry*, *46*, 129–135. https://doi.org/10.1016/j.soilbio.2011.11.022

Amougou, N., Bertrand, I., Cadoux, S., & Recous, S. (2012). Miscanthus × giganteus leaf senescence, decomposition and C and N inputs to soil. *GCB Bioenergy*, *4*(6), 698–707. https://doi.org/10.1111/j.1757-1707.2012.01192.x

Amougou, N., Bertrand, I., Machet, J. M., & Recous, S. (2011). Quality and decomposition in soil of rhizome, root and senescent leaf from Miscanthus x giganteus, as affected by harvest date and N fertilization. *Plant and Soil*, *338*(1), 83–97. https://doi.org/10.1007/s11104-010-0443-x

Anayah, F. M., & Kaluarachchi, J. J. (2014). Improving the complementary methods to estimate evapotranspiration under diverse climatic and physical conditions. *Hydrology and Earth System Sciences*, *18*, 2049–2064. https://doi.org/10.5194/hess-18-2049-2014

Archer, D., Eby, M., Brovkin, V., Ridgwell, A., Cao, L., Mikolajewicz, U., Caldeira, K., Matsumoto, K., Munhoven, G., Montenegro, A., & Tokos, K. (2009). Atmospheric Lifetime of Fossil Fuel Carbon Dioxide. *Annual Review of Earth and Planetary Sciences*, *37*, 117–134. https://doi.org/10.1146/annurev.earth.031208.100206

Arnold, J. G., Kiniry, J. R., Srinivasan, R., Williams, J. R., Haney, E. B., & Neitsch, S. L. (2012). Input/Output Documentation. *Soil and Water Assessment Tool "SWAT,"* 1068–1068. Retrieved from http://link.springer.com/10.1007/978-0-387-35973-1_1231

Arnold, J. G., Srinivasan, R., Muttiah, R. S., & Williams, J. R. (1998). Large area hydrologic modeling and assessment Part 1: Model development. *Journal of the*

American Water Resources Association, *34*(1), 73–89.

Aronsson, P., Rosenqvist, H., & Dimitriou, I. (2014). Impact of Nitrogen Fertilization to Short-Rotation Willow Coppice Plantations Grown in Sweden on Yield and Economy. *Bioenergy Research*, *7*(3), 993–1001. https://doi.org/10.1007/s12155-014-9435-7

Arthington, A. H., Naiman, R. J., McClain, M. E., & Nilsson, C. (2010). Preserving the biodiversity and ecological services of rivers: New challenges and research opportunities. *Freshwater Biology*, *55*, 1–16. https://doi.org/10.1111/j.1365-2427.2009.02340.x

Ashman, C., Awty-Carroll, D., Mos, M., & Robson, P. (2018). Assessing seed priming, sowing date and mulch film to improve the germination and survival of direct sown Miscanthus sinensis in the UK. *GCB Bioenergy*. https://doi.org/10.1111/gcbb.12518

Ashworth, A. J., Taylor, A. M., Reed, D. L., Allen, F. L., Keyser, P. D., & Tyler, D. D. (2015). Environmental impact assessment of regional switchgrass feedstock production comparing nitrogen input scenarios and legume-intercropping systems. *Journal of Cleaner Production*, *87*, 227–234. https://doi.org/10.1016/j.jclepro.2014.10.002

Asner, G. P., Scurlock, J. M. O., & Hicke, J. A. (2003). Global synthesis of leaf area index observations: implications for ecological and remote sensing studies. *Global Ecology & Biogeography*, *12*, 191–205.

Aubinet, M., Vesala, T., & Papale, D. (Eds.). (2012). *Eddy Covariance A Practical Guide to Measurement and Data Analysis*. Springer, Dordrecht Heidelberg, London, New York.

Aylott, M. J., Casella, E., Tubby, I., Street, N. R., Smith, P., & Taylor, G. (2008). Yield and spatial supply of bioenergy poplar and willow short-rotation coppice in the UK. *New Phytologist*, *178*(2), 358–370. https://doi.org/10.1111/j.1469-8137.2008.02396.x

Baggs, E. M., Rees, R. M., Smith, K. A., & Vinten, A. J. A. (2000). Nitrous oxide emission from soils after incorporating crop residues. *Soil Use and*

Management, *16*, 82–87.

Baker, J. M., Ochsner, T. E., Venterea, R. T., & Griffis, T. J. (2007). Tillage and soil carbon sequestration-What do we really know? *Agriculture, Ecosystems and Environment*, *118*, 1–5. https://doi.org/10.1016/j.agee.2006.05.014

Balesdent, J., Chenu, C., & Balabane, M. (2000). Relationship of soil organic matter dynamics to physical protection and tillage. *Soil & Tillage Research*, *53*(3–4), 215–230. https://doi.org/10.1016/S0167-1987(99)00107-5

Balesdent, J., Mariotti, A., & Guillet, B. (1987). Natural 13C abundance as a tracer for studies of soil organic matter dynamics. *Soil Biology and Biochemistry*, *19*(1), 25–30.

Ballingall, M. (2014). *Weed Management in Grassland. Technical Note TN643*.

Balogh, J., Pintér, K., Fóti, S., Cserhalmi, D., Papp, M., & Nagy, Z. (2011). Dependence of soil respiration on soil moisture, clay content, soil organic matter, and CO2uptake in dry grasslands. *Soil Biology and Biochemistry*, *43*, 1006–1013. https://doi.org/10.1016/j.soilbio.2011.01.017

Balslev-Clausen, D., Dahl, T. W., Saad, N., & Rosing, M. T. (2013). Precise and accurate 13C analysis of rock samples using Flash Combustion-Cavity Ring Down Laser Spectroscopy. *Journal of Analytical Atomic Spectrometry*, *28*(4), 516–523. https://doi.org/10.1039/c2ja30240c

Barco, A., Maucieri, C., & Borin, M. (2018). Root system characterization and water requirements of ten perennial herbaceous species for biomass production managed with high nitrogen and water inputs. *Agricultural Water Management*, *196*, 37–47. https://doi.org/10.1016/j.agwat.2017.10.017

Bartlett, M. K., Scoffoni, C., & Sack, L. (2012). The determinants of leaf turgor loss point and prediction of drought tolerance of species and biomes: A global meta-analysis. *Ecology Letters*, *15*, 393–405. https://doi.org/10.1111/j.1461-0248.2012.01751.x

Barton, K. (2018). MuMIn: Multi-Model Inference. R package version 1.40.4. Retrieved from https://cran.r-project.org/package=MuMIn

Batjes, N. H. (1996). Total carbon and nitrogen in the soils of the world. *European*

Journal of Soil Science, *47*, 151–163.

Beale, C. V, Bint, D. A., & Long, S. P. (1996). Leaf photosynthesis in the C4-grass Miscanthus x giganteus, growing in the cool temperate climate of southern England. *Journal of Experimental Botany*, *47*(2), 267–273. https://doi.org/10.1093/jxb/47.2.267

Beale, C. V, & Long, S. P. (1997). Seasonal dynamics of nutrient accumulation and partitioning in the perennial C4 grasses Miscanthus x giganteus and Spartina cynosuroides. *Biomass and Bioenergy*, *12*(6), 419–428.

Beale, C. V, Morison, J. I., & Long, S. P. (1999). Water use efficiency of C4 perennial grasses in a temperate climate. *Agricultural and Forest Meteorology*, *96*(1–3), 103–115. https://doi.org/10.1016/S0168-1923(99)00042-8

Behnke, G. D., David, M. B., & Voigt, T. B. (2012). Greenhouse Gas Emissions, Nitrate Leaching, and Biomass Yields from Production of Miscanthus × giganteus in Illinois, USA. *Bioenergy Research*, *5*, 801–813. https://doi.org/10.1007/s12155-012-9191-5

BEIS (Department for Business Energy & Industrial Strategy). (2018a). *Electricity generation and supply figures for Scotland, Wales, Northern Ireland and England 2004 to 2017*. Retrieved from https://assets.publishing.service.gov.uk/government/uploads/system/uploads/attachment_data/file/770767/Electricity_regional_generation_2004-2017.xls

BEIS (Department for Business Energy & Industrial Strategy). (2018b). *UK Energy in Brief*. Retrieved from https://www.gov.uk/government/statistics/uk-energy-in-brief-2018

Belanger, G., Gastal, F., & Warembourg, F. R. (1994). Carbon Balance of Tall Fescue (Festuca arundinacea Schreb.): Effects of Nitrogen Fertilization and the Growing Season. *Annals of Botany*, *74*, 653–659.

Bell, M. J., Jones, E., Smith, J., Smith, P., Yeluripati, J., Augustin, J., Juszczak, R., Olejnik, J. & Sommer, M. (2012). Simulation of soil nitrogen, nitrous oxide emissions and mitigation scenarios at 3 European cropland sites using the ECOSSE model. *Nutrient Cycling in Agroecosystems*, *92*, 161–181.

https://doi.org/10.1007/s10705-011-9479-4

Bellamy, P. H., Loveland, P. J., Bradley, R. I., Lark, R. M., & Kirk, G. J. D. (2005). Carbon losses from all soils across England and Wales 1978-2003. *Nature*, *437*(7056), 245–248. https://doi.org/10.1038/nature04038

Bequet, R., Campioli, M., Kint, V., Vansteenkiste, D., Muys, B., & Ceulemans, R. (2011). Leaf area index development in temperate oak and beech forests is driven by stand characteristics and weather conditions. *Trees*, *25*(5), 935–946. https://doi.org/10.1007/s00468-011-0568-4

Berg, B., & Matzner, E. (1997). Effect of N deposition on decomposition of plant litter and soil organic matter in forest systems. *Environmental Reviews*, *5*(1), 1–25. Retrieved from https://doi.org/10.1139/a96-017

Best, M. J., Pryor, M., Clark, D. B., Rooney, G. G., Essery, R. . L. H., Ménard, C. B., Edwards, J.M., Hendry, M.A., Porson, A., Gedney, N., Mercado, L.M., Sitch, S., Blyth, E., Boucher, O., Cox, P.M., Grimmond, C.S.B. & Harding, R. J. (2011). The Joint UK Land Environment Simulator (JULES), model description – Part 1: Energy and water fluxes. *Geoscientific Model Development*, *4*, 677–699. https://doi.org/10.5194/gmd-4-677-2011

Blanco-Canqui, H. (2010). Energy crops and their implications on soil and environment. *Agronomy Journal*, *102*(2), 403–419. https://doi.org/10.2134/agronj2009.0333

Borek, R., Faber, A., & Kozyra, J. (2010). Water implications of selected energy crops cultivated on a field scale. *Journal of Food Agriculture & Environment*, *8*(3–4), 1345–1351.

Bouchet, R. J. (1963). Evapotranspiration reelle et potentielle, signification climatique. *International Association of Hydrological Sciences Publ.*, *62*, 134–142.

Bouwman, A. F., Boumans, L. J. M., & Batjes, N. H. (2002). Emissions of N2O and NO from fertilized fields: Summary of available measurement data. *Global Biogeochemical Cycles*, *16*(4), 1–13. https://doi.org/10.1029/2001GB001811

Bowen, I. S. (1926). The ratio of heat losses by conduction and by evaporation from

any water surface. *Physical Review*, (14), 743–787.

Brady, N. C., & Weil, R. R. (2001). *The nature and properties of soil* (13th ed.). Prentice Hall, London & Upper Saddle River, NJ.

British Geological Survey Materials (c) NERC 2018. Open Government Licence V3. (2018). Soil Parent Material. Retrieved September 22, 2018, from https://www.bgs.ac.uk/products/onshore/soilPMM.html

Bronstert, A., Niehoff, D., & Brger, G. (2002). Effects of climate and land-use change on storm runoff generation: Present knowledge and modelling capabilities. *Hydrological Processes*, *16*, 509–529. https://doi.org/10.1002/hyp.326

Brosse, N., Dufour, A., Meng, X., Sun, Q., & Ragauskas, A. (2012). Miscanthus: a fast-growing crop for biofuels and chemicals production. *Biofuels, Bioproducts and Biorefining*, *6*, 580–598. https://doi.org/10.1002/bbb.1353

Brown, P. (2018). *UK Greenhouse Gas Inventory, 1990 to 2016 Annual Report for Submission under the Framework Convention on Climate Change*.

Bullard, M. J., Mustill, S. J., Carver, P., & Nixon, P. M. I. (2002). Yield improvements through modification of planting density and harvest frequency in short rotation coppice Salix spp. - 2. Resource capture and use in two morphologically diverse varieties. *Biomass and Bioenergy*, *22*(1), 27–39. https://doi.org/10.1016/S0961-9534(01)00055-1

Bunn, S. E., & Arthington, A. H. (2002). Basic principles and ecological consequences of altered flow regimes for aquatic biodiversity. *Environmental Management*, *30*(4), 492–507. https://doi.org/10.1007/s00267-002-2737-0

Burgy, R. H., & Pomeroy, C. R. (1958). Interception losses in grassy vegetation. *Transactions, American Geophysical Union*, *39*(6), 1095–1100. https://doi.org/10.1029/TR039i006p01095

Burt, T. P., & Slattery, M. C. (2005). Land Use and Land Cover Effects on Runoff Processes: Agricultural Effects. In M. G. Anderson & J. J. McDonnell (Eds.), *Encyclopedia of hydrological science*. John Wiley & Sons, Ltd.

Butterbach-Bahl, K., Baggs, E. M., Dannenmann, M., Kiese, R., & Zechmeister-

Boltenstern, S. (2013). Nitrous oxide emissions from soils: how well do we understand the processes and their controls? *Philosophical Transactions of the Royal Society B: Biological Sciences*, *368*(1621), 20130122–20130122. https://doi.org/10.1098/rstb.2013.0122

Cadoux, S., Riche, A. B., Yates, N. E., & Machet, J. (2012). Nutrient requirements of Miscanthus x giganteus: Conclusions from a review of published studies. *Biomass and Bioenergy*, *38*, 14–22.

Cadoux, S., Riche, A. B., Yates, N. E., & Machet, J. M. (2012). Nutrient requirements of Miscanthus x giganteus: Conclusions from a review of published studies. *Biomass and Bioenergy*, *38*, 14–22. https://doi.org/10.1016/j.biombioe.2011.01.015

Cassida, K. A., Muir, J. P., Hussey, M. A., & Read, J. C. (2005). Biomass yield and stand characteristics of switchgrass in south central US environments. *Crop Science*, *45*, 673–681.

Centre for Ecology & Hydrology (CEH). (n.d.). UK Lakes Portal. Retrieved February 1, 2018, from https://eip.ceh.ac.uk/apps/lakes/

Chadwick, D. R., Cardenas, L., Misselbrook, T. H., Smith, K. A., Rees, R. M., Watson, C. J., McGeough, K.L., Williams, J.R., Cloy, J.M., Thorman, R.E. & Dhanoa, M. S. (2014). Optimizing chamber methods for measuring nitrous oxide emissions from plot-based agricultural experiments. *European Journal of Soil Science*, *65*(2), 295–307. https://doi.org/10.1111/ejss.12117

Chapuis-Lardy, L., Wrage, N., Metay, A., Chotte, J. L., & Bernoux, M. (2007). Soils, a sink for N2O? A review. *Global Change Biology*, *13*, 1–17. https://doi.org/10.1111/j.1365-2486.2006.01280.x

Chatskikh, D., & Olesen, J. E. (2007). Soil tillage enhanced CO2 and N2O emissions from loamy sand soil under spring barley. *Soil and Tillage Research*, *97*(1), 5–18. https://doi.org/10.1016/j.still.2007.08.004

Cheng, W. (2009). Rhizosphere priming effect: Its functional relationships with microbial turnover, evapotranspiration, and C-N budgets. *Soil Biology and Biochemistry*, *41*(9), 1795–1801. https://doi.org/10.1016/j.soilbio.2008.04.018

Chow, V. T. (1959). *Open-channel hydraulics*. McGraw-Hill, New York.

Christen, B., & Dalgaard, T. (2013). Buffers for biomass production in temperate European agriculture: A review and synthesis on function, ecosystem services and implementation. *Biomass and Bioenergy*, *55*, 53–67. https://doi.org/10.1016/j.biombioe.2012.09.053

Christian, D. G., & Riche, A. B. (1998). Nitrate leaching losses under Miscanthus grass planted on a silty clay loam soil. *Soil Use and Management*, *14*(May 1993), 131–135. https://doi.org/10.1111/j.1475-2743.1998.tb00136.x

Christopher, S. F., & Lal, R. (2007). Nitrogen management affects carbon sequestration in North American cropland soils. *Critical Reviews in Plant Sciences*, *26*, 45–64. https://doi.org/10.1080/07352680601174830

Chum, H., Faaij, A., Moreira, J., Berndes, G., Dhamija, P., Dong, H., Gabrielle, B., Goss Eng, A., Lucht, W., Mapako, M., Masera Cerutti, O., McIntyre, T., Minowa, T. & Pingoud, K. (2011). *Chapter 2: Bioenergy*. *In IPCC Special Report on Renewable Energy Sources and Climate Change Mitigation*. (O. Edenhofer, R. Pichs-Madruga, Y. Sokona, K. Seyboth, P. Matschoss, S. Kadner, T. Zwickel, P. Eickemeier, G. Hansen, S. Schlömer, C. von Stechow, Ed.). Cambridge University Press, Cambridge, United Kingdom and New York, NY, USA. Retrieved from https://www.ipcc.ch/report/renewable-energy-sources-and-climate-change-mitigation/

Cibin, R. A. J., Trybula, E., Chaubey, I., & Brouder, S. M. (2016). Watershed-scale impacts of bioenergy crops on hydrology and water quality using improved SWAT model. *GCB Bioenergy*, 1–12. https://doi.org/10.1111/gcbb.12307

Claussen, M., Brovkin, V., & Ganopolski, A. (2001). Biophysical versus biogeochemical feedbacks of large-scale land cover change. *Geophysical Research Letters*, *28*(6), 1011–1014. https://doi.org/10.1029/2000GL012471

Clifton-Brown, J. C., Breuer, J., & Jones, M. B. (2007). Carbon mitigation by the energy crop, Miscanthus. *Global Change Biology*, *13*(11), 2296–2307. https://doi.org/10.1111/j.1365-2486.2007.01438.x

Clifton-Brown, J. C., & Lewandowski, I. (2000). Water use efficiency and biomass

partitioning of three different Miscanthus genotypes with limited and unlimited water supply. *Annals of Botany*, *86*(1), 191–200. https://doi.org/10.1006/anbo.2000.1183

Clifton-Brown, J. C., Lewandowski, I., Bangerth, F., & Jones, M. B. (2002). Comparative responses to water stress in stay-green, rapid and slow senescing genotypes of the biomass crop, Miscanthus. *New Phytologist*, *154*(2), 335–345. https://doi.org/10.1046/j.1469-8137.2002.00381.x

Clifton-Brown, J. C., Stampfl, P. F., & Jones, M. B. (2004). Miscanthus biomass production for energy in Europe and its potential contribution to decreasing fossil fuel carbon emissions. *Global Change Biology*, *10*(4), 509–518. https://doi.org/10.1111/j.1529-8817.2003.00749.x

Clifton-Brown, J., Hastings, A., Mos, M., McCalmont, J. P., Ashman, C., Awty-Carroll, D., Cerazy, J., Chian, Y., Ino, S., Cracroft-Eley, W., Scurlock, J., Donnison, I., Glover, C., Golab, I., Greef, J., Gwyn, J., Harding, G., Hayes, C., Helios, W., Hsu, T., Huang, L., Jezowski, S., Kim, D., Kiesel, A., Kotecki, A., Krzyzak, J., Lewandowski, I., Lim, S., Liu, J., Loosely, M., Meyer, H., Murphy-Bokern, D., Nelson, W., Pogrzeba, M., Robinson, G., Robson, P., Rogers, C., Scalici, G., Schuele, H., Shafiei, R., Shevchuk, O., Schwarz, K., Squance, M., Swaller, T., Thornton, J., Truckses, T., Botnari, V., Vizir, I., Wagner, M., Warren, R., Webster, R., Yamada, T., Youell, S., Xi, Q., Zong, J. & Flavell, R. (2017). Progress in upscaling Miscanthus biomass production for the European bio-economy with seed-based hybrids. *GCB Bioenergy*, *9*(1). https://doi.org/10.1111/gcbb.12357

Clifton-Brown, J., Robson, P., Sanderson, R., Hastings, A., Valentine, J., & Donnison, I. (2011). Thermal requirements for seed germination in Miscanthus compared with Switchgrass (Panicum virgatum), Reed canary grass (Phalaris arundinaceae), Maize (Zea mays) and perennial ryegrass (Lolium perenne). *GCB Bioenergy*, *3*(5), 375–386. https://doi.org/10.1111/j.1757-1707.2011.01094.x

Clifton-Brown, J., Schwarz, K. U., & Hastings, A. (2015). History of the development of Miscanthus as a bioenergy crop: From small beginnings to potential realisation. *Biology and Environment*, *115B*(1), 1–13.

https://doi.org/10.3318/BIOE.2015.05

Collier, S. M., Ruark, M. D., Oates, L. G., Jokela, W. E., & Dell, C. J. (2014). Measurement of Greenhouse Gas Flux from Agricultural Soils Using Static Chambers. *Journal of Visualized Experiments*, (90), 1–8. https://doi.org/10.3791/52110

Collura, S., Azambre, B., Finqueneisel, G., Zimny, T., & Weber, J. V. (2006). Miscanthus x giganteus straw and pellets as sustainable fuels. Combustion and emission tests. *Environmental Chemistry Letters*, 4, 75–78. https ://doi.org/10.1007/s10311-006-0036-3

Committee on Climate Change (CCC). (2018a). *Biomass in a low-carbon economy*. Retrieved from www.theccc.org.uk/publications

Committee on Climate Change (CCC). (2018b). *Land use: Reducing emissions and preparing for climate change*. Retrieved from www.theccc.org.uk/publications

Committee on Climate Change (CCC). (2019). *Reducing UK emissions. 2019 Progress Report to Parliament.* Retrieved from www.theccc.org.uk/publications

Conant, R. T., Easter, M., Paustian, K., Swan, A., & Williams, S. (2007). Impacts of periodic tillage on soil C stocks: A synthesis. *Soil and Tillage Research*, *95*(1–2), 1–10. https://doi.org/10.1016/j.still.2006.12.006

Conrad, R. (2009). The global methane cycle: Recent advances in understanding the microbial processes involved. *Environmental Microbiology Reports*, *1*(5), 285–292. https://doi.org/10.1111/j.1758-2229.2009.00038.x

Counsell, C., & Hess, T. (2000). IWASRI WaSim User Manual. Retrieved from https://dspace.lib.cranfield.ac.uk/bitstream/handle/1826/2455/user_manual.pdf?sequence=1&isAllowed=y

Cristiano, P. M., Posse, G., & Di Bella, C. M. (2015). Total and aboveground radiation use efficiency in C3 and C4 grass species influenced by nitrogen and water availability. *Grassland Science*, *61*(3), 131–141. https://doi.org/10.1111/grs.12086

Crow, P., & Houston, T. J. (2004). The influence of soil and coppice cycle on the

rooting habit of short rotation poplar and willow coppice. *Biomass and Bioenergy*, *26*(6), 497–505. https://doi.org/10.1016/j.biombioe.2003.09.002

Cuello, J. P., Hwang, H. Y., Gutierrez, J., Kim, S. Y., & Kim, P. J. (2015). Impact of plastic film mulching on increasing greenhouse gas emissions in temperate upland soil during maize cultivation. *Applied Soil Ecology*, *91*, 48–57. https://doi.org/10.1016/j.apsoil.2015.02.007

Cunniff, J., Purdy, S. J., Barraclough, T. J. P., Castle, M., Maddison, A. L., Jones, L. E., Shield, I.F, Gregory, A.S., & Karp, A. (2015). High yielding biomass genotypes of willow (Salix spp.) show differences in below ground biomass allocation. *Biomass and Bioenergy*, *80*(0), 114–127. https://doi.org/10.1016/j.biombioe.2015.04.020

Dale, V. H. (1997). The Relationship Between Land-Use Change and Climate Change. *Ecological Applications*, *7*(3), 753–769.

Dauber, J., Jones, M. B., & Stout, J. C. (2010). The impact of biomass crop cultivation on temperate biodiversity. *GCB Bioenergy*, *2*, 289–309. https://doi.org/10.1111/j.1757-1707.2010.01058.x

Davis, M. P., David, M. B., Voigt, T. B., & Mitchell, C. A. (2015). Effect of nitrogen addition on Miscanthus ×giganteus yield, nitrogen losses, and soil organic matter across five sites. *GCB Bioenergy*, *7*(6), 1222–1231. https://doi.org/10.1111/gcbb.12217

Davis, S. C., Parton, W. J., Dohleman, F. G., Smith, C. M., Del Grosso, S., Kent, A. D., & DeLucia, E. H. (2010). Comparative biogeochemical cycles of bioenergy crops reveal nitrogen-fixation and low greenhouse gas emissions in a Miscanthus × giganteus agro-ecosystem. *Ecosystems*, *13*, 144–156. https://doi.org/10.1007/s10021-009-9306-9

DeFries, R., & Eshleman, K. N. (2004). Land-use change and hydrologic processes: a major focus for the future. *Hydrological Processes*, *18*(11), 2183–2186. https://doi.org/10.1002/hyp.5584

Dengel, S., Levy, P.E., Grace, J., Jones, S.K., Skiba, U.M. (2011). Methane emissions from sheep pasture, measured with an open-path eddy covariance

system. *Global Change Biology*, 17, 3524–3533. doi: 10.1111/j.1365-2486.2011.02466.x

Department for Environment Food & Rural Affairs (DEFRA). (2002). *Growing Short Rotation Coppice: Best practice guidelines*. DEFRA Publications, London. Retrieved from http://adlib.everysite.co.uk/resources/000/023/833/src-guide.pdf

Department for Environment Food & Rural Affairs (DEFRA). (2017a). *Agriculture in the UK 2016*. Retrieved from https://www.gov.uk/government/statistics/agriculture-in-the-united-kingdom-2016

Department for Environment Food & Rural Affairs (DEFRA). (2017b). *Farming Statistics Provisional crop areas, yields and livestock populations at June 2017 - United Kingdom*.

Department for Environment Food & Rural Affairs (DEFRA). (2017c). *The British Survey of Fertiliser Practise (2016)*. Retrieved from https://www.gov.uk/government/collections/fertiliser-usage

Dhillon, R. S., & von Wuehlisch, G. (2013). Mitigation of global warming through renewable biomass. *Biomass and Bioenergy*, *48*, 75–89. https://doi.org/10.1016/j.biombioe.2012.11.005

Dickinson, R. E. (1984). Modeling evapotranspiration for three-di- mensional global climate models. In J. E. Hansen & T. Takahashi (Eds.), *Climate processes and climate sensitivity* (pp. 58–72). Geophys Mon- ogr 29, Am Geophys Union, Washington, D.C.

Dickmann, D. I. (2006). Silviculture and biology of short-rotation woody crops in temperate regions: Then and now. *Biomass and Bioenergy*, *30*, 696–705. https://doi.org/10.1016/j.biombioe.2005.02.008

Dile, Y. T., Daggupati, P., George, C., Srinivasan, R., & Arnold, J. (2016). Introducing a new open source GIS user interface for the SWAT model. *Environmental Modelling and Software*, *85*, 129–138. https://doi.org/10.1016/j.envsoft.2016.08.004

Dile, Y. T., Srinivasan, R., & George, C. (2018). *QGIS Interface for SWAT (QSWAT)*. Retrieved from https://swat.tamu.edu/software/qswat/

Dingman, S. L. (2002). *Physical Hydrology* (2nd ed.). Prentice-Hall, Inc., Upper Saddle River, New Jersey.

Dobbie, K., & Smith, K. (2003). Nitrous oxide emission factors for agricultural soils in Great Britain: the impact of soil water filled pore space and other controlling variables. *Global Change Biology*, *99*, 204–218. https://doi.org/10.1046/j.1365-2486.2003.00563.x

Dobbs, T.L. & Pretty, J. (2008). Case study of agri-environmental payments: The United Kingdom. *Ecological Economics*, 65(4), 765-775, doi: 10.1016/j.ecolecon.2007.07.030

Dondini, M., Jones, E. O., Richards, M., Pogson, M., Rowe, R. L., Keith, A. M., Perks, M.P., McNamara, N.P., Smith, J. U., & Smith, P. (2015). Evaluation of the ECOSSE model for simulating soil carbon under short rotation forestry energy crops in Britain. *GCB Bioenergy*, *7*(3), 527–540. https://doi.org/10.1111/gcbb.12154

Dondini, M., Richards, M. I. A., Pogson, M., McCalmont, J., Drewer, J., Marshall, R., Morrison, R., Yamulki, S., Harris, Z.M., Alberti, G., Siebicke, L., Taylor, G., Perks, M., Finch, J., McNamara, N.P., Smith, J.U., & Smith, P. (2016). Simulation of greenhouse gases following land-use change to bioenergy crops using the ECOSSE model: a comparison between site measurements and model predictions. *GCB Bioenergy*, *8*(5), 925–940. https://doi.org/10.1111/gcbb.12298

Dondini, M., Richards, M., Pogson, M., Jones, E. O., Rowe, R. L., Keith, A. M., McNamara, N.P., Smith, J.U., & Smith, P. (2016). Evaluation of the ECOSSE model for simulating soil organic carbon under Miscanthus and short rotation coppice-willow crops in Britain. *GCB Bioenergy*, *8*(4), 790–804. https://doi.org/10.1111/gcbb.12286

Donnelly, A., Styles, D., Fitzgerald, J., & Finnan, J. (2011). A proposed framework for determining the environmental impact of replacing agricultural grassland with Miscanthus in Ireland. *GCB Bioenergy*, *3*, 247–263. https://doi.org/10.1111/j.1757-1707.2010.01086.x

Donnison, I. S., & Fraser, M. D. (2016). Diversification and use of bioenergy to maintain future grasslands. *Food and Energy Security*, *5*(2), 67–75. https://doi.org/10.1002/fes3.75

Drewer, J., Anderson, M., Levy, P. E., Scholtes, B., Helfter, C., Parker, J., Rees, R.M. & Skiba, U. M. (2017). The impact of ploughing intensively managed temperate grasslands on N2O, CH4 and CO2 fluxes. *Plant and Soil*, *411*(1–2), 193–208. https://doi.org/10.1007/s11104-016-3023-x

Drewer, J., Finch, J. W., Lloyd, C. R., Baggs, E. M., & Skiba, U. (2012). How do soil emissions of N2O, CH4 and CO2 from perennial bioenergy crops differ from arable annual crops? *GCB Bioenergy*, *4*(4), 408–419. https://doi.org/10.1111/j.1757-1707.2011.01136.x

Duncan, D. S., Oates, L. G., Gelfand, I., Millar, N., Robertson, G. P., & Jackson, R. D. (2018). Environmental factors function as constraints on soil nitrous oxide fluxes in bioenergy feedstock cropping systems. IN PRESS. *GCB Bioenergy*. https://doi.org/10.1111/gcbb.12572

Dunkerley, D. (2000). Measuring interception loss and canopy storage in dryland vegetation: a brief review and evaluation of available research strategies. *Hydrological Processes*, *14*, 669–678.

Ellert, B. H., & Bettany, J. R. (1995). Calculation of organic matter and nutrients stored in soils under contrasting management regimes. *Canadian Journal of Soil Science*, *75*, 529–538. https://doi.org/10.4141/cjss95-075

Emmett, B. A., Frogbrook, Z. L., Chamberlain, P. M., Giffiths, R., Pickup, R., Poskitt, J., Reynolds, B., Rowe, E., Spurgeon, D., Rowland, P., Wilson, J. & Wood, C. M. (2008). *Countryside Survey: Soils Manual v1.0*.

Emmett, B. A., Reynolds, B., Chamberlain, P. M., Rowe, E., Spurgeon, D., Brittain, S. A., Frogbrook, Z., Hughes, S., Lawlor, A. J., Poskitt, J., Potter, E., Robinson, D. A., Scott, A., Wood, C. & Woods, C. (2010). *Countryside Survey: Soils Report from 2007. Technical Report No. 9/07*.

Energy Technologies Institute (ETI). (2015). *Bioenergy Delivering greenhouse gas emission savings through UK bioenergy value chains*.

Engel, B., Chaubey, I., Thomas, M., Saraswat, D., Murphy, P., & Bhaduri, B. (2010). Biofuels and water quality: Challenges and opportunities for simulation modeling. *Biofuels*, *1*(3), 463–477. https://doi.org/10.4155/bfs.10.17

Environment Agency. (2014). WFD River Basin Districts Cycle 2 (Open Government Licence v3.0). Retrieved February 1, 2018, from https://data.gov.uk/dataset

Environment Agency. (2015). *Energy crops and floodplain flows*. Environment Agency, Bristol.

Essery, R., Best, M., & Cox, P. (2001). MOSES 2.2 Technical Documentation. Met Office. Retrieved from http://jules.jchmr.org/sites/default/files/HCTN_30.pdf

European Academies Science Advisory Council (EASAC). (2012). *The current status of biofuels in the European Union, their environmental impacts and future prospects*. Retrieved from www.easac.eu

European Commission. (n.d.a). 2030 climate & energy framework. Retrieved October 4, 2018, from https://ec.europa.eu/clima/policies/strategies/2030_en

European Commission. (n.d.b). Agricultural and Rural Development. Less Favoured Areas Scheme. Retrieved March 15, 2019, from https://ec.europa.eu/agriculture/rural-development-previous/2007-2013/less-favoured-areas-scheme_en

European Commission. (n.d.c). Paris Agreement. Retrieved February 9, 2016, from https://ec.europa.eu/clima/policies/international/negotiations/paris_en

European Commission. (2017a). *Second Report on the State of the Energy Union*. Retrieved from https://ec.europa.eu/commission/sites/beta-political/files/2nd-report-state-energy-union_en.pdf

European Commission. (2017b). The future of food and farming. European Commission. Retrieved from https://ec.europa.eu/agriculture/future-cap_en

European Commission. (2018). *A Clean Planet for all A European strategic long-term vision for a prosperous, modern, competitive and climate neutral economy*. Retrieved from https://ec.europa.eu/clima/sites/clima/files/docs/pages/com_2018_733_en.pdf

European Commission Joint Research Centre. (n.d.). ESDAC European Soil Database Maps. Retrieved February 11, 2019, from https://esdac.jrc.ec.europa.eu/resource-type/european-soil-database-maps#

European Environment Agency. (2012). Average annual precipitation in the EEA area. Retrieved January 27, 2019, from https://www.eea.europa.eu/data-and-maps/figures/average-annual-precipitation

European Environment Agency. (2014). *National adaptation policy processes across European countries — 2014*. https://doi.org/10.2800/21394

Eurostat. (2018a). Agri-environmental indicator - cropping patterns. Retrieved May 29, 2018, from http://ec.europa.eu/eurostat/statistics-explained/index.php?title=Agri-environmental_indicator_-_cropping_patterns

Eurostat. (2018b). Agricultural accounts and prices. Retrieved from http://ec.europa.eu/eurostat/statistics-explained/index.php?title=Agricultural_accounts_and_prices

Falkowski, P., Scholes, R. J., Boyle, E., Canadell, J., Canfield, D., Elser, J., Gruber, N., Hibbard, K., Hogberg, P., Linder, S., Mackenzie, F.T., Moore, B., Pedersen, T., Rosenthal., Seitzinger, S., Smetacek, V. & Steffen, W. (2000). *The Global Carbon Cycle: A Test of Our Knowledge of Earth as a System*. *Source: Science* (Vol. 290).

Felten, D., Fröba, N., Fries, J., & Emmerling, C. (2013). Energy balances and greenhouse gas-mitigation potentials of bioenergy cropping systems (Miscanthus , rapeseed , and maize) based on farming conditions in Western Germany. *Renewable Energy*, *55*, 160–174. https://doi.org/10.1016/j.renene.2012.12.004

Feng, Q., Chaubey, I., Cibin, R., Engel, B., Sudheer, K. P., & Volenec, J. (2017). Simulating Establishment Periods of Switchgrass and Miscanthus in the Soil Water and Assessment Tool (SWAT). *Transactions of the ASABE*, *60*(5), 1621–1632. https://doi.org/10.13031/trans.12227

Feng, Q., Chaubey, I., Cibin, R., Engel, B., Sudheer, K. P., Volenec, J., & Omani, N. (2018). Perennial biomass production from marginal land in the Upper

Mississippi River Basin. *Land Degradation and Development*, *29*(6), 1748–1755. https://doi.org/10.1002/ldr.2971

Fera Science Ltd. (2018). Pesticide Usage Surveys. Retrieved February 1, 2018, from https://secure.fera.defra.gov.uk/pusstats/

Ferrarini, A., Fornasier, F., Serra, P., Ferrari, F., Trevisan, M., & Amaducci, S. (2017). Impacts of willow and miscanthus bioenergy buffers on biogeochemical N removal processes along the soil–groundwater continuum. *GCB Bioenergy*, *9*, 246–261. https://doi.org/10.1111/gcbb.12340

Finch, H. J. S., Samuel, A. M., & Lane, G. P. F. (2002). *Lockhart and Wiseman's Crop Husbandry* (8th Editio). Woodhead Publishing Ltd, Cambridge, England.

Finch, J. W., Hall, R. L., Rosier, P. T. W., Clark, D. B., Stratford, C., Davies, H. N., Marsh, T.J., Roberts, J.M., Riche, A. & Christian, D. (2004). *The hydrological impacts of energy crop production in the UK*.

Finch, J. W., & Riche, A. B. (2010). Interception losses from Miscanthus at a site in south-east England-an application of the Gash model. *Hydrological Processes*, *24*(18), 2594–2600. https://doi.org/10.1002/hyp.7673

Flattery, P., Fealy, R., Fealy, R. M., Lanigan, G., & Green, S. (2018). Simulation of soil carbon efflux from an arable soil using the ECOSSE model: Need for an improved model evaluation framework? *Science of the Total Environment*, *622–623*, 1241–1249. https://doi.org/10.1016/j.scitotenv.2017.12.077

Flechard, C. R., Ambus, P., Skiba, U., Rees, R. M., Hensen, A., van Amstel, A., van den Pol-van Dasselaar, A., Soussana, J-F., Jones, M., Clifton-Brown, J., Raschi, A., Horvath, L., Neftel, A., Jocher, M., Ammann, C., Leifeld, J., Fuhrer, J., Calanca, P., Thalman, E., Pilegaard, K., Di Marco, C., Campbell, C., Nemitz, E., Hargreaves, K.J., Levy, P.E., Ball, B.C., Jones, S.K., van de Bulk, W.C.M., Groot T., Blom M., Domingues, R., Kasper, G., Allard, V., Ceschia E., Cellier, P., Laville, P., Henault, C., Bizouard, F., Abdalla, M., Williams, M., Baronti, S., Berretti, F. & Grosz, B. (2007). Effects of climate and management intensity on nitrous oxide emissions in grassland systems across Europe. *Agriculture, Ecosystems and Environment*, *121*(1–2), 135–152. https://doi.org/10.1016/j.agee.2006.12.024

Foereid, B., De Neergaard, A., & Høgh-Jensen, H. (2004). Turnover of organic matter in a Miscanthus field: Effect of time in Miscanthus cultivation and inorganic nitrogen supply. *Soil Biology and Biochemistry*, *36*(7), 1075–1085. https://doi.org/10.1016/j.soilbio.2004.03.002

Foley, J. A., DeFries, R., Asner, G. P., Barford, C., Bonan, G., Carpenter, S. R., Chapin, F., Coe, M.T., Daily, G., Gibbs., H., Helkowski, J.H., Holloway., T., Howard, E.A., Kucharik, C.J., Monfreda, C., Patz, J., Prentice., C., Ramankutty, N. & Snyder, P. K. (2005). Global Consequences of Land Use. *American Association for the Advancement of Science*, *309*(5734), 570–574. https://doi.org/10.1126/science.1111772

Food and Agriculture Orangisation of the United Nations (UNFAO). (n.d.). Sustainable Development Goals, Land and Soil. Retrieved February 14, 2018, from http://www.fao.org/sustainable-development-goals/overview/fao-and-the-post-2015-development-agenda/land-and-soils/en/

Food and Agriculture Orangisation of the United Nations (UNFAO) (c) FAO/UNESCO 1995 All rights reserved worldwide. (2003). The Digital Soil Map of the World v3.6. Retrieved February 1, 2018, from http://www.waterbase.org/download_data.html

Forestry Commission. (2011). *Biomass in live woodland trees in Britain: National Forest Inventory Report*.

Forestry Commission. (2017). *Woodland Areas and Planting*. *Forestry statistics 2017*. https://doi.org/10.1016/S0733-8619(03)00096-3

Fox, J., & Weisberg, S. (2011). *An {R} Companion to Applied Regression* (Second). Thousand Oaks CA: Sage. Retrieved from http://socserv.socsci.mcmaster.ca/jfox/Books/Companion

Freibauer, A., Rounsevell, M. D. A., Smith, P., & Verhagen, J. (2004). Carbon sequestration in the agricultural soils of Europe. *Geoderma*, *122*, 1–23. https://doi.org/10.1016/j.geoderma.2004.01.021

Fritsche, U. R., Hennenberg, K. J., Wiegeman, K., Herrera, R., Franke, B., Köppen, S., Reinhardt, G., Domburg, V., Faaij, A. & Smeets, E. (2010). *Bioenergy*

Environmental Impact Analysis (BIAS): Analytical Framework. Retrieved from www.fao.org/nr

Garbulsky, M. F., Peñuelas, J., Papale, D., Ardö, J., Goulden, M. L., Kiely, G., Richardson, A.D., Rotenberg, E., Veenedaal, E. & Filella, I. (2010). Patterns and controls of the variability of radiation use efficiency and primary productivity across terrestrial ecosystems. *Global Ecology and Biogeography*, *19*(2), 253–267. https://doi.org/10.1111/j.1466-8238.2009.00504.x

Gardner, W. R., & Ehlig, F.C. (1963). The influence of soil water on transpiration by plants. *Journal of Geophysical Research*, 68(20), 5719-5724

Gash, J. H. C., Lloyd, C. R., & Lachaud, G. (1995). Estimating sparse forest rainfall interception with an analytical model. *Journal of Hydrology*, *170*(1–4), 79–86. https://doi.org/10.1016/0022-1694(95)02697-N

Gash, J. H. C., Valente, F., & David, J. S. (1999). Estimates and measurements of evaporation from wet, sparse pine forest in Portugal. *Agricultural and Forest Meteorology*, *94*, 149–158.

Gassman, P. W., Valcu-Lisman, A. M., Kling, C. L., Mickelson, S. K., Panagopoulos, Y., Cibin, R., … Schilling, K. E. (2017). Assessment of Bioenergy Cropping Scenarios for the Boone River Watershed in North Central Iowa, United States. *Journal of the American Water Resources Association*, *53*(6), 1336–1354. https://doi.org/10.1111/1752-1688.12593

Gauder, M., Butterbach-Bahl, K., Graeff-Hönninger, S., Claupein, W., & Wiegel, R. (2012). Soil-derived trace gas fluxes from different energy crops - results from a field experiment in Southwest Germany. *GCB Bioenergy*, *4*(3), 289–301. https://doi.org/10.1111/j.1757-1707.2011.01135.x

Gebler, S., Hendricks Franssen, H. J., Putz, T., Post, H., Schmidt, M., & Vereecken, H. (2015). Actual evapotranspiration and precipitation measured by lysimeters: A comparison with eddy covariance and tipping bucket. *Hydrology and Earth System Sciences*, *19*(5), 2145–2161. https://doi.org/10.5194/hess-19-2145-2015

Genever, L., & Buckingham, S. (2016). Planning grazing strategies for Better Returns. *Beef and Sheep Better Returns Programme Manual*, 26.

Gibon, A. (2005). Managing grassland for production, the environment and the landscape. Challenges at the farm and the landscape level. *Livestock Production Science*, *96*, 11–31. https://doi.org/10.1016/j.livprodsci.2005.05.009

Gonzalez, M., Augusto, L., Gallet-Budynek, A., Xue, J., Yauschew-Raguenes, N., Guyon, D., Trichet, P., Delerue, F., Niollet, S., Andreasson, F., Achat, D. & Bakker, M. R. (2013). Contribution of understory species to total ecosystem aboveground and belowground biomass in temperate Pinus pinaster Ait. forests. *Forest Ecology and Management*, *289*, 38–47. Retrieved from http://dx.doi.org/10.1016/j.foreco.2012.10.026

Gopalakrishnan, G., Cristina Negri, M., & Salas, W. (2012). Modeling biogeochemical impacts of bioenergy buffers with perennial grasses for a row-crop field in Illinois. *GCB Bioenergy*, *4*, 739–750. https://doi.org/10.1111/j.1757-1707.2011.01145.x

GRACE. (n.d.). GRowing Advanced industrial Crops on marginal lands for biorEfineries. Retrieved July 13, 2018, from https://www.grace-bbi.eu/

Granger, R. J., & Gray, D. M. (1989). Evaporation from natural nonsaturated surfaces. *Journal of Hydrology*, *111*, 21–29.

Grave, R. A., Nicoloso, R. da S., Cassol, P. C., da Silva, M. L. B., Mezzari, M. P., Aita, C., & Wuaden, C. R. (2018). Determining the effects of tillage and nitrogen sources on soil N2O emission. *Soil and Tillage Research*, *175*(September 2017), 1–12. https://doi.org/10.1016/j.still.2017.08.011

Greef, J. M., & Deuter, M. (1993). Syntaxonomy of Miscanthus× giganteus GREEF et DEU. *Angewandte Botanik*, *67*, 87–90.

Green, W. H., & Ampt, G. A. (1911). Studies on soil physics, 1. The flow of air and water through soils. *Journal of Agricultural Sciences*, *4*, 11–24.

Gregory, A. S., Dungait, J. A. J., Shield, I. F., Macalpine, W. J., Cunniff, J., Durenkamp, M., White, R., Joynes, A. & Richter, G. M. (2018). Species and Genotype Effects of Bioenergy Crops on Root Production, Carbon and Nitrogen in Temperate Agricultural Soil. *Bioenergy Research*, *11*, 382–397. https://doi.org/10.1007/s12155-018-9903-6

Gregory, P. J. (2006). *Plant roots: growth, activity, and interaction with soils*. Blackwell Publishing Ltd, Oxford.

Grutzmacher, P., Puga, A.P., Bibar, M.P.S., Coscione, A.R., Packer, A.P., & de Andrade, C.A. (2018). Carbon stability and mitigation of fertilizer induced N2O emissions in soil amended with biochar. *Science of The Total Environment*, 625, 1459-1466, doi: 10.1016/j.scitotenv.2017.12.196

Guo, D., & Westra, S. (2016). Evapotranspiration: Modelling Actual, Potential and Reference Crop Evapotranspiration. R package. Retrieved from https://cran.r-project.org/package=Evapotranspiration

Guo, L. B., & Gifford, R. M. (2002). Soil carbon stocks and land use change: A meta analysis. *Global Change Biology*, *8*(4), 345–360. https://doi.org/10.1046/j.1354-1013.2002.00486.x

Guo, T., Cibin, R., Chaubey, I., Gitau, M., Arnold, J. G., Srinivasan, R., Kiniry, J.R. & Engel, B. A. (2018). Evaluation of bioenergy crop growth and the impacts of bioenergy crops on streamflow, tile drain flow and nutrient losses in an extensively tile-drained watershed using SWAT. *Science of the Total Environment*, *613–614*, 724–735. https://doi.org/10.1016/j.scitotenv.2017.09.148

Guo, T., Engel, B. A., Shao, G., Arnold, J. G., Srinivasan, R., & Kiniry, J. R. (2015). Functional Approach to Simulating Short-Rotation Woody Crops in Process-Based Models. *Bioenergy Research*, *8*, 1598–1613. https://doi.org/10.1007/s12155-015-9615-0

Gurnell, A. M., Bertoldi, W., & Corenblit, D. (2012). Changing river channels: The roles of hydrological processes, plants and pioneer fluvial landforms in humid temperate, mixed load, gravel bed rivers. *Earth-Science Reviews*, *111*, 129–141. https://doi.org/10.1016/j.earscirev.2011.11.005

Hall, R. L., & Allen, S. J. (1982). Water use of poplar clones grown as short-rotation coppice at two sites in the United Kingdom. *Aspects of Applied Biology*, (No. 49), 163–172. Retrieved from https://www.cabdirect.org/cabdirect/abstract/19970607864

Hansen, E. M., Christensen, B. T., Jensen, L. S., & Kristensen, K. (2004). Carbon sequestration in soil beneath long-term Miscanthus plantations as determined by13C abundance. *Biomass and Bioenergy*, *26*(2), 97–105. https://doi.org/10.1016/S0961-9534(03)00102-8

Hargreaves, G. L., & Samani, Z. A. (1985). Evapotranspiration from temperature. *Applied Engineering in Agriculture*, *1*(2), 96–99.

Harris, Z. M., Spake, R., & Taylor, G. (2015). Land use change to bioenergy: A meta-analysis of soil carbon and GHG emissions. *Biomass and Bioenergy*, *82*, 27–39.

Hartwich, J., Schmidt, M., Bölscher, J., Reinhardt-Imjela, C., Murach, D., & Schulte, A. (2016). Hydrological modelling of changes in the water balance due to the impact of woody biomass production in the North German Plain. *Environmental Earth Sciences*, *75*(14). https://doi.org/10.1007/s12665-016-5870-4

Hastings, A., Clifton-Brown, J., Wattenbach, M., Mitchell, C. P., & Smith, P. (2009). The development of MISCANFOR , a new Miscanthus crop growth model : towards more robust yield predictions under different climatic and soil conditions. *GCB Bioenergy*, *1*, 154–170. https://doi.org/10.1111/j.1757-1707.2009.01007.x

Hastings, A., Clifton-Brown, J., Wattenbach, M., Stampfl, P., Mitchell, C. P., & Smith, P. (2008). Potential of Miscanthus grasses to provide energy and hence reduce greenhouse gas emissions. *Agronomy for Sustainable Development*, *28*(4), 465–472. https://doi.org/10.1051/agro:2008030

Hastings, A., Mos, M., Yesufu, J. A., McCalmont, J., Schwarz, K., Shafei, R., Ashman, C., Nunn, C., Schuele, H., Cosentino, S., Scalici, G., Scordia, D., Wagner, M., & Clifton-Brown, J. (2017). Economic and Environmental Assessment of Seed and Rhizome Propagated Miscanthus in the UK. *Frontiers in Plant Science*, *8*(June), 1–16. https://doi.org/10.3389/fpls.2017.01058

Hastings, A., Tallis, M. J., Casella, E., Matthews, R. W., Henshall, P. A., Milner, S., Smith, P. & Taylor, G. (2014). The technical potential of Great Britain to produce ligno-cellulosic biomass for bioenergy in current and future climates.

GCB Bioenergy, *6*(2), 108–122. https://doi.org/10.1111/gcbb.12103

Hay, C. H., & Irmak, S. (2009). Actual and reference evaporative losses and surface coefficients of a maize field during nongrowing (dormant) periods. *Journal of Irrigation and Drainage Engineering*, *135*(3), 313–322. https://doi.org/10.1061/(ASCE)IR.1943-4774.0000001

Heilig, G. K. (1994). *The Greenhouse Gas Methane (CH4): Sources and Sinks, the Impact of Population Growth, Possible Interventions*. *Population and Environment: A Journal of Interdisciplinary Studies* (Vol. 16).

Herbst, M., Rosier, P. T. W., McNeil, D. D., Harding, R. J., & Gowing, D. J. (2008). Seasonal variability of interception evaporation from the canopy of a mixed deciduous forest. *Agricultural and Forest Meteorology*, *148*(11), 1655–1667. https://doi.org/10.1016/j.agrformet.2008.05.011

Hess, T. M., Holman, I. P., Rose, S. C., Rosolova, Z., & Parrott, A. (2010). Estimating the impact of rural land management changes on catchment runoff generation in England and Wales. *Hydrological Processes*, *24*(10), 1357–1368. https://doi.org/10.1002/hyp.7598

Hickman, G. C., Vanloocke, A., Dohleman, F. G., & Bernacchi, C. J. (2010). A comparison of canopy evapotranspiration for maize and two perennial grasses identified as potential bioenergy crops. *GCB Bioenergy*, *2*(4), 157–168. https://doi.org/10.1111/j.1757-1707.2010.01050.x

Hillier, J., Whittaker, C., Dailey, G., Aylott, M., Casella, E., Richter, G. M., Riche, A., Murphy, R., Taylor, G., & Smith, P. (2009). Greenhouse gas emissions from four bioenergy crops in England and Wales: Integrating spatial estimates of yield and soil carbon balance in life cycle analyses. *GCB Bioenergy*, *1*(4), 267–281. https://doi.org/10.1111/j.1757-1707.2009.01021.x

Holder, A. J., McCalmont, J. P., McNamara, N. P., Rowe, R., & Donnison, I. S. (2018). Evapotranspiration model comparison and an estimate of field scale Miscanthus canopy precipitation interception. *GCB Bioenergy*, *10*(5), 353–366. https://doi.org/10.1111/gcbb.12503

Holder, A. J., McCalmont, J. P., Rowe, R., McNamara, N. P., Elias, D., & Donnison,

I. S. (2019). Soil N2O emissions with different reduced tillage methods during the establishment of Miscanthus in temperate grassland. *GCB Bioenergy*, *11*(3), 539–549. https://doi.org/10.1111/gcbb.12570

Holland, J. M. (2004). The environmental consequences of adopting conservation tillage in Europe: Reviewing the evidence. *Agriculture, Ecosystems and Environment*, *103*(1), 1–25. https://doi.org/10.1016/j.agee.2003.12.018

Hopkins, F., Gonzalez-Meler, M. A., Flower, C. E., Lynch, D. J., Czimczik, C., Tang, J., & Subke, J.-A. (2013). Ecosystem-level controls on root-rhizosphere respiration. *New Phytologist*, *199*(2), 339–351. https://doi.org/10.1111/nph.12271

Hörmann, G., Branding, A., Clemen, T., Herbst, M., Hinrichs, A., & Thamm, F. (1996). Calculation and simulation of wind controlled canopy interception of a beech forest in Northern Germany. *Agricultural and Forest Meteorology*, *79*(3), 131–148. https://doi.org/10.1016/0168-1923(95)02275-9

Hothorn, T., Bretz, F., & Westfall, P. (2008). Simultaneous Inference in General Parametric Models. *Biometrical Journal*, *50*(3), 346–363.

Hu, Y., Schäfer, G., Duplay, J., & Kuhn, N. J. (2018). Bioenergy crop induced changes in soil properties: A case study on Miscanthus fields in the Upper Rhine Region. *PLoS ONE*, 1–15. https://doi.org/10.1371/journal.pone.0200901

Huang, Y., Ren, W., Wang, L., Hui, D., Grove, J.H., Yang, X., Tao, B., & Goff, B. (2018). Greenhouse gas emissions and crop yield in no-tillage systems: A meta-analysis. *Agriculture, Ecosystems and Environment*, 268, 144-153, doi: 10.1016/j.agee.2018.09.002

Huang, Y., Zou, J., Zheng, X., Wang, Y., & Xu, X. (2004). Nitrous oxide emissions as influenced by amendment of plant residues with different C:N ratios. *Soil Biology and Biochemistry*, *36*(6), 973–981. https://doi.org/10.1016/j.soilbio.2004.02.009

Hurtado-Uria, C., Hennessey, D., Shalloo, L., O'Connor, D., & Delaby, L. (2013). Relationships between meterological data and grass growth over time in the south of Ireland. *Irish Geography*, 46 (3), 175-201.

International Renewable Energy Agency (IRENA). (2018). *Global Energy Transformation: A Roadmap to 2050*. International Renewable Energy Agency, Abu Dhabi. https://doi.org/Doi 10.1002/(Sici)1097-0029(19990915)46:6<398::Aid-Jemt8>3.0.Co;2-H

IPCC. (2006). Emissions from livestock and manure management, chapter 10. In: Guidelines for National Greenhouse Gas Inventories, Vol 4, Prepared by the *National Greenhouse Gas Inventories Programme* (Dong, H., Mangino, J., McAllister, T.A., Hatfield, J.L., Johnson, D.E., Lassey, K.R., de Lima, M.A., Romanovskaya, A.; eds Eggleston HS, Buendia L, Miwa K, Ngara T, Tanabe K), pp. 10.7–10.84. IGES, Japan.

IPCC. (2007). *Climate Change 2007: Synthesis Report. Contribution of Working Groups I, II and III to the Fourth Assessment Report of the Intergovernmental Panel on Climate Change.* (Core Writing Team, R. K. Pachauri & A. Reisinger, Eds.). IPCC, Geneva, Switzerland.

IPCC. (2013). *Climate Change 2013: The Physical Science Basis. Contribution of Working Group I to the Fifth Assessment Report of the Intergovernmental Panel on Climate Change*. (Stocker, T.F., D. Qin, G.-K. Plattner, M. Tignor, S.K. Allen, J. Boschung, A. Nauels, Y. Xia, V. Bex & P.M. Midgley Ed.). Cambridge University Press, Cambridge, United Kingdom and New York, NY, USA.

IPCC. (2014). *Summary for Policymakers*. (Edenhofer, O., R. Pichs-Madruga, Y. Sokona, E. Farahani, S. Kadner, K. Seyboth, A. Adler, I. Baum, S. Brunner, P. Eickemeier, B. Kriemann, J. Savolainen, S. Schlömer, C. von Stechow, T. Zwickel and J.C. Minx Ed.), *Summary for Policymakers. In: Climate Change 2014: Mitigation of Climate Change. Contribution of Working Group III to the Fifth Assessment Report of the Intergovernmental Panel on Climate Change*. Cambridge University Press, Cambridge, United Kingdom and New York, NY, USA. https://doi.org/10.1017/CBO9781107415324

Isselstein, J., Jeangros, B., & Pavlu, V. (2005). Agronomic aspects of biodiversity targeted management of temperate grasslands in Europe-A review. *Agronomy Research*, *3*(2), 139–151.

Jensen, K. D., Beier, C., Michelsen, A., & Emmett, B. A. (2003). Effects of experimental drought on microbial processes in two temperate heathlands at contrasting water conditions. *Applied Soil Ecology*, *24*, 165–176. https://doi.org/10.1016/S0929-1393(03)00091-X

Jones, S. K., Famulari, D., Di Marco, C. F., Nemitz, E., Skiba, U. M., Rees, R. M., & Sutton, M. A. (2011). Nitrous oxide emissions from managed grassland: A comparison of eddy covariance and static chamber measurements. *Atmospheric Measurement Techniques*, *4*(10), 2179–2194. https://doi.org/10.5194/amt-4-2179-2011

Jones, S. K., Rees, R. M., Skiba, U. M., & Ball, B. C. (2005). Greenhouse gas emissions from a managed grassland. *Global and Planetary Change*, *47*, 201–211. https://doi.org/10.1016/j.gloplacha.2004.10.011

Joo, E., Zeri, M., Hussain, M. Z., Delucia, E. H., & Bernacchi, C. J. (2017). Enhanced evapotranspiration was observed during extreme drought from Miscanthus, opposite of other crops. *GCB Bioenergy*, 1306–1319. https://doi.org/10.1111/gcbb.12448

Jorgensen, RN., Jorgensen, BJ., Nielsen, NE, Maag, M. & Lind, A. (1997). N20 Emission From Energy Crop Fields of Miscanthus " Giganteus" and Winter Rye. *Atmospheric Environment*, *31*(18), 2899–2904. https://doi.org/1352-2310/97

Jurasinski, G., Koebsch, F., Guenther, A., & Beetz, S. (2014). flux: Flux rate calculation from dynamic closed chamber measurements. R package version 0.3-0. Retrieved from https://cran.r-project.org/package=flux

Kahlon, M. S., Lal, R., & Ann-Varughese, M. (2013). Twenty two years of tillage and mulching impacts on soil physical characteristics and carbon sequestration in Central Ohio. *Soil and Tillage Research*, *126*, 151–158. https://doi.org/10.1016/j.still.2012.08.001

Keymer, D. P., & Kent, A. D. (2014). Contribution of nitrogen fixation to first year Miscanthus × giganteus. *GCB Bioenergy*, *6*(5), 577–586. https://doi.org/10.1111/gcbb.12095

Kiely, G., McGoff, N. M., Eaton, J. M., Xu, X., Leahy, P., & Carton, O. (2009). SoilC – Measuring and Modelling of Soil Carbon Stocks and Stock Changes in Irish Soils. STRIVE Report Series No. 35.

Kim, G. W., Das, S., Hwang, H. Y., & Kim, P. J. (2017). Nitrous oxide emissions from soils amended by cover-crops and under plastic film mulching: Fluxes, emission factors and yield-scaled emissions. *Atmospheric Environment*, *152*, 377–388. https://doi.org/10.1016/j.atmosenv.2017.01.007

Knapp, A. K., Briggs, J. M., & Koelliker, J. K. (2001). Frequency and extent of water limitation to primary production in a mesic temperate grassland. *Ecosystems*, *4*, 19–28. https://doi.org/10.1007/s100210000057

Kort, J., Collins, M., & Ditsch, D. (1998). A review of soil erosion potential associated with biomass crops. *Biomass and Bioenergy*, *14*(4), 351–359. https://doi.org/10.1016/S0961-9534(97)10071-X

Kørup, K., Lærke, P. E., Baadsgaard, H., Andersen, M. N., Kristensen, K., Münnich, C., Didion, T., Jensen, E., Mårtensson, L. & Jørgensen, U. (2018). Biomass production and water use efficiency in perennial grasses during and after drought stress. *GCB Bioenergy*, *10*, 12–27. https://doi.org/10.1111/gcbb.12464

Krol, D. J., Jones, M. B., Williams, M., Ní Choncubhair, & Lanigan, G. J. (2019). The effect of land use change from grassland to bioenergy crops Miscanthus and reed canary grass on nitrous oxide emissions. *Biomass and Bioenergy*, *120*, 396–403. https://doi.org/10.1016/j.biombioe.2018.11.033

Kucharik, C. J., & Brye, K. R. (2003). Integrated BIosphere Simulator (IBIS) Yield and Nitrate Loss Predictions for Wisconsin Maize Receiving Varied Amounts of Nitrogen Fertilizer. *Journal of Environmental Quality Abstract - Plant and Environment Interactions*, *32*(1), 247–268.

Kuzyakov, Y. (2010). Priming effects: Interactions between living and dead organic matter. *Soil Biology and Biochemistry*, *42*(9), 1363–1371. https://doi.org/10.1016/j.soilbio.2010.04.003

Kuzyakov, Y., & Domanski, G. (2000). Carbon inputs by plants into the soil. Review. *Journal of Plant Nutrition and Soil Science*, *163*(4), 421–431.

https://doi.org/10.1002/1522-2624(200008)163

La Scala Jr., N., Lopes, A., Spokas, K., Bolonhezi, D., Archer, D. W., & Reicosky, D. C. (2008). Short-term temporal changes of soil carbon losses after tillage described by a first-order decay model. *Soil and Tillage Research*, *99*(1), 108–118. https://doi.org/10.1016/j.still.2008.01.006

Lal, R. (2004). Soil Carbon Sequestration Impacts on Global Climate Change and Food Security. *Science*, *304*(5677), 1623–1627. https://doi.org/10.1126/science.1097396

Lal, R. (2011). Sequestering carbon in soils of agro-ecosystems. *Food Policy*, *36*, S33–S39. https://doi.org/10.1016/j.foodpol.2010.12.001

Lal, R. (2019). Managing soils for resolving the conflict between agriculture and nature: The hard talk. *European Journal of Soil Science*, 1-9, doi: 10.1111/ejss.12857

Lal, R., Reicosky, D. C., & Hanson, J. D. (2007). Evolution of the plow over 10,000 years and the rationale for no-till farming. *Soil and Tillage Research*, *93*(1), 1–12. https://doi.org/10.1016/j.still.2006.11.004

Langeveld, H., Quist-Wessel, F., Dimitriou, I., Aronsson, P., Baum, C., Schulz, U., Bolte, A., Baum, S., Kohn, J., Weih, M., Gruss, H., Leinweber, P., Lamersdorf, N., Schmidt-Walter, P., & Berndes, G. (2012). Assessing Environmental Impacts of Short Rotation Coppice (SRC) Expansion: Model Definition and Preliminary Results. *Bioenergy Research*, *5*, 621–635. https://doi.org/10.1007/s12155-012-9235-x

Larsen, S. U., Jørgensen, U., Kjeldsen, J. B., & Lærke, P. E. (2014). Long-Term Miscanthus Yields Influenced by Location, Genotype, Row Distance, Fertilization and Harvest Season. *Bioenergy Research*, *7*, 620–635. https://doi.org/10.1007/s12155-013-9389-1

Lask, J., Wagner, M., Trindade, L. M., & Lewandowski, I. (2018). Life cycle assessment of ethanol production from miscanthus: A comparison of production pathways at two European sites. *GCB Bioenergy*, 1–20. https://doi.org/10.1111/gcbb.12551

Le Maitre, D. C., Scott, D. F., & Colvin, C. (1999). A review of information on interactions between vegetation and groundwater. *Water SA*, *25*(2), 137–152. https://doi.org/http://www.wrc.org.za

Legates, D. R., & McCabe Jr., G. J. (2005). Evaluating the Use of "Goodness of Fit" Measures in Hydrologic and Hydroclimatic Model Validation. *Water Resources Research*, *35*(1), 233–241. https://doi.org/10.1029/1998WR900018

Leonard, R. A., Knisel, W. G., & Still, D. A. (1987). GLEAMS: Groundwater Loading Effects on Agricultural Management Systems. *Trans. ASAE*, *30*(5), 1403–1428.

Lewandowski, I., Clifton-Brown, J. C., Scurlock, J. M. O., & Huisman, W. (2000). Miscanthus: European experience with a novel energy crop. *Biomass and Bioenergy*, *19*, 209–227.

Lewandowski, I., Clifton-Brown, J., Trindade, L. M., van der Linden, G. C., Schwarz, K.-U., Müller-Sämann, K., Anisimov, A., Chen, C.-L., Dolstra, O., Donnison, I.S., Farrar, K., Fonteyne, S., Harding, G., Hastings, A., Huxley, L.M., Iqbal, Y., Khokhlov., N., Kiesel, A., Lootens, P., Meyer, H., Mos, M., Muylle, H., Nunn, C., Ozguven, M., Roldan-Ruiz, I., Schule, H., Tarakanov, I., van der Weijde, T., Wagner, M., Xi, Q., & Kalinina, O. (2016). Progress on Optimizing Miscanthus Biomass Production for the European Bioeconomy: Results of the EU FP7 Project OPTIMISC. *Frontiers in Plant Science*, *7*, 1620. https://doi.org/10.3389/fpls.2016.01620

Lewandowski, I., & Schmidt, U. (2006). Nitrogen, energy and land use efficiencies of miscanthus, reed canary grass and triticale as determined by the boundary line approach. *Agriculture, Ecosystems and Environment*, *112*, 335–346. https://doi.org/10.1016/j.agee.2005.08.003

Li, C. (2007). Quantifying greenhouse gas emissions from soils: Scientific basis and modeling approach. *Soil Science and Plant Nutrition*, *53*(4), 344–352. https://doi.org/10.1111/j.1747-0765.2007.00133.x

Li, S. X., Wang, Z. H., Li, S. Q., Gao, Y. J., & Tian, X. H. (2013). Effect of plastic sheet mulch, wheat straw mulch, and maize growth on water loss by evaporation in dryland areas of China. *Agricultural Water Management*, *116*,

39–49. https://doi.org/10.1016/j.agwat.2012.10.004

Lim, K.-J., Engel, B. A., Kim, K.-S., & Choi, J.-D. (2003). Nutrient Enabled National Agricultural Pesticide Risk Analysis (NAPRA) WWW Decision Support System for Agricultural Best Management Practices. *Journal of Korean Society of Rural Planning*, *9*(1), 85–93.

Lindegaard, K. N., Adams, P. W. R., Holley, M., Lamley, A., Henriksson, A., Larsson, S., von Engelbrechten, H.-G., Lopez, G.E., & Pisarek, M. (2016). Short rotation plantations policy history in Europe: Lessons from the past and recommendations for the future. *Food and Energy Security*, *5*(3), 125–152. https://doi.org/10.1002/fes3.86

Linderson, M. L., Iritz, Z., & Lindroth, A. (2007). The effect of water availability on stand-level productivity, transpiration, water use efficiency and radiation use efficiency of field-grown willow clones. *Biomass and Bioenergy*, *31*(7), 460–468. https://doi.org/10.1016/j.biombioe.2007.01.014

Liu, W., Mi, J., Song, Z., Yan, J., Li, J., & Sang, T. (2014). Long-term water balance and sustainable production of Miscanthus energy crops in the Loess Plateau of China. *Biomass and Bioenergy*, *62*, 47–57. https://doi.org/10.1016/j.biombioe.2014.01.018

Lovett, A. A., Sunnenberg, G. M., Richter, G. M., Dailey, A. G., Riche, A. B., & Karp, A. (2009). Land use implications of increased biomass production identified by gis-based suitability and yield mapping for miscanthus in england. *Bioenergy Research*, *2*(1–2), 17–28. https://doi.org/10.1007/s12155-008-9030-x

Lovett, A., Sünnenberg, G., & Dockerty, T. (2014). The availability of land for perennial energy crops in Great Britain. *GCB Bioenergy*, *6*(2), 99–107. https://doi.org/10.1111/gcbb.12147

Luo, Y., Wan, S., Hui, D., & Wallace, L. L. (2001). Acclimatization of soil respiration to warming in a tall grass prairie. *Nature*. https://doi.org/10.1038/35098065

Maag, M., & Vinther, F. P. (1996). Nitrous oxide emission by nitrification and denitrification in different soil types and at different soil moisture contents and

temperatures. *Applied Soil Ecology*, *4*(1), 5–14. https://doi.org/10.1016/0929-1393(96)00106-0

Mann, J. J., Barney, J. N., Kyser, G. B., & DiTomaso, J. M. (2013). Root System Dynamics of Miscanthus × giganteus and Panicum virgatum in Response to Rainfed and Irrigated Conditions in California. *Bioenergy Research*, *6*, 678–687. https://doi.org/10.1007/s12155-012-9287-y

Marriott, C.A., Hood, K., Fisher, J.M. & Pakeman, R.J. (2009). Long-term impacts of extensive grazing and abandonment on the species composition, richness, diversity and productivity of agricultural grassland. *Agriculture, Ecosystems & Environment*, 134(3-4), 190-200, doi: 10.1016/j.agee.2009.07.002

Marshall, M. R., Francis, O. J., Frogbrook, Z. L., Jackson, B. M., McIntyre, N., Reynolds, B., Solloway, I., Wheater, H.S., & Chell, J. (2009). The impact of upland land management on flooding: results from an improved pasture hillslope. *Hydrological Processes*, *23*, 464–475. https://doi.org/10.1002/hyp.7157

Marshall, T. J., Holmes, J. W., & Rose, C. W. (1996). *Soil Physics* (3rd ed.). Cambridge University Press, Cambridge, United Kingdom and New York, NY, USA.

McCalmont, J. P., Hastings, A., McNamara, N. P., Richter, G. M., Robson, P., Donnison, I. S., & Clifton-Brown, J. (2017). Environmental costs and benefits of growing Miscanthus for bioenergy in the UK. *GCB Bioenergy*, *9*(3), 489–507. https://doi.org/10.1111/gcbb.12294

McCalmont, J. P., McNamara, N. P., Donnison, I. S., Farrar, K., & Clifton-Brown, J. C. (2017). An interyear comparison of CO2 flux and carbon budget at a commercial-scale land-use transition from semi-improved grassland to Miscanthus x giganteus. *GCB Bioenergy*, *9*(1), 229–245. https://doi.org/10.1111/gcbb.12323

McCalmont, J. P., Rowe, R., Elias, D., Whitaker, J., McNamara, N. P., & Donnison, I. S. (2018). Soil nitrous oxide flux following land-use reversion from Miscanthus and SRC willow to perennial ryegrass, (May). https://doi.org/10.1111/gcbb.12541

McGowan, A. R., Roozeboom, K. L., & Rice, C. W. (2018). Nitrous Oxide Emissions from Annual and Perennial Biofuel Cropping Systems. *Agronomy Journal*, *110*(6), 84–92. https://doi.org/10.2134/agronj2018.03.0187

McMahon, T. A., Peel, M. C., Lowe, L., Srikanthan, R., & McVicar, T. R. (2013). Estimating actual, potential, reference crop and pan evaporation using standard meteorological data: A pragmatic synthesis. *Hydrology and Earth System Sciences*, *17*(4), 1331–1363. https://doi.org/10.5194/hess-17-1331-2013

McManus, M. C., & Taylor, C. M. (2015). The changing nature of life cycle assessment. *Biomass and Bioenergy*, *82*, 13–26. https://doi.org/10.1016/j.biombioe.2015.04.024

Met Office. (n.d.a). Gogerddan station. Retrieved October 9, 2018, from https://www.metoffice.gov.uk/public/weather/climate/gcm4k8cnp

Met Office. (n.d.b). UK Meterological Data: 30 year averages. Retrieved June 14, 2018, from https://www.metoffice.gov.uk/public/weather/climate/gcm1y0vvu

Met Office. (2014). Climate Stations. Retrieved February 1, 2018, from https://www.metoffice.gov.uk/climate

Met Office. (2016a). Climate Summaries. Retrieved August 24, 2017, from http://www.metoffice.gov.uk/climate/uk/summaries

Met Office. (2016b). Past weather events. Retrieved August 24, 2017, from http://www.metoffice.gov.uk/climate/uk/interesting

Miller, J. N., VanLoocke, A., Gomez-Casanovas, N., & Bernacchi, C. J. (2016). Candidate perennial bioenergy grasses have a higher albedo than annual row crops. *GCB Bioenergy*, *8*(4), 818–825. https://doi.org/10.1111/gcbb.12291

Mills, S. (2016). *Wetland Conservation Biomass to Bioenergy: End User Report*. Retrieved from https://ecosystemsknowledge.net/sites/default/files/wp-content/uploads/DECC Biomass to Bioenergy End User Report_0.pdf

Milne, J. A., Pakeman, R. J., Kirkham, F. W., Jones, I. P., & Hossell, J. E. (2002). Biomass production of upland vegetation types in England and Wales. *Grass and Forage Science*, *57*(4), 373–388. https://doi.org/10.1046/j.1365-2494.2002.00339.x

Milner, S., Holland, R. A., Lovett, A., Sunnenberg, G., Hastings, A., Smith, P., Wang, S. & Taylor, G. (2016). Potential impacts on ecosystem services of land use transitions to second-generation bioenergy crops in GB. *GCB Bioenergy*, *8*(2), 317–333. https://doi.org/10.1111/gcbb.12263

Mintz, Y., & Walker, G. K. (1993). Global Fields of Soil-Moisture and Land-Surface Evapotranspiration Derived from Observed Precipitation and Surface Air-Temperature. *Journal of Applied Meteorology*. https://doi.org/Doi 10.1175/1520-0450(1993)032<1305:Gfosma>2.0.Co;2

Mohr, A., & Raman, S. (2013). Lessons from first generation biofuels and implications for the sustainability appraisal of second generation biofuels. *Energy Policy*, *63*, 114–122. https://doi.org/10.1016/j.enpol.2013.08.033

Monteith, J. L. (1965). Evaporation and Environment. In *The State and Movement of Water in Living Organisms (Proceedings of 19th Symposium of the Society of Experimental Biology, Swansea 1964)* (pp. 205–234). Academic Press, Cambridge, UK.

Monteith, J. L., & Unsworth, M. H. (2008). *Principles of Environmental Physics* (3rd ed.). Academic Press, London.

Monti, A., & Zatta, A. (2009). Root distribution and soil moisture retrieval in perennial and annual energy crops in Northern Italy. *Agriculture, Ecosystems and Environment*, *132*, 252–259. https://doi.org/10.1016/j.agee.2009.04.007

Morton, F. I. (1965). Potential evaporation and river basin evaporation. *ASCE J. Hydraul. Eng.*, *102*, 275–291.

National Assembly for Wales. (2017). The Record of Proceedings, 6. Statement: Energy. Retrieved January 24, 2019, from http://www.assembly.wales/en/bus-home/pages/rop.aspx?meetingid=4644&assembly=5&c=Record of Proceedings#C494225

National Centers for Environmental Prediction (NCEP). (n.d.). Global Weather Data for SWAT. Retrieved February 1, 2018, from http://www.waterbase.org/download_data.html

Natural Environment Research Council (NERC), & Centre for Ecology &

Hydrology (CEH). (n.d.). National River Flow Archive 2018. Retrieved February 1, 2018, from https://nrfa.ceh.ac.uk

Natural Resources Wales (NRW). (2018). GB Lakes Inventory © Natural Resources Wales and Database Right. All rights Reserved. Contains Ordnance Survey Data. Ordnance Survey Licence number 100019741. Crown Copyright and Database Right. Retrieved February 1, 2018, from http://lle.gov.wales/catalogue/item/GBLakesInventoryEnglandWales/?lang=en

Neff, J. C., Townsend, A. R., Gleixner, G., Lehman, S. J., Turnbull, J., & Bowman, W. D. (2002). Variable effects of nitrogen additions on the stability and turnover of soil carbon. *Nature*, *419*, 915–917. https://doi.org/10.1038/nature01136

Neitsch, S. L., Arnold, J. G., Kiniry, J. R., & Williams, J. R. (2011). SWAT Theoretical Documentation Version 2009. *Texas Water Resources Institute*, 1–647. https://doi.org/10.1016/j.scitotenv.2015.11.063

Neukirchen, D., Himken, M., Lammel, J., Czypionka-Krause, U., & Olfs, H.-W. (1999). Spatial and temporal distribution of the root system and root nutrient content of an established Miscanthus crop. *European Journal of Agronomy*, *11*, 301–309.

Ng, T. L., Eheart, J. W., Cai, X., & Miguez, F. (2010). Modeling miscanthus in the Soil and Water Assessment Tool (SWAT) to simulate its water quality effects as a bioenergy crop. *Environmental Science and Technology*, *44*(18), 7138–7144. https://doi.org/10.1021/es9039677

Nguyen, T. L. T., & Hermansen, J. E. (2015). Life cycle environmental performance of miscanthus gasification versus other technologies for electricity production. *Sustainable Energy Technologies and Assessments*, *9*, 81–94. https://doi.org/10.1016/j.seta.2014.12.005

Nisbet, T. (2005). Water Use by Trees - Forestry Commission Information Note FCIN065, 1–8. Retrieved from https://www.forestry.gov.uk/pdf/FCIN065.pdf/$file/FCIN065.pdf%0Ahttp://www.forestry.gov.uk/pdf/fcin065.pdf

Nishimura, S., Komada, M., Takebe, M., Yonemura, S., & Kato, N. (2012). Nitrous oxide evolved from soil covered with plastic mulch film in horticultural field. *Biology and Fertility of Soils*, *48*(7), 787–795. https://doi.org/10.1007/s00374-012-0672-7

Nunn, C., Hastings, A. F. S. J., Kalinina, O., Özgüven, M., Schüle, H., Tarakanov, I. G., Van Der Weijde, T., Anisimov, A.A., Iqbal, Y., Kiesel, A., Khokhlov, N.F., McCalmont, J.P., Meyer, H., Mos, M., Schwarz, K., Trindade, L.m., Lewandowski, I & Clifton-Brown, J. C. (2017). Environmental Influences on the Growing Season Duration and Ripening of Diverse Miscanthus Germplasm Grown in Six Countries. *Frontiers in Plant Science*, *8*(May), 1–14. https://doi.org/10.3389/fpls.2017.00907

Oak Ridge National Laboratory Distributed Active Archive Center (ORNL DAAC). (n.d.). A Global Database of Field-observed Leaf Area Index in Woody Plant Species, 1932-2011. Retrieved February 1, 2018, from https://daac.ornl.gov/VEGETATION/guides/LAI_Woody_Plants.html

Oates, L. G., Duncan, D. S., Gelfand, I., Millar, N., Robertson, G. P., & Jackson, R. D. (2016). Nitrous oxide emissions during establishment of eight alternative cellulosic bioenergy cropping systems in the North Central United States. *GCB Bioenergy*, *8*(3), 539–549. https://doi.org/10.1111/gcbb.12268

Oenema, O., Velthof, G. L., Yamulki, S., & Jarvis, S. C. (1997). Nitrous oxide emissions from grazed grassland. *Soil Use and Management*. https://doi.org/10.1111/j.1475-2743.1997.tb00600.x

Olave, R. J., Forbes, E. G. A., Munoz, F., Laidlaw, A. S., Easson, D. L., & Watson, S. (2017). Performance of Miscanthus x giganteus (Greef et Deu) established with plastic mulch and grown from a range of rhizomes sizes and densities in a cool temperate climate. *Field Crops Research*, *210*(December 2016), 81–90. https://doi.org/10.1016/j.fcr.2017.05.020

Ordnance Survey. (2018). OS Terrain 50 & OS Open Rivers (c) Crown copyright and database right 2018. Retrieved February 1, 2018, from https://www.ordnancesurvey.co.uk/business-and-government/products/terrain-

50.html

Organisation for Economic Co-operation and Development (OECD). (2016). *Mitigating Droughts and Floods in Agriculture: Policy Lessons and Approaches*. OECD Publishing, Paris. Retrieved from https://dx.doi.org/10.1787/9789264246744-en

Ostle, N. J., Smith, P., Fisher, R., Ian Woodward, F., Fisher, J. B., Smith, J. U., Galbraith, D., Levy, P., Meir, P., McNamara, N.P. & Bardgett, R. D. (2009). Integrating plant-soil interactions into global carbon cycle models. *Journal of Ecology*, *97*, 851–863. https://doi.org/10.1111/j.1365-2745.2009.01547.x

Pallipparambil, G. R., Raghu, S., & Wiedenmann, R. N. (2015). Energy for Sustainable Development Modeling the biomass production of the biofuel crop Miscanthus x giganteus , to understand and communicate benefits and risks in cultivation. *Energy for Sustainable Development*, *27*, 63–72. https://doi.org/10.1016/j.esd.2015.04.005

Palmer, M. M., Forrester, J. A., Rothstein, D. E., & Mladenoff, D. J. (2014). Conversion of open lands to short-rotation woody biomass crops: Site variability affects nitrogen cycling and N2O fluxes in the US Northern Lake States. *GCB Bioenergy*, *6*(4), 450–464. https://doi.org/10.1111/gcbb.12069

Panagopoulos, Y., Gassman, P. W., Kling, C. L., Cibin, R., & Chaubey, I. (2017). Water Quality Assessment of Large-scale Bioenergy Cropping Scenarios for the Upper Mississippi and Ohio-Tennessee River Basins. *Journal of the American Water Resources Association*, *53*(6), 1355–1367. https://doi.org/10.1111/1752-1688.12594

Parajuli, P. B., & Duffy, S. E. (2013). Quantifying Hydrologic and Water Quality Responses to Bioenergy Crops in Town Creek Watershed in Mississippi. *Journal of Sustainable Bioenergy Systems*, *3*, 202–208. https://doi.org/10.4236/jsbs.2013.33028

Parkin, T. B., & Venterea, R. T. (2010). Chamber-Based Trace Gas Flux Measurements. In *USDA-ARS GRACEnet project protocol; chapter 3*. (pp. 1–39). https://doi.org/10.2134/jeq2009.0231

Pellis, A., Laureysens, I., & Ceulemans, R. (2004). Growth and production of a short rotation coppice culture of poplar I. Clonal differences in leaf characteristics in relation to biomass production. *Biomass and Bioenergy*, *27*(1), 9–19. https://doi.org/10.1016/j.biombioe.2003.11.001

Pielke, R. A., Marland, G., Betts, R. A., Chase, T. N., Eastman, J. L., Niles, J. O., Niyogi, D. & Running, S. W. (2002). The influence of land-use change and landscape dynamics on the climate system: Relevance to climate-change policy beyond the radiative effect of greenhouse gases. *Philosophical Transactions of the Royal Society A*. https://doi.org/10.1098/rsta.2002.1027

Pinheiro, J., Bates, D., DebRoy, S., Sarkar, D., & R Core Team. (2017). nlme: Linear and Nonlinear Mixed Effects Models. R package version 3.1-131. Retrieved from https://cran.r-project.org/package=nlme

Pitman, A. J., De Noblet-Ducoudré, N., Cruz, F. T., Davin, E. L., Bonan, G. B., Brovkin, V., Claussen, M., Delire, C., Ganzeveld., L., Gayler., V., van den Hurk, B., Lawrence, P., van der Molen, M., Muller, C., Reick, C., Seneviratne, S., Strengers, B & Voldoire, A. (2009). Uncertainties in climate responses to past land cover change: First results from the LUCID intercomparison study. *Geophysical Research Letters*, *36*, 1–6. https://doi.org/10.1029/2009GL039076

Poeplau, C., & Don, A. (2014). Soil carbon changes under Miscanthus driven by C4 accumulation and C3 decompostion - toward a default sequestration function. *GCB Bioenergy*, *6*(4), 327–338. https://doi.org/10.1111/gcbb.12043

Poff, N. L., Richter, B. D., Arthington, A. H., Bunn, S. E., Naiman, R. J., Kendy, E., Acreman, M., Apse, C., Bledsoe, B., Freeman, M., Henriksen, J., Jacobson, R., Kennen, J., Merritt, D., O'Keeffe, J., Olden, J., Rogers, K., Tharme, R. & Warner, A. (2010). The ecological limits of hydrologic alteration (ELOHA): A new framework for developing regional environmental flow standards. *Freshwater Biology*, *55*, 147–170. https://doi.org/10.1111/j.1365-2427.2009.02204.x

Poff, N. L., & Zimmerman, J. K. H. (2010). Ecological responses to altered flow regimes: A literature review to inform the science and management of environmental flows. *Freshwater Biology*, *55*, 194–205.

https://doi.org/10.1111/j.1365-2427.2009.02272.x

Post, M., & Kwon, K. C. (2000). Soil Carbon Sequestration and Land-Use Change: Processes and Potential. *Global Change Biology*, *6*, 317–328. https://doi.org/10.1046/j.1365-2486.2000.00308.x

Powlson, D. S., Whitmore, A. P., & Goulding, K. W. T. (2011). Soil carbon sequestration to mitigate climate change: A critical re-examination to identify the true and the false. *European Journal of Soil Science*, *62*, 42–55. https://doi.org/10.1111/j.1365-2389.2010.01342.x

Priestley, C. H. B., & Taylor, R. J. (1972). On the assessment of surface heat flux and evaporation using large scale parameters. *Monthly Weather Review*, *100*, 81–92.

QGIS (Development Team). (2014). QGIS Geographic Information System. Open Source Geospatial Foundation Project. Retrieved from http://qgis.osgeo.org

Qin, Z., Dunn, J. B., Kwon, H., Mueller, S., & Wander, M. M. (2016). Soil carbon sequestration and land use change associated with biofuel production: Empirical evidence. *GCB Bioenergy*, *8*(1), 66–80. https://doi.org/10.1111/gcbb.12237

Quaye, A. K., & Volk, T. A. (2013). Biomass production and soil nutrients in organic and inorganic fertilized willow biomass production systems. *Biomass and Bioenergy*, *57*, 113–125. https://doi.org/10.1016/j.biombioe.2013.08.002

R Core Team. (2015). R: A language and environment for statistical computing. R Foundation for Statistical Computing, Vienna, Austria. URL https://www.R-project.org/.

Raghunath, H. M. (2006). *Hydrology* (Second Edi). New Age International (P) Ltd, New Delhi.

Rana, G., & Katerji, N. (2000). Measurement and estimation of actual evapotranspiration in the field under Mediterranean climate: A review. *European Journal of Agronomy*, *13*, 125–153. https://doi.org/10.1016/S1161-0301(00)00070-8

Rathmann, R., Szklo, A., & Schaeffer, R. (2010). Land use competition for

production of food and liquid biofuels: An analysis of the arguments in the current debate. *Renewable Energy*, *35*(1), 14–22. https://doi.org/10.1016/j.renene.2009.02.025

Ravishankara, A. R., Daniel, J. S., & Portmann, R. W. (2009). Nitrous Oxide (N_20): The Dominant Ozone-Depleting Substance Emitted in the 21st Century. *Science*, *326*(5949), 123–125. https://doi.org/10.1126/science.ll76758

Reay, D. S., Davidson, E. A., Smith, K. A., Smith, P., Melillo, J. M., Dentener, F., & Crutzen, P. J. (2012). Global agriculture and nitrous oxide emissions. *Nature Climate Change*, *2*(6), 410–416. https://doi.org/10.1038/nclimate1458

Reay, D. S., Hewitt, C. N., Smith, K. A., & Grace, J. (2007). *Greenhouse Gas Sinks*. CABI, Oxford UK and Cambridge USA.

Reicosky, D. C., & Lindstrom, M. J. (1995). Impact of fall tillage on short term carbon dioxide flush. In R. Lal, J. Kimble, E. Levine, & B. A. Stewart (Eds.), *Soils and Global Change*. CRC Press Inc., Florida.

Richards, M., Pogson, M., Dondini, M., Jones, E. O., Hastings, A., Henner, D. N., Tallis, M.J., Casella, E., Matthews, R.W., Henshall, P.A., Milner, S., Taylor, G., McNamara, N.P., Smith, J.U., & Smith, P. (2017). High-resolution spatial modelling of greenhouse gas emissions from land-use change to energy crops in the United Kingdom. *GCB Bioenergy*, *9*(3), 627–644. https://doi.org/10.1111/gcbb.12360

Riche, A. B., & Christian, D. G. (2001). Rainfall interception by mature Miscanthus grass in SE England. *Aspects of Applied Biology*, *65*, 143–146.

Richter, G. M., Agostini, F., Redmile-Gordon, M., White, R., & Goulding, K. W. T. (2015). Sequestration of C in soils under Miscanthus can be marginal and is affected by genotype-specific root distribution. *Agriculture, Ecosystems and Environment*, *200*, 169–177. https://doi.org/10.1016/j.agee.2014.11.011

Richter, G. M., Riche, A. B., Dailey, A. G., Gezan, S. A., & Powlson, D. S. (2008). Is UK biofuel supply from Miscanthus water-limited? *Soil Use and Management*, *24*(3), 235–245. https://doi.org/10.1111/j.1475-2743.2008.00156.x

Robertson, A. D., Davies, C. A., Smith, P., Dondini, M., & McNamara, N. P. (2015). Modelling the carbon cycle of Miscanthus plantations: Existing models and the potential for their improvement. *GCB Bioenergy*, *7*(3), 405–421. https://doi.org/10.1111/gcbb.12144

Robertson, A. D., Whitaker, J., Morrison, R., Davies, C. A., Smith, P., & McNamara, N. P. (2017). A Miscanthus plantation can be carbon neutral without increasing soil carbon stocks. *GCB Bioenergy*, *9*(3), 645–661. https://doi.org/10.1111/gcbb.12397

Robinson, E. L., Blyth, E. M., Clark, D. B., Finch, J., & Rudd, A. C. (2017). *Trends in atmospheric evaporative demand in Great Britain using high-resolution meteorological data*. *Hydrology and Earth System Sciences* (Vol. 21). https://doi.org/10.5194/hess-21-1189-2017

Rochette, P. (2008). No-till only increases N2O emissions in poorly-aerated soils. *Soil and Tillage Research*, *101*(1–2), 97–100. https://doi.org/10.1016/j.still.2008.07.011

Roth, B., Jones, M., Burke, J., & Williams, M. (2013). The Effects of Land-Use Change from Grassland to Miscanthus x giganteus on Soil N2O Emissions. *Land*, *2*(3), 437–451. https://doi.org/10.3390/land2030437

Rowe, R. L., Keith, A. M., Elias, D., Dondini, M., Smith, P., Oxley, J., & McNamara, N. P. (2016). Initial soil C and land-use history determine soil C sequestration under perennial bioenergy crops. *GCB Bioenergy*, *8*(6), 1046–1060. https://doi.org/10.1111/gcbb.12311

Rowe, R. L., Street, N. R., & Taylor, G. (2009). Identifying potential environmental impacts of large-scale deployment of dedicated bioenergy crops in the UK. *Renewable and Sustainable Energy Reviews*, *13*(1), 271–290. https://doi.org/10.1016/j.rser.2007.07.008

Rowell, D. L. (1994). *Soil Science: Methods and Applications*. Longman, Harlow.

Rowland, C. S., Morton, R. D., Carrasco, L., McShane, G., O'Neil, A. W., & Wood, C. M. (2017). Land Cover Map 2015 (25m raster, GB). *NERC Environmental Information Data Centre.* Retrieved from https://doi.org/10.5285/bb15e200-

9349-403c-bda9-b430093807c7

Ruf, T., & Emmerling, C. (2018). Site-adapted production of bioenergy feedstocks on poorly drained cropland through the cultivation of perennial crops. A feasibility study on biomass yield and biochemical methane potential. *Biomass and Bioenergy*, *119*, 429–435. https://doi.org/10.1016/j.biombioe.2018.10.007

Rumpel, C., Amiraslani, F., Koutika, L.-S., Smith, P., Whitehead, D., & Wollenberg, E. (2018). Put more carbon in soils to meet Paris climate pledges. *Nature*, *564*, 32–34. https://doi.org/10.1029/2018GL079362

Sage, R. F. (2014). Preface: Photosynthetic efficiency and carbon concentration in terrestrial plants: The C4 and CAM solutions. *Journal of Experimental Botany*, *65*(13), 3323–3325. https://doi.org/10.1093/jxb/eru262

Saha, D., Rau, B. M., Kaye, J. P., Montes, F., Adler, P. R., & Kemanian, A. R. (2017). Landscape control of nitrous oxide emissions during the transition from conservation reserve program to perennial grasses for bioenergy. *GCB Bioenergy*, *9*(4), 783–795. https://doi.org/10.1111/gcbb.12395

Samadi, S. Z. (2017). Assessing the sensitivity of SWAT physical parameters to potential evapotranspiration estimation methods over a coastal plain watershed in the southeastern United States. *Hydrology Research*, *48*(2), 395–415. https://doi.org/10.2166/nh.2016.034

Saxton, K. E., & Rawls, W. J. (2006). Soil Water Characteristic Estimates by Texture and Organic Matter for Hydrologic Solutions. *Soil Science Society of America Journal*, *70*(5), 1569. https://doi.org/10.2136/sssaj2005.0117

Schmidt-Walter, P., & Lamersdorf, N. P. (2012). Biomass Production with Willow and Poplar Short Rotation Coppices on Sensitive Areas-the Impact on Nitrate Leaching and Groundwater Recharge in a Drinking Water Catchment near Hanover, Germany. *Bioenergy Research*, *5*(3), 546–562. https://doi.org/10.1007/s12155-012-9237-8

Schneckenberger, K., & Kuzyakov, Y. (2007). Carbon sequestration under Miscanthus in sandy and loamy soils estimated by natural 13C abundance. *Journal of Plant Nutrition and Soil Science*, *170*(4), 538–542.

https://doi.org/10.1002/jpln.200625111

Sellers, P. J., Mintz, Y., Sud, Y. C., & Dalcher, A. (1986). A Simple Biosphere Model (SiB) for Use within General Circulation Models. *Journal of the Atmospheric Sciences*, *43*(6), 505–531.

Semere, T., & Slater, F. M. (2007). Ground flora, small mammal and bird species diversity in miscanthus (Miscanthus×giganteus) and reed canary-grass (Phalaris arundinacea) fields. *Biomass and Bioenergy*, *31*, 20–29. https://doi.org/10.1016/j.biombioe.2006.07.001

Sen, S., & Ganguly, S. (2017). Opportunities, barriers and issues with renewable energy development – A discussion. *Renewable and Sustainable Energy Reviews*, *69*(May 2016), 1170–1181. https://doi.org/10.1016/j.rser.2016.09.137

Shafroth, P. B., Wilcox, A. C., Lytle, D. A., Hickey, J. T., Andersen, D. C., Beauchamp, V. B., Hautzinger, A., McMullen, L.E. & Warner, A. (2010). Ecosystem effects of environmental flows: modelling and experimental floods in a dryland river. *Freshwater Biology*, *55*, 68–85. https://doi.org/10.1111/j.1365-2427.2009.02271.x

Shuttleworth, W. J., & Wallace, J. S. (1985). Evaporation from sparse crops-an energy combination theory. *Quarterly Journal of the Royal Meteorological Society*, *111*(469), 839–855.

Smit, H. J., Metzger, M. J., & Ewert, F. (2008). Spatial distribution of grassland productivity and land use in Europe. *Agricultural Systems*, *98*(3), 208–219. https://doi.org/10.1016/j.agsy.2008.07.004

Smith, C. M., David, M. B., Mitchell, C. A., Masters, M. D., Anderson-Teixeira, K. J., Bernacchi, C. J., & DeLucia, E. H. (2013). Reduced Nitrogen Losses after Conversion of Row Crop Agriculture to Perennial Biofuel Crops. *Journal of Environmental Quality*, *42*(1), 219–228. https://doi.org/10.2134/jeq2012.0210

Smith, J., Gottschalk, P., Bellarby, J., Chapman, S., Lilly, A., Towers, W., Bell, J., Coleman, K., Nayak, D., Richards, M., Hillier, J., Flynn, H., Wattenbach, M., Aikenhead, M., Yeluripati, J., Farmer, J., Milne, R., THomson, A., Evans, C., Whitmore, A., Falloon, P., & Smith, P. (2010). Estimating changes in Scottish

soil carbon stocks using ECOSSE. I. Model description and uncertainties. *Climate Research*, *45*(1), 179–192. https://doi.org/10.3354/cr00902

Smith, K. A., Ball, T., Conen, F., Dobbie, K. E., Massheder, J., & Rey, A. (2003). Exchange of greenhousegases between soil and atmosphere: interactions of soil physical factors and biological processes. *European Journal of Soil Science*, *54*(December), 779–791. https://doi.org/10.1046/j.1365-2389.2003.00567.x

Smith, K. A., Dobbie, K. E., Ball, B. C., Bakken, L. R., Sitaula, B. K., Hansen, S., Brumme, R., Borken, W., Christensen, S., Prieme, A., Fowler, D., MacDonald, J., Skiba, U., Klemedtsson, L., Kasmir-Klemedtsson, A., Degorska, A. & Orlanski, P. (2000). Oxidation of atmospheric methane in Northern European soils, comparison with other ecosystems, and uncertainties in the global terrestrial sink. *Global Change Biology*, *6*, 791–803. https://doi.org/10.1046/j.1365-2486.2000.00356.x

Smith, P., Chapman, S. J., Scott, W. A., Black, H. I. J., Wattenbach, M., Milne, R., Campbell, C.D., Lilly, A., Ostle, N., Levy, P.E., Lumsdon, D.G., Millard, P., Towers, W., Zaehle, S. & Smith, J. U. (2007). Climate change cannot be entirely responsible for soil carbon loss observed in England and Wales, 1978–2003. *Global Change Biology*, *13*(12), 2605–2609. https://doi.org/10.1111/j.1365-2486.2007.01458.x

Smith, P., Martino, D., Cai, Z., Gwary, D., Janzen, H., Kumar, P., McCarl, B., Ogle, S., O'Mara, F., Rice, C., Scholes, B., Sirotenko, O., Howden, M., McAllister, T., Pan, G., Romanenkov, V., Schneider, U., Towprayoon, S., Wattenbach, M. & Smith, J. (2008). Greenhouse gas mitigation in agriculture. *Philosophical Transactions of the Royal Society B: Biological Sciences*, *363*(1492), 789–813. https://doi.org/10.1098/rstb.2007.2184

Snyder, C. S., Bruulsema, T. W., Jensen, T. L., & Fixen, P. E. (2009). Review of greenhouse gas emissions from crop production systems and fertilizer management effects. *Agriculture, Ecosystems and Environment*, *113*, 247–266. https://doi.org/10.1016/j.agee.2009.04.021

Soil Conservation Service. (1976). Section 4: Hydrology. In *National Engineering Handbook*. SCS.

Soussana, J. F., Allard, V., Pilegaard, K., Ambus, P., Amman, C., Campbell, C., Ceschia, E., Clifton-Brown, J., Czobel, S., Domingues, R., Flechard, C., Fuhrer, J., Hensen, A., Horvath, L., Jones, M., Kasper, G., Martin, C., Nagy, Z., Neftel, A., Raschi, A., Baronti, S., Rees, R. M., Skiba, U., Stefani, P., Manca, G., Sutton, M., Tuba, Z. & Valentini, R. (2007). Full accounting of the greenhouse gas (CO2, N2O, CH4) budget of nine European grassland sites. *Agriculture, Ecosystems and Environment*, *121*, 121–134. https://doi.org/10.1016/j.agee.2006.12.022

Srinivasan, R., & Arnold, J. G. (1994). Integration of a basin-scale water quality model with GIS. *Journal of the American Water Resources Association*, *30*(3), 453–562. https://doi.org/https://doi.org/10.1111/j.1752-1688.1994.tb03304.x

Stephens, W., Hess, T., & Knox, J. (2001). *Review of the effects of energy crops on hydrology*. Retrieved from https://dspace.lib.cranfield.ac.uk/handle/1826/3368

Stephens, W., Hess, T. M., & Knox, J. W. (2001). The effect of energy crops on hydrology. *Aspects of Applied Biology*, *65*, 101–108.

Surendran Nair, S., Kang, S., Zhang, X., Miguez, F. E., Izaurralde, R. C., Post, W. M., Dietze, Michael C., Lynd, Lee R. & Wullschleger, S. D. (2012). Bioenergy crop models: Descriptions, data requirements, and future challenges. *GCB Bioenergy*, *4*, 620–633. https://doi.org/10.1111/j.1757-1707.2012.01166.x

SWAT. (n.d.). Soil & Water Assessment Tool. Retrieved December 14, 2017, from http://swat.tamu.edu/

SWAT 2012 Input/Output. (n.d.). Retrieved February 1, 2018, from https://swat.tamu.edu/docs/

Tabari, H. (2010). Evaluation of reference crop evapotranspiration equations in various climates. *Water Resources Management*, *24*(10), 2311–2337. https://doi.org/10.1007/s11269-009-9553-8

Tardieu, F., & Simonneau, T. (1998). Variability among species of stomatal control under fluctuating soil water status and evaporative demand: modelling isohydric and anisohydric behaviours. *Journal of Experimental Botany*, *49*, 419–432.

Taube, F., Gierus, M., Hermann, A., Loges, R., & Schönbach, P. (2014). Grassland and globalization - challenges for north-west European grass and forage research. *Grass and Forage Science*, *69*(1), 2–16. https://doi.org/10.1111/gfs.12043

Terravesta Ltd. (2018). Retrieved November 23, 2018, from https://www.terravesta.com

The Oak Ridge National Laboratory Distributed Active Archive Center (ORNL DAAC). (n.d.). A Global Database of Field-observed Leaf Area Index in Woody Plant Species, 1932-2011. Retrieved February 1, 2018, from https://daac.ornl.gov/VEGETATION/guides/LAI_Woody_Plants.html

Thomas, M. A., Ahiablame, L. M., Engel, B. A., & Chaubey, I. (2014). Modeling Water Quality Impacts of Growing Corn, Switchgrass, and Miscanthus on Marginal Soils. *Journal of Water Resource and Protection*, *6*, 1352–1368. https://doi.org/10.4236/jwarp.2014.614125

Triana, F., Nassi o Di Nasso, N., Ragaglini, G., Roncucci, N., & Bonari, E. (2015). Evapotranspiration, crop coefficient and water use efficiency of giant reed (Arundo donax L.) and miscanthus (Miscanthus × giganteus Greef et Deu.) in a Mediterranean environment. *GCB Bioenergy*, *7*(4), 811–819. https://doi.org/10.1111/gcbb.12172

Trybula, E. M., Cibin, R., Burks, J. L., Chaubey, I., Brouder, S. M., & Volenec, J. J. (2015). Perennial rhizomatous grasses as bioenergy feedstock in SWAT: Parameter development and model improvement. *GCB Bioenergy*, *7*(6), 1185–1202. https://doi.org/10.1111/gcbb.12210

Ubierna, N., Sun, W., Kramer, D. M., & Cousins, A. B. (2013). The efficiency of C4 photosynthesis under low light conditions in Zea mays, Miscanthus x giganteus and Flaveria bidentis. *Plant, Cell and Environment*, *36*, 365–381. https://doi.org/10.1111/j.1365-3040.2012.02579.x

United Nations Framework Convention on Climate Change (UNFCCC). (n.d.). New Era of Global Climate Action To Begin Under Paris Climate Change Agreement. Retrieved December 18, 2018, from https://unfccc.int/news/new-era-of-global-climate-action-to-begin-under-paris-climate-change-agreement-0

United States Department of Agriculture (USDA). (1986). *Urban Hydrology for Small Watersheds - TR55*. *Technical Release 55*. https://doi.org/Technical Release 55

Van Dijk, A. I. J. M., Gash, J. H., Van Gorsel, E., Blanken, P. D., Cescatti, A., Emmel, C., Gielen, B., Harman, I.N., Kiely, G., Merbold, L., Montagnani, L., Moors, E., Sottocornola, M., Varlagin, A., Williams, C.A. & Wohlfahrt, G. (2015). Rainfall interception and the coupled surface water and energy balance. *Agricultural and Forest Meteorology*, *214–215*, 402–415. https://doi.org/10.1016/j.agrformet.2015.09.006

Van Weyenberg, S., Ulens, T., De Reu, K., Zwertvaegher, I., Demeyer, P., & Pluym, L. (2015). Feasibility of Miscanthus as alternative bedding for dairy cows. *Veterinarni Medicina*, *60*(3), 121–132. https://doi.org/10.17221/8059-VETMED

Vanloocke, A., Bernacchi, C. J., & Twine, T. E. (2010). The impacts of Miscanthus x giganteus production on the Midwest US hydrologic cycle. *Global Change Biology Bioenergy*, *2*(4), 180–191. https://doi.org/DOI 10.1111/j.1757-1707.2010.01053.x

Verlinden, M. S., Broeckx, L. S., Van den Bulcke, J., Van Acker, J., & Ceulemans, R. (2013). Comparative study of biomass determinants of 12 poplar (Populus) genotypes in a high-density short-rotation culture. *Forest Ecology and Management*, *307*, 101–111. https://doi.org/10.1016/j.foreco.2013.06.062

Wagle, P., Kakani, V. G., & Huhnke, R. L. (2016). Evapotranspiration and ecosystem water use efficiency of switchgrass and high biomass sorghum. *Agronomy Journal*, *108*(3), 1007–1019. https://doi.org/10.2134/agronj2015.0149

Wang, D., Li, J. S., & Rao, M. J. (2006). Winter wheat canopy interception under sprinkler irrigation. *Scientia Agricultura Sinica*, *39*(9), 1859–1864.

Wang, G., Jager, H. I., Baskaran, L. M., & Brandt, C. C. (2018). Hydrologic and water quality responses to biomass production in the Tennessee river basin. *GCB Bioenergy*, (May), 877–893. https://doi.org/10.1111/gcbb.12537

Weih, M., & Nordh, N. E. (2002). Characterising willows for biomass and phytoremediation: Growth, nitrogen and water use of 14 willow clones under different irrigation and fertilisation regimes. *Biomass and Bioenergy*, *23*(6), 397–413. https://doi.org/10.1016/S0961-9534(02)00067-3

Welsh Government. (n.d.). Agricultural Land Classification Map. Retrieved November 27, 2018, from https://beta.gov.wales/agricultural-land-classification-predictive-map

Welsh Government. (2018a). *Farming Facts and Figures, Wales 2017*. Retrieved from https://gov.wales/docs/statistics/2017/170620-farming-facts-figures-2017-en.pdf

Welsh Government. (2018b). *Welsh Agricultural Statistics 2016*. https://doi.org/10.1039/c0mt00106f

Wendt, J. W., & Hauser, S. (2013). An equivalent soil mass procedure for monitoring soil organic carbon in multiple soil layers. *European Journal of Soil Science*, *64*(1), 58–65. https://doi.org/10.1111/ejss.12002

Whitaker, J., Field, J. L., Bernacchi, C. J., Cerri, C. E. P., Ceulemans, R., Davies, C. A., Delucia, E.H., Donnison, I.S., McCalmont, J.P., Paustian, K., Rowe, R.L., Smith, P., Thornley, P., & McNamara, N. P. (2018). Consensus, uncertainties and challenges for perennial bioenergy crops and land use. *GCB Bioenergy*, *10*(3), 150–164. https://doi.org/10.1111/gcbb.12488

Williams, D., & Scott, R. L. (2009). Vegetation-Hydrology Interactions: Dynamics of Riparian Plant Water Use. In J. C. Stromberg & B. J. Tellman (Eds.), *Ecology and Conservation of the San Pedro River* (pp. 37–56). Tuscon: University of Arizona Press.

Williams, J. R. (1975). Sediment-yield prediction with universal equation using runoff energy factor. In *Present and prospective technology for predicting sediment yield and sources: Proceedings of the Sediment yield workshop*. USDA Sedimentation Lab., Oxford.

Williams, J. R., Jones, C. A., & Dyke, P. T. (1984). A modeling approach to determining the relationship between erosion and soil productivity. *Trans.*

ASAE, *27*, 129–144.

Wu, Y., & Liu, S. (2012). Impacts of biofuels production alternatives on water quantity and quality in the Iowa River Basin. *Biomass and Bioenergy*, *36*, 182–191. https://doi.org/10.1016/j.biombioe.2011.10.030

Wu, Q., & Vos, P. (2018) *Chapter 6 Inference and Predition in Handbook of Statistics Volume 38*. Elsevier, Oxford UK.

Wynne-Jones, S. (2016). Flooding and media storms – controversies over farming and upland land-use in the UK. *Land Use Policy*, *58*, 533–536. https://doi.org/10.1016/j.landusepol.2016.08.007

Xu, C. Y., & Chen, D. (2005). Comparison of seven models for estimation of evapotranspiration and groundwater recharge using lysimeter measurement data in Germany. *Hydrological Processes*, *19*(18), 3717–3734. https://doi.org/10.1002/hyp.5853

Xue, S., Lewandowski, I., & Kalinina, O. (2017). Miscanthus establishment and management on permanent grassland in southwest Germany. *Industrial Crops and Products*, *108*, 572–582. https://doi.org/10.1016/j.indcrop.2017.07.024

Yang, Q., & Zhang, X. (2016). Improving SWAT for simulating water and carbon fluxes of forest ecosystems. *Science of the Total Environment*, *569–570*, 1478–1488. https://doi.org/10.1016/j.scitotenv.2016.06.238

Yang, Y. (2015). *Evapotranspiration Over Heterogeneous Vegetated Surfaces. Models and Applications.* Springer, Dordrecht Heidelberg, London, New York.

Zambrano-Bigiarini, M. (2017). hydroGOF: Goodness-of-fit functions for comparison of simulated and observed hydrological time series.

Zang, H., Blagodatskaya, E., Wen, Y., Xu, X., Dyckmans, J., & Kuzyakov, Y. (2018). Carbon sequestration and turnover in soil under the energy crop Miscanthus: repeated13C natural abundance approach and literature synthesis. *GCB Bioenergy*, *10*(4), 262–271. https://doi.org/10.1111/gcbb.12485

Zatta, A., Clifton-Brown, J., Robson, P., Hastings, A., & Monti, A. (2014). Land use change from C3 grassland to C4 Miscanthus: Effects on soil carbon content and estimated mitigation benefit after six years. *GCB Bioenergy*, *6*(4), 360–370.

https://doi.org/10.1111/gcbb.12054

Zhuang, Q., Qin, Z., & Chen, M. (2013). Biofuel, land and water: Maize, switchgrass or Miscanthus? *Environmental Research Letters*, *8*, 6. https://doi.org/10.1088/1748-9326/8/1/015020

Zimmermann, J., Dauber, J., & Jones, M. B. (2012). Soil carbon sequestration during the establishment phase of Miscanthus × giganteus: A regional-scale study on commercial farms using13C natural abundance. *GCB Bioenergy*, *4*(4), 453–461. https://doi.org/10.1111/j.1757-1707.2011.01117.x

Appendix

A1 Chapter 2 Supplementary Information

A1.1 Determining the percentage area covered by each core sample position.

The same soil core sampling design was used in T_{12} (12 years after planting) as previously used in T_6 (six years after planting, Zatta *et al*., 2014). The design uses three soil cores taken from each plot to represent the areas covered by the plant centre (C_c), plant edge (C_e), and inter-row (C_i). For this study (T_{12}) the percentage area represented by each core location was determined by a field cover survey using three randomly placed 1 m^2 quadrats per plot. The survey was conducted after the spring 2017 harvest when the remaining stubble was used to give an above ground indication of the area covered by the *Miscanthus* plants. The results showed that the *Miscanthus* plants covered a mean area of 63.50 +/-1.96 % of each plot (Table A-24).

Table A-24 Results of the ground cover survey to determine the percentage area covered by *Miscanthus*. The percentage cover and standard error (SE) shown are the mean of the three 1 m^2 quadrats used per plot.

Plot	*Miscanthus* % cover	SE
1	56.67	3.33
2	58.33	10.14
3	63.33	6.01
4	50.00	10.00
5	63.33	9.28
6	63.33	8.33
7	55.00	18.93
8	48.33	1.67
9	53.33	6.67
10	61.67	10.14
11	58.33	8.33
12	66.67	18.56
13	75.00	5.00
14	63.33	6.67
15	80.00	0.00
16	65.00	20.21
17	66.67	8.82
18	73.33	3.33
19	76.67	8.82
20	71.67	6.01
Mean	63.50	1.96

The distances between the three soil core locations within each plot were based on the original planting position, as it was not always possible to determine the location of individual plant edges due to the spreading nature of the mature plants. The soil core sample at C_c was taken at the point the plant was originally planted, C_i at 0.5 m along a diagonal between two plants (being the furthest distance), and C_e halfway between C_c and C_i (Figure A-27).

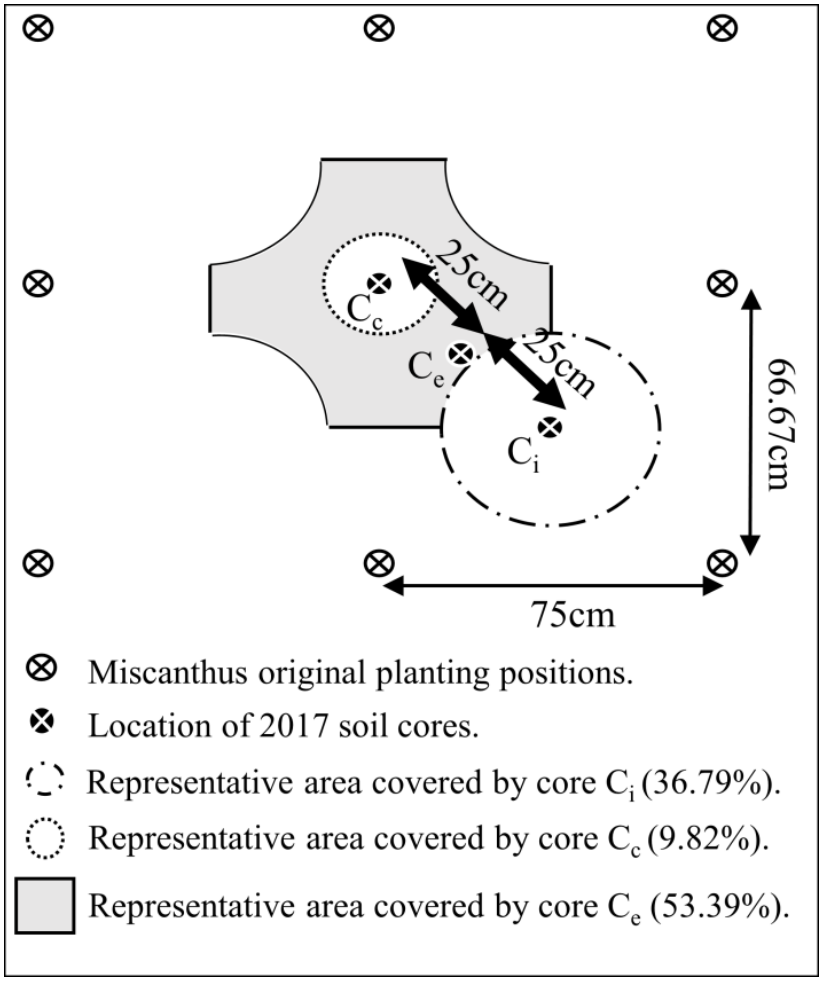

Figure A-27 Location of the three soil core positions taken within each plot, with the percentage area represented by the plant centre (C_c), plant edge (C_e) and inter-row (C_i).

Based on the original planting distance the zone relating to an individual plant was 0.50 m^2 (0.67 m x 0.75 m). The representative area covered by C_i of 0.18 m^2 (37% of the zone), was taken from the field survey as the area without *Miscanthus* stubble. The remaining 63% (covered by *Miscanthus*) was split as follows: the area represented by C_c was given an arbitrary diameter of 0.25 m (area 0.05 m^2) covering 10%; the remaining area of 0.27 m^2 (53%) was taken to represent C_e.

A1.2 Plot heterogeneity

To explore heterogeneity between individual plots, the “aov” function in the statistical program R (R Core Team, 2015) was used to check for differences in soil organic carbon (SOC) between individual plots at time points T_0, T_6, T_{12} and also for the change in SOC between T_6 and T_{12}. No statistical differences were found ($p>0.05$).

A2 Chapter 5 Supplementary Information

A2.1 Description of model evaluation statistics

The mean absolute error (MAE) calculates the average of the difference between simulated and measured values, measuring the closeness of the predictions. It is calculated using equation 30.

$$MAE = \sum_{t=1}^{n} |\hat{y}_t - y|/n \quad (30)$$

where n is the number of observations, t time, $\hat{y}_t$ the predicted values, and y the observed values.

The root mean square error (RMSE) calculates the standard deviation of the model prediction error, giving more weight to the largest errors. It is calculated using equation 31.

$$RMSE = \sqrt{\sum_{t=1}^{n}(\hat{y}_t - y)/n} \quad (31)$$

The coefficient of determination (R^2) between the observation and predicted values gives the degree of collinearity between observed data and model simulations and is calculated using equation 32.

$$R^2 = \left\{ \frac{\sum_i^n (Q_{m,i} - \bar{Q}_m)(Q_{s,i} - \bar{Q}_s)}{\left[\sum_i^n (Q_{m,i} - \bar{Q}_m)^2\right]^{0.5} \left[\sum_i^n (Q_{s,i} - \bar{Q}_s)^2\right]^{0.5}} \right\}^2 \quad (32)$$

where n is the number of observations, i the i^{th} measured or simulated data, Q_m and Q_s the measured or simulated variable respectively (e.g. evapotranspiration), with the overbar denoting the mean for the period.

R^2 only evaluates the linear relationship and therefore is insensitive to additive and proportional differences so other goodness of fit tests are also used to further evaluate the model performance. The modified Nash Sutcliffe Efficiency (mNSE, equation 33) and the modified index of agreement (md, equation 34) are sensitive to differences in measured and simulated means and variances and remove the sensitivity to extreme values due to the squaring of the difference terms in the unmodified versions (Legates & McCabe, 2005).

$$mNSE = 1 - \frac{\sum_i |Q_m - Q_s|_i^j}{\sum_i |Q_{m,i} - \bar{Q}_m|_i^j} \quad (33)$$

$$md = 1.0 - \frac{\sum_i |Q_m - Q_s|^j}{\sum_i (|Q_{s,i} - \bar{Q}_m| + |Q_{m,i} - \bar{Q}_m|)^j} \quad (34)$$

where j is an arbitrary power, for example if $j>2$ in the MNSE equation there is increased sensitivity to high values.

A2.2 Yearly model results

In accordance with the seasonal results, the yearly values over the whole time period (2012 to 2016) show the PMgrass formula to be performing well in both model agreement indexes (Table A-25).

Table A-25 Mean yearly evapotranspiration (2012 to 2016) with the standard deviation (SD), standard error of the mean (SEM), modified Index of Agreement (md) and modified Nash Sutcliffe Efficiency (mNSE). The models are: GG, Granger-Gray; PMsugarcane.adj, PMgrass adjusted with a water stress coefficient and the crop coefficient for sugarcane; PMsugarcane, PMgrass adjusted with the crop coefficient for sugarcane; PMgrass, Penman-Monteith (short grass); HS, Hargreaves-Samani; HS.adj, HS adjusted with a soil moisture function; PT, Priestley-Taylor; PT.adj, PT adjusted with a soil moisture function. Model results are compared to eddy covariance (EC).

	EC	**GG**	**PMsugar-cane.adj**	**PMsugar-cane**	**PM-grass**	**HS**	**HS.adj**	**PT**	**PT.adj**
Mean (mm yr^{-1})	491.80	424.28	335.18	541.37	534.71	692.11	363.61	536.49	319.50
SD (mm yr^{-1})	39.97	20.22	60.53	35.44	32.60	18.45	90.54	27.48	76.52
SEM (mm yr^{-1})	17.87	9.04	27.07	15.85	14.58	8.25	40.49	12.29	34.22
md [0-1]		0.32	0.17	0.25	0.25	0.14	0.23	0.25	0.16
mNSE [-INF- 1]		-1.10	-3.88	-0.60	-0.75	-5.24	-2.99	-0.77	-4.37

A3 Chapter 6 Supplementary Information

A3.1 Climate data

Daily weather data (covering the period 1999-2013) from the National Centers for Environmental Prediction (NCEP) Climate Forecast System Reanalysis (CFSR) (NCEP, n.d.) were used in the SWAT model. Climate reanalysis (observations combined with a numerical model simulating coupled atmosphere-ocean-land systems) provides comprehensive global records of climate states for long time periods. CFSR data was checked against UK Met Office historic and long term averages at four stations located within the watershed (Fig. A-28 – A-32).

SWAT provides a choice of methods for calculating potential evapotranspiration (Priestley-Taylor, Hargreaves, and Penman-Monteith for a 40 cm tall reference crop of alfalfa) as well as the ability to read in externally calculated values (Neitsch *et al*., 2011). Calculating potential evapotranspiration (PET) within SWAT gave a mean watershed PET of 0.35 (fraction of precipitation) or below, whereas values of around 0.45 are more realistic for the region (Nisbet, 2005). PET was therefore calculated on a daily basis outside of SWAT (using R (R Core Team, 2015) package 'Evapotranspiration' Penman Monteith formula for short grass (Guo & Westra, 2016) and the values were read in. The daily climate data required was taken from a representative weather location (see main document Fig. 22). Use of the read in values resulted in an average PET for the watershed of 0.44. Actual evapotranspiration was calculated by SWAT.

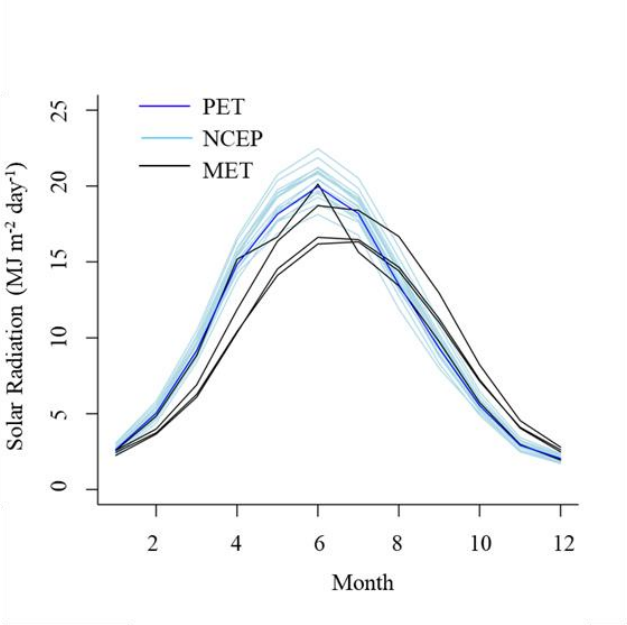

Figure A-28 Mean daily solar radiation for each month from 1999 to 2013 for NCEP (National Centres for Environment Prediction) data and from 1999-2010 for the MET (UK Met Office) data. The PET line highlights the climate location used in potential evapotranspiration calculations.

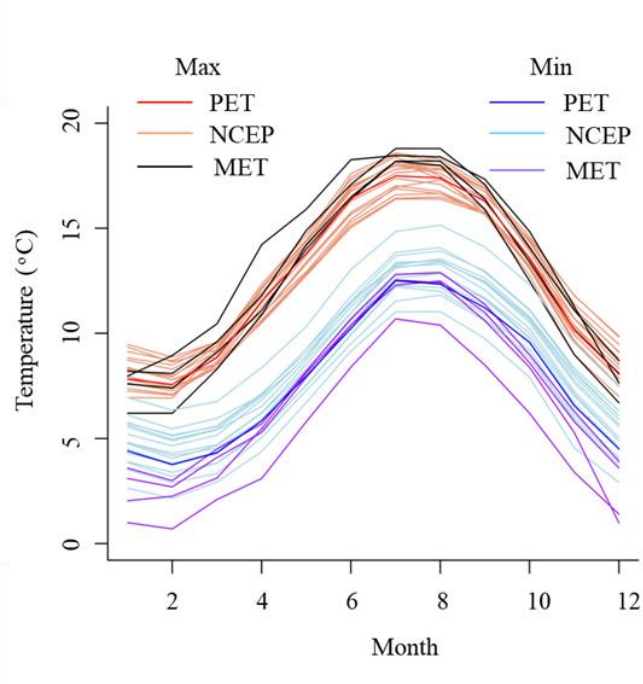

Figure A-29 Mean daily maximum (Max) and minimum (Min) air temperature for each month from 1999 to 2013 for NCEP (National Centers for Environment Prediction) data and from 1999-2010 for the MET (UK Met Office) data. The PET line highlights the climate location used in potential evapotranspiration calculations.

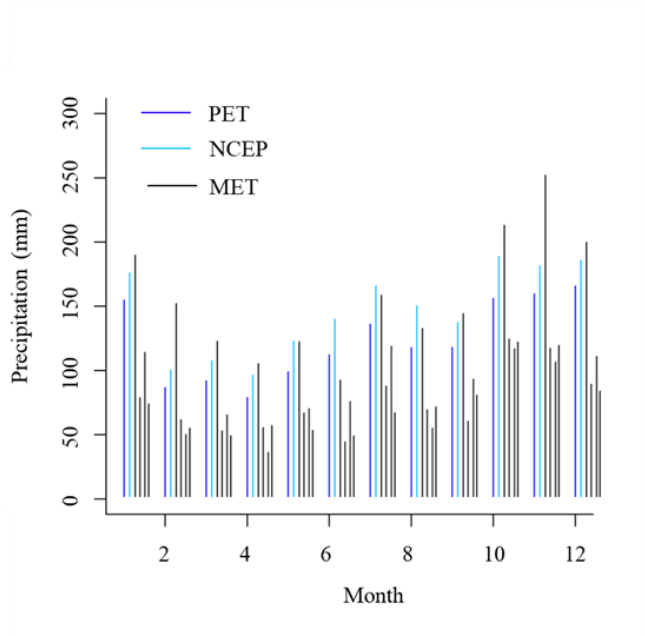

Figure A-30 Mean total monthly precipitation from 1999 to 2013 for NCEP (National Centers for Environment Prediction) data (only highest value from NCEP locations shown) and from 1999-2010 for the MET (UK Met Office) data. The PET line shows the mean values for the climate location used in potential evapotranspiration calculations.

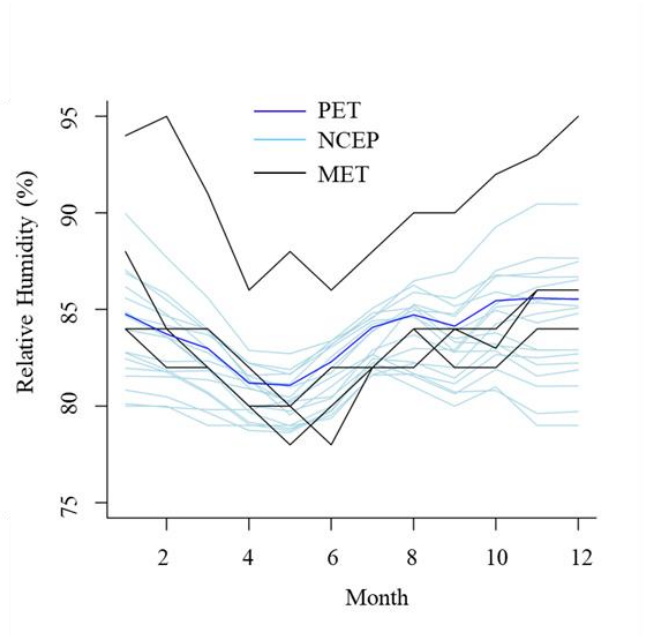

Figure A-31 Mean daily relative humidity for each month from 1999 to 2013 for NCEP (National Centers for Environment Prediction) data and from 1999-2010 for the MET (UK Met Office) data. The PET line highlights the climate location used in potential evapotranspiration calculations. The station with the highest humidity is located at Gogerddan (52.43°N, 4.02°W).

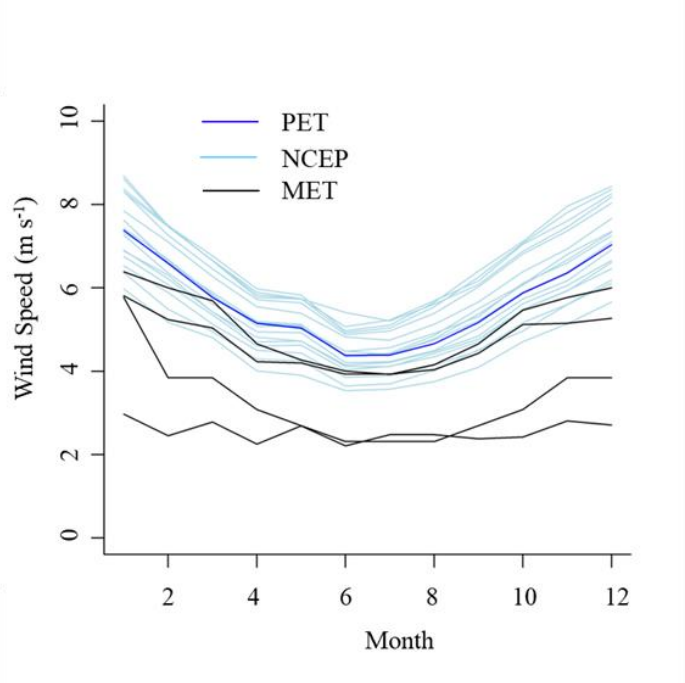

Figure A-32 Mean daily wind speed in each month from 1999 to 2013 for NCEP (National Centers for Environment Prediction) data and from 1999-2010 for the MET (UK Met Office) data. The PET line highlights the climate location used in potential evapotranspiration calculations. The stations with the lowest wind speeds are located at Cwmystwyth (52.35°N, 3.80°W) and Gogerddan (52.43°N, 4.02°W).

A3.2 Model calibration and validation

A3.2.1 Streamflow

Calibration and validation of the baseline scenario (representing existing land use) was completed using SWAT-CUP 2012 v.5.1.6 Sequential Uncertainty Fitting (SUFI2) procedure (Abbaspour, 2015). 700 simulations were run with the adjustment of a selection of basin level parameters (Table A-26) with the objective of achieving a Modified Nash Sutcliffe Efficiency (where p=3) of 0.5. The values used in the best simulation were used in all the modelled scenarios. Observed daily streamflow (NERC & CEH, n.d.) was converted to monthly mean values to correspond with the monthly time-step of the SWAT modelled streamflow outputs. Observed and modelled values were compared using R^2 and Nash Sutcliffe coefficients to assess goodness of fit. Satisfactory calibration was achieved for all calibration and validation locations with a Nash Sutcliffe value of 0.50 or above (Fig. A-33 – A-39).

Table A-26 SWAT input parameters (along with SWAT input code and file extension,(Arnold *et al*., 2012)) adjusted with SWAT-CUP Sequential Uncertainty Fitting routines and the resulting best value ranges. The values used in the best simulation (objective of achieving a Modified Nash Sutcliffe Efficiency (p=3) of 0.5) were used in the model.

SWAT input parameter	Best range	Best simulation value
Threshold depth of water in shallow aquifer for "revap"/percolation (REVAPMN .gw)	961-994	978
Groundwater "revap" coefficient (GW_REVAP .gw)	0.04-0.05	0.05
Threshold depth of water to shallow aquifer for return flow (GWQ_MN .gw)	114-359	236
Ground water delay time (GW delay .gw)	1.5-5.11	3.31
Baseflow alpha factor (Alpha_BF .gw)	0.47-0.77	0.61
Soil evaporation compensation factor (ESCO .bsn)	0.42-0.80	0.61
Plant uptake compensation factor (EPCO .bsn)	0.57-0.87	0.72
Surface runoff lag coefficient (SURLAG .bsn)	0.16-23	12

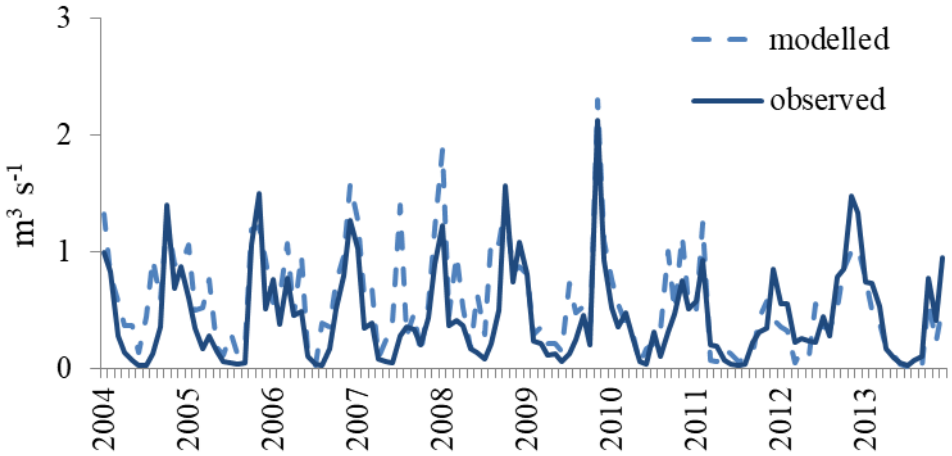

Figure A-33 Observed and modelled stream flow for location C1 (located on Anglesea at 53.26 °N and 4.35 °W). Correlation coefficients: R^2 0.65; Nash Sutcliffe Efficiency 0.50.

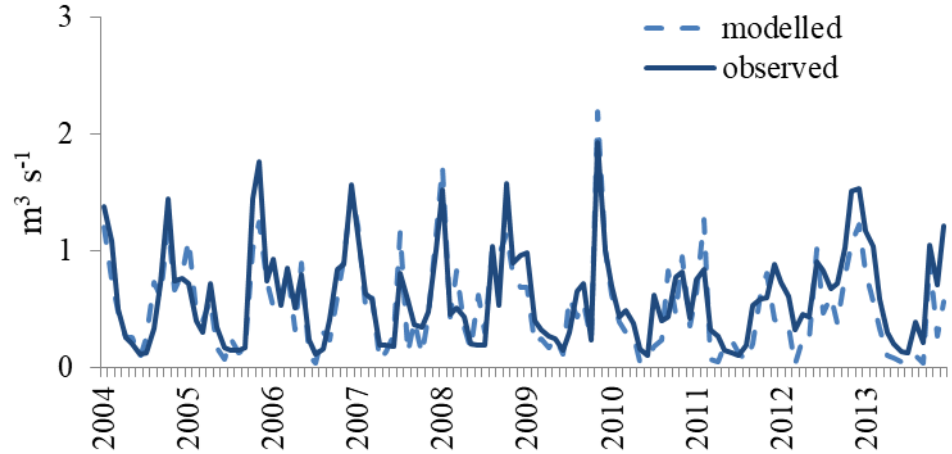

Figure A-34 Observed and modelled stream flow for location C2 (located at Erch, 53.93 °N and 4.38 °W). Correlation coefficients: R^2 0.73; Nash Sutcliffe Efficiency 0.67.

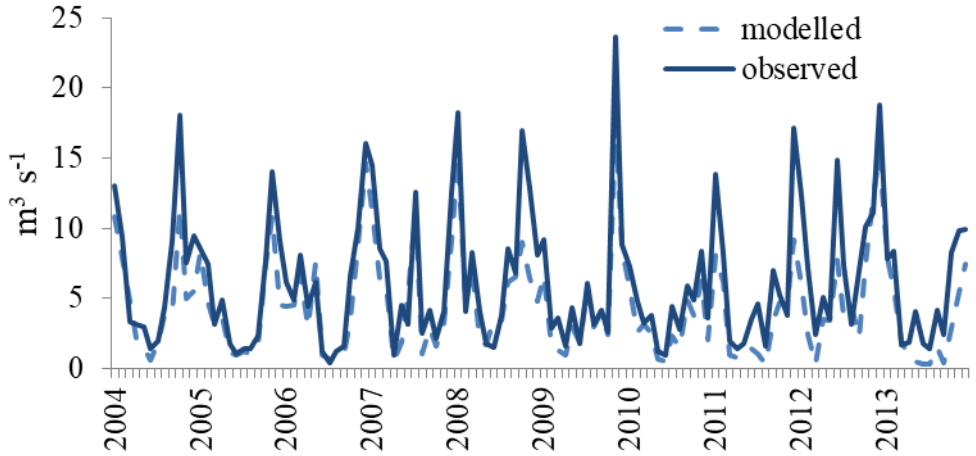

Figure A-35 Observed and modelled stream flow for location C3 (located at Ysywyth, 52.37 °N and 4.07 °W). Correlation coefficients: R^2 0.84; Nash Sutcliffe Efficiency 0.67.

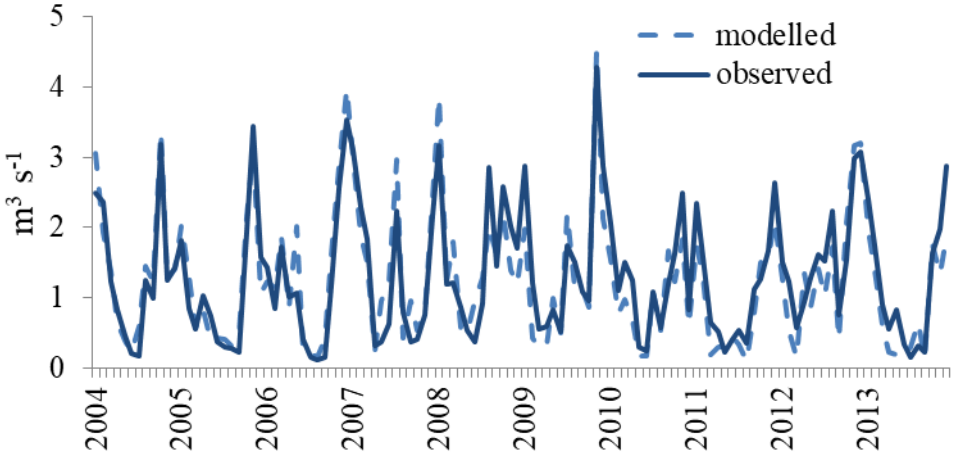

Figure A-36 Observed and modelled stream flow for location C4 (located at Dewi Fawr, 51.82 °N and 4.48 °W). Correlation coefficients: R^2 0.83; Nash Sutcliffe Efficiency 0.81.

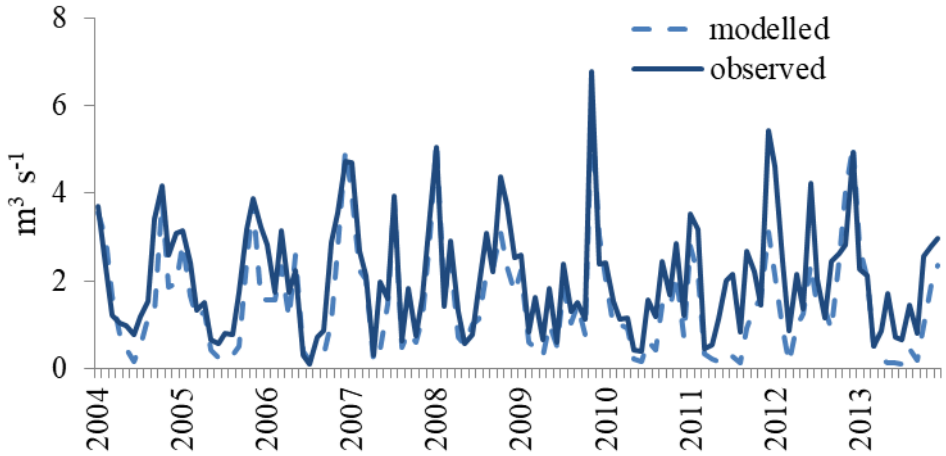

Figure A-37 Observed and modelled stream flow for location V1 (located at Cwmystwyth, 52.34 °N and 3.77 °W). Correlation coefficients: R^2 0.87; Nash Sutcliffe Efficiency 0.56.

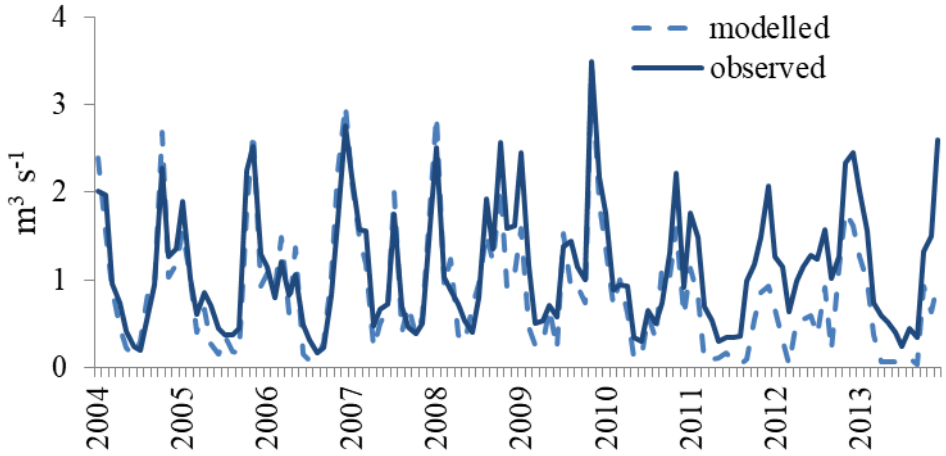

Figure A-38 Observed and modelled stream flow for location V2 (located at Gwaun, 51.97 °N and 4.90 °W). Correlation coefficients: R^2 0.76; Nash Sutcliffe Efficiency 0.59.

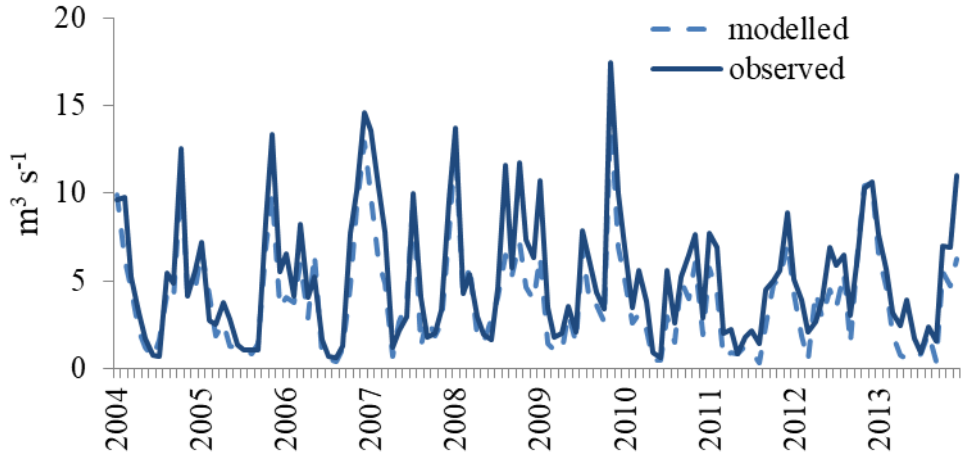

Figure A-39 Observed and modelled stream flow for location V3 (located at Gwii, 51.87 °N and 4.28 °W). Correlation coefficients: R^2 0.88; Nash Sutcliffe Efficiency 0.76.

A3.3 Crop growth time series

Simulated growth for all land cover plants types were checked against literature values for expected growth within the region (see Table 22 in the main document). Examples of the crop growth patterns for the main three crops (taken from the same hydrological response unit (HRU)) used in each scenario are shown below (Fig. A-40, A-42 and A-43). The early growth spurt and increased biomass for the grass pasture seen in 2012 is likely to be as a result of the warm winter with high air temperatures and solar radiation early in the year (Fig. A-41) promoting a growth spurt before the start of grazing. Similar peaks are not seen with *Miscanthus* and SRC due to their later starting growing season.

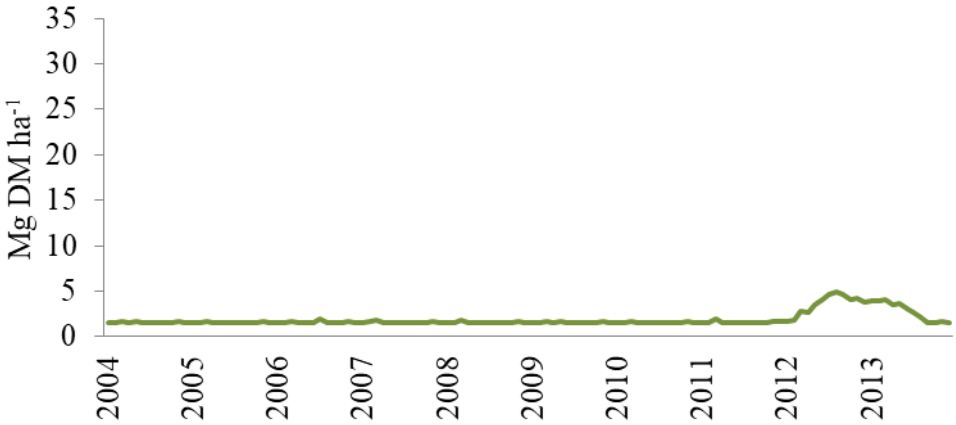

Figure A-40 Simulated improved pasture biomass growth (dry matter, DM). Sheep grazing is modelled from April to a minimum biomass of 1.5 Mg DM ha^{-1}.

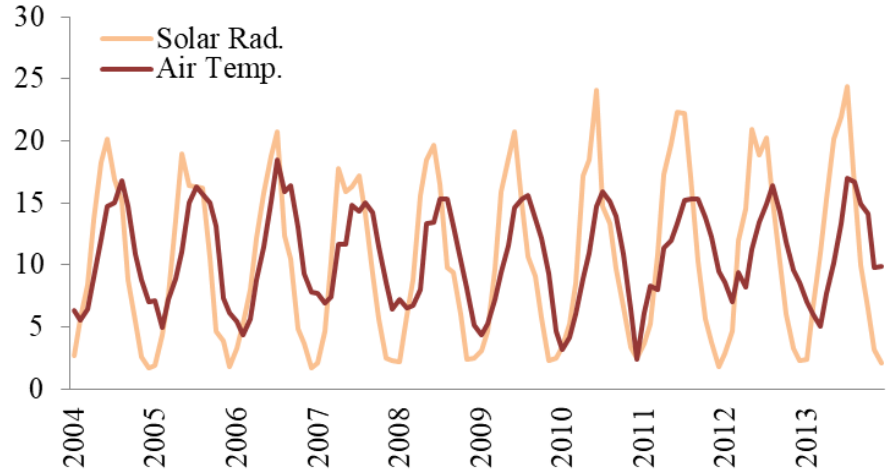

Figure A-41 Average daily air temperature and solar radiation for the crop growth series shown in Figures A-40, A-42 and A-43.

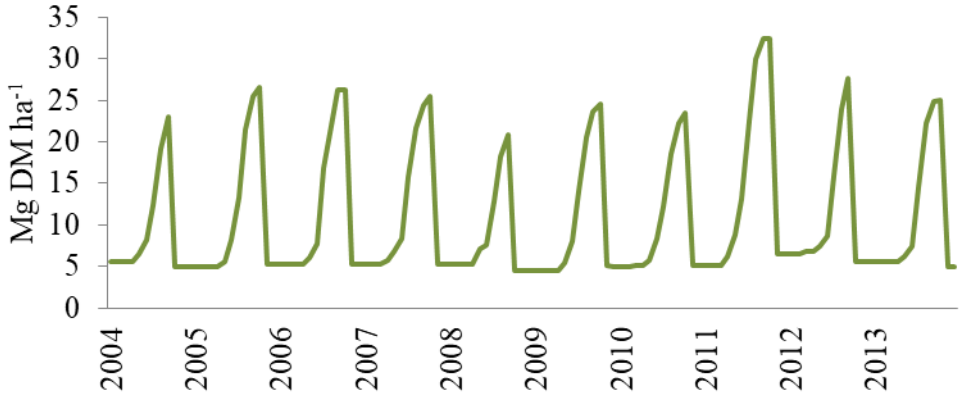

Figure A-42 Simulated *Miscanthus* biomass growth (dry matter, DM) with an autumn harvest.

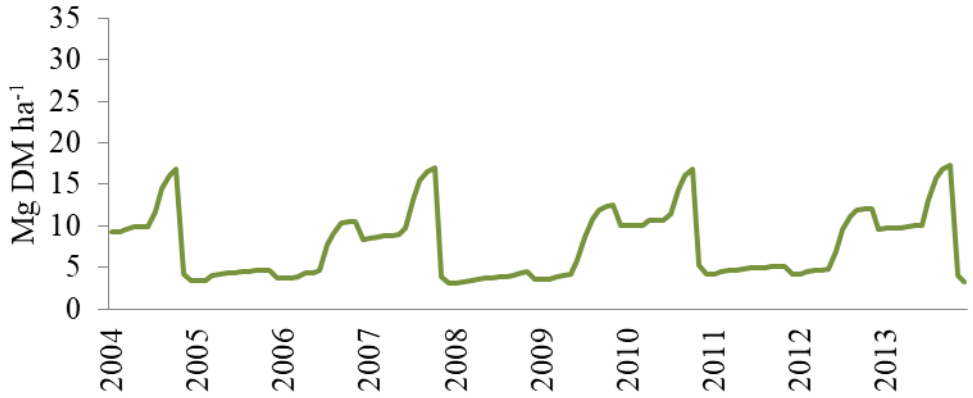

Figure A-43 Simulated short rotation coppice (SRC) biomass growth (dry matter, DM) with autumn harvests on a three year cycle.

A3.4 Wald chi square

The Wald chi square test for significance of fixed factors in mixed effects models does not require two models for comparison (as needed for likehood ratio tests, LRT). It uses an assumption of asymptotic distribution and whilst mixed models do not have classic asymptotic distributions useful inferences can still be made. It is calculated by taking the square of the distance between the maximum likelihood estimate and the value under the null hypothesis divided by the estimated variance (equation 35).

$$Wald\ x^2 = \frac{(\hat{\theta} - \theta_o)^2}{\hat{v}(\hat{\theta})} = I(\hat{\theta})(\hat{\theta} - \theta_o)^2 \qquad (35)$$

where $\hat{\theta}$ is the maximum likelihood estimator, θ_o the hypothesis value, $\hat{v}$ the variance and $I(\hat{\theta})$ the Fisher Information number (evaluated at the maximum likelihood estimator) (Wu & Vos, 2018).

A4 Conversions

A4.1 Conversion using molecular weights

- Conversion from kg C in CO_2 to CO_2:

1kg CO_2-C = x (44/12) = 3.67 kg CO_2

- Conversion from kg N in N_2O to N_2O:

1 kg N_2O-N = x (44/28) = 1.57 kg N_2O

Conversion from kg C in CH_4 to CH_4:

1kg CH_4-C = x (16/12) = 1.33 kg CH_4

(IPCC, 2006)

A4.2 Conversion from hourly flux (µg N_2O m^{-2} hr^{-1}) to Mg N_2O ha^{-1} day^{-1}

µg N_2O m^{-2} hr^{-1} x 24 = µg N_2O m^{-2} day^{-1}

µg N_2O m^{-2} day^{-1} x 10^{-6} = g N_2O m^{-2} day^{-1}

g N_2O m^{-2} day^{-1} x 10^{-2} = Mg N_2O ha^{-1} day^{-1}

A4.3 Conversions to CO_2-eq

- Carbon

Mg C ha^{-1} x 3.67 = Mg CO_2-eq ha^{-1}

- Nitrous oxide

Mg N_2O ha^{-1} x 298 = Mg CO_2-eq ha^{-1}

A4.4 Conversion from Mg CO_2-eq ha^{-1} to g CO_2-eq MJ^{-1}

Mg CO_2-eq ha^{-1} / GJ ha^{-1} = Mg CO_2-eq GJ^{-1}

Mg CO_2-eq GJ^{-1} x 10^6 = g CO_2-eq GJ^{-1}

g CO_2-eq GJ^{-1} x 10^{-3} = g CO_2-eq MJ^{-1}

A4.5 Soil organic carbon to fixed depth

C concentration (kg Mg^{-1}) x Bulk density (Mg m^{-3}) x Depth of sample (m) x 10^4 (m^2 ha^{-1})